BINGE ALCOHOL DRINKING ALTERS THE DIFFERENTIAL CONTROL OF CHOLINERGIC INTERNEURONS OVER NUCLEUS ACCUMBENS MEDIUM SPINY NEURONS

A Dissertation Presented

By

JENYA KOLPAKOVA

Submitted to the Faculty of the

University of Massachusetts Graduate School of Biomedical Sciences, Worcester

in partial fulfillment of the requirements for the degree of

DOCTOR OF PHILOSOPHY

MAY 6, 2022

NEUROSCIENCE

BINGE ALCOHOL DRINKING ALTERS THE DIFFERENTIAL CONTROL OF CHOLINERGIC INTERNEURONS OVER NUCLEUS ACCUMBENS MEDIUM SPINY NEURONS

A Dissertation Presented

By

JENYA KOLPAKOVA

This work was undertaken in the Graduate School of Biomedical Sciences

Neuroscience Program

Under the mentorship of

Gilles Martin, Ph.D., Thesis Advisor

Kensuke Futai, Ph.D., Member of Committee

Andrew Tapper, Ph.D., Member of Committee

David Weaver, Ph.D., Member of Committee

Scott Steffensen, Ph.D., External Member of Committee

Haley Melikian, Ph.D., Chair of Committee

Mary Ellen Lane, Ph.D.,

Dean of the Graduate School of Biomedical Sciences

May 6, 2022

Acknowledgements and Dedication

I would like to firstly acknowledge my mentor, Dr. Gilles Martin. He has been there for me for the past six years and mentored me on everything, from electrophysiological techniques to hypothesis testing to important life wisdom. I greatly appreciate all the effort he put into turning me into a real scientist, always inspiring me to be curious and also really acknowledging my effort, which shaped me into a confident and insightful scientist. Next, I would like to acknowledge my thesis and dissertation committee, Dr. Kensuke Futai, Dr. Andrew Tapper, Dr. Dave Weaver and Dr. Haley Melikian, who is also my Thesis Chair, who guided my research for the past 6 years and taught me to think critically and always to keep questioning. Lastly I would like to acknowledge my family, my daughter Victoria Espinosa, my father Pavel Kolpakov and my mother Olga Kolpakova, who always supported me and believed in me, and my partner Dr. Vincent van der Vinne, who always acknowledges my strengths and at the same time keeps encouraging me to be the best version of myself. And especially I would like to acknowledge my grandmother, Lubov Ivanovna Jeltova, who used to live in Mariupol, Ukraine and is now displaced into Donetsk Republic, and my uncle, Alexander Zaitsev, who was killed while trying to evacuate from Mariupol. I have left Ukraine as a teenager and only saw them once per few years, but they always believed in me and taught me to never give up. This thesis is for them.

Abstract

Striatal cholinergic interneurons (ChIs) play a central role in basal ganglia function by regulating associative learning and reward processing. Drug addiction, such as alcoholism, is often described to hijack the natural reward system. In the nucleus accumbens (NAc), a brain region that mediates rewarding properties of substance of abuse, ChIs regulate glutamatergic, dopaminergic, and GABAergic neurotransmission. However, it is unclear how ChIs orchestrate the control of these neurotransmitters to determine the excitability of medium spiny neurons (MSNs), the NAc output neurons that translate accumbens electrical activity into behavior. Combining *ex vivo* electrophysiology, fast scan cyclic voltammetry and optogenetics approaches, I have demonstrated that stimulating NAc ChIs decreases the spontaneous excitatory postsynaptic currents (sEPSCs) frequency of both D1- and D2-MSNs through different mechanisms. While this effect in D1-MSNs was mediated by dopamine, it resulted from a direct control of glutamate release by ChIs in D2-MSNs. Interestingly, after two weeks of binge alcohol drinking, the effect of ChI stimulation on glutamate release was reversed in D1-MSNs, while its effect on D2-MSNs remained unchanged. Finally, *in vivo* optogenetic stimulation of NAc ChIs significantly increased alcohol consumption compared to unstimulated mice, but failed to alter mouse locomotor activity and saccharine or water consumption. Together, these results identify ChIs as a key modulator of NAc circuit activity and as a potential therapeutic target for alcohol use disorder.

Table of Contents

List of Tables

Chapter II

List of Figures

Chapter IV

List of Symbols, Abbreviations or Nomenclature

ACh	acetylcholine
AChRs	acetylcholine receptors
ACSF	artificial cerebrospinal fluid
Atr	atropine
AUD	alcohol use disorder
BLA	basolateral amygdala
BNST	bed nucleus of the stria terminalis
CeA	central amygdala
ChIs	cholinergic interneurons
ChR2	channelrhodopsin-2
ChrimsonR	chrimson opsin
CIE	chronic intermittent ethanol
D1	dopamine 1 receptor
D1-D5	dopamine 1-5 receptors
D1-MSN	dopamine receptor 1-medium spiny neuron
D2	dopamine 2 receptor
D2-MSN	dopamine 2 receptor-medium spiny neuron
DA	dopamine
DID	drinking in the dark
DS	dorsal striatum
DSM-5	Diagnostic and Statistical Manual of Mental Disorders
eEPSC	evoked excitatory post-synaptic current
eEPSP	evoked excitatory post-synaptic potential
EPHierStats	statistical tool to model the hierarchical relationships in electrophysiological data
EPSC	excitatory post-synaptic current
EPSP	excitatory post-synaptic potential
EtOH	ethanol
FS	fast-spiking
FSCV	fast-scan cyclic voltammetry
GLM	general linear model
GP	globus pallidus
GPCR	G protein-coupled receptors
IEI	inter-event interval
IN	interneuron
IPSC	inhibitory post-synaptic current
IPSP	inhibitory post-synaptic potential
K-S	Kolmogorov-Smirnov test
LTD	long-term depression
LTP	long-term potentiation
LTS	low-threshold spiking

mAChR	muscarinic acetylcholine receptors
Mec	mecamylamine
mEPSC	miniature spontaneous excitatory post-synaptic current
mEPSP	miniature spontaneous excitatory post-synaptic potential
mGluR	metabotropic glutamatergic receptor
mIPSC	miniature spontaneous inhibitory post-synaptic currents
mIPSP	miniature spontaneous inhibitory post-synaptic potential
MM GLM	mixed model general linear model
MSNs	medium spiny neuron
NAc	nucleus accumbens
nAChR	nicotinic acetylcholine receptor
nNOS	neuronal nitric oxide synthase
oEPSC	optogenetically-evoked excitatory post-synaptic current
oEPSP	optogenetically-evoked excitatory post-synaptic potential
PFCx	prefrontal cortex
PPD	paired-pulse depression
PPF	paired-pulse facilitation
PPR	paired-pulse ratio
PTX	picrotoxin
RDL	reverse-dark-light conditions
SCH	SCH-23390
sEPSC	spontaneous excitatory post-synaptic current
sEPSP	spontaneous excitatory post-synaptic potential
SNc	substantia nigra pars compacta
SNr	substantia nigra pars reticulata
SPN	spiny principal neurons
STDP	spike-timing dependent plasticity
STN	sub-thalamic nucleus
Sulp	sulpiride
TTX	tetrodotoxin
VGCC	voltage-gated calcium channel
VM	ventral mesencephalon
VP	ventral pallidum
VTA	ventral tegmental area

Preface

The work presented in Chapter II was previously published in:

Kolpakova J, van der Vinne V, Gimenez-Gomez P, Le T, You IJ, Zhao-Shea R, Velazquez-Marrero C, Tapper AT, Martin GE (2021) Binge alcohol drinking alters synaptic processing of executive and emotional information in core nucleus accumbens medium spiny neurons. *Front Cell Neurosci* 15:742207.

The work presented in Chapter III is deposited in biorxiv.org:

Kolpakova J, Marvel-Zuccola JD, Futai K, Martin GE, van der Vinne V (2022) EPHierStats: a statistical tool to model the hierarchical relationships in electrophysiological data. *BioRxiv* doi: https://doi.org/10.1101/2022.03.23.485501

The work presented in Chapter IV is modified from the manuscript submitted for publication:

Kolpakova J, van der Vinne V, Gimenez-Gomez P, Le T, Martin GE (2022) Binge alcohol drinking alters the differential control of cholinergic interneurons over nucleus accumbens D1 and D2 medium spiny neurons. *In review in Biological Psychiatry*

Chapter I

Introduction

Chapter I: Introduction

Addiction and Reward Circuitry

Addiction stages and mechanism

The Diagnostic and Statistical Manual of Mental Disorders (DSM-5) defines substance-use disorder as “a recurrent use of alcohol or other drugs that causes clinically and functionally significant impairment, such as health problems, disability, and failure to meet major responsibilities at work, school, or home”. Depending on the level of severity, this disorder is classified as mild, moderate, or severe. The term addiction is used to indicate the most severe, chronic stage of substance-use disorder, in which there is a substantial loss of self-control, as indicated by compulsive drug taking despite the desire to stop taking the drug (DSM-5, 2013)

When using animal model to study drug addiction, it is impossible to capture all aspects of addiction, therefore a heuristic understanding of addiction has evolved. It is described as a chronically relapsing disorder that involves drug binges, loss of control in limiting intake, and a subsequent negative emotional state (Koob & Volkow, 2010). Thus, drug addiction has been characterized by a cycle composed of three stages: 1) Binge/intoxication, 2) Withdrawal/negative affect and 3) Preoccupation/anticipation (i.e., craving) (Koob et al., 2004). These stages interact with each other, intensify over time, and through loss of control of the escalation of consumption, lead to the pathological state of addiction (Koob & Le Moal, 1997). The progression between the stages is accompanied by a shift from

positive reinforcement driving the consumption behavior to a negative reinforcement driven by the avoidance of dysphoria and automaticity during the motivated behavior (Koob et al., 2004). The occasional drug use that does not lead to escalation and compulsion is clinically distinct from chronic drug use and the transition from occasional to chronic drug use involves neuroplasticity (Koob & Volkow, 2010).

The physiology of addiction can be explained in part as the dysregulation of the reward pathway where drugs of abuse distort the response to natural reinforcers leading to continued drug use (Volkow & Morales, 2015). Natural reward response involves stimulus-response learning such as conditioned reinforcement and motivation (Di Chiara, 2002). Natural, unconditioned stimuli, such as food or predator, evoke a response when it is of biological value, such as reward or punishment, and are salient. These responses can be extended to other stimuli, such as drugs of abuse, that carry pleasurable valence through stimulus-reward contingencies, thus Pavlovian learning takes place (Di Chiara, 2002). By means of this associative learning, the enhanced incentive salience state drives the person to focus specifically on drug-related stimuli, leading to escalating compulsion for seeking and taking drugs (Robinson & Berridge, 1993; Koob & Volkow, 2010). These processes take place in the basal ganglia group of nuclei, and through the mesocorticolimbic reward pathway, the monoamine, dopamine (DA) has been shown to be the primary neurotransmitter modulating reward and motivation (Wise, 2002; Berridge, 2007; Humphries & Prescott, 2010).

Basal ganglia overview

The basal ganglia consists of the ventral striatum (mainly nucleus accumbens, NAc), dorsal striatum (DS), globus pallidus (GP), ventral pallidum (VP), sub-thalamic nucleus (STN), the substantia nigra pars reticulata and compacta (SNr/SNc), and the ventral tegmental area (VTA); these structures connect with cortex and thalamus in parallel circuit loops (Alexander & Crutcher, 1990; Haber, 2003). Different series of loops exist for the dorsal and ventral striatum, although they both synapse with the thalamus (Hikida, Morita, & Macpherson, 2016). Dorsal striatum receives dopaminergic inputs from SNc and sends projections to SNr, directly, or through GP and STN (Graybiel, 2000). Ventral striatum receives dopaminergic inputs from VTA and sends projections either to the VTA or to the VP, which, in turn, projects to both mediodorsal thalamus and SNr (Kupchik et al., 2015). In addition to anatomical differences, dorsal and ventral striatum differ in a number of functional aspects. While dorsal striatum is implicated in sensorimotor function, habit, and performance of learned instrumental tasks, ventral striatum is associated with higher functions such as reward and aversive learning, social behavior and motivation (Robinson & Berridge, 1993; Lim, Kang, & McGehee, 2014; Hikida et al., 2016).

Neural circuitry of addiction

Although a full discussion of the neural circuitfy of addiction is beyond the scope of this thesis, a review by Koob and Volkow provides an overview of the brain areas involved in the addiction cycle (Koob & Volkow, 2010). The simplified schematic in **Figure 1.1** shows three stages (binge/intoxication, withdrawal/negative affect and preoccupation/activipation “craving”) and their corresponding brain areas.

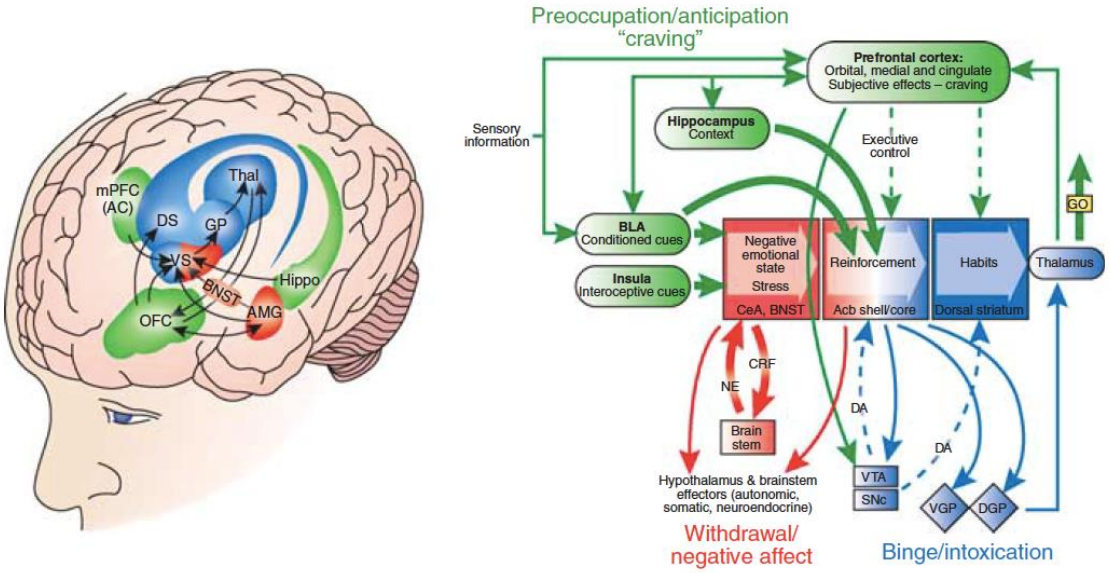

Figure 1.1 | Circuitry of stages of addiction. (a), blue, binge/intoxication stage, (b), red, withdrawal/negative affect stage, (c), green, preoccupation/anticipation “craving” stage. Adopted from Koob and Volkow (2010).

The first, binge stage (a), or the initial action of drug reward is hypothesized to involve activation of the NAc. DA, glutamate and opioid peptides originating in the VTA release in the NAc, GABA systems in NAc and VP. Second, the withdrawal/negative affect stage (b), engages the activation of extended amygdala

(composed of central amygdala, CeA, bed nucleus of the stria terminalis, BNST and the shell of NAc), involves corticotropin-releasing factor, norepinephrine, and dynorphin that function in negative reinforcement. Third (c), the preoccupation/anticipation and craving stage is thought to involve the processing of conditioned reinforcement in the basolateral amygdala (BLA) and the processing of contextual information by the hippocampus. Glutamate is thought to be involved in the craving stage and is localized in projections from frontal cortex and BLA to the ventral striatum. Human studies of drug craving with functional imaging show activation of the orbital and anterior cingulate cortices and the temporal lobe, including the amygdala (Franklin et al., 2007).

Alcohol Use Disorder and its Targets

Binge drinking stage

Alcohol use disorder (AUD) is the third major cause of preventable mortality in the world, globally causing 3.3 million deaths annually (5.9% of all deaths) and 5.1% of the burden of disease and injury, with an economic burden of ~$250 billion annually in the United States (WHO, 2014) (Sacks, Gonzales, Bouchery, Tomedi, & Brewer, 2015). Despite such devastating effects, the treatment options are very scarce, and available medications are effective at treating only 20-30% of patients, with significant side effects (Spanagel, 2009). Interestingly, the comorbidity of alcohol and other drugs of abuse is very high (Wu, Gao, & Taylor, 2014). Alcohol and nicotine usage have been well documented: 96% of alcoholics were found to

be smokers, and recently, smoking cessation anticholinergic drugs started being used to treat alcohol dependence and modulate alcohol drinking behavior (Wu, Gao, & Taylor, 2014).

Binge alcohol drinking, as originally described by Tomsovic in the 1970s, involves repeated period of heavy drinking, followed by a period of abstinence (Tomsovic, 1974). This pattern of ingesting large quantities over a short period of time is exhibited primarily by late adolescent and young adults, with roughly 40% of college students reporting binge drinking behavior (Krieger, Young, Anthenien, & Neighbors, 2018). An updated definition stipulates that binge alcohol drinking brings blood alcohol level to 0.08% and typically corresponds to $\geq$5 drinks for males and $\geq$4 drinks for females in a 2-hour period (NIAAA, 2004). Importantly, binge drinkers, contrary to light drinkers, typically display a strong response to early euphoric effects, but are less sensitive to the sedative effects of alcohol, indicative of a predisposition for the development of alcohol addiction (Schuckit, 1994; Schuckit et al., 2008). There is strong evidence that long-lasting adaptations of the strength of synaptic connections are responsible for the addictive properties of alcohol (Lüscher & Malenka, 2011; Zorumski, Mennerick, & Izumi, 2014). This has led to a hypothesis that synaptic plasticity is affected by binge alcohol drinking (Stephens & Duka, 2008). There is solid evidence that the alteration of neuronal plasticity by drugs of abuse is a conduit for their addictive properties (Hyman, Malenka, & Nestler, 2006; Kauer & Malenka, 2007).

Molecular targets of alcohol

Humans consume and abuse alcohol, and ethanol (EtOH), its main constituent, interacts with biomolecules in our body via hydrogen bonding and weak hydrophobic interactions. It is well established that ethanol is a nonspecific drug with myriad of targets and is known to directly alter membrane protein functions (McClintick et al., 2016; Abrahao, Salinas, & Lovinger, 2017). Although many have been implicated in alcohol effects, those listed in **Figure 1.2** have been validated and causally associated with alcohol effects. Some of the most common targets associated with synaptic transmission are described below.

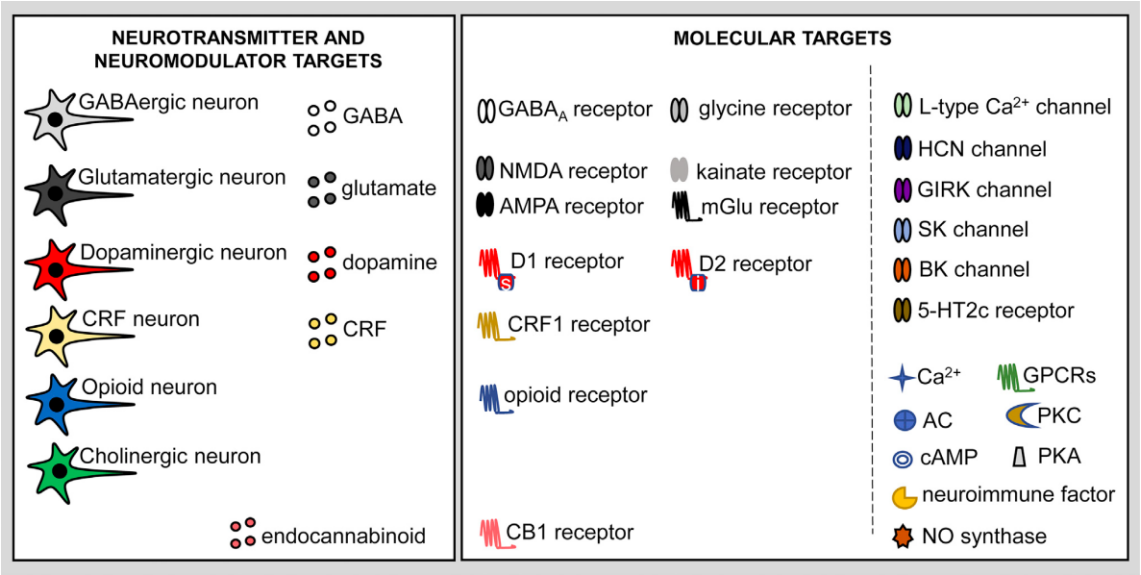

Figure 1.2 | Direct and indirect targets of alcohol effect on the brain. Taken from Abrahao et al. 2017

Alcohol is known to potentiate GABAergic synaptic transmission and glycine receptors throughout the brain, while mostly inhibiting glutamate receptors (Weiner & Valenzuela, 2006; Lovinger & Roberto, 2013; Söderpalm, Lidö, &

Ericson, 2017; Abrahao et al., 2017). The open probability of ion channels, including calcium- and voltage-gated potassium channels, also known as BK cannels, is increased by acute EtOH (Martin, 2010; Dopico, Bukiya, & Martin, 2014), while a decrease in calcium-activated small potassium channels (SK channels) function following ethanol administration has been reported (Hopf et al., 2010). Channels involved in neuron firing have been shown to be enhanced by alcohol, such as G-protein-coupled inwardly rectifying K+ (GIRK) (Bodhinathan & Slesinger, 2013) and hyperpolarization-activated and cyclic nucleotide-gated (HCN) channels (McDaid, McElvain, & Brodie, 2008). nAChRs are well known to be affected by alcohol (Hendrickson, Guildford, & Tapper, 2013). Although differing by subunit composition, the typical effect of alcohol is to potentiate nAChR by stabilization of the open channel state of the receptor (Hendrickson, Guildford, & Tapper, 2013), while inhibiting the mAChR (Costa & Guizzetti, 1999; VanDemark, Guizzetti, Giordano, & Costa, 2009). Finally, alcohol has been shown to downregulate central D2-like receptors (Heinz et al., 2004; Martinez et al., 2005; Coleman, He, Lee, Styner, & Crews, 2011; Trantham-Davidson et al., 2014) and increase the number of surface D1-like receptors (Lograno et al., 1993).

Importantly, when examining the effect of alcohol on ion channel/receptor function, it is crucial to consider that the efficacy of action differs by channels and receptors. As summarized by Gao and collegues (Gao et al., 2019), EC_{50} concentrations of EtOH for the the cannels and receptors are: 37 mM for modulation of L-type Ca^{2+} channels (Mullikin-Kilpatrick & Treistman, 1994), 30–

100 mM for NMDA receptors (Lovinger, White, & Weight, 1989; Weight, Lovinger, & White, 1991), 220 mM for kainate receptors (Weight, Peoples, Wright, Lovinger, & White, 1993), 75 mM for a blockade of α4β2-nAChRs (Zuo, Kuryatov, Lindstrom, Yeh, & Narahashi, 2002) and 75 mM for GABA-induced chloride currents (Nishio & Narahashi, 1990; Gao et al., 2019).

Nucleus Accumbens Functional Anatomy

NAc cell composition

The NAc consists of core and shell regions that do not have a clear neuroanatomical distinction, however, the core region appears to be anatomically similar to the dorsal striatum, while the shell region has shown to have characteristics of the extended amygdala (Humphries & Prescott, 2010). NAc is composed predominantly of GABAergic medium spiny neurons (MSNs, sometimes called spiny principal neurons, SPN), which compose 90-95% of the NAc neuronal population, and are the sole output neurons of the striatum. MSNs are divided into subpopulations of dopamine receptor 1- and 2-expressing medium spiny neurons (D1-/D2-MSNs) (Gerfen & Surmeier, 2011). D1-MSNs co-express dynorphin and substance P, while D2-MSNs express enkephalin, neurotensin, and A2a adenosine receptors (Le Moine & Bloch, 1995; Lobo, Karsten, Gray, Geschwind, & Yang, 2006). The remaining 5–10% of neurons are either GABAergic or cholinergic interneurons. GABAergic interneurons (INs) are composed of several subtypes, including parvalbumin-, somatostatin/

neuropeptide Y/ neuronal nitric oxide synthase (nNOS)/-, and calretinin-expressing INs (Tepper, Tecuapetla, Koós, & Ibáñez-Sandoval, 2010). GABAergic INs that co-express parvalbumin were identified physiogically as the fast-spiking (FS) neuron class (Kawaguchi, Wilson, Augood, & Emson, 1995), while those INs that co-express nitric oxide, somatostatin, and neuropeptide Y were identified physiologically as the low-threshold spiking (LTS) neuron class (Kawaguchi, Wilson, Augood, & Emson, 1995). Cholingergic interneurons (ChIs) release acetylcholine, comprise a single population expressing ChAT (Bolam, Wainer, & Smith, 1984) and are known as tonically active neurons (TANs) (Aosaki, Kimura, & Graybiel, 1995). In addition to neurons, NAc contains glial cells such as astrocytes that are known to increase the extracellular glutamate concentration via coordinated uptake and release (Malarkey & Parpura, 2008; Scofield & Kalivas, 2014).

NAc afferent signals

NAc is a primary input nucleus of the basal ganglia and receives a plethora of afferent signals via glutamate, DA, GABA, serotonin neurotransmission among others (Haber, 2003). The neurotransmitter that has the biggest impact on MSN excitability is glutamate, and glutamatergic inputs originate primarily from cortex, BLA, hippocampus and thalamus (Humphries & Prescott, 2010).

Glutamatergic inputs to NAc that originate from cortical areas (prefrontal cortex, PFCx) (Brog, Salyapongse, Deutch, & Zahm, 1993), are thought to be

responsible for “executive” functions such as planning and attentional control (Miller, 2000). NAc receives projections from medial paralimbic medial (prelimbic and anterior cingulate) and lateral (dorsal and ventral anterior insular) PFCx (Scofield et al., 2016). The amygdala is often considered the seat of basic emotions (LeDoux, 2000), and NAc glutamatergic inputs that originate from the central and caudal basolateral amygdala are thought to encode the value of an unconditioned stimulus associated with a learned conditioned stimulus (Cardinal & Everitt, 2004; Scofield et al., 2016). The hippocampal formation has a key role in episodic memory and spatial navigation and sends glutamatergic projections to the NAc shell and core from the subiculum CA1 area and entorhinal cortex (Humphries & Prescott, 2010). Thalamus, a region known as the relay station between cortex and the sensory signals, sends projections from paraventricular and interlaminar nuclei to NAc MSNs (Vertes & Hoover, 2008; Humphries & Prescott, 2010) and cholinergic interneurons (Ding, Guzman, Peterson, Goldberg, & Surmeier, 2010).

VTA sends dense dopaminergic projections to the NAc, with minor projections from SNc (Joel & Weiner, 2000; Owesson-White, Cheer, Beyene, Carelli, & Wightman, 2008; Tritsch & Sabatini, 2012; Granger, Wallace, & Sabatini, 2017). Dopaminergic afferents to the NAc are well characterized, but must be considered carefully, as DA neurons exhibit tonic and phasic burst firing, with each firing pattern having different functional consequences. Phasic firing is traditionally associated with the modulation of synaptic plasticity in the striatum, while tonic

firing modulates short-term striatal neuron excitability (Humphries & Prescott, 2010). Interestingly, a small sub-populations of VTA dopaminergic inputs to the NAc have also been reported to co-release glutamate or GABA, emphasizing complex role of DA projections in reward-based learning (Stuber, Hnasko, Britt, Edwards, & Bonci, 2010; Tritsch, Ding, & Sabatini, 2012; Granger et al., 2017).

Other neurotransmitters have also been shown to be released into the NAc, including GABA via inputs from the VP (Scofield et al., 2016), VTA (Brown et al., 2012; Taylor et al., 2014; Yorgason et al., 2022) and lateral septum (Brog et al., 1993). Also, serotonergic projections from the dorsal raphe (Brown & Molliver, 2000), and noradrenergic projections from locus coeruleus and nucleus of the solitary tract (Delfs, Zhu, Druhan, & Aston-Jones, 1998) have been reported. Additionally, cholinergic inputs from the brainstem, including the pedunculopontine and laterodorsal tegmental nuclei innervate the NAc (Dautan et al., 2014), however, these inputs do not gate DA release, unlike the local cholinergic interneurons (Brimblecombe et al., 2018).

NAc efferents: direct/indirect pathways

As mentioned above, the only output neurons of the NAc are MSNs, and they are divided into D1, substance P-expression neurons and D2, Enk-expressing neurons, with only 6% showing co-expression of both receptors (Lu, Ghasemzadeh, & Kalivas, 1998). D1- and D2-MSNs, as the only output neurons, have been postulated to promote and inhibit behavior, respectively (Kravitz, Tye, & Kreitzer,

2012). Although initially a strict separation has been described between direct “go” pathway through the D1-MSNs and indirect “no-go” pathway through the D2-MSNs, recent reports challenge this assumption (Kupchik & Kalivas, 2017). The canonical concept described by Albin et al. (Albin, Young, & Penney, 1989) for dorsal striatum posits that D1-MSNs project to ventral mesencephalon (VM) neurons and directly inhibit them, thus disinhibiting the thalamus and promoting motivated behavior (Watabe-Uchida, Zhu, Ogawa, Vamanrao, & Uchida, 2012; Chuhma, Tanaka, Hen, & Rayport, 2011; Macpherson, Morita, & Hikida, 2014), while D2-MSNs project inhibit the ventral pallidum, which inhibits the VM, resulting in inhibition of thalamus and repressed motivated behavior. However, the initial assumption that ventral striatum may be identical to dorsal striatum has been disproven (Voorn, Vanderschuren, Groenewegen, Robbins, & Pennartz, 2004) using modern cell-type specific tools such as transgenic lines expressing fluorescent reporters under D1/D2-promoters to differentiate D1- and D2-MSNs. A newer view posits that D1-MSNs, just like D2-MSNs synapse on VP neurons that project to the VM, thus comprising the indirect pathway (Kupchik et al., 2015). Also, D2-MSNs target VP neurons that innervate the thalamus directly, thus contributing to the direct pathway through the VP to disinhibit the thalamus (Kupchik et al., 2015). Moreover, it was shown that the input to the VP (rather than to the VM) promotes goal-directed behavior and can directly inhibit the thalamus (Root, Melendez, Zaborszky, & Napier, 2015).

However, despite these different pathways' convergence, many studies still find that stimulation or inhibition of D1- and D2-MSNs in the NAc have opposing effects on motivated behavior in rodent models; and optogenetic manipulation of their excitability, such as during glutamatergic plasticity has been causally linked to reward-seeking behaviors (Surmeier, Ding, Day, Wang, & Shen, 2007; Ma et al., 2014; Renteria, Maier, Buske, & Morrisett, 2017; Ma et al., 2018). In NAc, activation of D1-MSNs increased cocaine preference in mice, while activation of D2-MSNs attenuated cocaine preference and suppressed cocaine reward (Lobo et al., 2010). Moreover, activation of D1-MSNs and inhibition of D2-MSNs increase alcohol drinking behavior (Strong et al., 2020). The explanation of these results may lay in a better definition of "go" and "no-go" behavior: not just in terms of initiating or stopping an action, but in different aspects of motivated behavior. For example, it was shown that in NAc, the activation of D1 receptors in the direct pathway is essential for animals to acquire reward-based learning, while D2 receptors inactivation is necessary for learning flexibility to switch from the previously learned behavior (Yawata, Yamaguchi, Danjo, Hikida, & Nakanishi, 2012).

Medium Spiny Neurons in the Striatum

Overview and characteristics

In anesthetized animals, intracellular recordings showed that medium spiny neurons (MSNs) are bistable cells, with their membrane potential in a silent,

hyperpolarized “down” state around -77±7 mV, or in a burst firing depolarized “up” state (i.e., around 63±7 mV) (O’Donnell & Grace, 1995). The transition from downstate to upstate is primarily controlled by glutamatergic inputs from the hippocampus, with cortical afferents playing a minor role in the transition from downstate to upstate (O’Donnell & Grace, 1995). Extracellular recordings in freely moving rats showed that NAc MSNs typically fire between 1 and 10 Hz in freely moving animals (Carelli & Ijames, 2000; Hollander, Ijames, Roop, & Carelli, 2002), which results from glutamatergic incoming signals that fire at similar frequencies (Rosenkranz & Grace, 1999; Margrie, Brecht, & Sakmann, 2002). In slice preparations, where incoming afferents are severed, MSNs resting membrane potential remains in a downstate, they are silent (no action potentials firing), but spontaneous glutamate release can still be recorded (Kasanetz & Manzoni, 2009).

Glutamatergic synaptic transmission

Glutamatergic synaptic neurotransmission from multiple origins converging onto the same MSN (O’Donnell & Grace, 1995; Kolpakova et al., 2021) has been shown to reinforce instrumental (Britt et al., 2012), and drive goal-directed behavior (Goto & Grace, 2008). In order to study how neurons influence their targets, one needs to understand the synaptic transmission. Neurotransmission is canonically known to be initiated by the action potential arriving at the presynaptic terminal, triggering presynaptic calcium influx and resulting in the synaptic vesicle fusion with the presynaptic membrane and neurotransmitter release (Katz, 1969; Südhof, 2013;

Guzikowski & Kavalali, 2021). However, more recently, three different modes of neurotransmission are categorized based on their time scale relative to a stimulus and calcium dependence (Kavalali, 2015; Guzikowski & Kavalali, 2021). The action-potential dependent or evoked release, which is subdivided into synchronous and asynchronous phases; and spontaneous release, which is independent of the action potentials on the presynaptic neuron (Kavalali, 2015; Guzikowski & Kavalali, 2021). Interestingly, although individual synapses can participate in both, evoked and spontaneous glutamatergic neurotransmission, highly active synapses show a preference for one mode of transmission (Peled, Newman, & Isacoff, 2014). Indeed, these different modes of transmission have been found to encode different physiological response (Chanaday & Kavalali, 2018). Synchronous release relays the specific activity pattern given its fidelity to the precise timing of the arriving action potential, while asynchronous release compliments synchronous release during repetitive activity and maintains neurotransmission strength (Otsu et al., 2004; Chanaday & Kavalali, 2018). Spontaneous neurotransmission regulates synaptic strength independent of activity and influence dendritic arbor complexity (Cho et al., 2015; Andreae & Burrone, 2015; Chanaday & Kavalali, 2018).

To measure glutamatergic transmission, the most common approach is whole-cell patch-clamp recording, which measures ionic currents in individual isolated living cells, tissue sections, or patches of cell membrane (Sakmann & Neher, 1984). This technique is used to record spontaneous and evoked excitatory

postsynaptic currents and potentials (EPSCs and EPSPs, respectively), paired-pulse ratio (PPR) as a measure of probability of vesicular release at synapses, and long-term changes of synaptic strength in slice preparation. Additionally, *in vivo* extracellular recordings in anesthetized animals are performed to measure neuron firing associated with specific tasks and behaviors in freely moving animals. These techniques can often distinguish whether the glutamatergic synaptic transmission is altered at pre or postsynaptic sites.

Synaptic Plasticity: LTP/LTD

When we experience memory formation, cognition, or sensory-motor processes, our brains change. Every environmental stimulus and experience cause dynamic change in the neuronal networks by changing the strength of synaptic transmission, which takes place in part through continuous insertion or removal of glutamatergic AMPA receptors, changes accompanied by synaptic formation and morphological refinements (Malenka & Bear, 2004). Importantly, alterations of these synaptic mechanisms called synaptic plasticity may also lead to numerous brain pathologies (Kauer & Malenka, 2007). The most studied form of synaptic plasticity takes place at excitatory synapses following alterations of the strength of glutamate transmission resulting either in long-term depression (LTD) or long-term potentiation (LTP) (Malenka & Bear, 2004; Lau & Zukin, 2007). Although LTP and LTD, and their molecular and cellular underpinnings, have been extensively studied in CA1 and CA3 pyramidal neurons, it is believed most neurons in most

brain regions undergo similar changes (Scofield et al., 2016; Kauer & Malenka, 2007).

While LTP is traditionally evoked using high-frequency stimulation (100 Hz) (Bliss & Lomo, 1973), this stimulation fails to consistently evoke LTP in NAc MSNs (Kombian & Malenka, 1994; Robbe, Alonso, Chaumont, Bockaert, & Manzoni, 2002). This may reflect the fact that neurons that synapse onto MSNs, such as cortical pyramidal neurons fire at extremely low frequency (<1Hz) in freely moving animals. To circumvent this limitation, a different stimulation protocol, termed spike-timing dependent plasticity (STDP) was developed (Song, Miller, & Abbott, 2000). Under this protocol, the repeated pairing of MSN action potential with EPSPs at low frequency (i.e., 1 Hz) induces robust LTP and LTD in the NAc (Ji & Martin, 2012; Ji, Saha, & Martin, 2015; Ji et al., 2017). Interestingly, the occurrence of LTP vs LTD in MSNs in NAc is dependent upon the origin of glutamatergic input and the type of MSNs, D1 or D2-MSNs. It was shown that LTP is absent at cortical synapses, but not at amygdala or hippocampal inputs (Ji et al., 2015), and D1-MSNs mostly showing LTD, while D2-MSNs displaying predominantly LTP (Ji et al., 2017). These findings emphasize that in NAc, D1- and D2-MSNs differentially encode incoming glutamatergic inputs.

MSNs and dopamine

Synaptic transmission that changes MSN excitability is mostly controlled by the release of glutamate from afferents originating in the PFCx, BLA, hippocampus

and thalamus, and GABA from local GABAergic interneurons. While there is accumulating evidence indicating that many neuromodulators (e.g., serotonin, cannabinoid and opioid receptors) regulate both glutamatergic and GABAergic synaptic transmission, DA has received considerable amount of attention. The unique role of DA in the NAc from early studies implicate DA to be responsible for the rewarding properties of all drugs of abuse, including alcohol (Wise, 2002; Clarke & Adermark, 2015). However, a wealth of evidence over the past two decades has shown that its role is much more complex and has now been extended to other functions like encoding novelty and discrepancy between actual and expected reward (Volkow, Koob, & McLellan, 2016; Cox & Witten, 2019). Nevertheless, mechanisms underpinning DA release and its role in modulating neuronal excitability in the NAc remain the focus of intense research. The ability of DA to control neuronal excitability is very extensive due in part to the fact that, upon its release from VTA afferents, DA activates D1-like and D2-like receptors expressed on cholinergic and GABAergic interneurons as well as on glutamatergic terminals and MSNs (Nicola, Surmeier, & Malenka, 2000; Surmeier et al., 2007; Shen, Flajolet, Greengard, & Surmeier, 2008).

Dopamine receptors are G protein-coupled receptors (GPCRs), and are divided into D1-like receptors (D1 and D5) and D2-like receptors (D2, D3 and D4) (Beaulieu & Gainetdinov, 2011). D1-like and D2-like receptor mechanisms typically have opposing actions on neuron excitability. As described by Beaulieu and Gainetdinov, DA receptors have direct and indirect effects on neuron excitability

(Beaulieu & Gainetdinov, 2011). D1-type receptors are coupled to the $G\alpha_{s/olf}$ family of G-proteins that activate adenylyl cyclase to stimulate cAMP production, thus activating downstream signaling cascades via cAMP-dependent protein kinase and other cAMP-dependent proteins, which regulate gene expression via transcription factors including cAMP response element binding protein (CREB) (Beaulieu & Gainetdinov, 2011). The D2-type receptors couple to $G\alpha_{i/o}$ proteins that inhibit adenylyl cyclase and cAMP production, resulting in directly opposing effects on intracellular signaling and gene expression (Spano, Govoni, & Trabucchi, 1978; Kebabian & Calne, 1979; Beaulieu & Gainetdinov, 2011). In addition to signaling cascades, DA receptors also affect sodium channels, either directly, or through cAMP-dependent protein kinase pathways (Zhang, Hu, & White, 1998).

Despite the opposing roles of DA receptor downstream pathways, both D1 and D2 receptors seem to decrease MSN excitability. DA decreases both, spontaneous glutamatergic and GABAergic release onto MSNs via presynaptic D1 receptors (Pennartz, Dolleman-Van der Weel, Kitai, & Lopes da Silva, 1992; Nicola, Kombian, & Malenka, 1996; Nicola & Malenka, 1997), while electric stimulation of DA fibers in the VTA decreased evoked glutamatergic potentials (Brady & O'Donnell, 2004). Moreover, D1 receptors are shown to attenuate action potentials by inhibiting sodium channels (Surmeier et al., 1992), as well as voltage-gated N-, and P/Q-type calcium channels (Surmeier, Bargas, Hemmings, Nairn, & Greengard, 1995). D2 receptors are also shown to inhibit sodium and calcium channels and depress MSNs excitability (Greif, Lin, Liu, & Freedman, 1995;

Hernandez-Lopez et al., 2000; Olson et al., 2005), and D2 receptor agonist quinpirole is found to inhibit MSN firing (Perez, White, & Hu, 2006). However, activation of D1 receptors located in glutamatergic presynaptically terminals were also found to increase glutamate release (Wang et al., 2012b). Therefore, the location of the receptors (pre- vs post-synaptic and whether they are located on inhibitory vs excitatory synapses) is key to understanding DA effects on NAc excitability (Tritsch & Sabatini, 2012).

Cholinergic Interneurons (ChIs) in the striatum

Intrinsic properties and anatomy

ChIs constitute 1-5% of the neuronal population in the NAc (Aosaki et al., 1995; Zhou, Wilson, & Dani, 2002; Bonsi et al., 2011; Lim et al., 2014) and are responsible for this region having the highest brain ACh concentration. Their neurochemical identification is due to the expression of ChAT, the biosynthetic enzyme for ACh. ChIs are characterized morphologically by a large polygonal soma (20–50 μm), and thick widespread dendritic and axonal fields (Bolam et al., 1984; Aosaki et al., 1995; Bennett & Wilson, 1999). ChIs send dense innervations throughout striatum with each interneuron forming more than 500,000 axonal varicosities (Lim et al., 2014). While most ChIs fire spontaneously *in vivo*, some are silent or display burst firing (Bennett & Wilson, 1999; Bennett, Callaway, & Wilson, 2000). This excitability, or firing pattern, was found to be intrinsic in origin, pacemaker-like, and not caused by synaptic input (Bennett, Callaway, & Wilson,

2000). The spontaneous pacemaking firing of ChIs is driven by Na^+, K^+, Ca^{2+} and HCN (I_H current) channels (Bennett et al., 2000). Specifically, spontaneous firing results from the combined action of sodium current and the hyperpolarization-activated cation current (I_H), which together ensure membrane potential return to an action potential-initiation threshold. Calcium entry triggered by the action potential, shapes the falling phase of the waveform by activating SK and and BK classes of calcium-dependent potassium channels (Bennett et al., 2000).

Interestingly, *in vitro* studies indicate that DAergic and glutamatergic synaptic activities change the firing patterns in ChIs (Ding et al., 2010; Wieland et al., 2014). Notably, a “pause” or “burst-pause” pattern of firing is the mechanism that has been implicated in the conditioning response (Aosaki, Miura, Suzuki, Nishimura, & Masuda, 2010; Ding et al., 2010). During transitioning to pause-burst firing pattern the slow spike afterhyperpolarization is blocked via SK channels (Bennett et al., 2000).

As discussed above, the basal ganglia are involved in behavioral learning and reward. Studies by Aosaki and colleagues in the 1990s showed that striatal ChIs are temporally coordinated during sensorimotor learning and undergo changes in firing reflecting the reward values of salient environmental stimuli: ChIs showed a pause in firing only after several trials of pairings between stimulus and reward (Aosaki et al., 1994; Aosaki et al., 1995; Aosaki et al., 2010). These observations were later confirmed and their function elucidated in NAc by the observation that unlike MSNs, that were virtually insensitive to reinforcement

signals, ChIs generate unique bidirectional outcome responses during reward-based learning, signaling both positive (reward) and negative (reward omission) outcomes (Atallah, McCool, Howe, & Graybiel, 2014). Over time, ChIs were found to play a central role in basal ganglia function by regulating associative learning, reward processing, and motor control (Schulz & Reynolds, 2013). Anticholinergic drugs have been used as the therapeutic targets in Parkinson's and dystonia diseases (Duvoisin, 1967; Pisani et al., 2006; Pisani, Bernardi, Ding, & Surmeier, 2007; Ding et al., 2011; Bonsi et al., 2011), as well as schizophrenia, depression, and particularly in drug addiction disorders (Lim et al., 2014; Warner-Schmidt et al., 2012).

Nicotinic and muscarinic cholinergic receptors in striatum

ChI firing releases ACh and exerts its action on adjacent cells by activating nicotinic and muscarinic acetylcholine receptors (nAChR and mAChR, respectively). Nicotinic receptors are fast ionotropic ligand-gated cation channels, activating in microseconds. nAChRs are homo- or heteromeric receptors consisting of α and β subunits (Albuquerque, Pereira, Alkondon, & Rogers, 2009). In the striatum, the most common nAChR subunits are the α4, α6, α7, β2, and β3 (Lim et al., 2014). Subunit composition determines the channel's ion permeability, rate and extent of desensitization subcellular localization (McGehee & Role, 1995; Albuquerque et al., 1995). Although nAChRs are expressed on the soma, they also are often located on presynaptic terminals where activation facilitates

neurotransmitter release. Since the nAChR is a non-selective cation channel, it is permeable to positively charged ions such as Na^+ (entering cell) and K^+ (exiting cell), resulting in net depolarization of the membrane (Albuquerque et al., 2009). Additionally, Ca^{2+} entry through nAChRs in presynaptic terminals can induce transmitter release or long-term changes in cellular function through activation of Ca^{2+} dependent intracellular cascades (Exley & Cragg, 2008; Albuquerque et al., 2009). Interestingly, it was also shown there are physical interactions between nAChR and D2 autoreceptors which likely form a single complex that modulates DA release (Quarta et al., 2007).

In contrast to nAChRs, muscarinic acetylcholine receptors (mAChRs) are metabotropic G protein-coupled receptors that mediate their effects through second messenger pathways. mAChRs are either excitatory or inhibitory and are considered slow-activating receptors (milliseconds to seconds) (Eglen, 2005). Excitatory mAChRs, consisting of M1, M3 and M5, couple to $G_{q/11}$ and induce activation of the phospholipase C pathway (Lin, Chung, de Castro, Funk, & Lipski, 2004). M2 and M4 inhibitory receptors are coupled to $G_{i/o}$ proteins and decrease activity of adenylyl cyclase (Wess, 1996). Although all five mAChRs express in the striatum (Yan, Flores-Hernandez, & Surmeier, 2001), M1 and M4 receptors are predominantly expressed in the striatum with a small presence of M2, M3 and M5 expression (Yasuda et al., 1993). In the NAc, M2 and M3 receptors are located on presynaptic glutamatergic terminals, M5 on dopaminergic terminals, and M1 and M4 located on postsynaptic MSN dendrites. ChIs express M2 and M4 auto-

inhibitory receptors (Lim et al., 2014; Loftén, Adermark, Ericson, & Söderpalm, 2020).

Reciprocal regulation of ACh and DA

ACh and DA imbalance is implicated as a key mechanism in basal ganglia disorders such as Parkinson's disease, dystonia, depression and drug addiction (Warner-Schmidt et al., 2012; Gonzales & Smith, 2015). Much research has been devoted to understanding ACh and DA interactions, which are involved in many aspects of physiological processes, such as goal-directed behavior, learning and motivation. ChIs and DA neurons regulate each other's neurotransmitter release in the striatum, with causality seemingly impossible to establish (Exley & Cragg, 2008; Aosaki et al., 2010; Surmeier & Graybiel, 2012; Myslivecek, 2021). While, initially, activation of the DAergic input from the VTA to the NAc has been considered the main response to environmental salient stimuli with ChIs just filtering and amplifying DA signal (Joshua, Adler, Mitelman, Vaadia, & Bergman, 2008; Aosaki et al., 2010), recent evidence suggests that ChIs directly regulate DA release in the striatum (Threlfell et al., 2012; Cachope et al., 2012; Yorgason, Zeppenfeld, & Williams, 2017). Several pharmacological studies support the notion that DA receptors are expressed in ChIs where they either increase ChIs' firing rate through D1-like receptors (Maurice et al., 2004; Pisani et al., 2006), or decrease ChIs' firing rate through D2-like receptors (Bennett & Wilson, 1998). On the other hand, ACh receptors that are expressed on DA terminals (Zhou, Liang, & Dani,

2001; Exley, Clements, Hartung, McIntosh, & Cragg, 2008; Grilli et al., 2008; Threlfell et al., 2010; Shin, Adrover, Wess, & Alvarez, 2015), regulate DA release through nAChRs (Threlfell et al., 2012) and mAChRs (Grilli et al., 2008). Moreover, activation of mAChRs decreases DA release when DA terminals are stimulated at <20 Hz but increases DA release with >25 Hz stimulation (Threlfell & Cragg, 2011). The likely functional explanation for this phenomenon is that different stimuli and behaviors likely activate different pathways: ChIs gate the expression of cue-motivated behavior evoked by DA release, such that mAChR activity was found to blunt, while nAChR inactivation to augment cue-evoked DA release (Collins, Aitken, Greenfield, Ostlund, & Wassum, 2016).

Cholinergic interneuron modulation of MSNs

Since MSNs are the only output neurons of the striatum, modulation of their excitability is critical to affect behavioral output. As mentioned above, MSNs receive glutamatergic inputs from incoming terminals and GABAergic inputs from local interneurons that increase and decrease their excitability, respectively. Therefore, neuromodulators, such as DA and ACh can either directly depolarize or hyperpolarize MSN membranes, or alter the release of glutamate and GABA onto the MSNs. It is important to note that our understanding of the effects of ACh on MSNs excitability is limited in pharmacological studies, and interpretation of the effects of AChRs is potentially clouded by caveats like agonists/antagonists binding to all target receptors, regardless of their location. Also, pharmacological

compounds are present for much longer time than endogenous ligands would be, thus potentially producing desensitization, such as in the case of nicotine application. Therefore, such results must be interpreted with caution.

ChIs have been shown to regulate MSN excitability by controlling both glutamatergic and GABAergic inputs. Both AChR agonists and optogenetic ChI stimulation decrease glutamatergic neurotransmission while also increasing GABAergic neurotransmission, thus acting through both pathways to decrease overall NAc MSN excitability (de Rover, Lodder, Kits, Schoffelmeer, & Brussaard, 2002; Pakhotin & Bracci, 2007; Witten et al., 2010). However, these studies did not differentiate D1- and D2-MSNs and the mechanism and receptor identity underlying effects on excitability remain unknown.

There is little ambiguity about the fact that activation of mAChRs in the striatum decreases glutamatergic transmission onto MSNs (Pakhotin & Bracci, 2007). Several studies showed that mAChRs inhibit glutamatergic synaptic transmission in both D1- and D2-MSNs (Ding et al., 2010) through presynaptic M4 mAChRs (Calabresi, Centonze, Gubellini, Pisani, & Bernardi, 2000; Pancani et al., 2014), and decreases both release probability and glutamate concentration in the synaptic cleft (Higley, Soler-Llavina, & Sabatini, 2009). However, nAChR contributions to MSN excitability has proven to be more controversial. An initial study by de Rover and colleagues showed that nicotine application has no effect on EPSC parameters, while increasing amplitude and frequency of IPSCs (de Rover et al., 2002). In contrast, a later study by Licheri and colleagues found

nicotine to have no effect on IPSCs, but a decrease in EPSC frequency (de Rover et al., 2002; Licheri et al., 2018). Furthermore, microdialysis-based measurements of glutamate release in the striatum showed α7 nAChR antagonists decreased glutamate release (Carpenedo et al., 2001) and the application of ACh provided tonic excitation at cortico-striatal terminals through α7* and β2* (* denotes other unidentified nAChR subunits co-assemble with the indicated subunit) nicotinic receptors (Wang et al., 2013). The differences could be due to the length of the antagonist application, concentration of the antagonists used, as well as the recording conditions of the electrophysiological measurements. Therefore, further studies are required to unequivocally elucidate the ChI effect on MSN excitability.

ChIs and cocaine

Out of all drugs of abuse, cocaine effects on the brain are perhaps best described as being modulated by ChIs. Cholinergic interneurons are activated by cocaine self-administration (Lee et al., 2020), and blocking muscarinic and nicotinic cholinergic receptors with atropine and mecamylamine, respectively, blocks cocaine reinforcement (Berlanga et al., 2003; Crespo, Sturm, Saria, & Zernig, 2006), and ChI ablation in the NAc increased cocaine sensitivity (Hikida et al., 2001). It was also shown that cocaine increased ChI firing rate, and optogenetic ChI stimulation enhanced cocaine place preference, while optogenetic ChI inhibition showed a decrease in cocaine-induced place preference (Witten et al., 2010). Interestingly the acquisition of drug reinforcement was accompanied by an

increase in ACh, but not DA (Crespo et al., 2006), therefore additional research is necessary to elucidate the role of ChIs in drugs of abuse mechanisms.

Effect of Alcohol on NAc excitability

Alcohol effects on inhibitory and excitatory transmission onto MSNs

Modulation of GABAergic synaptic transmission by alcohol in the NAc is complex and depends on the type of the GABAergic interneurons that innervate MSNs. Acute EtOH hyperpolarizes low-threshold spiking striatal interneurons (LTS) while it depolarizes fast-spiking (FSIs) interneurons (Blomeley, Cains, Smith, & Bracci, 2011). *In vivo* electrophysiological recordings show that acute ethanol increases the firing rate of FSIs in the NAc, a phenomenon that mirrors the depolarization observed *in vitro* (Burkhardt & Adermark, 2014). Interestingly, acute EtOH (50 mM) similarly inhibits the release of GABA in dorso-lateral striatum MSNs. However, this effect disappeared after six weeks of binge alcohol drinking (Wilcox et al., 2014), possibly indicating the development of tolerance to the drug. Surprisingly, the same study showed that acute EtOH in MSNs of naïve mice enhanced the frequency of mIPSCs in the dorsomedial striatum.

EtOH effects on glutamatergic synaptic transmission are similarly complex. While acute alcohol increased glutamate release in the NAc (Nona & Nobrega, 2018), four days of 24-hour alcohol exposure promoted increased extracellular glutamate (Griffin, Haun, Hazelbaker, Ramachandra, & Becker, 2014). Twenty days of alcohol consumption increased glutamatergic neurotransmission by

increasing the frequency of mEPSCs and paired-pulse depression (PPD) (Spiga et al., 2014), and an increase in basal glutamate levels after seven weeks of alcohol exposure (Pati, Kelly, Stennett, Frazier, & Knackstedt, 2016). However, acute alcohol also caused depression of excitatory synaptic input and hyperpolarized MSNs, (Adermark, Clarke, Söderpalm, & Ericson, 2011b; Blomeley et al., 2011).

Synaptic plasticity, including LTP and LTD, have been measured to evaluate the effects of alcohol on glutamatergic neurotransmission. Acute ethanol application blocks LTP, and has differential effects on LTD (Yin, Park, Adermark, & Lovinger, 2007; Clarke & Adermark, 2010; McCool, 2011). Acute EtOH inhibits NMDAR-dependent LTD in the NAc shell in an MSN-subtype-specific manner (Jeanes, Buske, & Morrisett, 2014). In the NAc core, acute ethanol impairs LTP via effects on metabotropic glutamate receptors (mGluRs) (Mishra, Zhang, & Chergui, 2012). In chronic alcohol exposure studies, it was demonstrated that EtOH exposure leads to a loss of dendritic spines on MSNs in the NAc (Spiga et al., 2014), hampering or blocking of LTD formation at excitatory synapses (Cui et al., 2011; DePoy et al., 2013; Renteria et al., 2017), and facilitation of cortico-striatal LTP formation (Xia et al., 2006; Wang et al., 2012a). The mechanism proposed involves potentiation of AMPA- and NMDA-mediated transmission at the mPFC inputs and increased glutamate release from BLA afferents (Ma, Barbee, Wang, & Wang, 2017).

Importantly, it has been determined that LTP or LTD formation is dependent on the type of MSN (D1 vs D2), where in naïve mice, D1-MSNs showed LTD and D2-MSNs showed LTP, as measured by the low-frequency plasticity induction (Ji et al., 2017). However, 1-2 weeks of alcohol exposure induces glutamatergic facilitation in D1-MSNs (LTP induction, or loss of LTD), and glutamatergic inhibition for D2-MSNs (LTD induction) (Jeanes et al., 2014; Ji et al., 2017; Renteria et al., 2017). In addition to MSN type, alcohol was also found to have differential effect in dorsal vs ventral striatum: in dorsal striatum alcohol potentiated MSN output, while inhibited the net MSN output in the ventral striatum, thus promoting an imbalance between associative and sensorimotor circuits (Cuzon Carlson et al., 2011; Wilcox et al., 2014; Abrahao et al., 2017).

Alcohol and DA

Several decades of research leave little doubt about the role of DA in mediating acute and chronic effects of drugs of abuse (Lüscher & Malenka, 2011), and given the aforementioned differential effect of alcohol on D1 and D2 receptor-expressing MSNs, the effect of alcohol on DA concentration is necessary to delineate. However, this aspect seems to be especially complex, given the variety of modes of dopamine release (tonic, phasic, spontaneous, evoked) observed in the NAc.

As shown by a number of human studies, acute alcohol consumption increases DA release in the NAc (Boileau et al., 2003; Aalto et al., 2015). The increased DA level in the NAc (Löf, Ericson, Stomberg, & Söderpalm, 2007;

Adermark et al., 2011a) is associated with increased DAergic neurons firing in the VTA (Yoshimoto, McBride, Lumeng, & Li, 1992; Ericson, Blomqvist, Engel, & Söderpalm, 1998; Liu, Zhao-Shea, McIntosh, & Tapper, 2013b). This effect has been found using both active and passive alcohol administration routes (Bassareo, Cucca, Frau, & Di Chiara, 2017). Moreover, Yorgason and colleagues reported that alcohol-mediated inhibition of DA release in the NAc was greater in C57 compared to DBA mice (Yorgason, Rose, McIntosh, Ferris, & Jones, 2015). Indeed, the DA concentration following alcohol exposure seems to depend on several factors including the time frame of DA measurement (seconds vs tens of minutes, and measured with voltammetry vs microdialysis), concentration of ethanol administered, and the previous alcohol exposure history of the animal. When assessing the effect of EtOH on DA levels, if DA is measured on the order of seconds, with fast-scan cyclic voltammetry (FSCV) for example, DA levels decrease (Budygin, Phillips, Wightman, & Jones, 2001; Schilaty et al., 2014; Yorgason et al., 2022). However, when DA is measured in tens of minutes using microdialysis, EtOH administration increases DA levels (Nestby et al., 1999; Adermark et al., 2011a; Loftén et al., 2020), but see (Yorgason et al., 2022). Additionally, 40-150 mM, but not 20mM of EtOH changed DA transients at high frequency (<20 Hz) stimulation (Yorgason, Ferris, Steffensen, & Jones, 2014). These findings emphasize the important differences when considering alcohol effects on DA, with lower doses increasing dopamine and higher doses inhibiting release (Abrahao et al., 2017; Gao et al., 2019), and exemplified by opposing

effects of alcohol when measuring tonic or phasic DA neurotransmission (Robinson, Howard, McConnell, Gonzales, & Wightman, 2009).

Alcohol and ChIs

A direct effect of alcohol application on ChIs has not been well documented, and most studies involve either chronic alcohol exposure or application of anticholinergic treatments to determine ChI involvement in alcohol effects. One study reported that in the dorsal striatum acute alcohol application decreased ChI firing rate (Blomeley et al., 2011), while another study in NAc reported an increase in ChI firing rate with alcohol application (Yorgason et al., 2022). An increase in the percentage of Fos-immunoreactive ChIs was observed after EtOH intraperitoneal injection (Herring, Mayfield, Camp, & Alcantara, 2004). After 2-week alcohol administration increased ACh release was observed (Nestby et al., 1999). However, after 6 months of drinking the density of ChAT-IR varicosities was decreased, which could be potentially caused by compensatory mechanisms (Pereira et al., 2014).

In terms of the cholinergic effects on alcohol consumption behavior, systemic administration of nicotinic receptor antagonists decreases EtOH consumption and conditioned place preference in numerous studies (Hendrickson, Zhao-Shea, & Tapper, 2009; Rahman & Prendergast, 2012), and after 3 months of drinking, application of nAChR agonist varenicline into the NAc decreased EtOH intake (Feduccia, Simms, Mill, Yi, & Bartlett, 2014). Importantly, specifically α6-

and α4-containing nAChR are especially sensitive EtOH potentiation of ACh-induced activation (Liu et al., 2013b; Liu et al., 2013a; Gao et al., 2019). However, these effects were observed on a systemic level, and cannot be attributed to only ChIs in the striatum.

ChIs mediate alcohol effects on DA release

Despite the variety of alcohol effects on DAergic signaling, cholinergic transmission appears to participate in this mechanism. Striatal ChIs are the main regulators of increased DA levels in the NAc following alcohol administration (Adermark et al., 2011b; Clarke & Adermark, 2015). One of the ways that ChIs regulate alcohol is by acting on nAChR and mAChRs located on DAergic terminals (Söderpalm, Ericson, Olausson, Blomqvist, & Engel, 2000; Williams & Adinoff, 2008). Accordingly, alcohol-induced increase in DA release was shown to be regulated by muscarinic and nicotinic receptors in NAc (Tuesta, Fowler, & Kenny, 2011; Shin et al., 2015). Specifically, alcohol-induced increase of spontaneous DA release is mediated by α6 subunit-containing nAChRs (Schilaty et al., 2014; Gao et al., 2019). A combination of both nicotinic and muscarinic receptors is shown to be necessary to evoke alcohol-mediated DA release (Loftén et al., 2020). Therefore, alcohol-mediated increase in ChI firing and activation of AChR could alter DA levels both directly, and via GABAergic transmission (Yorgason et al., 2022).

Summary and Hypothesis

As outlined above, conflicting effects on MSN excitability by acute and chronic alcohol emphasize that much remains to be discovered regarding the mechanisms underpinning the regulation of synaptic transmission in MSNs by alcohol, as well as the differentiation between D1- and D2-MSN function.

DA release in NAc following acute EtOH administration has been well documented (Clarke & Adermark, 2015), and EtOH is known to modulate glutamatergic signaling onto MSNs through DA receptors (Ji et al., 2017). However, cholinergic interneurons (ChIs) have been found to gate DA release (Threlfell et al., 2012) and ACh regulates alcohol-dependent changes in DA level (Loftén et al., 2020). However, whether ChIs control alcohol effects on MSN excitability, and whether there are D1-/D2-MSN differences in response to ACh is completely unknown.

Therefore, I hypothesized, 1) ChI stimulation modulates glutamatergic synaptic transmission in MSNs by modulating the release of DA in a D1/D2 receptor-specific manner, 2) binge alcohol drinking modulates the effects of ChIs on glutamatergic synaptic transmission, and 3) ChI activity is necessary and sufficient to alter binge alcohol drinking in mice. The following chapters address these hypotheses.

Chapter II

Binge alcohol drinking alters synaptic processing of executive and emotional information in core nucleus accumbens medium spiny neurons

Chapter II: Binge alcohol drinking alters synaptic processing of executive and emotional information in core nucleus accumbens medium spiny neurons

Jenya Kolpakova[1,4], Vincent van der Vinne[2], Pablo Giménez-Gómez[1], Timmy Le[1,4], In-Jee You[1], Rubing Zhao-Shea[1], Cristina Velazquez-Marrero[3], Andrew R. Tapper[1,4] and Gilles E. Martin[1,4]

This work is published in: *Frontiers Cellular Neuroscience* (2021) *15*, 742207

1. Department of Neurobiology, The Brudnick Neuropsychiatric Research Institute, University of Massachusetts Chan Medical School, Worcester, MA, United States,

2. Department of Biology, Williams College, Williamstown, MA, United States,

3. Institute of Neurobiology, University of Puerto Rico Medical Sciences Campus, San Juan, PR, United States

4. Graduate Program in Neuroscience, Morningside Graduate School of Biomedical Sciences, UMass Chan Medical School

Roles of authors

JK GEM designed research, JK GEM carried out experiments, JK GEM VvdV analyzed data, GEM JK VvdV wrote the paper, PGG TL INY RZS CVM helped out with data collection, ART helped out with research design

Abstract

The nucleus accumbens (NAc) is a forebrain region mediating the positive-reinforcing properties of drugs of abuse, including alcohol. It receives glutamatergic projections from multiple forebrain and limbic regions such as the prefrontal cortex (PFCx) and basolateral amygdala (BLA), respectively. However, it is unknown how NAc medium spiny neurons (MSNs) integrate PFCx and BLA inputs, and how this integration is affected by alcohol exposure. Because progress has been hampered by the inability to independently stimulate different pathways, we implemented a dual wavelength optogenetic approach to selectively and independently stimulate PFCx and BLA NAc inputs within the same brain slice. This approach functionally demonstrates that PFCx and BLA inputs synapse onto the same MSNs where they reciprocally inhibit each other pre-synaptically in a strict time-dependent manner. In alcohol-naïve mice, this temporal gating of BLA-inputs by PFCx afferents is stronger than the reverse, revealing that MSNs prioritize high-order executive processes information from the PFCx. Importantly, binge alcohol drinking alters this reciprocal inhibition by unilaterally strengthening BLA inhibition of PFCx inputs. In line with this observation, we demonstrate that in vivo optogenetic stimulation of the BLA, but not PFCx, blocks binge alcohol drinking escalation in mice. Overall, our results identify NAc MSNs as a key integrator of executive and emotional information and show that this integration is dysregulated during binge alcohol drinking.

Introduction

Binge drinking is a potentially dangerous pattern of ingesting large quantities of alcohol over a short period of time that effects primarily late adolescents and young adults with roughly 40% of college students in the United States reporting binge drinking (Krieger et al., 2018). The nucleus accumbens (NAc) is a forebrain region that has long been regarded as a key mediator of the effects of all drugs of abuse, including alcohol (D'Souza, 2015). It receives robust glutamatergic inputs from multiple limbic regions [e.g., basolateral amygdala (BLA) and ventral hippocampus] and from the medial and lateral prefrontal cortex (PFCx) (Groenewegen, Wright, Beijer, & Voorn, 1999; Ikemoto, 2007). While the PFCx is responsible for planning, evaluating long-term consequences and is instrumental in retrieving drug-associated memories (Dalley, Cardinal, & Robbins, 2004; Zhang et al., 2019), the BLA encodes emotions that shape impulsive behavior and the response to associative learning (Gallagher & Chiba, 1996; Cardinal, Parkinson, Hall, & Everitt, 2002; Lalumiere, 2014). Importantly, PFCx and BLA send converging synaptic inputs onto single GABAergic medium-spiny neurons (MSNs) (O'Donnell & Grace, 1995; Finch, 1996; French & Totterdell, 2002), the only output cells of the NAc that represent up to 95% of the NAc neuronal population (Meredith & Totterdell, 1999).

Although it has been hypothesized that drug addiction develops as a consequence of imbalances in processing of executive (cortical) and emotional (amygdala) information in the NAc (Bechara, 2005), there are currently no data at the cellular level supporting this theory. Efforts to test this hypothesis at the cellular

level have been hampered by the inability to evoke synaptic responses independently from different pathways converging on NAc MSNs using traditional approaches. To circumvent this limitation, we implemented a double-optogenetics approach developed by Klapoetke et al. (2014) using injections of viral-mediated gene expression of Channelrhodopsin-2 and the red-shifted ChrimsonR opsin to evoke excitatory post-synaptic potentials and currents (EPSPs/EPSCs) independently from PFCx and BLA pathways in the same brain slice (Klapoetke et al., 2014). We found that NAc MSNs favor the transmission of information from the PFCx in alcohol-naïve mice. Importantly, in binge alcohol drinking mice, NAc MSNs appear to favor BLA information. Also, when tested in freely behaving mice, optogenetic activation of the BLA, but not PFCx, prevented the escalation of alcohol consumption typically observed in mouse models of binge drinking. These data suggest that alteration of the processing of PFCx-driven executive and BLA-driven emotional information by MSNs may be a key cellular mechanism underpinning the role of the NAc in controlling binge alcohol drinking.

Materials and Methods

Animals

All experiments were performed using male C57Bl/6J mice. All mice were handled according to the American Association for the Accreditation of Laboratory Animal Care guideline. The protocol was approved by the Institutional Animal Care and Use Committee of University of Massachusetts Medical School. Mice were maintained at constant temperature (22±1°C) and humidity with a 12 h:12 h light–dark cycle. Water and food were provided *ad libitum*.

Surgeries

We bilaterally (0.6 μl/side) injected 26- to 28-day-old (15–20 g) C57Bl/6J mice with pAAV2-EF1a-hChR2(H134R)-eYFP virus (a gift from Karl Deisseroth, Stanford University, CA) in the PFCx, using a 26G 10-μl neurosyringe (701N; Hamilton) into the prelimbic PFCx (AP +2.0 mm, ML ±0.35 mm, DV -2.6 mm from Bregma). In the same animals, we also bilaterally injected 0.8 μl AAV2-Syn-ChrimsonR-tdTomato (a gift from Edward Boyden; MIT, MA) into the BLA (AP +0.7 mm, ML ±3.3 mm, DV -5.5 mm from Bregma). The injectors were left in place for 5 min following injection and subsequently raised slowly during an additional 5–8 min. We returned mice to their home cages for 28 days before performing electrophysiological experiments. In a subset of mice (n = 6), we injected pAAV2-EF1a-hChR2(H134R)-eYFP (3 mice) and AAV2-Syn-ChrimsonR-tdTomato (3 mice) directly into the NAc (AP +1.5, ML ±1.5, DV -4.3 mm from Bregma) to test

the cross stimulation between the two opsins. For both opsins (i.e., ChR2 and ChrimsonR), we chose the AAV serotype 2 to circumscribe infection to the injection sites and to minimize viral spread (Aschauer, Kreuz, & Rumpel, 2013) (**Figure 2.2B, C**).

Drinking in the Dark Paradigm (DID)

Two days following brain viral injection, individually housed mice were allowed to adapt to a reversed light-dark cycle (OFF at 7AM, ON at 7PM) for one week. Mice were given water bottles with sipper tubes before the experiment to allow habituation and reduce the novelty effect once the ethanol bottle, containing a similar sipper tube, was presented. The total habituation time for the reverse light-dark cycle was 2 weeks before the experiment began. Ethanol exposure started 2 hrs into the dark phase and lasted for 2 hrs (Rhodes, Best, Belknap, Finn, & Crabbe, 2005; Hendrickson et al., 2009; Ji et al., 2017). At the start of the experiment, each water bottle was removed and replaced with a pre-weighed 50-mL conical tube containing 20% ethanol with a rubber stopper and double-ball bearing sipper tube. Mice were allowed to drink for 2 hrs, and then the ethanol bottles were removed, weighed and the water bottles were returned. Ethanol consumed was measured as grams ethanol divided by mouse body weight in kilograms. This protocol was repeated 5 days a week with 2 days off (water only) after each 5-day span. Drip controls were used to account for evaporation and dripping, and experimental bottle weights were corrected using these control

values. On average, mice steadily increased their consumption of alcohol before reaching a maximum around 7 g/Kg of 20% alcohol per drinking session at the end of a 2-week period. All electrophysiological recordings were performed 24 hrs after the last drinking bout during the 4^{th} or 5^{th} post-surgery weeks.

Slice Preparation

We prepared coronal slices from fresh brain tissue of 8 – 9-weeks old mice. Following intracardiac perfusion with an ice-cold N-methyl-D-glucamine-based solution (see below), we rapidly removed and transferred the brain in an ice cold oxygenated (95% O_2 / 5% CO_2) cutting solution of the following composition (in mM): 92 N-methyl-D-glucamine (NMDG), 2.5 KCl, 1.25 $NaH_2PO_4.H_2O$, 30 $NaHCO_3$, 20 HEPES, 25 glucose, 2 thiourea, 5 Na^+-ascorbate, 3 Na^+-pyruvate, 0.5 $CaCl_2.2H_2O$, 10 $MgSO_4.7H_2O$, to cut slices (300 µm) with a Vibroslicer (VT1200, Leica MicroInstrutments; Germany). Slices were immediately transferred in an incubation chamber and left to recuperate in the NMDG-based solution for 22 min at 32°C before being moved into a chamber containing an artificial cerebrospinal fluid (ACSF; in mM): 126 NaCl, 2.5 KCl, 1.25 $NaH_2PO_4.H_2O$, 1 $MgCl_2$, 2 $CaCl_2$, 26 $NaHCO_3$, 10 D-glucose, at room temperature. Slices were left in this chamber for at least one hour before being placed in a recording chamber and perfused with ACSF at a constant rate of 2–3 ml/min at room temperature (~21°C). We visualized neurons in infrared differential interference contrast (60x, IR-DIC) videomicroscopy using a fully motorized upright microscope (Scientifica; Spain).

Electrophysiology

Slices were prepared according to methods previously described (Ji et al., 2015, Ji et al., 2017). Whole-cell patch clamp recordings were performed in the absence of GABA receptor antagonists (Ji et al., 2017). Briefly, borosilicate glass electrodes (1.5 mm OD, 5–7 Mohms resistance) were filled with an internal solution containing (mM): 120 K-methanesulfonate; 20 KCl; 10 HEPES; 2 ATP, 1 GTP, and 12 phosphocreatine. Following seal rupture, series resistance was 18.3±1.1 MOhms in a randomly selected sample of 23 MSNs, fully compensated in current clamp recording mode, and periodically monitored throughout recording sessions. Recordings with changes of series resistance larger than 20% were rejected, as were MSNs with a resting membrane potential more positive than -80 mV. Voltage and current traces in whole cell patch-clamp were acquired with an EPC10 amplifier (HEKA Elektronik; Germany). Sampling was performed at 10 kHz and digitally filtered voltage and current traces were acquired with PatchMaster 2.15 (HEKA Elektronik; Germany) at 2 kHz. All traces were subsequently analyzed off-line with FitMaster 2.15 (HEKA Electronik; Germany). EPSP/Cs were evoked optically by flashing 1 ms-long 450 nm blue and 610 nm red lights through the light path of a microscope 60x objective using independent high-powered LEDs (pE-100 470 and 610 nm CooLED, NY, United States) under the control of the acquisition software (PatchMaster, HEKA, Germany). To rapidly switch (i.e., milliseconds) between blue and red lights, single bandpass filters (450/50 and

620/50 from Chroma, Bellows Falls, VT) were placed directly in front of the optical path of each light source mounted on a two-way exchanger (CooLED, NY, United States) at the back of the microscope. Light intensity was measured at slice level. Although gating strength was not a function of the amplitude of the first EPSPs (see **Figure 2.3**), we adjusted the light intensity to evoke synaptic events of at least 5 mV in amplitude. However, if more than 35 mW was necessary to evoke ChR2-driven EPSPs, recordings were rejected based on the sensitivity of ChrimsonR to blue light (**Figure 2.1B**). Ethanol was obtained from Sigma-Aldrich (Saint Louis, MO, United States).

Optogenetic Stimulation in Freely Moving Mice

28–32 days old mice were injected with 0.6 μl of pAAV5-CaMKII-hChR2(H134R)-eGFP or AAV-eGFP (UNC viral core) bilaterally either in the prelimbic PFCx or BLA and on the same day implanted with a fiber optic fiber (Doric Lenses, CA) located above the NAc (AP +1.5, ML ±1.5, DV -4.0 mm from Bregma). Injection sites and fiber optics placement was verified at the end of experiments. Mice were allowed to recover for 9 days before being transferred into the testing chamber. Three days after transfer, mice were connected to the fiber optic cables. For habituation purposes, mice remained tethered to the fiber optic cables and LED drivers. Following 4 days of habituation, mice were exposed to alcohol according to the Drinking in the Dark (DID) protocol as described above. Alcohol drinking behavior was quantified by measuring licks of the drinking spout. Drinking behavior

(number and timing of licks) was measured in mice exposed to 2 hrs of the DID paradigm. Following 4 days of drinking without stimulation, the PFCx or BLA was optogenetically stimulated (ChR2, 5 mW 5 ms-long 470 nm light pulses at 10 Hz with alternating 2-min stimulation ON and 2-min stimulation OFF) throughout the 2 hrs drinking interval. The comparison was made between the last day of alcohol drinking without stimulation (Day 4) and the last day of alcohol drinking with stimulation (Day 8). We chose 10 Hz based on the capacity of glutamatergic terminals to follow this frequency (**Figure 2.7B**; 10 Hz). In contrast, 20 Hz stimulation evoked failures to transmit glutamate. For saccharin control experiment, 0.3% saccharin (Fisher Scienfitic) solution was made and consumption measured during the same optogenetic stimulation protocol. Drinking bouts of alcohol and saccharin were measured using a closed-circuit loop connected to a drinkometer (Lafayette Instruments, Lafayette, IN, USA). Timing of licks was measured as counts of licks per second.

Locomotor Activity during Optogenetic Stimulation in Freely Moving Mice

To test mouse locomotor activity during optogenetic stimulation mice were implanted with optic fibers and optogenetically stimulated as described above. During stimulation mice were tethered to the fiiber optic cables and placed into an open field arena (17 x 17 inches, created by the Scripps FL Behavior Core) and locomotor behavior was measured for 30 mins (after 15 mins of habituation). All experimental sessions were conducted under red light illumination. The locomotor

activity (velocity and time spent in the center) was conducted and recorded by a computerized video-tracking software program EthoVision XT (Noldus Information Technology, Leesburg, VA).

Analysis

EPSP/Cs maximum amplitude was measured in a 20 ms time window 10 ms after the onset of the stimulus. In each experimental condition, 10 consecutive EPSP/Cs evoked every 15 s were measured. Data are expressed as mean ±SEM. Electrophysiological and behavioral data were analyzed with Prism 7.0 (Graphpad, United States) Statistics package using either Student's t tests or one- and two-way ANOVAs (**Figures 2.3–5**) or with mixed-model general linear model (MM-GLM) (**Figures 2.2, 2.6, 2.7**; SAS JMP 7.0) to account for random effect variables such as cell ID, direction of stimulation, and alcohol treatment, as indicated in the text. The drinking behavior of freely moving mice was quantified by summing the number of drinking spout licks per 2-min interval with intermittent optogenetic stimulation LED light ON or OFF. Statistical comparisons assessed the total number of licks over the 2 hrs drinking interval per day. The variance is calculated by taking the average of squared deviations from the mean. The criterion for statistical significance was $p < 0.05$ for all comparisons.

Results

Selective Responses of Accumbens Core Medium Spiny Neurons to Stimulation of ChR2 and ChrimsonR

The present study necessitated independent stimulation of ChR2 and ChrimsonR in the same brain slices with minimal stimulation overlap. In view of this requirement, the selectivity of blue light to evoke ChR2- and red light to evoke ChrimsonR-mediated responses was optimized in brain slices of mice injected in the NAc with one of the viral plasmids. Accumbens core MSNs from injected mice had a mean resting membrane potential and membrane input resistance of −86.7 ± 0.6 mV and of 117.47 ± 14 MOhm, respectively, indicative of healthy neurons. As expected, low intensity (i.e., <5 mW) 470 nm blue light readily evoked rapid (~300–400 μs delay) non-synaptic depolarizations of MSNs in slices of mice injected with pAAV2-EF1a-hChR2(H134R)-eYFP. Depolarization increased in amplitude with increasing light intensities (**Figure 2.1A**, graph, open circles). Importantly, 610 nm red light failed to elicit responses, even at the highest intensity (i.e., 120 mW) tested (**Figure 2.1A** top panel, red traces), demonstrating strong selectivity of ChR2 for blue light (**Figure 2.1A**, graph, solid red circles). A different group of mice were injected with AAV2-Syn-ChrimsonR-tdTomato into the NAc. Short (1 ms) red light pulses evoked depolarizations with a rapid onset with a similar timecourse as ChR2-mediated responses (**Figure 2.1B**). However, 470 nm blue light also evoked ChrimsonR-mediated depolarization when the intensity was higher than 30 mW (**Figure 2.1B**, graph, open circles), showing that both blue and

red light could activate ChrimsonR. To decrease the sensitivity of ChrimsonR to blue light, the blue light was left-shifted by replacing the blue light filter (470/20 nm) with a single bandpass filter (450/50 nm). Although this new filter did not totally render ChrimsonR insensitive to the left-shifted blue light, it markedly decreased its sensitivity. Thus, only blue light with an intensity greater than 40 mW and higher excited ChrimsonR (**Figure 2.1B**, solid blue circles). We then tested ChrimsonR-mediated excitatory post-synaptic potentials' (EPSPs) sensitivity to 450 and 610 nm light at PFCx synapses in the NAc. We found that their sensitivity is very similar to that of non-synaptic ChrimsonR (**Figure 2.1B**), with blue light evoking small amplitude EPSPs at light intensity higher than 40 nm (**Figure 2.1C**, top traces and **D**, solid blue circles). In contrast, red light evoked large synaptic responses (**Figure 2.1C**, bottom traces and **D**, solid red circles). Also, we compared these synaptic responses to ChR2-mediated EPSPs at the same synapse. We found that 450 nm stimulation evoked robust EPSPs at very low intensity (**Figure 2.1D**, open blue square). In a random sample of 12 MSNs, we measured ChR2- and ChrimsonR-EPSC kinetics and found no statistical differences between the two groups, with ChR2-EPSCs decay being 7.72 ± 0.42 ms while that of ChrimsonR was 7.58 ± 0.37 ms. This result suggests that the populations of AMPA receptors activated by cortical and amygdala inputs are likely similar in terms of their subunit composition.

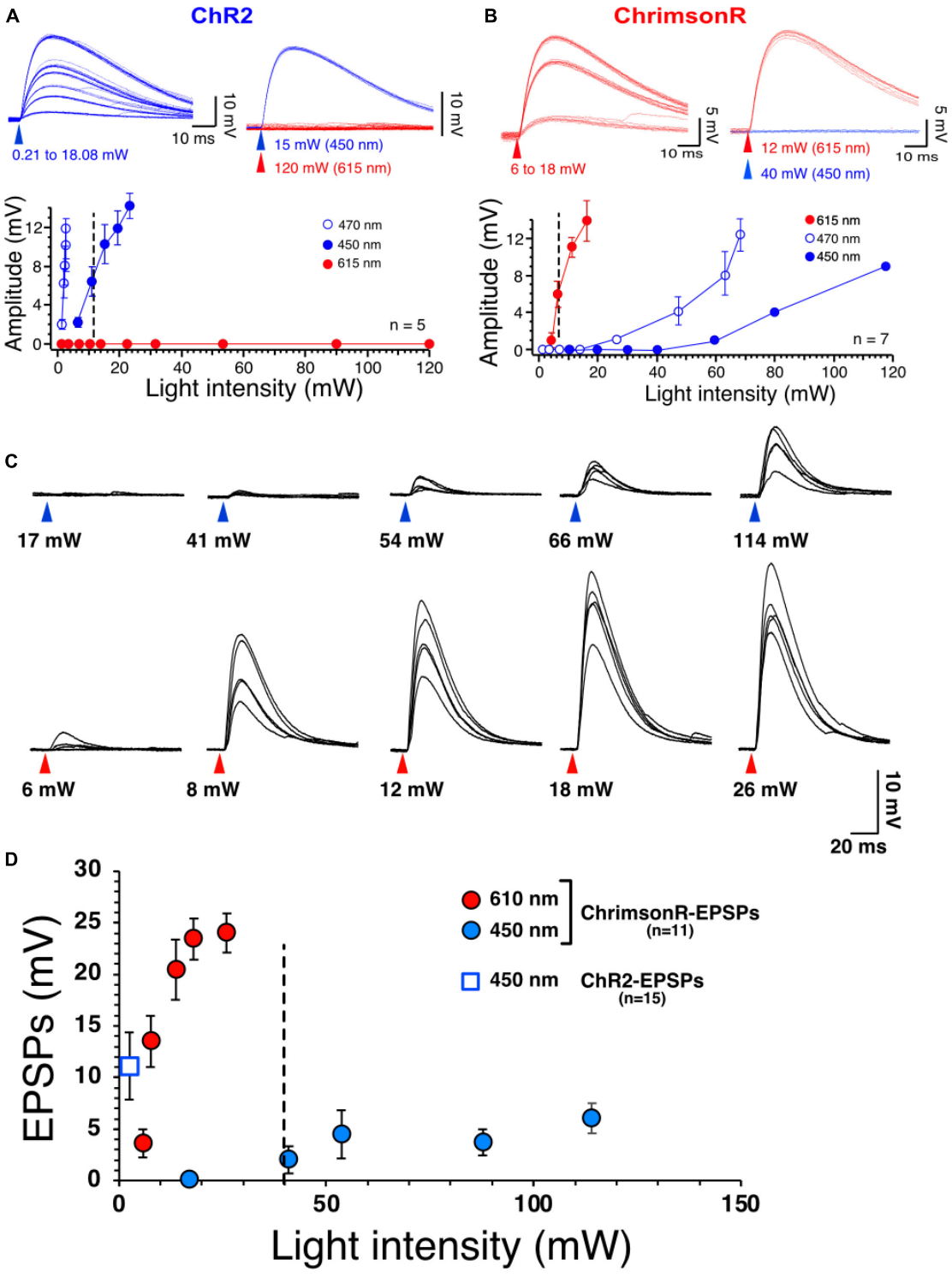

Figure 2.1 | Selective stimulation of ChR2 and ChrimsonR. A, Voltage responses of ChR2 expressed in NAc MSNs to increasing intensities of 450 nm blue light (blue traces)

and 615 nm red light (red traces, top right panel). Bottom panel shows graph of ChR2-mediated voltage responses as a function of light intensity at 450 nm (solid blue circles, n = 5), 470 nm (open blue circles, n = 5) and 615 nm light intensity (solid red circles, n = 5). Note the lack of sensitivity of ChR2 to red light. **B**, Voltage responses of ChrimsonR expressed in NAc MSNs to increasing intensities of 615 nm (red traces, n = 7) and 450 nm blue light (blue traces, top right panel, n = 7). Bottom panel shows graph of ChrimsonR-mediated voltage responses as a function of light intensity at 450 nm (solid blue circles, n = 7), 470 nm (open blue circles) and 615 nm light intensity (solid red circles). Average values in graphs are expressed as mean ± standard error (SEM). **C**, Representative EPSPs following injection of AAV-ChrimsonR in PFCx in response to increase intensity to 450 nm (blue triangles) and 610 nm (red triangles) light. Note that blue light evokes EPSPs at intensity higher than 40 mW. **D**, Graph showing ChrimsonR-mediated EPSP amplitude as a function of increasing light (450 – solid blue squares and 610 nm – solid red squares) intensities. Open blue square shows the average amplitude of ChR2-mediated EPSPs as a function of low 450 nm light intensity (0.78 mW).

Synaptic Gating Between Cortical and Amygdala Inputs in the Core Nucleus Accumbens of Alcohol-Naïve Mice

To test whether cortical inputs gate BLA-mediated EPSPs, we bilaterally injected AAV2-ChR2-eYFP and AAV2-ChrimsonR-tdTomato into the PFCx and BLA areas, respectively, and recorded from NAc MSNs receiving both PFCx and BLA inputs (**Figure 2.2A**). The spread of the virus was well contained to the injection sites and only terminals in the NAc were activated (**Figures 2.2B, C**). We employed a protocol where we evoked PFCx-EPSPs (**Figure 2.2D**, blue triangles) followed by BLA-EPSPs (PFCx → BLA gating; **Figure 2.2D**, P2 - red triangles) at different time intervals (i.e., 40, 65, 115, and 165 ms). For each interval, we averaged 10 consecutives traces recorded with 15 s between trials. As a control, 10 BLA-EPSPs were evoked in the absence of PFCx-EPSPs (**Figure 2.2D**, P1 - red triangle, bottom traces) with changes in BLA-EPSP amplitude represented as the ratio of P2/P1 × 100%. At a short (40 ms) interval, BLA-EPSPs were almost

completely inhibited by preceding stimulation of the PFCx pathway (**Figure 2.2D** top traces and **G**, 4.9 ± 1.5% of control). As intervals lengthened, the amplitude of BLA-EPSPs increased, with amplitudes returning to control levels at a 165 ms interval (**Figure 2.2D** lower traces and **G**, 97.3 ± 1.9% of control). This pattern was consistently and repeatedly observed in each of the 6 MSNs recorded. As the length of the interval between the PFCx and BLA stimulation increased, the inhibitory effects of PFCx inputs on BLA-induced EPSPs became significantly weaker (**Figure 2.2G**; $F(3,15) = 132.7$, $p < 0.0001$, mixed-model general linear model (GLM), with cell ID as random variable). Tukey post hoc test showing 40 ms interval being significantly different from all other intervals. This result demonstrates that PFCx afferents exert a powerful but narrow time-dependent inhibition of BLA projections synapsing on core NAc MSNs.

Using the same protocol, the stimulation order was subsequently reversed with BLA-EPSPs preceding PFCx-EPSPs (BLA → PFCx gating). PFCx-EPSPs evoked 40 ms after BLA-EPSPs were similarly strongly inhibited in some MSNs (**Figure 2.2E**) although this effect was not observed in all cells. Indeed, in some MSNs, the gating was either weaker or simply lacking at the same 40 ms interval (**Figure 2.2F**). When averaged over 13 MSNs, the mean inhibition of BLA → PFCx gating was 56.7 ± 10.81% of control at a 40 ms interval, and 90.6 ± 2.9% at 165 ms. There was also significant difference between the intervals tested (**Figure 2.2H**; $F(3,36) = 10.4$, $p < 0.0001$, GLM with cell ID as a random variable), with

Tukey post hoc test revealing significant difference between 40 and 115 ms intervals and 40–165 ms intervals.

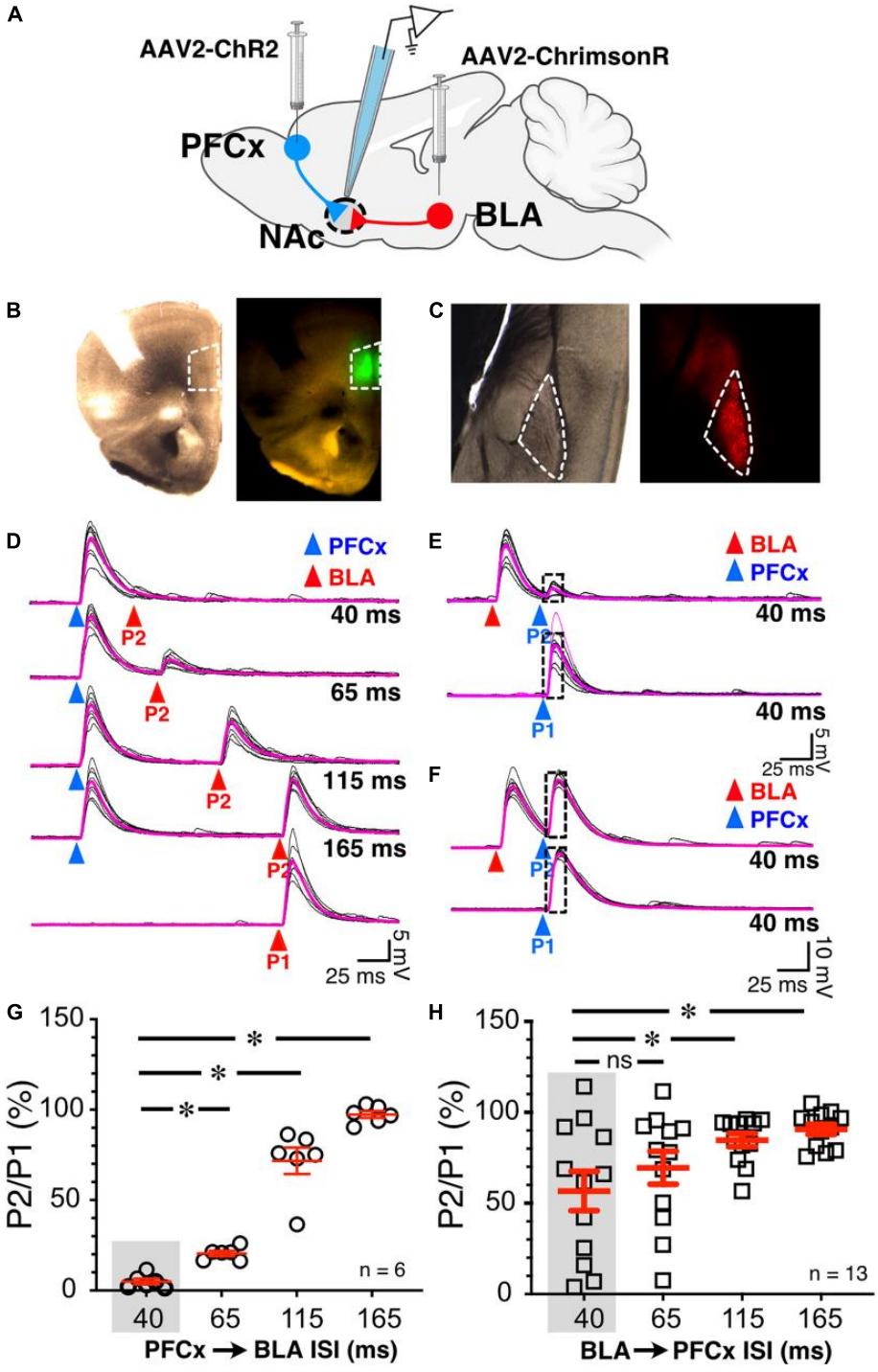

Figure 2.2 | Synaptic gating between BLA and PFCx inputs is bidirectional and asymmetric in alcohol-naïve mice in NAc MSNs. A, Cartoon illustrating the injections and the recording sites. **B**, Bright field (left panel) and epifluorescence of AAV2-ChR2-eYFP injected in the prelimbic prefrontal cortex area outlined by white broken line. **C**, Bright field (left panel) and epifluorescence of AAV2-ChrimsonR-tdTomato injected in the amygdala area outlined by white broken line. Note that the infection is confined to the targeted areas. **D**, 10 overlaid traces of PFCx-EPSPs (blue arrowheads) evoked before stimulation of the BLA pathway (red arrowheads, P2) at increasing interstimulus intervals (from 40 to 165 ms, ISI). As a control, the lowest traces (red P1) show BLA-EPSPs evoked in the absence of PFCx-EPSPs. **E,F** 10 overlaid traces of BLA- EPSPs (red arrowheads) evoked before PFCx-EPSPs (blue arrowheads, P2) at a 40 ms interval. While BLA-EPSPs inhibit PFCx-EPSPs in some MSNs (B) at this short interval, it fails to do so in others (C). **G**, Circles show the magnitude of the gating of BLA-EPSPs (P2) by PFCx inputs (PFCx → BLA) at various intervals expressed as percent relative to control (P1) in 6 MSNs. **H**, Square symbols show magnitude of the gating of PFCx-EPSPs (P2) by BLA inputs (BLA → PFCx) at various intervals relative to control (P1) in 13 MSNs. Each symbol presents a MSN. Average values in graphs are expressed as mean ± standard error (SEM). ∗ $p < 0.01$. Purple traces show averaged EPSPs in panels (D–F).

Interestingly, the BLA → PFCx gating response was significantly different from that observed in PFCx → BLA gating (**Figures 2.2G vs. H**). When comparing the interaction between the interval and the stimulation order, we found a significant interaction effect [$F(3,54.9) = 8.9$, $p < 0.0001$, GLM with cell ID as a random variable], with Tukey post hoc tests revealing BLA → PFCx significantly weaker inhibition than PFCx → BLA gating at 40 and 65 ms intervals.

Next, we tested whether the magnitude of PFCx → BLA gating depended on the size of PFCx-EPSPs. Stimulation of BLA inputs alone evoked large EPSPs (**Figure 2.3A** top traces), that were robustly inhibited by large PFCx-EPSPs (**Figure 2.3A** middle traces). Interestingly, lowering the intensity of blue light reduced the amplitude of PFCx-EPSPs without altering gating efficacy (**Figure 2.3A** bottom traces), a pattern observed in all 8 recorded MSNs (**Figure 2.3B**). Furthermore, we found no correlation between the amplitude of PFCx- and BLA-

EPSPs with a slope was not significantly different from zero (40 ms delay; **Figure 2.3C**). Overall, this shows that the magnitude of gating, at least at BLA synapses, does not appear to be a function of the strength of PFCx synaptic transmission.

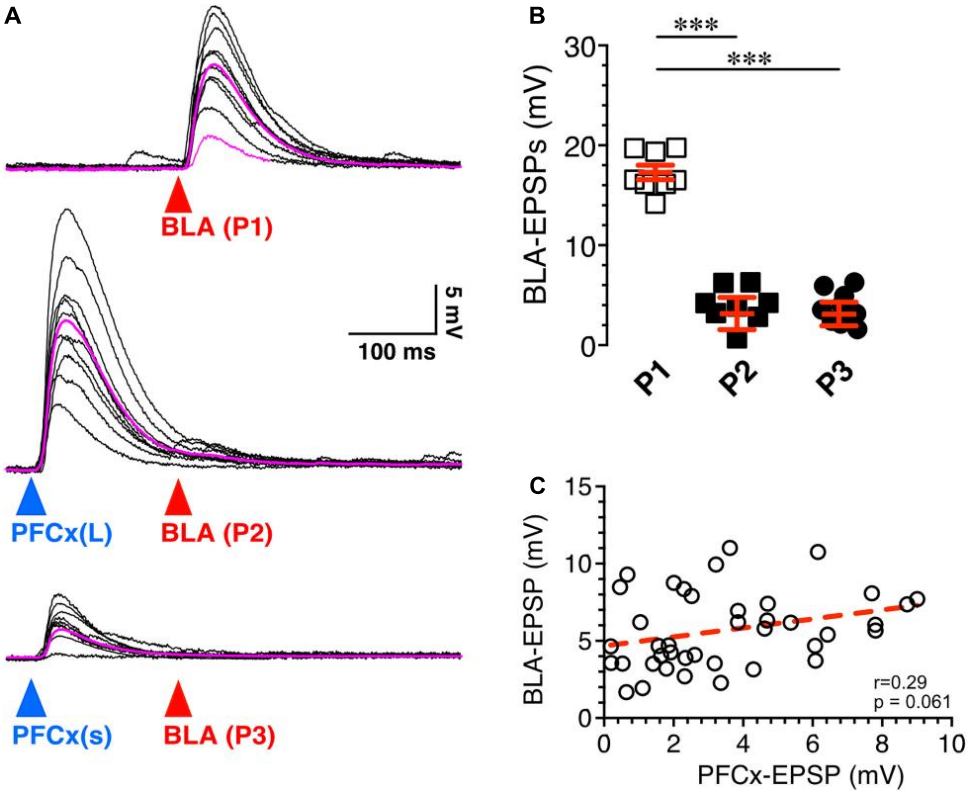

Figure 2.3 | Synaptic gating is a sensitive phenomenon. A, Ten overlaid BLA EPSPs (red arrowhead) evoked in absence (top traces) and in presence of large (middle traces) and small (bottom traces) PFCx-EPSPs (blue arrowheads) in the same MSN (n = 8). Purple traces show averaged EPSPs. **B**, Amplitude of BLA-EPSPs in absence (open squares) and in presence of large (solid black squares, P2) and small (solid circles, P3) PFCx-EPSPs. **C**, Relationship between amplitude of BLA-EPSPs as a function of PFCx-EPSPs amplitudes. Average values in graphs are expressed as mean ± standard error (SEM). *** $p < 0.001$

Synaptic Gating Between Cortical and Amygdala Inputs Is a Pre-synaptic Phenomenon

Since paired-pulse ratio (PPR) is a protocol commonly used to assess the probability of release (Dobrunz & Stevens, 1997), we hypothesized that if gating is pre-synaptic, stimulation of one pathway should alter the PPR of the other. To that end, the probability of release of cortical afferents was assessed by evoking PFCx-EPSCs 100 ms apart (**Figure 2.4A**). For each MSN, 8 consecutive current traces were recorded with a delay of 15 s between traces. Confirming previous findings (Ji et al., 2015), stimulation of the PFCx pathway with an inter-stimulus interval of 100 ms led to a paired pulse depression (PPD) with the second EPSCs being smaller than the first (**Figure 2.4Ai**), indicative of an initial high probability of release (Dobrunz & Stevens, 1997). When averaged over 7 MSNs, the PPR of S2/S1 was 0.57 ± 0.03 (**Figure 2.4C**). Interestingly, when the PPR at PFCx synapses was preceded by stimulation of BLA inputs (red arrowhead, **Figure 2.4Aii**) with an delay of 65 ms, a value we chose based on Figure 2.2H showing that this interval induces a roughly 50% reduction of PFCx-EPSPs by BLA inputs, the paired-pulse depression significantly switched to paired-pulse facilitation (PPF, **Figure 2.4Aii**), with a S2/S1 ratio of 1.37 ± 0.10 (**Figure 2.4C**, n = 7; $F(2,12) = 75.6$, $p < 0.0001$, RM one-way ANOVA), an effect that was reversed when stimulation of the BLA inputs was turned off (**Figures 2.4Aiii, C,** $p = 0.71$, Tukey test). This result is in line with the hypothesis that BLA inputs synapse pre-

synaptically on PFCx afferents and decrease the probability of release of glutamate.

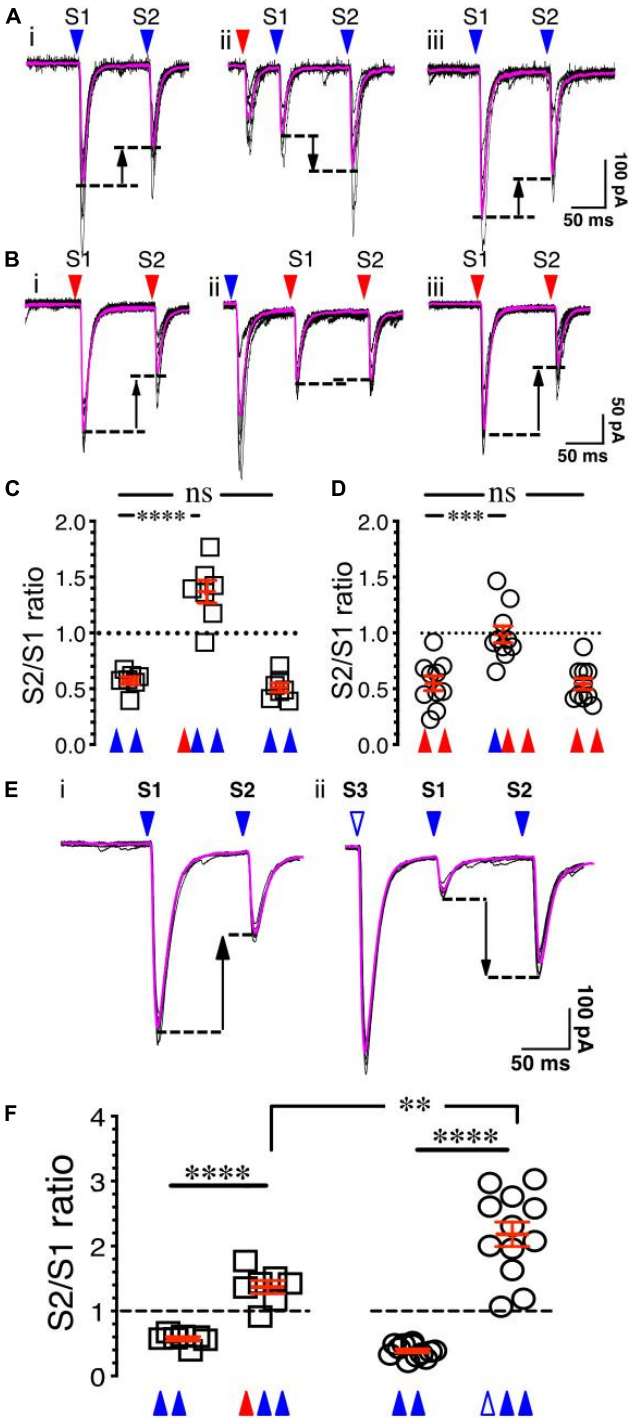

Figure 2.4 | Synaptic gating is a pre-synaptic phenomenon. Ai, Eight overlaid traces of PFCx-EPSCs (blue arrowheads) evoked 100 ms apart (S1 and S2). **Aii**, Same as in i with stimulation of the BLA afferents (red arrowhead) preceding PFCx-EPSCs. **Aiii,** Shows in the same recording that paired pulse depression returned to control level when stimulation of BLA afferents was turned off. **B**, Stimulation order was reversed from panel (A). **C**, Graph showing the switch from depression to facilitation following stimulation of BLA inputs (n = 7). **D**, Graph showing the loss of depression following stimulation of PFCx inputs (n = 10). Note that the magnitude of the switch is not similar. **Ei**, Eight overlaid traces of PFCx-EPSCs (blue arrowheads) evoked 100 ms apart (S1 and S2). **Eii**, PFCx inputs were stimulated 70 ms before the PPR protocol (S3). Purple lines show average traces. **F**, Graphs showing the switch from depression to facilitation when the PPR at PFCx synapses is preceded by stimulation of the BLA (circles) or PFCx (squares) pathways (n = 11). Average values in graphs are expressed as mean ± standard error (SEM). ∗∗ $p < 0.01$, ∗∗∗ $p < 0.001$, **** $p < 0.0001$. Purple traces show averaged EPSCs in panels (A,B,E).

Whether PFCx inputs similarly affected PPR at BLA synapses was tested subsequently. Stimulating BLA afferents 100 ms apart led to a robust depression with a S2/S1 ratio of 0.54 ± 0.03 (**Figures 2.4Bi, D**, n = 10). Interestingly, preceding PFCx-EPSCs, with a delay of 80 ms (a value based on data of Figure 2.2G), essentially blocked the depression at BLA synapses [**Figure 2.4D**; $F(2,18) = 19.4$, $p < 0.0001$, RM one-way ANOVA], but this time without inducing facilitation (**Figures 2.4Bii, D**), with a S2/S1 ratio of 0.98 ± 0.07 (**Figure 2.4D**). As with the control of PFCx PPR by BLA inputs, this effect quickly dissipated when stimulation of PFCx inputs was turned off (**Figures 2.4Biii, D**). This demonstrates that pre-synaptic control of BLA glutamate release by PFCx inputs was significantly weaker than the control of PFCx glutamate release by BLA afferents (PPR = 0.98 ± 0.7 for BLA vs. PPR = 1.37 ± 0.10 for PFCx; $t = 3.1$, $df = 15$, $p = 0.0072$, Student's t test).

To assess whether the changes in synaptic gating underlying the pre-synaptic control of glutamate release from PFCx terminals by the BLA are similar to the changes in PPR, stimulation of BLA inputs (**Figure 2.4Aii**) was replaced with

stimulation of PFCx afferents. Although three consecutive blue light pulses led to a similar reversal of the PPR from depression to facilitation (**Figures 2.4Ei** vs. **ii, F**, $t = 9.5$, $df = 11.5$, $p < 0.0001$, Welch-corrected t test), the magnitude of the effect was markedly larger compared to what was observed following BLA pathway stimulation (**Figure 2.4F**). Thus, while BLA stimulation induced a paired-pulse facilitation with a S2/S1 ratio of 1.37 ± 0.10 (n = 7, **Figure 2.4F**, red triangle), this effect was significantly larger ($t = 3.8$, $df = 15.9$, $p = 0.0016$, Welch-corrected t test) when BLA stimulation was replaced with stimulation of PFCx afferents (**Figure 2.4F**, S2/S1 ratio of 2.31 ± 0.24, white triangle). These observations show that gating appears to induce an increase in PPR that indicates decreased probability of release. It also suggests that a partial, but not full overlap in mechanisms or it might simply be attributable to the fact that direct depolarization of the PFC input is likely more efficacious at engaging the exact same mechanisms that are engaged by BLA stimulation.

Pre-synaptic Dopamine and Metabotropic Glutamate Receptors Do Not Control Synaptic Gating in Nucleus Accumbens Medium Spiny Neurons

In light of the findings showing that gating is pre-synaptic, we investigated its nature by testing the putative involvement of dopamine and type 2/3 metabotropic glutamate receptors, two families of receptor known to control glutamate release (Pennartz et al., 1992; Manzoni, Michel, & Bockaert, 1997; Martin, Nie, & Siggins, 1997; Nicola & Malenka, 1997; Wang et al., 2012b). We measured the strength of

gating at 40 and 165 ms intervals before (Ctrl) and during exposure to 100 μM EGLU, a selective mGluR2/3 antagonist when stimulation of PFCx pathway preceded that of BLA inputs (PFCx → BLA, **Figure 2.5A**), and the reverse (BLA → PFCx, **Figure 2.5B**). We observed no statistically significant change in gating strength in either condition. In a different group of mice, we tested the effects of dopamine D1 and D2 receptor antagonist 5 μM SCH 23390 and 1 μM sulpiride. Like with EGLU, the combination of both antagonists failed to significantly alter synaptic gating in both directions (i.e., PFCx → BLA; **Figure 2.5C** and BLA → PFCx; **Figure 2.5D**). These results indicate that gating is not mediated by dopamine or mGluRs.

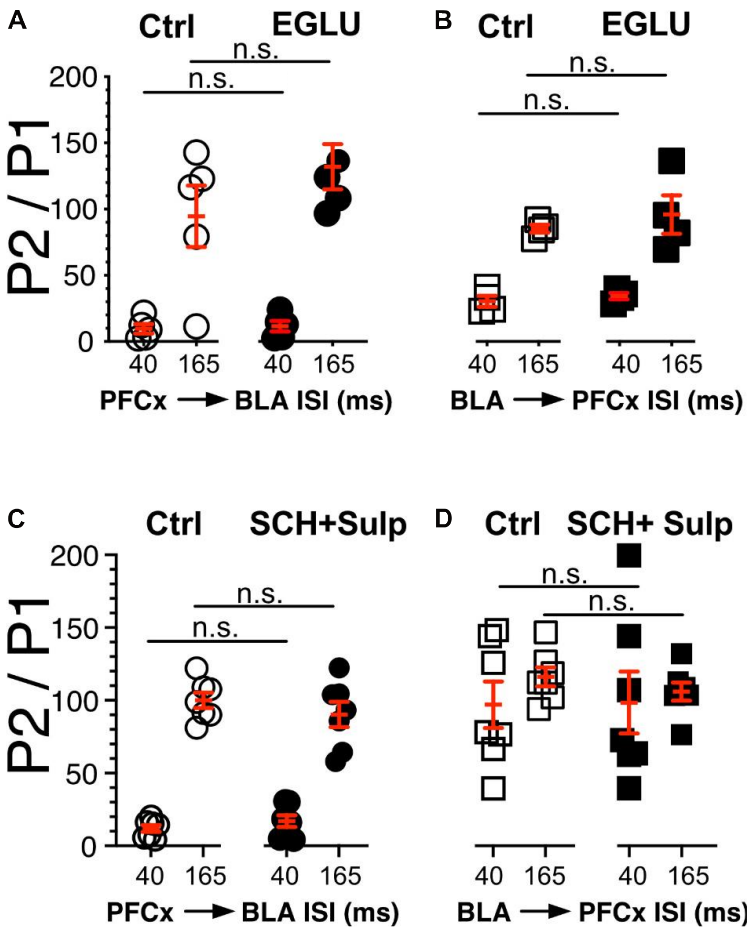

Figure 2.5 | Neither DA nor metabotropic receptors control synaptic gating. A,B Circles show the magnitude of the gating of BLA-EPSPs (P2) by PFCx inputs (PFCx → BLA) at various intervals expressed as percent relative to control (P1) in 5 MSNs before and during exposure to EGLU. Square symbols show the magnitude of the gating of PFCx-EPSPs (P2) by BLA inputs (BLA → PFCx) at various intervals expressed as percent relative to control (P1) in 5 MSNs before and during exposure to EGLU. **C,D** Same as panels (A,B) in presence of SCH-23390 and sulpiride.

Binge Alcohol Drinking Alters Synaptic Gating in an Input Specific Manner

Having established the basic principles and mechanisms underlying synaptic gating of PFCx and BLA inputs to NAc MSNs, gating sensitivity was subsequently assessed in mice exposed to repeated binge alcohol drinking. Following a 2-week period of binge alcohol drinking, and 24 hrs after the last drinking bout, the

reciprocal control of glutamate synaptic transmission in NAc MSNs was examined at PFCx and BLA synapses. First, BLA → PFCx gating was measured at the same intervals of 40, 65, 115, and 165 ms. Interestingly, BLA → PFCx gating was substantially altered by alcohol exposure. Strikingly, at 165 ms interval many DID cells never reached 100% P2/P1 ratio (**Figures 2.6Ai,ii**), a feature that distinguished it from all other cells measured. At the shortest interval of 40 ms, the inhibition in DID mice was variable, ranging from 2.3 to 106.3%, with an average of 56.7 ± 10.9% (**Figure 2.6Bii**, DID), mirroring that of alcohol-naïve mice that ranged from 1.13 to 121.8% of control with an average of 39.8 ± 8.5% (**Figure 2.6Bi**, Control). However, at longer intervals (i.e., 115 and 165 ms), inhibition of PFCx-EPSPs by BLA afferents in DID mice remained highly variable with some MSNs showing weak inhibition of PFCx-EPSPs (**Figures 2.6Ai,ii, Bii**); a result that contrasted sharply with synaptic gating at the same interval in alcohol-naïve mice where only a consistently weak inhibition was observed (**Figure 2.6Bi**). Thus, in some MSNs from DID mice, the inhibition persisted at the longest interval of 165 ms, while it was nearly absent in other MSNs (**Figure 2.6Bii**). At 165 ms interval recorded from alcohol-exposed mice, the inhibition ranged from 18.7 to 107.9% (**Figure 2.6Bii**), with an average value of 63.8 ± 7.6% of control, showing a stronger inhibition than that of alcohol-naive mice (93.6 ± 2.4% of control, compare **Figure 2.6Bi** (Control) and **ii** (DID)). Accompanying the stronger inhibition, we observed a significantly larger variance at intervals 110 and 165 ms. Additionally, in DID BLA → PFCx gating, a significant positive correlation was detected between

the magnitude of the EPSP inhibition at 40 ms and 165 ms [**Figure 2.6D**; $F(1,12) = 30.69$; $p < 0.0001$], indicating a faithful gating mechanism throughout different interval progression.

Next, PFCx → BLA gating was measured. As in water-drinking mice (**Figure 2.6Biii,** Control), PFCx inputs robustly and consistently inhibited BLA-EPSPs to 10.6 ± 2.0% of control (n = 7) at the shortest interval tested in DID mice (40 ms. **Figure 2.6Biv**); a value that was similar to control mice (10.5 ± 3.7% of control, **Figure 2.6Biii**). Inhibition got weaker with longer intervals and was absent at 165 ms (103.4 ± 9.7% of control; **Figure 2.6Biv**). PFCx → BLA gating was thus mostly unaffected by binge alcohol drinking. However, when analyzing the variance at each interval between Control and DID mice, we found a significant effect of binge drinking on the variability in PFCx gating of BLA inputs at all but 40 ms intervals between Control and DID mice (**Table 1**). While binge alcohol drinking does not on average alter the gating of BLA inputs by PFCx, it does increase the variability at 65, 115 and 165 ms intervals, suggesting an effect, albeit smaller than the one observed for gating of PFCx inputs by BLA.

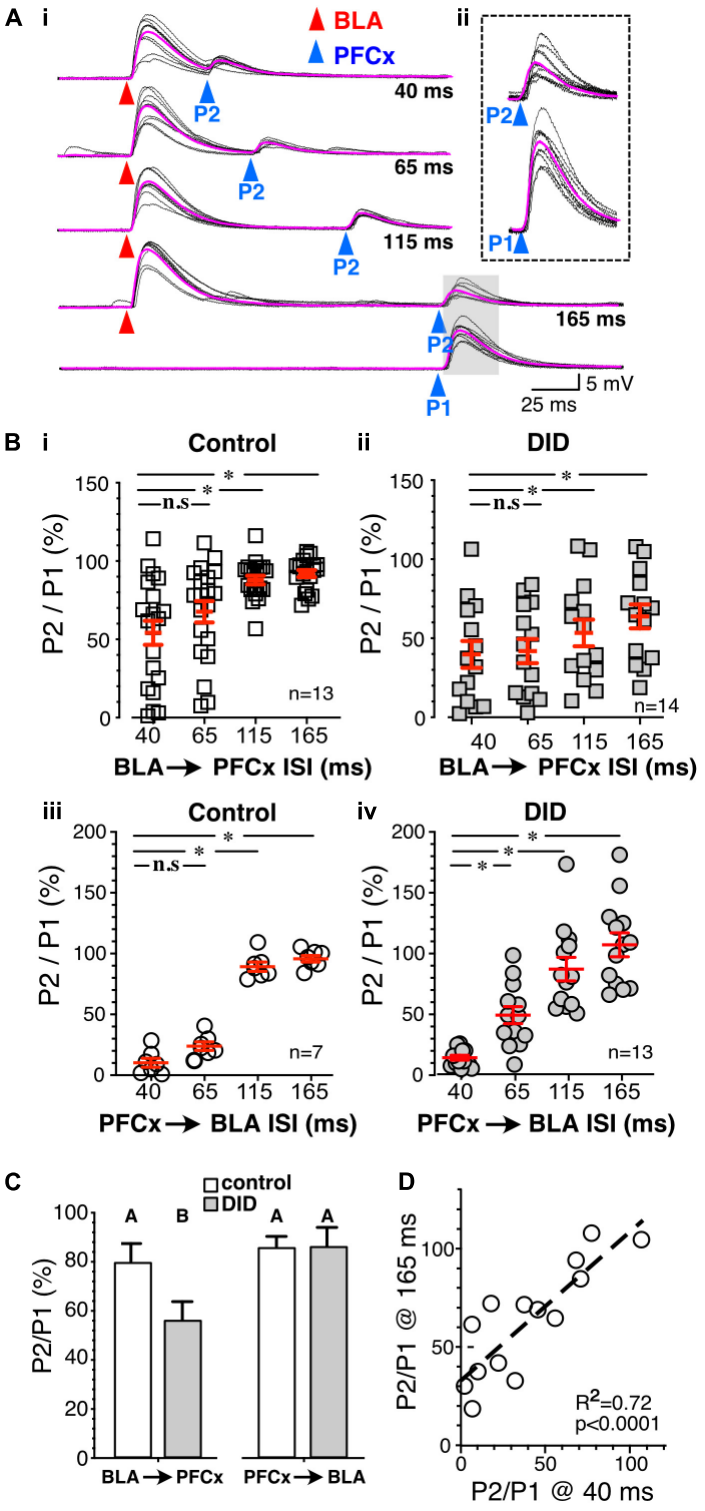

Figure 2.6 | Binge drinking strengthens BLA-driven inhibition of PFCx inputs. Ai, Ten overlaid traces of PFCx-evoked EPSPs (blue arrowheads) in absence (P1-bottom

panel) or presence of BLA-EPSPs (red arrowheads) in the same MSN from an EtOH drinking mouse. Purple traces show average EPSPs. **Aii**, Enlarged PFCx-EPSPs traces evoked 165 ms after BLA-EPSPs (P2) or in its absence (P1) as shown in shaded area in panel (Ai). Note the persistent gating at 165 ms interval indicated by the vertical arrow. **Bi,ii** Magnitude of gating of BLA → PFCx inputs in water-drinking (Control) and Drinking-in-the-Dark mice (DID) at various intervals relative to control expressed as percent relative to control (P1) in 13 and 14 MSNs, respectively. **Biii,iv** Magnitude of gating of PFCx → BLA inputs in water-drinking mice (Control) and Drinking-in-the-Dark mice (DID) at various intervals relative to control in 7 and 13 MSNs, respectively. **C**, Summary statistics of Panel (B) for 165 ms interval. Change in EPSP amplitude (P2/P1) resulting from BLA → PFCx and PFCx → BLA gating is altered by binge alcohol drinking (DID). Averages and SEMs represent GLM model estimates of the effects of gating direction and alcohol exposure. Groups identified with different letters are significantly different. **D**, Correlation between the magnitude of inhibition of PFCx-EPSPs by BLA at 40 ms and that measured at 165 ms interval in DID mice. Average values in graphs are expressed as mean ± standard error (SEM). $*p < 0.01$.

TABLE 1 | *F*-test of Two-Sample Variance.

		Mean		Variance			
		DID	**Control**	**DID**	**Control**	***F* value**	***p*-value**
BLAx → PFC	*40 ms*	39.8	56.7	1012.5	1568.9	0.65	0.2220
BLAx → PFC	*65 ms*	41.9	65.0	808.9	843.9	0.96	0.4676
BLAx → PFC	*115 ms*	53.4	88.4	992.9	141.2	7.03	0.0009
BLAx → PFC	*165 ms*	63.8	93.6	801.3	74.3	10.78	0.0001
PFCx → BLA	*40 ms*	10.6	10.6	52.9	95.9	0.55	0.1793
PFCx → BLA	*65 ms*	45.6	24.2	645.3	83.6	7.72	0.0100
PFCx → BLA	*115 ms*	83.4	89.5	1208.6	101.4	11.92	0.0031
PFCx → BLA	*165 ms*	103.5	96.1	1244.5	52.7	23.63	0.0005

To compare all the groups in **Figure 2.6B** and to determine whether alcohol treatment alters the weight between PFCx and BLA inputs, we tested for the interaction between the order of stimulation and the presence of alcohol treatment. We indeed observed a significant interaction between the order of stimulation

(PFCx or BLA first) and alcohol treatment, (**Figures 2.6B, C**; F(1,162.2) = 10.9, p = 0.0012, MM-GLM). Tukey post hoc revealed significant differences between control and EtOH BLA → PFCx groups, but no differences between Control and EtOH PFCx → BLA groups. We did not observe the effect of alcohol on the intervals (p = 0.56).

In summary, we have found that 2-week EtOH DID treatment significantly affected weight contribution between PFCx and BLA inputs by altering the overall strength of BLA → PFCx gating but not that of PFCx → BLA gating, while additionally significantly affecting the variability in both pathways.

Suppression of Binge Alcohol Drinking by Optogenetic Basolateral Amygdala Activation in Freely Moving Mice

Next, we wanted to determine whether activation of PFCx or BLA pathways to NAc has behavioral significance. Although we could not recapitulate the in vitro double stimulation “gating” protocol, we wanted to know whether single pathway stimulation would be sufficient to alter mouse binge alcohol consumption. We injected mice with pAAV5-CaMKII-hChR2(H134R)-eGFP (AAV-ChR2) either into the PFCx or BLA nuclei, with controls injected with a GFP-expressing AAV (AAV-GFP) into the PFCx and fiber optic probes placed in the NAc core (**Figure 2.7A**). Optogenetic stimulation of PFCx and BLA pathways was achieved via delivery of 10 Hz 470 nm light, 2 min on, 2 min off (**Figure 2.7B**). As described previously (Ji et al., 2017), alcohol access over a 2-week period produces an escalation in

consumption. When we repeated this experiment over eight consecutive days, we also saw a significant increase between day 4 and day 8 of alcohol consumption in a group of n = 8 mice that did not undergo surgery (**Figure 2.7C**; t = 2.5, df = 14, p = 0.0235). Since we have observed this increase in consumption, we exposed mice to 20% EtOH for 4 days, and then optogenetically stimulated during EtOH drinking days 5–8 (**Figure 2.7A**). Binge alcohol drinking behavior was quantified by recording the number and timing of licks of the drinking spout on day 4 of EtOH consumption (last day before stimulation) and day 8 (last day of stimulation). Like mice that did not undergo surgery (**Figure 2.7C**, inset), mice injected with AAV-GFP showed an increase of EtOH consumption on day 8 after stimulation (Opto Stim, patterned columns) compared to day 4 without stimulation (No Stim; **Figure 2.7D**, GFP). Injection of AAV-ChR2 into the PFCx showed a pattern like GFP controls: an escalation of drinking on stimulation day 8 (Opto Stim, patterned columns) compared to day 4 without stimulation (No Stim; **Figure 2.7D**, PFCx). Interestingly, in mice injected with AAV-ChR2 into the BLA using the same paradigm, optogenetic stimulation prevented this escalation in EtOH consumption on day 8 (Opto Stim; **Figure 2.7D** BLA). We found a significant interaction between light presence and the brain area injected (**Figure 2.7D**; $F(2,17.6) = 3.6$, $p = 0.0497$, with Day and Mouse ID as random variables, GLM). Post hoc Student's t test showed significant differences in PFCx and GFP groups between day 4 (no stimulation day) and day 8 (stimulation day), with no differences in BLA-injected mice. This finding was in line with our patch clamp data showing an increased

efficiency of the gating of PFCx-EPSPs by BLA activation. Also, on Day 4 there are no differences among GFP, PFCx, and BLA groups. Finally, comparison of alcohol consumption at Day 8 between the GFP, PFCx, and BLA groups showed a highly significant difference between GFP and BLA but not between GFP and PFCx groups. This effect was not due to a general depression of behavioral activity in BLA-stimulated mice, as no differences in movement velocity (**Figure 2.7E**; $F(1,12) = 0.4885$, $p = 0.625$) and time spent in the center (**Figure 2.7F**; $F(2,12) = 0.4103$, $p = 0.672$) were observed in an open-field test. Importantly, 0.3% saccharin drinking behavior was unaffected by PFC- or BLA-stimulation (**Figure 2.7G**; $F(2,12) = 1.256$, $p = 0.319$), thus demonstrating the BLA-specific inhibition of alcohol drinking as an alcohol-specific effect.

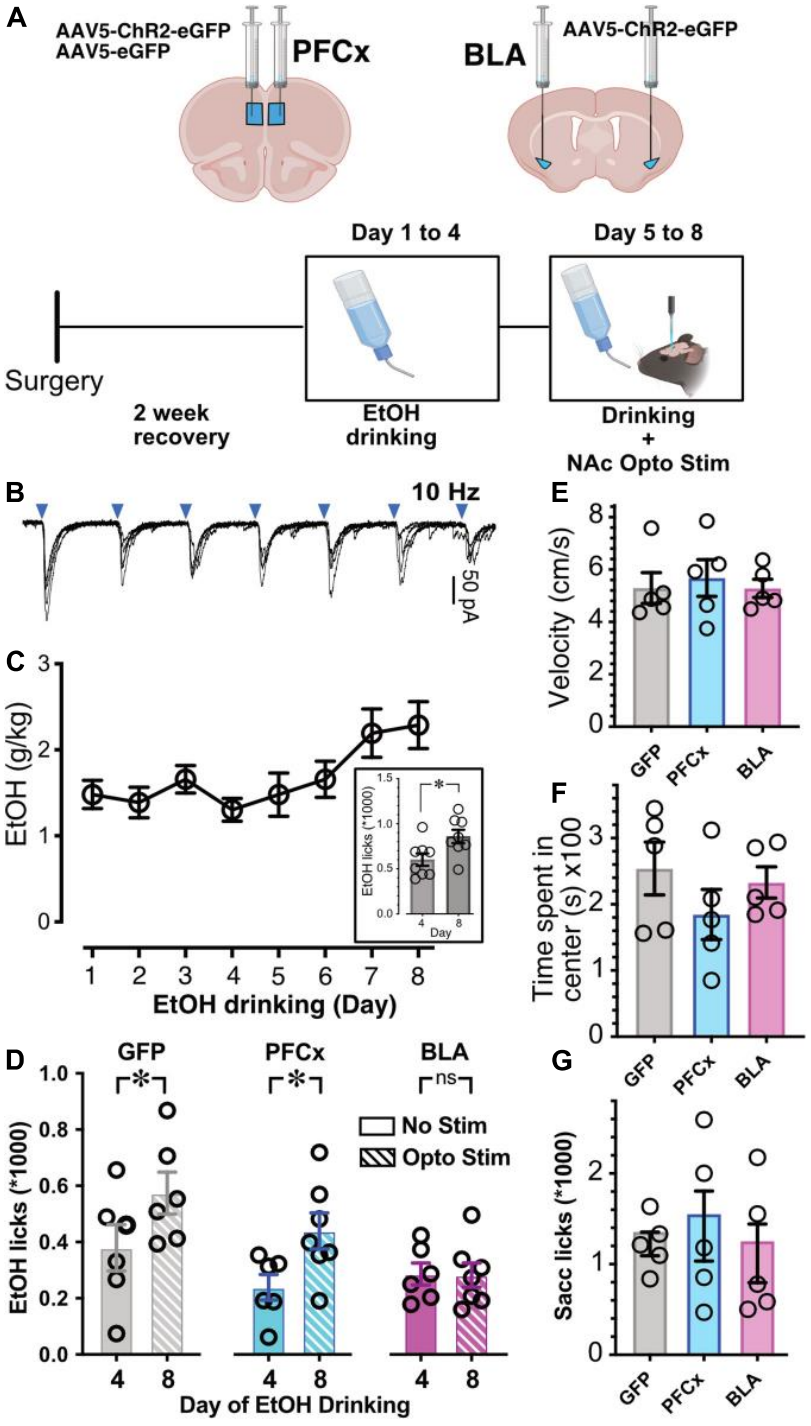

Figure 2.7 | Effects of optogenetic activation of PFCx or BLA inputs on EtOH drinking. A, Schematic illustrating the sites of bilateral injections and the timeline of the behavioral experiments. **B**, Synaptic responses to 10 Hz light stimulation of PFCx afferents. Blue triangles indicate time of stimulations. **C**, EtOH consumption over a period

of 8 consecutive days. Note the escalation between the 4th and 8th day. Graph in inset shows the corresponding number of licks at Day 4 and 8. **D**, Number of licks measured over a 2 h period at Day 4 and 8 in mice injected with GFP in the PFCx (GFP, gray columns), with ChR2 in the PFCx (PFCx, blue columns), or in the BLA (BLA, pink columns) in absence (solid columns, no stim) or presence of light stimulation (hatched columns, Opto Stim). **E,** Velocity measured in mice injected with GFP (GFP) or ChR2 (BLA; PFCx). **F**, Time spent in center of field in mice injected with GFP (GFP) or ChR2 (BLA; PFCx). Average values in graphs are expressed as mean ± standard error (SEM). Each symbol represents a mouse. **G**, Number of licks of 0.3% saccharin (Sacc) in 2 h in mice injected with GFP (GFP) or ChR2 (BLA; PFCx). $*$ $P < 0.01$.

Discussion

The NAc is considered to be a key mediator of the effects of drugs of abuse such as alcohol (Scofield et al., 2016). Within the NAc, MSNs serve as integrators of potentially conflicting drives (Lara & Wallis, 2015; Wassum & Izquierdo, 2015; Klenowski, 2018) and receive inputs from different brain regions such as the PFCx and BLA while projecting to the effector cells (Humphries & Prescott, 2010). The present study confirms this function of NAc MSNs as integrators of different inputs with the PFCx and BLA synapsing onto the same core NAc MSNs. Importantly, the relative timing of input signals determines the subsequent MSN output. BLA and PFCx inputs reciprocally inhibit each other, but the strength of this reciprocal inhibition is asymmetric, with PFCx → BLA gating stronger than the reverse. The interactions underlying PFCx → BLA and BLA → PFCx gating occur pre-synaptically. Surprisingly, previous exposure to binge alcohol drinking uni-directionally strengthens BLA → PFCx gating in a selective manner (**Figure 2.6**). Overall, these findings suggest the integration of different inputs in the MSNs as a potential target for modifying substance abuse behaviors. In line with this suggestion, optogenetic activation of BLA inputs in the NAc does indeed result in an inhibition of the increase in alcohol drinking behavior observed during the first week of alcohol exposure in mice.

The idea that afferents originating in the cortex, amygdala, hippocampus and thalamus converge onto the same NAc MSNs is supported by multiple anatomical studies (French & Totterdell, 2002; French & Totterdell, 2003) and

electrophysiological recordings in anesthetized rats (O'Donnell & Grace, 1995; Finch, 1996; Brady, Glick, & O'Donnell, 2005; Calhoon & O'Donnell, 2013), and in acute tissue slices (Stuber et al., 2011). However, the degree of convergence remains unclear with some studies showing convergence of these inputs in less than 5% of MSNs (Callaway, Hakan, & Henriksen, 1991; Finch, 1996) while others reported a strong convergence in nearly all MSNs (O'Donnell & Grace, 1995), a discrepancy that may be attributed to the use of different recording methods (i.e., intra vs. extracellular recordings). Our data supports strong convergence since we found that the vast majority (i.e., ~81%) of core NAc MSNs received inputs from both the PFCx and the BLA.

The current work illustrates that a key feature of synaptic gating between PFCx and BLA afferents is its bidirectionality, with inhibition of synaptic transmission of one pathway by the other being mirrored when the stimulation order is reversed. This phenomenon is reminiscent of findings by Calhoon and O'Donnell showing a similar bidirectional gating between thalamic and PFCx afferents in anesthetized rats (Calhoon & O'Donnell, 2013). Furthermore, the delay of 50 ms at which inhibition was the strongest in their study was similar to the one reported in our study (i.e., 40 ms), suggesting that synaptic gating of PFCx-, BLA-, and thalamic-inputs converging onto NAc MSNs shares characteristics at least in terms of its timing. One major difference, however, is the need for high frequency stimulation to induce gating in the intact brain while a single EPSP was sufficient to obtain similar strong inhibition in our in vitro slice study. This difference might

reflect a higher efficiency to evoke synaptic events in slices compared to the intact brain. Surprisingly, our data shows that not only is a single PFCx-EPSP sufficient to block the transmission of BLA information, but that this inhibition can even be induced by very small PFCx-EPSPs, illustrating the high sensitivity of synaptic gating between cortical and amygdala inputs in NAc MSNs. A possible explanation for the apparent discrepancy between slice- and intact-brain recordings is that seemingly small somatic EPSPs are much larger at their point of inception (i.e., the synapse). As EPSPs travel to the soma following synaptic induction distally, they get subjected to the strong filtering by the dendrites' cable properties, resulting in a depression of the detected EPSPs amplitude (Rall, 1959). Overall, the current findings demonstrate the bidirectional nature of gating different inputs to the NAc and underscores the extreme sensitivity of this process.

Our efforts to identify the pre-synaptic mechanism responsible led to the conclusion that neither DA receptors and mGluRs nor NMDA receptors are necessary for synaptic gating. This is not entirely surprising considering synaptic gating kinetics that is characterized by a very fast onset, with one input blocking the other within a few ms before disappearing after 165 ms. This time course is rather incompatible with slower acting G protein-coupled receptor / second messenger system. Because this result suggested the participation of pre-synaptic ionotropic receptors, we were surprised to observe the lack of effects of the NMDA receptor antagonist d-APV. Therefore, it is likely that pre-synaptic control is mediated by AMPA receptors. Unfortunately, testing this hypothesis would require

neutralizing these receptors, which we cannot do without blocking EPSPs altogether.

Bechara (2005) proposed that an underlying cause for drug addiction is the hyperactivity in the amygdala system that overrides the reflective system of the prefrontal cortex (Bechara, 2005). The present study examined how MSNs reconcile drastically different information originating specifically from the medial prelimbic PFCx and the BLA. To determine whether the integration of these conflicting inputs has physiological relevance, binge alcohol drinking was assessed in freely behaving mice with optogenetically activated PFCx- or BLA-inputs to the NAc. Stimulation of BLA projections, but not PFCx inputs, in the NAc abolished the increase in alcohol drinking behavior over days 4 to 8 of alcohol exposure. Interestingly, using a Pavlovian conditioning protocol, Millan et al. (2017) reported that activation of the BLA to NAc pathway similarly blocked alcohol consumption triggered by cue-conditioned alcohol seeking (Millan, Kim, & Janak, 2017). Additionally, in an interesting parallel, our electrophysiological data shows that alcohol exposure that strengthens BLA control of PFC inputs has lesser effect on PFCx gating of BLA. The alteration of BLA input to the NAc responsible for modifying alcohol consumption behavior might be the result of changes in direct synapses with MSNs or the inhibition of PFCx projecting inputs to MSNs. While our in vivo experiment could not distinguish between these two modes, our electrophysiological data showed that alcohol exposure disrupts the sensitive balance underlying the integration of PFCx and BLA information by NAc MSNs.

Based on these electrophysiological observations, we hypothesize that BLA activation can modify alcohol drinking behavior through the inhibition of PFCx inputs to MSNs in the NAc. It is important to note that the interpretation of our behavioral data is limited by the fact that we could not replicate the gating protocol (i.e., double stimulation) used in in vitro slice recordings. In particular, the 10 Hz frequency could alter synaptic transmission in a way unrelated to the gating mechanism unveiled in slices (Pascoli, Cahill, Bellivier, Caboche, & Vanhoutte, 2014) and may cause a suppression of BLA synaptic efficacy possibly accounting for the confounding effect on binge drinking (i.e., blockade instead of increase of alcohol consumption **Figure 2.7D**). Further studies recruiting both pathways with stimulation intervals based on our electrophysiological findings in freely moving mice are needed to fully understand the respective roles of PFCx and BLA pathways in controlling binge alcohol drinking. Another limitation of our behavioral design was that we could not distinguish between the effect of time and stimulation on binge alcohol drinking. Additional studies need to be performed to tease apart their respective influence.

Acknowledgment

This work was supported by the National Institute on Alcohol Abuse and Alcoholism AA020501 (GM) and the National Institute of General Medical Sciences T32GM135751 (TL).

Chapter III

EPHierStats: a statistical tool to model the hierarchical relationships in electrophysiological data

Chapter III: EPHierStats: a statistical tool to model the hierarchical relationships in electrophysiological data

Jenya Kolpakova[1,2], Jonathan D. Marvel-Zuccola[3], Kensuke Futai[1,2], Gilles E. Martin[1,2], Vincent van der Vinne[3]

This work is deposited into Bioarchives: *BioRxiv* doi: https://doi.org/10.1101/2022.03.23.485501

1. Brudnick Neuropsychiatric Research Institute, Department of Neurobiology, University of Massachusetts Chan Medical School, Worcester MA 01655, USA, Worcester MA 01655, USA
2. Graduate Program in Neuroscience, Morningside Graduate School of Biomedical Sciences, UMass Chan Medical School, Worcester MA 01655, USA, Worcester MA 01655, USA
3. Biology Department, Williams College, Williamstown MA 01247, USA

Roles of authors

JK VvdV designed research, JK GEM KF carried out experiments, JK VvdV KF analyzed data, JK VvdV wrote the paper, KF JDMZ helped out with research design

Abstract

Electrophysiological datasets are typically analyzed under the assumption that repeated measurements of the same unit of analysis (i.e. neuron or animal) can be treated as statistically independent. Recently, this assumption has been questioned and our data confirms and quantifies this skepticism using ex vivo slice recordings of synaptic currents in D1-MSNs in the NAc. We therefore present EPHierStats as a statistical framework to analyze electrophysiological datasets with large numbers of measurements (>100) per unit of analysis. This novel analysis framework enables encoding of the full hierarchical relationships between measurements in a mixed-effects general linear model while also analyzing the distribution of values in assessed variables. Our method can easily be adapted to analyze a wide range of repeated-measures electrophysiological experiments. Implementation of the EPHierStats tool will aid the adoption of modern statistical approaches that prevent pseudoreplication and its associated false discovery rate while enabling statistical assessments of the complex relationships inherent to the field of neuroscience.

Introduction

Electrophysiological recordings of the activity of neurons provide insight into the functioning of the brain at the level of its fundamental components (Kandel, Schwartz, Jessell, & Siegelbaum, 2000). Electrophysiological recordings of individual cells can be performed using a suite of different approaches, including the recording of action potentials, single channels, excitatory and inhibitory postsynaptic currents (EPSCs/IPSCs), and/or multi-electrode array recordings. All of these approaches can record the electrophysiological behavior of individual neurons and do so by performing (many) repeated measurements of each neuron. The repeated nature of electrophysiological measurements does however complicate the analysis of these recordings and commonly used analysis approaches are often overly conservative or unreliable due to pseudoreplication (Aarts, Verhage, Veenvliet, Dolan, & van der Sluis, 2014; Yu et al., 2021).

One of the most common analyses for electrophysiological datasets is to assess whether the average of an output parameter is different between treatment conditions. Since repeated measurements from the same neuron will typically be more alike compared to measurements from a different neuron (thus violating the homogeneity of variance assumption), analyses often calculate the average output parameter per cell and statistically analyze these average values (Aarts, Verhage, Veenvliet, Dolan, & van der Sluis, 2014). Although this approach circumvents the problem of pseudoreplication, the resulting analysis will suffer from an unnecessarily low statistical power. Also, with regression to the mean inherently

occurring in cells with more measurements, cells that were sampled less often will be more likely to have an extreme value (Stigler, 1997). Due to the normalizing at the level of individual cells, an outsized weight will thus be attached to these more extreme values. Finally, it is important to recognize that the distribution of electrophysiological values typically resembles a Poisson distribution, thus requiring either a non-parametric statistical test or transformation of the data to ensure that the residuals are normally distributed (Limpert, Stahel, & Abbt, 2001; Yu et al., 2021).

Another research question often addressed using electrophysiological measurements is whether the distribution of values is altered between treatments. An example of such an altered distribution can be observed in a dataset where one treatment results in an increase of activity at a specific part of the distribution of outcomes (Mao et al., 2018). A typically employed statistical test to assess changes in the distribution of values is the two-sample Kolmogorov-Smirnov test (Massey, 1951; Manabe, Renner, & Nicoll, 1992). This test does not account for the specific neuron that each measurement was taken from, and the test thus requires that the distribution of values is the same in each of the neurons included in a group. Conversely, in cases where the distribution of measurement values is dependent on the neuron from which the recording was taken (or another similarly confounding factor), the repeated measurements within those neurons cannot be considered as statistically independent and thus pseudoreplication will result in an overestimation of the statistical effect size. Finally, the Kolmogorov-Smirnov test

only assesses the value at which the two samples are most divergent and is thus incapable of assessing statistical differences at any other part of the distribution.

This paper first quantifies the statistical influences of the neuron, slice, animal, and experimenter levels on individual EPSC measurements of D1-MSNs in the nucleus accumbens of mice. These analyses of EPSC frequency and amplitude illustrate the necessity of incorporating the underlying hierarchical relationships in the statistical analysis of such an electrophysiological dataset. Subdivision of the repeated measurements of each neuron into multiple subsequent intervals provides a way to generate biological replicates that increase statistical power while also enabling assessment of the distribution of outcomes. We present a flow scheme to implement this analytical approach to a hierarchical electrophysiological dataset and demonstrate its utility by analyzing an existing dataset. Overall, this novel statistical framework enables the use of powerful mixed-effects general linear modeling approaches to analyze the complex relationships that are common in electrophysiological datasets.

Materials & Methods

Electrophysiological measurements

All animal experiments used 8 – 10-weeks old male Drd1a-tdTomato (Stock No. 016204; The Jackson Laboratory, Bar Harbor, ME) on the C57Bl/6J background as originally described (Ade, Wan, Chen, Gloss, & Calakos, 2011). Animal studies were approved by the Institutional Animal Care and Use Committee of the University of Massachusetts Chan Medical School. Mice were maintained at constant temperature (22 ± 1°C) and humidity in a 12 h:12 h light–dark cycle with water and food available *ad libitum*. Mouse acute brain slices were prepared according to methods previously described (Kolpakova et al., 2021). Whole-cell patch clamp recordings of spontaneous EPSCs were acquired from dopamine-1 receptor^{+} (D1) MSNs in the NAc and identified by tdTomato fluorescent reporter (Ade, Wan, Chen, Gloss, & Calakos, 2011). EPSCs were isolated by recording in the presence of 15 µM bicuculine (GABA receptor antagonist). Spontaneous EPSCs were acquired for 4-6 mins using gap-free recording at MSN resting membrane potential (Kolpakova et al., 2021). EPSC amplitude and interevent interval were determined using Clampfit (pClamp 11 software suite, Molecular Devices).

Data Analysis and Statistics

The interevent interval and amplitude of all EPSCs identified by Clampfit were associated with the corresponding mouse, experimenter, brain slice, neuron, and

time interval for each individual measurement. For each neuron, EPSCs occurring during three minutes of recording were included and were also subdivided into three one-minute time intervals for statistical analyses. Based on visual assessments of the distribution of residuals resulting from different transformations ($\sqrt[n]{x}$, with n = [1:400]) we concluded that the $\sqrt[40]{x}$ transformation was adequate and enabled the use of parametric statistical approaches. The partitioning of variance was assessed separately for interevent interval and amplitude in a series of mixed-effects general linear models incorporating all the independent variables listed above as random variables to determine the variance explained. The statistical significance of individual variables was assessed in a series of models with all variables included as random factors except for the assessed variable. In all these analyses, variables were nested to reflect the hierarchical relationships between biological levels of organization. All statistical analyses were performed using SAS JMP 7.0.

Assessments of the distribution of values were performed using different approaches to describe the distribution. In the traditional approach, all untransformed values were first averaged per neuron to describe the average response, while a cumulative distribution was calculated while ignoring the neuron from which each measurement was taken. Our novel approach first visualized the distribution of values in a subset of seven neurons taken from separate mice and measured by the same experimenter. The value closest to the 5^{th}, 25^{th}, median, 75^{th} and 95^{th} percentile was determined separately for each of the three-minute

sets of measurements in each neuron with means ± SEM calculated based on transformed values. The subsequent visualization of percentile values in individual neurons determined the value closest to the 5^{th}, 25^{th}, median, 75^{th} and 95^{th} percentile separately in each of the three one-minute intervals available in each neuron and presents the mean ± SEM based on the transformed values of these three values.

EPHierStats procedure

The EPHierStats approach aims to optimize a tradeoff between the most powerful statistical analysis of average responses and the ability to describe the distribution of outcomes. Subdividing measurements into biological replicates of 25 observations enables the selection of values corresponding exactly to the 6^{th}, 26^{th}, median, 74^{th}, and 94^{th} percentile values. These values were selected to represent the median, shoulders, and extreme values of the distribution we aimed to describe but could easily be replaced with other percentile values if appropriate. The inclusion of ten replicates of 25 measurements per condition enabled very powerful statistical comparisons but a lower number of replicate intervals will typically be sufficient to accurately quantify within-neuron variability. Selection of the five values per interval was accomplished here in MS Excel following organization of the dataset using the Sort command and can be accomplished easily in a wide range of software packages. Visual inspection of residuals of the various models confirmed that normalization using the $\sqrt[40]{x}$ transformation worked well for our

dataset and enabled us to use parametric statistical tests. Proper encoding of the hierarchical relationships between the measurements from biological replicates is done using a mixed-effects general linear model in which (at a minimum) neuron and time interval should be included as random variables. The percentile [6, 26, 50, 74, 94] of each included value should always be included as a categorical fixed main effect in the statistical model as well as the interaction between the percentile and the factor of interest (i.e. percentile*genotype). If this interaction term does not substantially reduce the unexplained variance in the model, the interpretation of the statistical results might be simplified by removing this interaction term from the model.

Validation of the EPHierStats analysis approach

The utility of the EPHierStats approach was assessed by re-analyzing a previously published dataset (Mao et al., 2018) that tested the involvement of the Chromatin reader L3mbtl1 in synaptic scaling induced by pharmacological treatments (Turrigiano, 2011). In line with traditional approaches to analyze a dataset like this, our initial statistical comparisons analyzed the average miniature EPSC (mEPSC) amplitude for each neuron. A second model described the hierarchical relationships between different neurons more extensively by adding Mouse ID as a random variable to the initial model. The final statistical model applied the EPHierStats approach outlined above and included Mouse ID, Neuron ID, and Time interval as random variables. All statistical comparisons were made using

mixed-effects general linear models with genotype, pharmacological treatment, and their interaction included in all models as fixed effects. The EPHierStats model also included percentile and its interactions as fixed effects. The criterion for statistical significance was $p<0.05$ for all experiments and post-hoc comparisons were made using Tukey-HSD tests.

Results

Repeated electrophysiological measurements are not statistically independent

Common analysis methods assessing changes in the average electrophysiological response of neurons to experimental treatments often assume that the repeated measurements taken from multiple neurons are statistically independent. Statistical independence is a core assumption underlying all statistical tests and it requires that the residual of one or a subset of datapoints cannot be used to predict the residual of any other datapoints (Grafen & Hails, 2002). The assumption of statistical independence is typically violated when repeated measurements are performed since measurements from the same neuron are likely to be more similar compared to measurements from a different neuron. To restore statistical independence in the analysis of a repeated-measurements dataset, it is necessary to properly encode the hierarchical relationships between measurements in the statistical analysis (e.g. repeated-measures ANOVA). Beyond the expected similarities between individual neurons, measurements taken from neurons in the same brain slice and/or the same animal might similarly result in violations of the assumption of statistical independence.

To establish which levels of biological organization should be incorporated in the statistical analysis of repeated electrophysical measurements in order to ensure statistical independence, repeated EPSC measurements were performed by 2 experimenters from 110 neurons on 36 brain slices derived from 8 mice (**Figure 3.1**). As expected, both the inter-event interval and amplitude of these

EPSCs were Poisson distributed (**Figure 3.1A, C**), thus requiring transformation ($\sqrt[40]{x}$) to enable the use of parametric statistical approaches (**Figure 3.1B, D**). Subdividing the recordings into one-minute intervals provided three biological replicates of repeated EPSCs for each neuron that illustrated the low within-neuron variability relative to the between-neuron variability of the EPSCs' mean interevent interval and amplitude (**Figure 3.1E, F**). Partitioning of the variance in interevent interval between the different levels of biological organization showed that the neuron ID and slice ID could explain 18.6 % ($F_{74,196.3} = 34.44$, $p < 0.0001$) and 9.5 % ($F_{28,38.02} = 3.916$, $p < 0.0001$) of the total variance, respectively (**Figure 3.1G**). The time interval (0.9 %, $F_{219,49592} = 2.856$, $p < 0.0001$), experimenter (1.5 %, $F_{1,32.33} = 2.562$, $p = 0.1192$), and mouse (1.9 %, $F_{7,25.1} = 1.413$, $p = 0.2438$) only marginally influenced the interevent interval duration. Analyzing the distribution of variance in EPSC amplitude demonstrated that neuron ID explained 23.8 % ($F_{74,225.1} = 49.52$, $p < 0.0001$) of variance, while slice (-0.9 %, $F_{28,1} = 2.092$, $p = 0.5050$), interval (0.7 %, $F_{219,50002} = 2.423$, $p < 0.0001$), experimenter (2.6 %, $F_{1,16.66} = 9.078$, $p = 0.0080$), and mouse (-0.7 %, $F_{7,18.06} = 0.4903$, $p = 0.8294$) barely affected amplitude (**Figure 3.1H**). In summary, these results show that repeated EPSC measurements are not statistically independent and that the neuron from which recordings are taken should be considered when analyzing this kind of electrophysiological recordings.

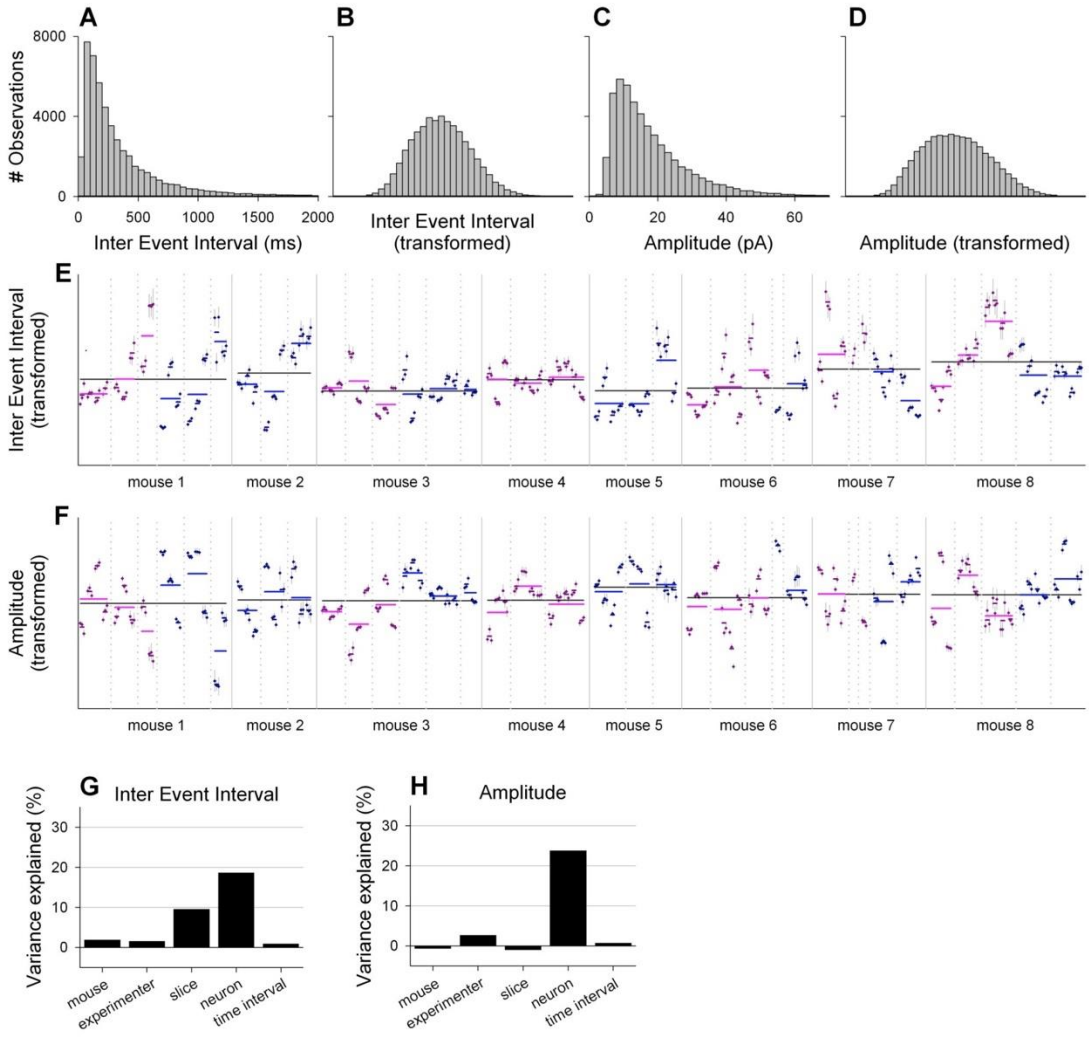

Figure 3.1 | Hierarchical relationships shape measurements of EPSCs interevent interval and amplitude. A, B Histograms of raw (A) and transformed ($\sqrt[40]{x}$, B) EPSCs interevent interval measurements. **C, D** Histograms of raw (C) and transformed ($\sqrt[40]{x}$, D) EPSCs amplitude measurements. **E**, Average ± SEM of transformed EPSCs interevent intervals for three one-minute intervals per neuron. Measurements taken from neurons on the same brain slice are separated by dotted vertical lines while continuous vertical lines separate mice. Recordings taken by two different experimenters are separated by color (red and blue). Averages per neuron (dark colored), slice (light colored), and mouse (black) are indicated by horizontal lines. **F**, Average ± SEM of transformed EPSCs amplitudes for three one-minute intervals per neuron. Drawing conventions are the same as in (E). **G, H** Proportion of variance in ESPCs interevent interval (G) and amplitude (H) explained by different model components.

Analyzing distributions of electrophysiological measurements

Describing the factors that influence EPSCs is a key element of most electrophysiological studies. Such characterizations are typically accomplished through a two-step process that describes both the overall average as well as the distribution of values of the parameter being measured. Comparisons of the average response of a group of neurons is traditionally done by describing the average response of each neuron using a single parameter, typically the mean or median response, and statistically analyzing these values (**Figure 3.2A, G**). Beyond assessing the average changes in interevent interval and amplitude, electrophysiological studies often assess the whole distribution of values to identify whether experimental manipulations specifically affect a subset of frequencies and/or strengths of EPSCs. Traditionally, such an analysis is performed by visually assessing the cumulative frequency probability curves of all measurements in a specific condition (**Figure 3.2B, H**). Statistically, this visual approach is supported by a two-sample Kolmogorov-Smirnov test that assesses whether the maximal difference between two curves is larger than a statistical threshold (Massey, 1951). This statistical comparison does however ignore all points of sub-maximal divergence and does not account for between-neuron differences.

Describing the distribution of measurements separately for each neuron enables both the partitioning of variance between the hierarchical levels shaping measurement outcomes as well as the statistical assessment of the whole distribution of values. In practice, such a comparison becomes very complicated

to interpret when each of a large number of observations (>100) is compared between neurons. We propose to calculate the 5^{th}, 25^{th}, 50^{th}, 75^{th}, and 95^{th} percentile values for each neuron as a way to describe the distribution of measurements for each neuron in sufficient detail to be both meaningful and comprehensible (**Figure 3.2C, I**). These values represent the median, shoulders, and extreme values of the distribution of responses. When transformed ($\sqrt[40]{x}$), the residuals at all the five assessed percentiles have comparable values and are normally distributed (**Figure 3.2D, J**), thus enabling statistical comparisons using parametric statistics. Plotting the group averages of each of the percentiles provides a convenient way to visually represent the average distribution of measurement outcomes (**Figure 3.2E, K**). Applying this visualization approach further illustrates the substantial variability between cells in both interevent interval (**Figure 3.2F**) and amplitude of EPSCs (**Figure 3.2L**), in line with the analysis of the same data presented in **Figures 3.1E and F**.

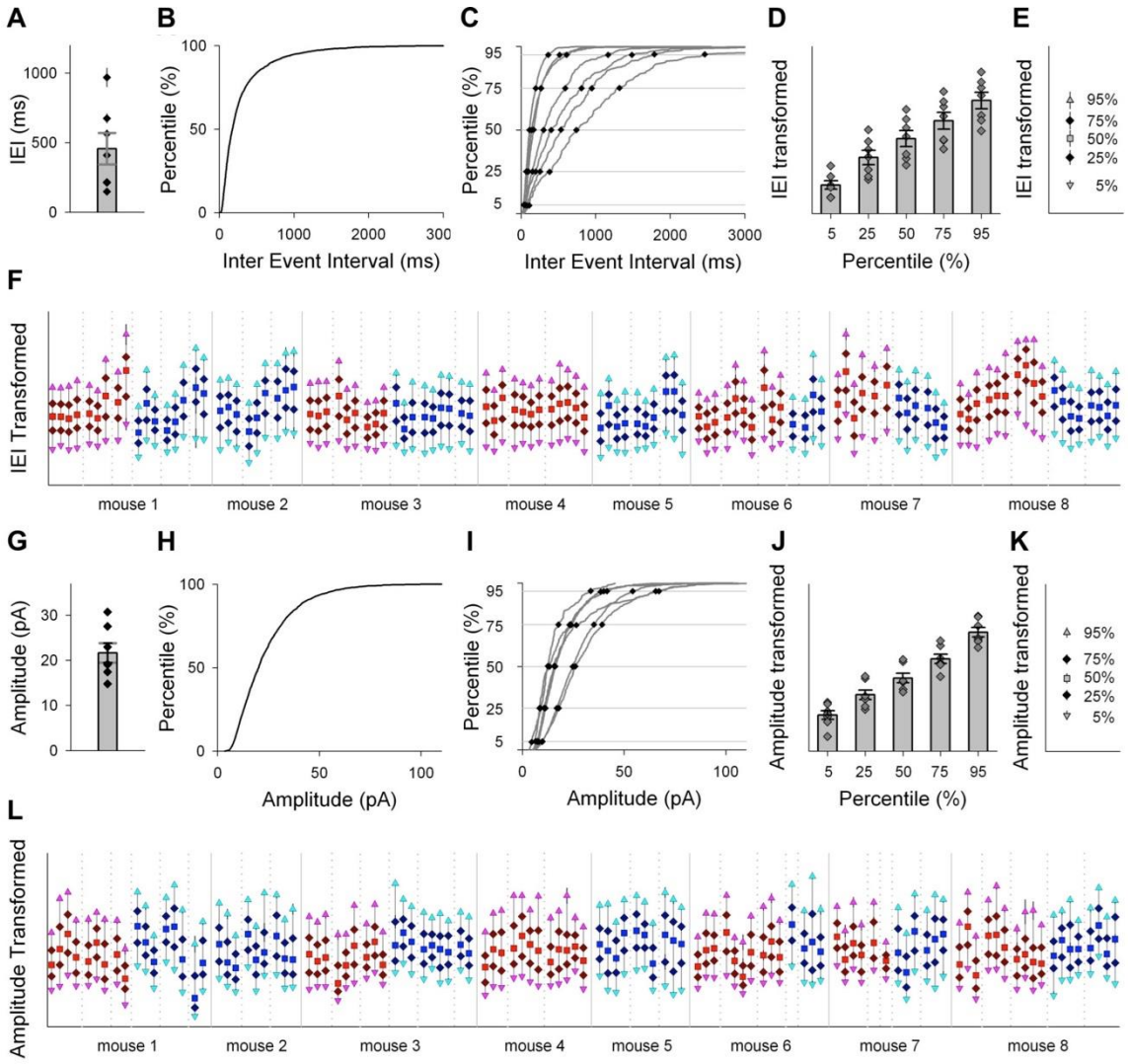

Figure 3.2 | Describing the distribution of EPSC measurements. A, G Bar graph representing the traditional method to depict average responses showing group mean ± SEM of ESPCs interevent interval (A) and amplitude (G) with individual neurons (mean ± SEM) plotted as dots. Data obtained from seven individual neurons is included (left most neuron of each mouse analyzed by experimenter Blue in Fig. 1E; same in elements B/H, C/I, D/J, and E/K). **B, H** Line graph representing the traditional method to depict the distribution of measurement values in a cumulative frequency distribution plot of the EPSCs interevent interval (B) and amplitude (H). **C, I** Cumulative frequency distribution curves of EPSCs interevent interval (C) and amplitude (I) calculated separately for each of the seven included neurons (gray lines). Black dots represent the EPSCs interevent interval (C) and amplitude (I) of individual neurons at the indicated percentiles. **D, J** Bar graphs (mean ± SEM) of transformed (40√x) EPSCs interevent interval (D) and amplitude (J) for five investigated percentiles. Dark gray dots (mean ± SEM) depict values for each of the seven neurons and correspond to black dots in C/I. **E, K** Mean ± SEM of transformed EPSCs interevent interval (E) and amplitude (K) at the indicated percentiles for seven

neurons. The five points correspond to the bars in D/J. **F, L** Distribution of transformed EPSCs interevent interval (F) and amplitude (L) measurements of all neurons as described by five selected percentiles. Points represent the mean ± SEM of the specified percentile value determined separately for the first-, second-, and third-minute recording of each neuron. Measurements taken from neurons on the same brain slice are separated by dotted vertical lines while continuous vertical lines separate animals. Recordings taken by two different experimenters are separated by color (red and blue).

All statistical analyses are based on the partitioning of variance between underlying independent variables. Statistical power can typically be increased by including biological replicates and the repeated measurements that are common in electrophysiological studies provide a convenient way to do so. As outlined above, the distribution of measurement outcomes can be described by the 5^{th}, 25^{th}, 50^{th}, 75^{th} and 95^{th} percentile values. Doing so based on the ~250 measurements that our lab typically uses to describe a neuron's characteristics provides a highly precise value describing the distribution of each individual neuron. However, from a statistical perspective, it is more powerful to subdivide this relatively large set of measurements into multiple biological replicates that, although each individually less precise, enables a more thorough partitioning of the variance in our dataset. We feel that subdivision into intervals of 25 events provides a sweet spot where the distribution of values can be meaningfully described with five percentile levels while the ten intervals allow for the estimation of within-neuron variance in these five values (**Figure 3.3**). This then allows separation of the substantial (see **Figure 3.1**) within-neuron variance from the unexplained variance, thus making statistical comparisons between neurons and especially within-neuron comparisons of experimental conditions much more powerful.

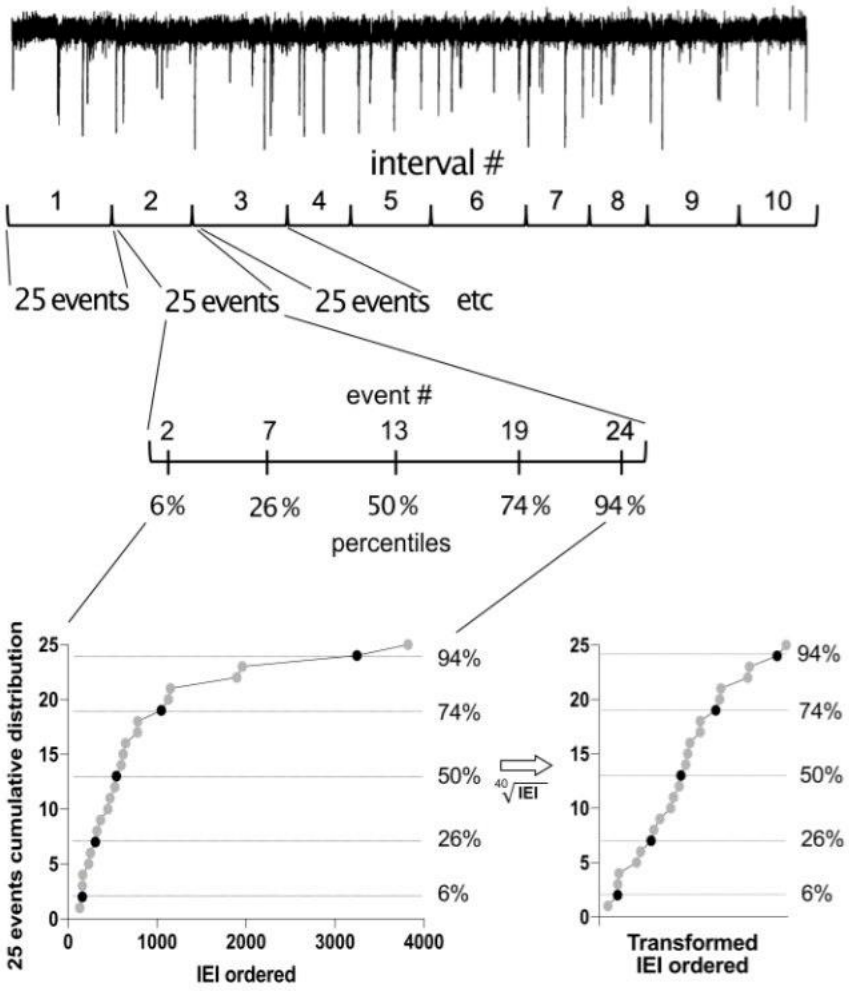

Figure 3.3 | Partitioning of EPSCs raw recording events for statistical analysis. Recording of 250 EPSC inter-event intervals is divided into 10 biological replicates of 25 events. Each replicate set of 25 values is ordered from smallest to largest and the 2nd (6th percentile), 7th (26th percentile), 13th (50th percentile), 19th (74th percentile), and 24th (94th percentile) are taken. Together these values describe the distribution of measurement values, representing the median (50%), shoulders (26 and 74%) and extremes (6 and 94%) of the distribution. Transformation of the Poisson-distributed raw values typically enables statistical analyses using parametric tests such as mixed-effects general linear models.

EPHierStats enables exposure of complex relationships in electrophysiological data

The utility of our novel statistical approach describing repeated electrophysiological measurements as a distribution of outcomes in a hierarchical statistical model was tested by re-analyzing a previously published dataset [Mao et al., 2018]. This dataset tested the involvement of the Chromatin reader L3mbtl1 in synaptic scaling that compensates for activity perturbation and maintains the excitatory and inhibitory balance. Hippocampal primary neurons were prepared from wildtype and L3mbtl1 knockout (KO) mice and synaptic scaling was induced by applying picrotoxin (PTX) or tetrodotoxin (TTX) that increased or decreased neuronal activity, respectively. Miniature EPSCs were recorded 48 hours after induction of synaptic scaling. The original analysis of this data was done by performing a series of two-sample Kolmogorov-Smirnov tests comparing pharmacological treatments with controls within both genotypes (**Figure 3.4A**). This showed that in wildtype mice, PTX and TTX treatment both altered at least some part of the distribution of mEPSC amplitudes, while in L3mbtl1-KO mice only TTX pre-exposure significantly shifted some part of the distribution of mEPSC amplitudes. Unfortunately, these statistical tests provide only very limited information about what parts of the distribution are affected, since the Kolmogorov-Smirnov test only assesses the amplitude with maximal divergence (indicated in **Figure 3.4A** by the vertical lines connecting the compared curves) and does not assess any other part of the distribution. Furthermore, the Kolmogorov-Smirnov

test does not account for the clustering of repeated measurements from the same neuron (see **Figures 3.1G, H**) and instead treats all measurements as statistically independent, thus likely overestimating the effect size and increasing the chance of making a type I error.

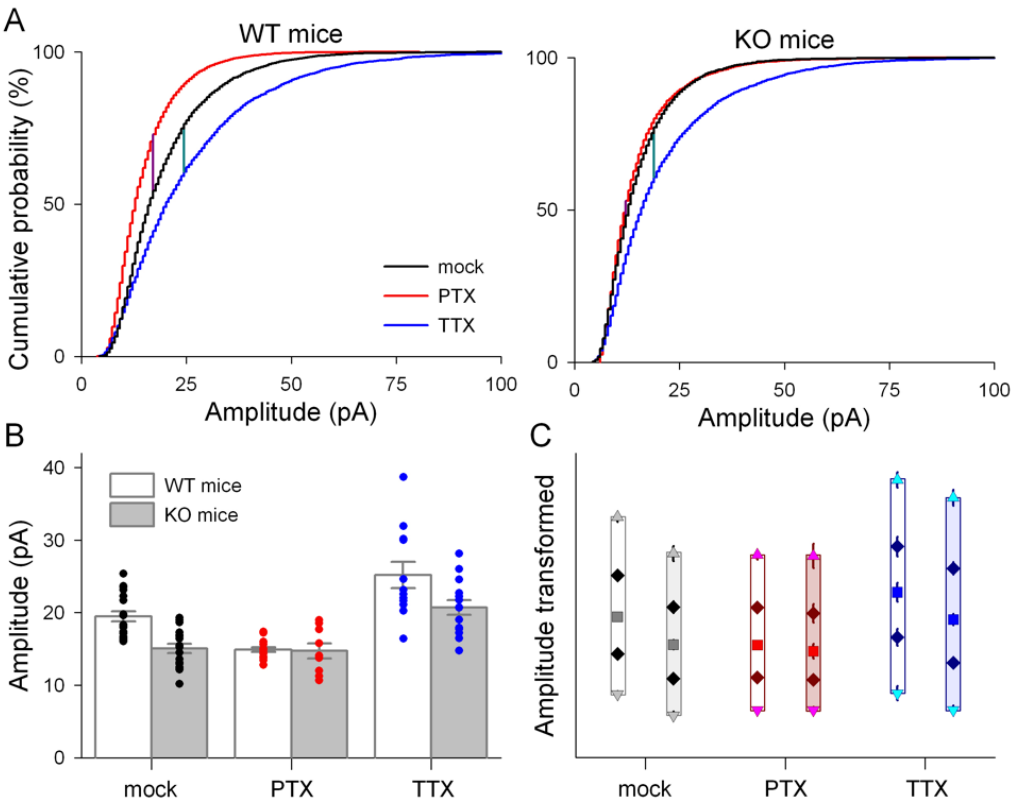

Figure 3.4 | Application of EPHierStats exposes relationships in electrophysiological dataset. A, Cumulative frequency distribution plots of mEPSC amplitude for wildtype (left) and L3mbtl1-KO mice (right) representing the traditional method for assessing differences in the distribution of measurements. Cumulative frequency distribution plots are depicted for all measurements from all neurons in each of the three treatment groups (mock, PTX, TTX). Vertical lines connecting cumulative distribution curves represent the test amplitude and the maximal percentile difference assessed by the two-sample Kolmogorov-Smirnov tests. **B**, Bar graphs representing the mean ± SEM mEPSCs amplitude for six groups defined by genotype and pre-exposure treatment. Dots represent the mean mEPSCs amplitude for individual neurons. **C**, The effects of L3mbtl1 genotype and pharmacological pre-treatment are most pronounced on mEPSCs with a larger amplitude. The 6^{th}, 26^{th}, 50^{th}, 74^{th}, and 94^{th} percentile of mEPSCs

amplitudes is depicted for each genotype and pre-treatment combination (mean ± SEM). Colors represent pharmacological pre-treatment and bar opacity indicates genotype (white: wildtype, darker: L3mbtl1-KO).

The effects of incorporating the hierarchical nature of electrophysiological measurements into the statistical assessment of the average change in mEPSC amplitude (**Figure 3.4B**) were analyzed by comparing three statistical models that became progressively more complex below. In line with the most common approach to analyze this type of dataset, model one described the response of each neuron by the mean amplitude and assumed that all neurons were statistically independent units. Based on this approach, the conclusion that the pharmacological treatment of neurons has divergent effects depending on the genotype of the mice would be justified (Genotype*Pharmacological treatment: $F_{2,81} = 3.121$, $p = 0.0495$). However, the second model showed that accounting for the relationships between neurons by adding the animal from which each neuron was derived as a random variable to the statistical model reduces both the degrees of freedom and the effect size. As a result, this model did not support the conclusion that the pharmacological treatment of neurons has divergent effects depending on the genotype of the mice (Genotype*Pharmacological treatment: $F_{2,73.4} = 2.657$, $p = 0.0769$).

The third statistical assessment of how the presence or absence of L3mbtl1 altered the mEPSC amplitude in response to PTX and TTX leveraged the repeated measures taken from each neuron and used the EPHierStats approach outlined in **Figure 3.3** to generate biological replicates describing the distribution of mEPSC

amplitudes. The hierarchical relationships between these repeated measurements were incorporated into the model by including the mouse, neuron, and interval of each assessed value. When assuming that the shape of the distribution of values was constant throughout the model (i.e. percentile was only included as a main effect), this third statistical model supports the original conclusion based on model 1: the effect of PTX on mEPSC amplitude was modulated by genotype (**Figure 3.4C**, Genotype*Pharmacological treatment: $F_{2,75.72} = 3.334$, $p = 0.0409$). Interestingly, a more complex statistical assessment demonstrated that the interaction between genotype and pharmacological manipulation was statistically different at the five assessed percentiles of the measurement distribution (Percentile*Genotype*Pharmacological treatment: $F_{8,5064} = 4.246$, $p < 0.0001$). Post-hoc comparisons of this relationship revealed that the differences between genotype and pharmacological treatment could not be detected in the smallest amplitude mEPSCs (6^{th} percentile) but become progressively more pronounced with larger mEPSC amplitudes (26^{th}, 50^{th}, 74^{th} and 94^{th} percentiles). In conclusion, our novel approach provides a way to properly account for the hierarchical nature of repeated electrophysiological measurements that increases statistical power while providing the ability to statistically compare specific parts of distributions of measurement values between conditions.

Discussion

The statistical analysis of most types of electrophysiological datasets is complicated by both the repeated nature as well as the hierarchical relationships between measurements. Traditional approaches to analyze these datasets typically rely on the implicit assumption that individual measurements are statistically independent (Aarts et al., 2014; Yu et al., 2021). Our demonstration that the interevent interval and amplitude of EPSCs is clustered around the mean of individual neurons demonstrates that this assumption is violated and illustrates the importance of using statistical models that reflect the hierarchical nature of electrophysiological datasets. Beyond the similarity of measurements taken from individual neurons, our assessment demonstrates that the slice from which recordings were made influences measurements in some cases while other factors (time interval, mouse, and experimenter) barely influenced the outcomes. Based on these findings, we propose that analyses of most electrophysiological datasets should, as a minimum, incorporate the neuron and slice level into their statistical model.

Beyond assessments of average responses, comparisons of electrophysiological changes often involve a description of the distribution of values. Traditionally, these assessments rely on the two-sample Kolmogorov-Smirnov test. Unfortunately, the two-sample Kolmogorov-Smirnov test only compares a single value per distribution and does not take the hierarchy underlying measurements into account. Our novel approach identifying multiple values that

together describe the distribution of values (i.e. the 6th, 26th, median, 74th, and 94th percentile values) enables a more structured and reliable method to assess responses in specific parts of the distribution of outcomes. The selection of these specific percentiles is somewhat arbitrary, but we feel that a set of five values provides an optimum in the trade-off between describing the distribution more fully and being able to interpret potential differences in outcome. It is of course possible to select a different set of percentile values if an experiment requires a more (or less) precise description of the distribution of outcomes.

Despite the complexities presented by datasets of hierarchically organized and repeated electrophysiological measurements, these datasets also offer the potential of high statistical power when analyzed correctly. Our new EPHierStats approach is designed to use the power of parametric mixed-effects general linear models to enable the description of complex hierarchical relationships while analyzing repeated-measurements datasets at the level of individual measurements. By not reducing large sets of measurements to a single value per neuron and by incorporating biological replicates within each neuron and experimental condition, statistical power is maximized. A further benefit of the use of mixed-effects general linear models is that it allows assessments of more complex (interacting) relationships between groups and conditions. When analyzing such relationships, the most powerful analyses will be those that compare within-neuron manipulations since measurements from the same neuron cluster together, but a host of other between-neuron comparisons can also be

assessed. Overall, the EPHierStats approach proposed here enables the description of hierarchical, repeated-measurements electrophysiological datasets in their full complexity and provides a powerful statistical tool to analyze the effects of experimental manipulations on the full distribution of measurement outcomes.

Acknowledgment

This work was supported by the National Institute on Alcohol Abuse and Alcoholism AA020501 (GM) and the National Institute of Neurological Disorders and Stroke NS085215 (KF).

Chapter IV

Binge alcohol drinking alters the differential control of cholinergic interneurons over nucleus accumbens D1 and D2 medium spiny neurons

Chapter IV: Binge alcohol drinking alters the differential control of cholinergic interneurons over nucleus accumbens D1 and D2 medium spiny neurons

Jenya Kolpakova[1,3], Vincent van der Vinne[2], Pablo Gimenez-Gomez[1], Timmy Le[1,3], Gilles E. Martin[1,3]

The work is modified from the manuscript submitted for publication in *Biological Psychiatry* (2022).

1. Brudnick Neuropsychiatric Research Institute, Department of Neurobiology, University of Massachusetts Chan Medical School, Worcester MA 01655, USA
2. Biology Department, Williams College, Williamstown MA 01247, USA
3. Graduate Program in Neuroscience, Morningside Graduate School of Biomedical Sciences, UMass Chan Medical School

Roles of authors

JK GEM designed research, JK GEM PGG carried out experiments, JK VvdV analyzed data, JK VvdV GEM wrote the paper, TL helped out with data collection

Abstract

Ventral striatal cholinergic interneurons (ChIs) play a central role in basal ganglia function by regulating associative learning, reward processing and reinforcing properties of drugs of abuse, including alcohol. In the nucleus accumbens (NAc), ChIs regulate glutamatergic, dopaminergic, and GABAergic neurotransmission. However, it is unclear how ChIs orchestrate the control of these neurotransmitters to determine the excitability of medium spiny neurons (MSNs), the NAc output neurons. Combining *ex vivo* electrophysiology, fast scan cyclic voltammetry and optogenetics demonstrates that NAc ChIs decrease the frequency of spontaneous excitatory postsynaptic currents (sEPSCs) in both D1- and D2-MSNs, though through different mechanisms. Interestingly, after two weeks of binge alcohol drinking, the effect of ChIs stimulation on glutamate release was reversed in D1-MSNs, while its effect on D2-MSNs remained unchanged. Finally, *in vivo* optogenetic stimulation of NAc ChIs significantly increased alcohol consumption. Together, these results identify ChIs as a key mediator for the regulation of NAc circuitry and as a potential future target for treatment of alcohol addiction.

Introduction

Addiction is a disorder of the reward system (Koob & Volkow, 2016) where drugs of abuse distort the response to natural reinforcers leading to continued drug use, which, in turn, impairs brain function by interfering with the capacity to exert self-control over drug-taking behaviors such as binge drinking (Koob & Volkow, 2016; Volkow & Morales, 2015; Berridge, 2007). Binge alcohol drinking is the main mode of alcohol consumption in late adolescents and young adults and often serves as a gateway to alcohol dependence later in life (Crabbe, Harris, & Koob, 2011). One of the main brain areas controlling drug taking behaviors is the nucleus accumbens (NAc), a forebrain region that encodes association between temporally unpredictable stimuli and the appropriate action to maximize reward or avoid punishment (Nicola, 2007). Medium spiny neurons expressing dopamine-1 and 2 receptors (D1- and D2-MSNs) are the sole output neurons of the NAc. D1- and D2-MSNs promote and inhibit reinforcement behavior, respectively (Kravitz et al., 2012), and optogenetic manipulation of their excitability has been causally linked to reward-seeking behaviors (Soares-Cunha et al., 2020; Ma et al., 2014). The role traditionally attributed to MSNs is that of integrators that receive a range of different inputs (glutamate, dopamine, acetylcholine, and GABA) from across the brain and determine the optimal behavioral response (Soares-Cunha et al., 2020; Humphries & Prescott, 2010; Francis, Yano, Demarest, Shen, & Bonci, 2019). In recent years, this view has been challenged by the observations that the integration of different inputs is mainly performed by a different cell population in the NAc: Cholinergic

interneurons (ChIs) (Lim et al., 2014; Abudukeyoumu, Hernandez-Flores, Garcia-Munoz, & Arbuthnott, 2019).

Cholinergic interneurons (ChIs) make up only 1-2% of all neurons in the striatum (Lim et al., 2014), but play an outsize role in regulating NAc GABAergic (Melendez-Zaidi, Lakshminarasimhah, & Surmeier, 2019), glutamatergic (Assous, 2021; Higley et al., 2011) and dopaminergic synaptic transmission (Collins et al., 2016; Threlfell et al., 2012) through their extensive projections (Lim et al., 2014). NAc ChIs generate unique bidirectional outcome responses during reward-based learning, signaling both positive (reward) and negative (reward omission) outcomes (Atallah et al., 2014). Cholinergic receptor signaling has been shown to alter alcohol and other drugs' consumption (Hendrickson et al., 2013; Rahman & Prendergast, 2012; Scofield et al., 2016). Currently, both the role played by ChIs in orchestrating dopamine (DA) and glutamatergic synaptic transmission to regulate D1- and D2-MSNs excitability, as well as how alcohol exposure modulates this connection remain to be elucidated. Here we combine *ex vivo* patch clamp, fast scan cyclic voltammetry (FSCV), optogenetics and behavioral recordings to answer these questions.

In alcohol-naïve mice, we demonstrate that optogenetic stimulation of ChIs decreases the frequency of spontaneous excitatory post-synaptic currents (sEPSCs), presumably through a presynaptic mechanism, in both D1- and D2-MSNs. However, this effect was mediated by DA only in D1-MSNs. Interestingly, binge alcohol drinking differentially altered ChIs control of glutamatergic synaptic

transmission in D1- and D2-MSNs. While the ChI-mediated decrease of sEPSCs frequency in D2-MSNs was unaffected, the ChI-induced inhibition of glutamatergic transmission in D1-MSNs seen in naïve mice was reversed and optogenetic stimulation became potentiating following alcohol exposure. Finally, optogenetic stimulation of ChIs *in vivo* significantly increased alcohol consumption in mice, while not altering locomotion or saccharin or water consumption.

Materials and Methods

Animals

All experiments were performed in male 6 – 10-week old mice on C57Bl/6J background. Drd1a-tdTomato (Stock No. 016204), ChAT.ChR2.eYFP (Stock No. 014546), and ChAT.IRES.Cre (Stock No. 006410) were purchased from Jackson Labs, were backgrossed to C57Bl/6J and bred in the UMass Chan Medical School animal facility. Drd1a-tdTomato were crossed to ChAT.ChR2.eYFP mice to generate Drd1a-tdTomato; ChAT.ChR2.eYFP mice that were selected using genotyping and used for all studies. All mice were handled according to the American Association for the Accreditation of Laboratory Animal Care guideline. The protocol was approved by the Institutional Animal Care and Use Committee of University of Massachusetts Chan Medical School. Mice were maintained at constant temperature (22 ± 1°C) and humidity with a reversed 12 h:12 h light–dark cycle. Water and food were provided *ad libitum*.

Immunostaining

Mice were euthanized using pentobarbital (120 mg/kg, i.p.) followed by transcardiac perfusion with 0.1 M sodium phosphate buffer followed by 4% paraformaldehyde (PFA) in 0.1 M sodium phosphate buffer (pH 7.4). Brains were removed, post-fixed in 4% PFA overnight and placed in 30% sucrose solution for 48 hrs. Coronal serial sections (20 µm) were sliced on a freezing microtome (Leica SM2000R, Leica Microsystems GmbH, Buffalo Grove, IL, United States) and

stored in a cryoprotective solution. Double-label immunofluorescence was performed on free-floating sections incubated overnight at 4°C with the following primary antibodies: chicken anti-GFP (1:250, ab13970, Abcam) and rabbit anti-RFP (1:250, ab185921, Abcam). Secondary antibodies used were goat anti-chicken Alexa Fluor 488 (1:500, A-11039, Thermo Fisher) and goat anti-rabbit Alexa Fluor 594 (1:500, A11007, Thermo Fisher). Sections were counter stained with 4', 6-diamidino-2-phenylindole (DAPI, 1:500, D9564, Sigma). After this incubation, sections were washed with PBS, mounted and coverslipped. Controls performed in parallel without primary antibodies showed very low levels of nonspecific staining. Image acquisition was performed with a laser-scanning confocal imaging system (Zeiss, Carl Zeiss MicroImaging, Inc., NY, United States) and image analysis was performed with the ZEN 2009 software (Zeiss, Carl Zeiss MicroImaging, Inc., NY, United States).

Ex Vivo Slice Preparation

Acute striatal brain slices were prepared according to method previously described (Kolpakova et al., 2021). Briefly, we prepared coronal slices from fresh brain tissue of 8 – 9-week old male mice. Following intracardiac perfusion with an ice-cold N-methyl-D-glucamine-based solution (see below), we rapidly removed and transferred the brain into ice-cold oxygenated (95% O_2 / 5% CO_2) cutting solution of the following composition (in mM): 92 N-methyl-D-glucamine (NMDG), 2.5 KCl, 1.25 $NaH_2PO_4.H_2O$, 30 $NaHCO_3$, 20 HEPES, 25 glucose, 2 thiourea, 5 Na^+-

ascorbate, 3 Na^+-pyruvate, 0.5 $CaCl_2.2H_2O$, 10 $MgSO_4.7H_2O$, pH 7.37. Slices were cut 200 µm thick with a Vibroslicer (VT1200, Leica MicroInstrutments; Germany). Slices were immediately transferred to an incubation chamber and left to recuperate in the NMDG-based solution for 20-30 mins at 32°C before being moved into a chamber containing oxygenated artificial cerebrospinal fluid (ACSF; in mM): 126 NaCl, 2.5 KCl, 1.25 $NaH_2PO_4.H_2O$, 1 $MgCl_2.H_2O$, 2 $CaCl_2.H_2O$, 26 $NaHCO_3$, 10 D-glucose, at room temperature. Slices were left in this chamber for at least one hour before being placed in a recording chamber and perfused with oxygenated ACSF at a constant rate of 2–3 ml/min at room temperature (~21°C).

Electrophysiology

Whole-cell patch clamp recordings of spontaneous excitatory post-synaptic currents (sEPSCs), and electrically evoked excitatory post-synaptic potentials (eEPSPs) in MSNs in the NAc core were performed in the presence of 15 µM GABA receptor antagonist bicuculine. NAc MSNs were visualized in infrared differential interference contrast videomicroscopy using a fully motorized microscope mounted with 10x and 60x objectives (Scientifica, Spain) and TdTomato-D1R MSNs were identified by fluorescence microscopy. Recordings were performed according to the method described previously (Kolpakova et al., 2021). Briefly, borosilicate glass electrodes (1.5 mm OD, 4–6 MOhm resistance) were filled with an internal solution containing (mM): 120 K-methanesulfonate; 20 KCl; 10 HEPES; 2 ATP, 1 GTP, and 12 phosphocreatine. Following seal rupture,

series resistance was assessed and fully compensated in current clamp recording mode, and periodically monitored throughout recording sessions. Recordings with changes of series resistance larger than 20% were rejected, as were MSNs with a resting membrane potential more positive than −80 mV. Voltage and current traces in whole-cell patch-clamp were acquired with an EPC10 amplifier (HEKA Elektronik, Germany). Sampling was performed at 10 kHz and digitally filtered voltage and current traces were acquired with PatchMaster 2.15 (HEKA Elektronik, Germany) at 2 kHz. All traces were subsequently analyzed off-line with FitMaster 2.15 (HEKA Elektronik, Germany). We analyzed sEPSCs amplitude and frequency with Clampfit (pClamp 11 Software suite, Molecular Devices, CA, United States). We monitored series resistance by comparing EPSPs decay time before and after induction using Clampfit event template analysis. Cholinergic Interneurons were stimulated optogenetically by flashing a train of five 1 ms-long pulses at 20 Hz every 20 seconds for 2 min at 470 nm through the light path of a microscope 60x objective using independent high-powered LEDs (pE-100 470 CooLED, NY, United States) under the control of the acquisition software PatchMaster 2.15 (HEKA, Elektronik; Germany). Spontaneous EPSCs were acquired for 4 mins before (Pre) and 4 mins after (Post) optogenetic stimulation using gap-free recording at MSN resting membrane potential. Antagonists were added to the recording bath at the final slice concentration of (in µM): 1 atropine, 5 mecamylamine, 5 SCH-23390, 1 sulpiride.

Fast Scanning Cyclic Voltammetry

Striatal slices were prepared as described for electrophysiological recordings above. Fast scanning cyclic voltammetry was performed using carbon-fibre microelectrodes, with tip length ~150 µm, constructed in house with 7 µm carbon fibre and glass electrodes (Warner Instruments, Hamden, CT, USA) and preconditioned in ASCF by applying triangular voltage ramps (−0.4 to +1.2 and back to −0.4 V at 400 V/s), delivered at 60 Hz for 1 hour. Recordings were performed at 10Hz. Electrodes were calibrated to a 1 µM DA standard prior to recording. Electrodes were positioned in NAc core and DA transients were evoked using 470 nm light stimulation of cholinergic interneurons in ChAT.ChR2.eYFP mice with pattern described above. Data were collected with a 3-electrode headstage, using an EPC10 amplifier (HEKA, Elektronik; Germany) after low-pass filter at 10 kHz and digitized at 100 kHz, using PatchMaster 2.15 (HEKA, Elektronik; Germany). Data were analyzed in Igor Pro, using the Wavemetrics FSCV plugin (gift of Veronica Alvarez, NIAAA). Peak amplitudes were measured for each individual DA transient.

Drinking in the Dark (DID) Paradigm

Alcohol (20% ethanol) was obtained from Sigma-Aldrich (Saint Louis, MO, United States). At 4 – 5-weeks old, individually housed mice were allowed to adapt to a reversed light-dark cycle (OFF at 7AM, ON at 7PM) for 2 weeks. Mice were given water bottles with sipper tubes before the experiment to allow habituation and

reduce the novelty effect in preparation for the ethanol bottle, containing a similar sipper tube, was presented. Ethanol exposure started 2 hrs into the dark phase and lasted for 2 hrs (Rhodes et al., 2005; Hendrickson et al., 2009; Kolpakova et al., 2021). At the start of the experiment, each water bottle was removed and replaced with a 25 mL serological pipette fitted with a drinking spout containing ethanol 20% (v/v). Body weights of mice and ethanol and water intake values were recorded daily. These data were used to calculate the self-administered ethanol dose (i.e., g/kg). Control mice were exposed to water at all times. This protocol was repeated 5 days a week with 2 days off (water only) after each 5-day span. On average, mice steadily increased their consumption of alcohol before reaching a maximum around 7 g/kg of 20% ethanol per drinking session at the end of a 2-week period. Electrophysiological recordings were performed 23-25 hrs after the last drinking bout.

Optogenetic Stimulation in Freely Moving Mice

4-week old male ChAT.ChR2.eYFP and ChAT.cre mice were anesthetized and implanted with an optic fiber cannula (Doric Lenses, CA, United States) located above the NAc (AP +1.5, ML ±1.5, DV −4.0 mm from Bregma). Optic fiber placements were verified at the end of experiments. Mice were allowed to recover for 2-3 weeks in the reversed light-dark cycle (OFF at 7AM, ON at 7PM). Mice were handled every day for 2 weeks prior to initiation of the experiment. 24 hours prior to the first alcohol exposure mice were connected to the fiber optic cable for

habituation purposes, however, during successive stimulation days mice were connected only for an hour prior to beginning of the stimulation each day. Mice received the same pattern of optogenetic stimulation as during the electrophysiologic recordings: a burst of five 2-ms long 470 nm light pulses at 20 Hz every 20 seconds. Initial stimulations started 2 mins prior to first alcohol exposure and then continued for the duration of alcohol drinking session of 1 hour. We limited alcohol consumption concurrent with stimulation to 1 hour, as the first hour of alcohol exposure contained the majority of alcohol consumption (Kolpakova et al., 2021). Mice were stimulated every day for 4 consecutive days. The comparison was made between the optogenetically stimulated ChAT.ChR2.eYFP mice, non-stimulated ChAT.ChR2.eYFP mice and optogenetically stimulated ChAT.cre mice. For water and saccharin control experiment, 0.3% saccharin (Fisher Scientific) solution was made and consumption measured during the same optogenetic stimulation protocol. To quantify the drinking bouts we measured the number and timing of alcohol, saccharin and water licks using a closed-circuit loop connected to a drinkometer (Lafayette Instruments, Lafayette, IN, USA). Timing of licks was measured as counts of licks per second.

Locomotor activity

Mice were handled every day for 2 weeks prior to initiation of the experiment. Locomotor activity was measured in ChAT.cre and ChAT.ChR2.eYFP mice using

a cage-rack photobeam system (PAS, San Diego Instruments) and the corresponding PAS software (PAS, San Diego Instruments). Mice were placed in a novel cage within the locomotor apparatus, and ambulation (locomotion) was measured as the breaking of two distinct beams 10 cm apart. Locomotor activity was recorded for 40 mins following 15 minutes of habituation.

Analysis

Results are reported as mean ± SEM. Specific statistical tests used are detailed within figure legends and main text. Electrophysiological and behavioral data were analyzed using either Student's paired t test, one-way ANOVAs (GraphPad Prism 7.0) or with mixed model general linear model (MM-GLM; SAS JMP 7.0) to assess the distribution of outcomes and account for random effect variables: experimenter, animal ID, cell ID; and fixed effect variables: percentile distribution, optogenetic treatment, antagonist treatment or alcohol treatment depending on the experiment (Kolpakova et al., 2022). In addition to this novel statistical approach, cumulative frequency distribution plots were also analyzed using the traditionally used two-sample Kolmogorov-Smirnov (K-S) test. The drinking behavior of freely moving mice was quantified by summing the number of drinking spout licks or g/kg quantity consumed per 1-hour drinking period of 20% alcohol, water or 0.3% saccharin. Statistical comparisons assessed the total number of licks over the drinking period for 4 days of stimulation. The criterion for statistical significance was $p < 0.05$ for all experiments.

Results

We first asked whether cholinergic transmission differentially impacted glutamatergic onto D1- *vs.* D2-MSNs. To do this we crossed ChAT.ChR2.eYFP and DrD1.TdTomato mice to allow for 1) ChR2 expression in ChIs for optogenetic ChI activation and 2) differentiation between D1- and D2-MSNs. Immunostaining showed the presence of eYFP and TdTomato reporters for ChIs and D1-MSNs, respectively, in the NAc (**Figure 4.1A**). eYFP-positive neurons were confirmed to be ChIs by injecting incremental current steps and recording voltage responses: current-voltage relationships presented the hallmarks of cholinergic interneurons, i.e., depolarized resting membrane potential (~-50 mV), large membrane resistance and sag, and spontaneous firing (**Figure 4.1B**). To verify that ChIs expressed functional ChR2 (**Figure 4.1C**), ChIs were stimulated with blue light (five light pulses at 20 Hz every 20 seconds for 2 minutes). This pattern faithfully evoked action potentials in all (n = 8) neurons tested (**Figure 4.1D**)

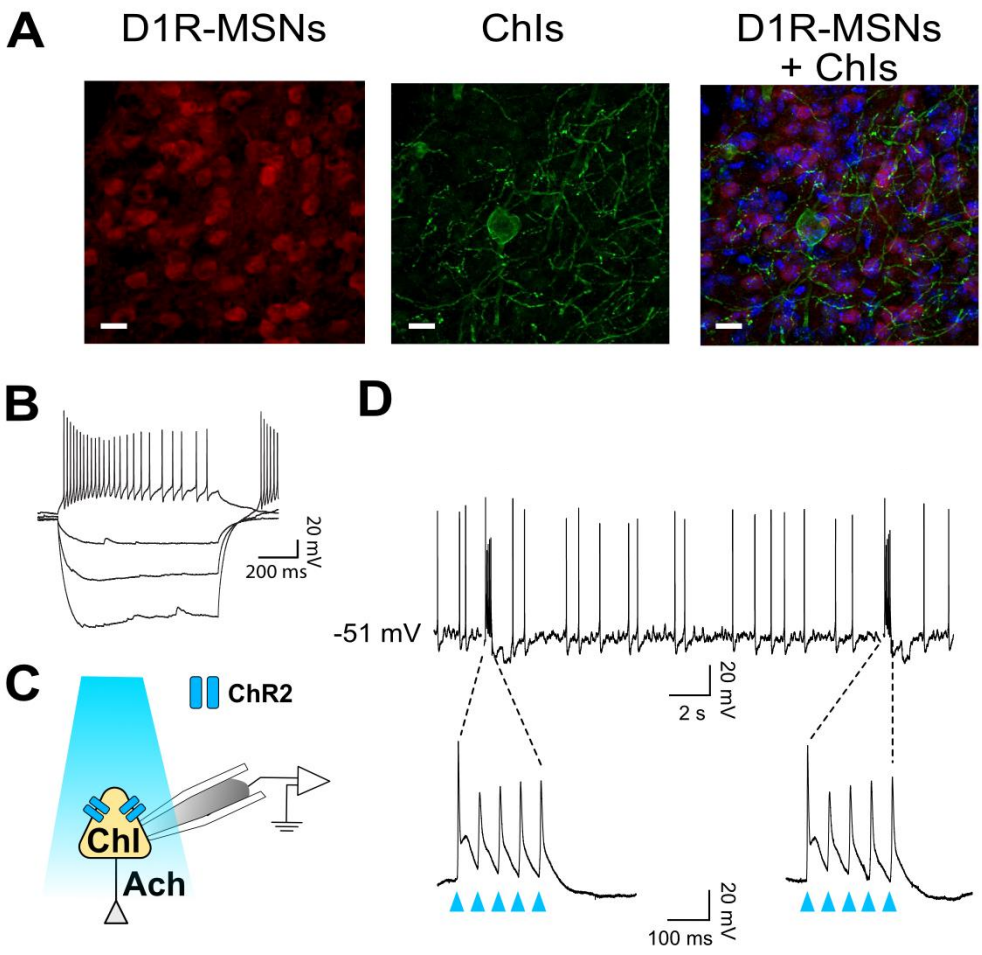

Figure 4.1 | ChAT-ChR2-eYFP x DrD1-tdTomato mouse line to optogenetically stimulate ChIs and differentiate core NAc D1- and D2-MSNs. A, Immunostaining in ChAT-ChR2-eYFP x DrD1-tdTomato mouse line of D1-MSNs (left panel, red-fluorescence) and cholinergic interneurons (middle panel, eYFP fluorescence) in the nucleus accumbens. Right panel shows overlaid left and middle panels. Scale bar 20 um. **B,** Representative voltage traces in response to incremental current steps (-150 pA to 0 in steps of 50) in a cholinergic interneuron. **C,** Schematic of ChI recording during optogenetic stimulation with blue light. **D,** Optogenetic stimulation (i.e., burst of five 20 Hz pulses every 20 seconds for 2 minutes) evokes action potentials in ChI.

Cholinergic interneurons decrease glutamate release in D1- and D2-MSNs.

To determine whether ChIs controlled spontaneous glutamate release onto D1-MSNs, sEPSCs were recorded in TdTomato-labeled neurons while ChIs were

simultaneously stimulated (**Figure 4.2A**) with a pattern described in **Figure 4.1**. Current-voltage relationships confirmed that all recorded red epifluorescent neurons (**Figure 4.2Biii**) were MSNs (**Figure 4.2Bi,ii**). Often, the cell body of ChIs could be detected in the vicinity of recorded MSNs (**Figure 4.2Biv**). sEPSCs were recorded at MSNs' resting membrane potential (-85 $\pm$ 0.7 mV in a random sample of 10 neurons) for 4 minutes (Pre-stim; **Figure 4.2Ci**) before stimulating ChIs for 2 minutes (**Figure 4.2Ci**, blue arrowheads), followed by recording sEPSCs for 4 minutes (Post-stim; **Figure 4.2Ci**). The inter-event intervals (IEIs) between sEPSCs lengthened during the Post-stim versus the Pre-stim interval (i.e., a decreased frequency; **Figure 4.2C**, $t(13) = 2.868$, $p = 0.0132$, paired t-test, $n = 14$). Interestingly, ChI stimulation did not affect the amplitude of D1-MSN sEPSCs in ChAT-ChR2 mice (**Figure 4.3A**, $t(13) = 2.04$, $p = 0.0619$, paired t-test, $n = 14$). To verify that these effects are specifically due to optogenetic ChI stimulation, D1-MSN sEPSCs were recorded in slices obtained from the DrD1.Tdtomato mouse line (**Figure 4.2Di**). These recordings demonstrating that optical stimulation did not significantly affect IEIs (**Figure 4.2Dii**, $t(9) = 0.2512$, $p = 0.8073$, paired t-test, $n = 10$) or amplitude (**Figure 4.3B**, $t(9) = 1.571$, $p = 0.1506$, paired t-test, $n = 10$).

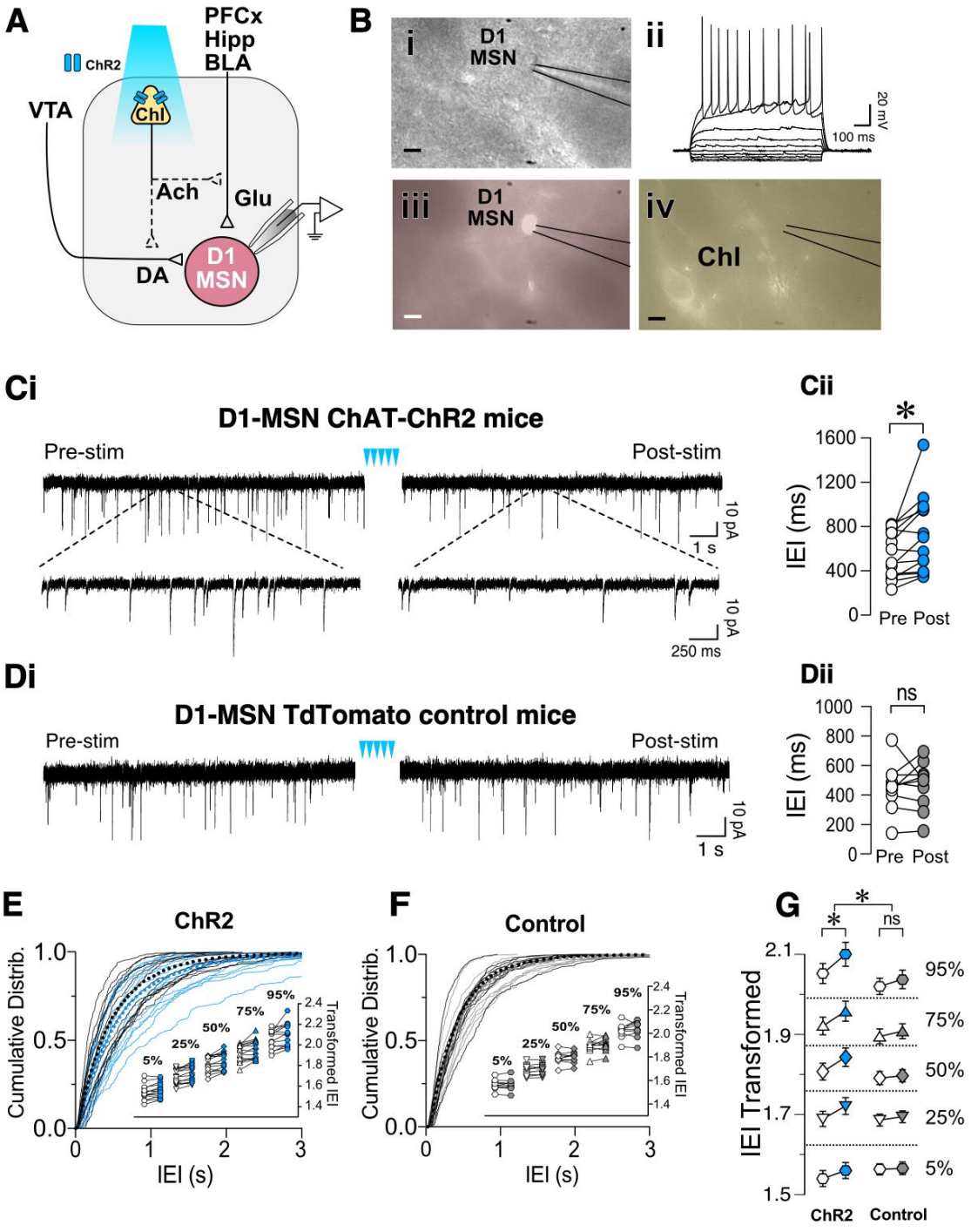

Figure 4.2 | Optogenetic stimulation of ChIs decreases sEPSCs frequency in D1-MSNs. A, Schematic of the experimental setup: whole cell recording of D1-MSNs sEPSC during optogenetic stimulation of ChIs. B. Same slice images of representative MSNs (**i**, DIC), corresponding IV traces to confirm MSN identity (**ii**), red-epifluorescence to verify

the cell is D1R+ (**iii**), and eYFP epifluorescence of ChI cell in proximity of the recording (**iv)**. Scale bar 10 um. **Ci**, Representative sEPSCs in D1-MSNs in ChAT-ChR2 mice before (Pre) and after (Post) ChI optogenetic stimulation (blue arrowheads). **Cii**, Average sEPSCs inter-event intervals (IEI) in Pre (white circles) and Post (blue circles) ChI optogenetic stimulation in ChAT-ChR2 D1-MSNs (n = 14). **Di**, Representative traces of sEPSCs in D1-MSNs of TdTomato control mice before (Pre) and after (Post) ChI stimulation. **Dii,** Average EPSCs inter-event intervals (IEI) in Pre (white circles) and Post (gray circles) ChI optogenetic stimulation in control TdTomato D1-MSNs (n = 10). **E**, Cumulative frequency distribution of D1-MSN sEPSCs IEI in ChAT-ChR2 mice group Pre (black traces) and Post (blue traces) ChI optogenetic stimulation. Each solid line represents a neuron. Average traces for Pre and Post conditions are shown in dotted black and blues lines, respectively. Inset. Cumulative distributions of ChAT-ChR2 D1-MSNs EPSCs IEIs broken into percentiles of distribution to quantify median (50%), shoulders (25 and 75%), and extreme values (5 and 95%) of distribution, that are $^{10}\sqrt{x}$ transformed to normalize the distribution. **F**, Cumulative frequency distribution of D1-MSNs inter-event intervals (IEI) of sEPSCs before (Pre, black lines) and after (Post, gray lines) ChI optogenetic stimulation in tdTomato control mice. Each solid line represents a neuron. Average traces are shown in dotted black and blues lines for Pre and Post conditions, respectively. Inset. Same as inset in E, but in TdTomato D1-MSN controls. **G**, Percentiles of cumulative distribution of transformed IEIs of EPSCs in ChAT-ChR2 D1-MSNs (Pre, white circles, Post, blue circles) and control TdTomato D1-MSNs (Pre, white circles, Post, gray circles). *p < 0.05, ns: no significant difference

Comparisons of IEI cumulative frequency distributions revealed a significant difference between Pre- and Post-ChI stimulation conditions in D1-MSNs ChAT.ChR2 mice (**Figure 4.2E,** D = 0.07492, p <0.0001, K-S test) but not in D1-MSN TdTomato control mice (**Figure 4.2F,** D = 0.03261, p = 0.0603, K-S test). Next, the relationship between sEPSCs' IEI size and the ChI-mediated effect was assessed. To address this relationship, sets of 25 consecutive IEIs were ordered by IEI and the 50 (median), 25 and 75 (shoulders), as well as the 5 and 95 (extremes) percentile values were analyzed (Kolpakova et al., 2022). No effect of different IEI size distribution on ChI-mediated IEI increase was observed (**Figure 4.2E** inset, F(4, 907) = 0.3362, p = 0.85, Mixed-model general linear modeling (MM GLM)), indicating that EPSCs are uniformly altered by ChIs. Finally, a significant

difference in response to ChI stimulation was observed between ChR2 and TdTomato groups (**Figure 4.2G**; $F(1,2265) = 25.58$, $p < 0.0001$, MM GLM, with Tukey Post-hoc tests revealing significant increases in IEI size between Pre- and Post-stimulation in ChR2 but not in TdTomato controls). Interestingly, ChI stimulation had no effect on electrically evoked EPSPs in D1-MSNs (**Figure 4.3C**, $F(2,10) = 0.973$, $p = 0.3785$, RM one-way ANOVA) and TdTomato control mice (**Figure 4.3D**, $F(2,6) = 1.7$, $p = 0.238$, RM one-way ANOVA). These results indicate that optogenetic stimulation of ChIs decreases only spontaneous glutamate release onto D1-MSNs, a likely presynaptic effect.

To further compare whether ChI might exert an effect during, as well as post-stimulation in a time-dependent manner, we analyzed the timeline of the effect of ChI stimulation on electrically evoked EPSPs (eEPSPs) in D1-MSN. As shown in **Figure 4.3**, ChI optogenetic stimulation did not have an effect on eEPSPs at any time point during or after the stimulation in ChAT-ChR2 (**Figure 4.3E**, $F(2,26.8) = 2.65$, $p = 0.090$, MM GLM) or TdTomato control D1-MSNs (**Figure 4.3F**, $F(2,21.9) = 1.73$, $p = 0.2$, MM GLM)

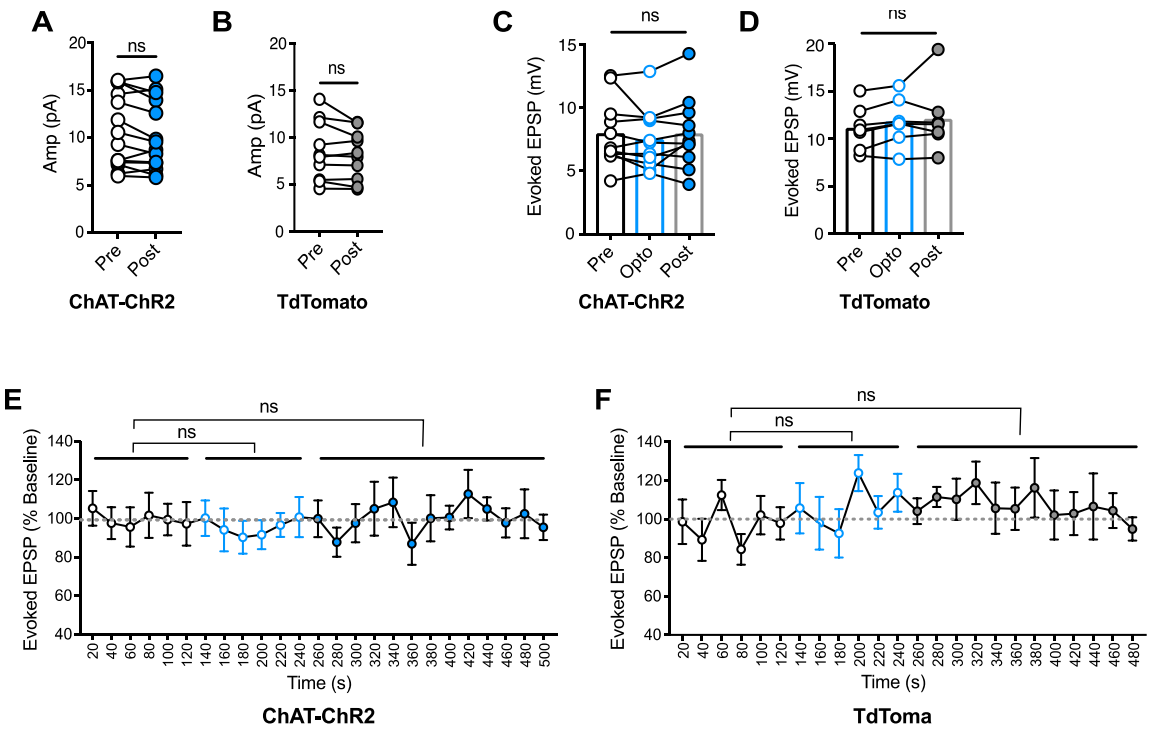

Figure 4.3 | D1-MSNs sEPSC and evoked EPSP measurements during and after ChI optogenetic stimulation. A. Average sEPSCs amplitudes before (Pre, white circles) and after (Post, blue circles) ChI optogenetic stimulation in D1-MSNs ChAT.ChR2 mice (n = 14). **B**. Average sEPSCs amplitudes before (Pre, white circles) and after (Post, gray circles) light stimulation of ChIs in D1-MSNs TdTomato mice. (n = 10). **C**. Electrically-evoked EPSPs in ChAT-ChR2 D1-MSNs before (Pre, white circles), during (white circles, blue bar) and after (Post, blue circles) ChI optogenetic stimulation (n = 10). **D**. Electrically-evoked EPSPs in TdTomato control D1-MSNs before (Pre, white circles), during (white circles, blue bar) and after (Post, gray circles) ChI optogenetic stimulation (n = 7). *p<0.05, ns: no significant difference. **E, F**. Timeline of electrically evoked EPSPs before, during (blue), and after ChI optogenetic stimulation over 8 minutes. EPSPs were invoked every 15 seconds, and calculated as % Baseline change taken for 5 minutes prior to ChI stimulation. Baseline, before ChI optogenetic stimulation (Pre, black circles), during ChI optogenetic stimulation (Opto, blue circles), and after ChI optogenetic stimulation (Post, blue-filled black circles). ns>0.05

To determine whether ChIs similarly regulated glutamatergic synaptic transmission in putative D2-MSNs, non-fluorescent MSNs were recorded while stimulating ChIs optogenetically (**Figures 4.4A and B**). Current-voltage relationships confirmed that all recorded neurons were MSNs (**Figure 4.4Bii**). As

with D1-MSNs, putative D2-MSNs' baseline sEPSCs was recorded for 4 minutes before (Pre) and after (Post) optogenetic ChIs stimulation. Similar to D1-MSNs, blue light stimulation significantly increased average IEIs (i.e., decrease frequency; **Figure 4.4C**, $t(11) = 2.27$, $p = 0.0443$, paired t-test, $n = 12$) in sliced obtained from ChAT-ChR2 mice but not in TdTomato control slices (**Figure 4.4D**, $t(8) = 0.604$, $p = 0.563$, paired t-test, $n = 9$). Likewise, significant increase of IEI sEPSCs cumulative frequency distribution in Pre vs Post groups in D2-MSNs of ChAT-ChR2 mice was observed (**Figure 4.4E,** $D = 0.048$, $p = 0.0011$, K-S test, $n = 12$), but not in D2-MSNs of TdTomato control mice (**Figure 4.4F**, $D = 0.0175$, $p = 0.7278$, K-S test, $n = 9$). As with D1-MSNs, significant increases of IEI were observed at all percentiles in D2-MSNs of ChAT-ChR2 (**Figure 4.4E** inset), but not TdTomato control mice (**Figure 4.4F**, inset). Finally, a significant difference in response to ChI stimulation between ChR2 and TdTomato control groups was observed (**Figure 4.4G**; $F(1,1915) = 18.05$, $p<0.0001$, MM GLM, with Tukey post-hoc tests showing significant increase in IEI duration between Pre- and Post-intervals in ChR2 but not in TdTomato controls).

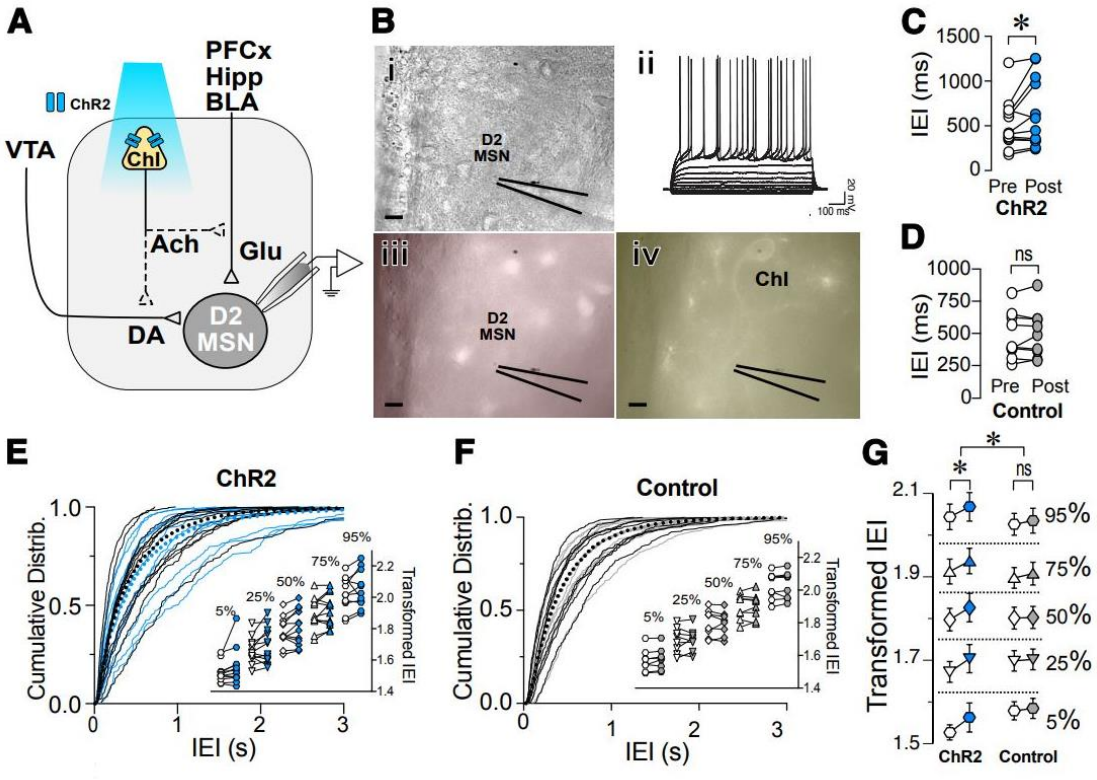

Figure 4.4 | Optogenetic stimulation of ChIs decreases sEPSCs frequency in D2-MSNs. A. Schematic of the experimental setup: whole cell sEPSC recording of D2-MSNs during optogenetic stimulation of ChIs. **B**. Same slice images of representative MSNs (**i,** DIC), corresponding IV traces to confirm MSN identity (**ii**), lack of red-epifluorescence to verify the cell is D1R(-) (**iii**), and eYFP epifluorescence of ChI cell in the proximity of the recording (**iv**). Scale bar 10 um. **C**. Average sEPSCs IEI before (Pre, white circles) and after (Post, blue circles) optogenetic stimulation of ChIs in ChAT-ChR2 D2-MSNs (n = 12). **D**. Average sEPSCs IEI before (Pre, white circles) and after (Post, gray circles) optogenetic stimulation of ChIs in tdTomato control mice (n = 9). **E**. Cumulative frequency distribution of D2-MSN IEI of sEPSCs in ChAT-ChR2 mice before (Pre, black traces) and after (Post, blue traces) ChI optogenetic stimulation. Each solid line represents a neuron. Average traces are shown in dotted black and blues lines for Pre and Post conditions, respectively. Inset. Cumulative distributions of ChAT-ChR2 D2-MSNs EPSCs IEIs broken into percentiles of distribution to quantify median (50%), shoulders (25 and 75%), and extreme values (5 and 94%) of distribution, that are $^{10}\sqrt{x}$ transformed to normalize the distribution. **F**. Cumulative frequency distribution of D2-MSN IEI of sEPSCs in tdTomato mice before (Pre, black traces) and after (Post, blue traces) ChI optogenetic stimulation. Each solid line represents a neuron. Average traces are shown in dotted black and blues lines for Pre and Post conditions, respectively. Inset. Same as inset in E, but in TdTomato D2-MSN controls. **G**. Percentiles of cumulative distribution of transformed IEIs of EPSCs in ChAT-ChR2 D2-MSNs (Pre, white circles, Post, blue circles) and control TdTomato D2-MSNs (Pre, white circles, Post, gray circles). *p < 0.05, ns: no significant difference

No effect of ChI stimulation on D2-MSNs sEPSC amplitude was observed in ChR2 (**Figure 4.5A**, t(11) = 0.129, p = 0.8995, paired t-test), or TdTomato control group (**Figure 4.5B**, t(8) = 0.277, p = 0.789, paired t-test). Interestingly, electrically evoked EPSPs in D2-MSNs following ChI optogenetic stimulation had a significantly decreased amplitude in ChR2 groups both during the stimulation (Opto) and after (Post), compared to baseline (Pre) groups (**Figure 4.5C**, F(2,8) = 6.01, p = 0.0145, One-way ANOVA), but not in TdTomato control groups (**Figure 4.5D**, F(2,6) = 0.20, p = 0.742, One-way ANOVA).

Similarly to D1-MSNs, we also measured the timeline of ChI effect to determine whether the ChI-induced suppression of eEPSPs is time-dependent in D2-MSNs. As was already determined by average eEPSPs, during optogenetic treatment (Opto) and post-optogenetic treatment (Post) eEPSPs were significantly decreased compared to baseline (Pre) groups (**Figure 4.5E**, F(2,22.6) = 4.937, p = 0.017, MM GLM), with no differences in Td-Tomato D2-MSNs (**Figure 4.5F**, F(2,21.7) = 0.007, p = 0.99 MM GLM).

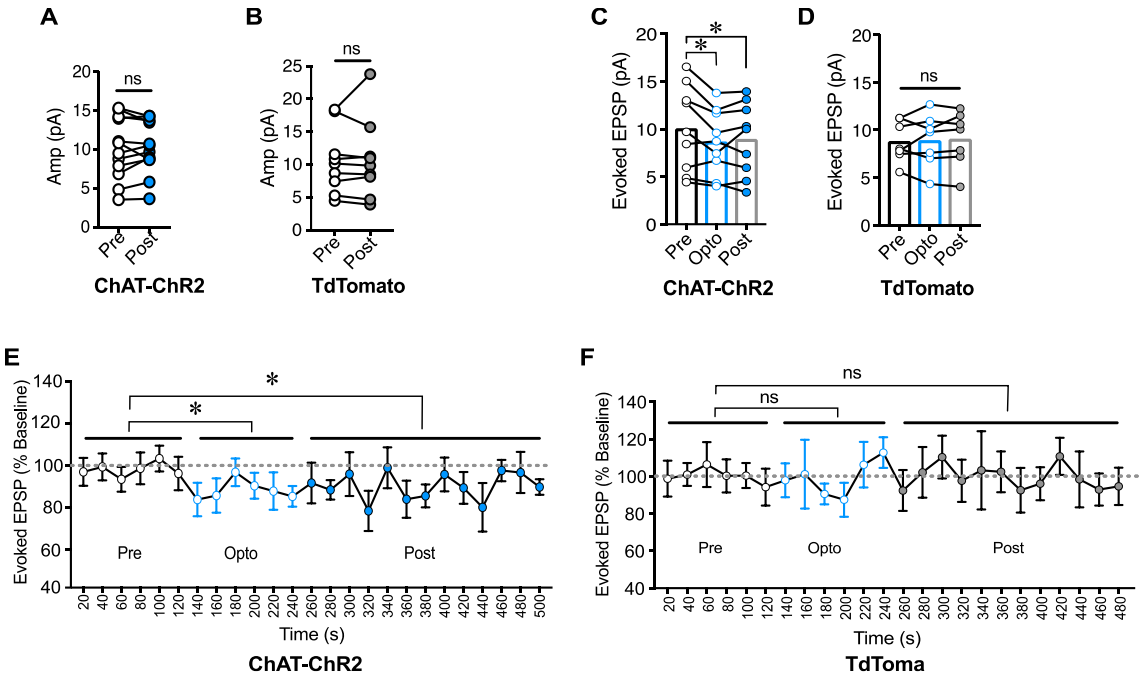

Figure 4.5 | D2-MSNs sEPSC and evoked EPSP measurements after ChI optogenetic stimulation. A. Average sEPSCs amplitudes **before (**Pre, white circles) and after (Post, blue circles) ChI optogenetic stimulation in D2-MSNs of ChAT.ChR2 mice (n = 11). **B.** Average sEPSCs amplitudes before **(**Pre, white circles) and after (Post, gray circles) light stimulation in D2-MSNs of TdTomato mice. (n = 9). **C.** Electrically-evoked EPSPs in ChAT-ChR2 D2-MSNs before (Pre, black circles), during (Opto, white circles, blue bar) and after (Post, blue circles) ChI optogenetic stimulation (n = 9). **D.** Same as C in TdTomato mice (n = 7). **E-F**. Timeline of electrically evoked D2-MSNs EPSPs before ChI optogenetic stimulation (Pre, black circles), during ChI optogenetic stimulation (Opto, blue circles), and after ChI optogenetic stimulation (Post, blue-filled black circles) in ChAT-ChR2 and TdTomato. *p<0.05, ns: no significant difference

Control of glutamate release by ChIs in D1- and D2-MSNs involves different mechanisms

Having shown that ChIs decrease the release of glutamate from presynaptic terminals synapsing on both D1- and D2-MSNs, we questioned whether these two neuronal populations shared the same mechanisms. There is strong evidence that ChIs induce DA release in the striatum (Threlfell et al., 2012; Cachope et al., 2012). Because DA regulates glutamate release (Wang et al., 2013), we tested the

hypothesis that ChIs' effects on glutamate release involved DA by examining ChAT.ChR2.eYFP x DrD1-TdTomato mice. First, we confirmed that optogenetic stimulation of ChIs indeed evoked DA release (**Figure 4.6Ai,ii**) measured with fast-scan cycling voltammetry (FSCV) when using the same stimulation pattern as used in our electrophysiological experiments. We then tested the putative role of DA in mediating ChIs-induced inhibition of glutamate release in D1-MSNs. ChI stimulation resulted in significantly longer IEIs in of D1-MSNs (**Figure 4.6B** ACSF group as already presented in **Figure 4.6G**). In the presence of dopamine D1- and D2-receptor antagonists IEIs were no longer lengthened by optogenetic ChI stimulation (**Figure 4.6B**, ACSF vs sulpiride+SCH-23390, $F(1,2514) = 32.12$, $p<0.0001$, MM GLM), with Tukey post-hoc tests revealing significant differences between Pre and Post conditions in ACSF condition, while the Pre- and Post-stimulation groups with dopamine antagonists were not significantly different. These findings show that the effect of ChI activity is DA-dependent in D1-MSNs with DA released by ChI stimulation likely acting on DA receptors expressed on glutamatergic terminals (Dumartin, Doudnikoff, Gonon, & Bloch, 2007; Wang et al., 2012b). Next, the dependency of the DA effect on nAChR activation was confirmed (**Figure 4.6B**, ACSF vs mecamylamine, $F(1,2562) = 28.25$, $p<0.0001$, MM GLM, with Tukey post-hoc tests showing no differences between Pre and Post conditions when nAChRs were blocked). Antagonizing mAChR signaling also prevented the ChI-activation mediated increase in IEI (**Figure 4.6B**, ACSF vs atropine, $F(1,2269) = 56.81$, $p<0.0001$, MM GLM, with Tukey post-hoc tests showing no differences

between atropine Pre and Post conditions). In line with the preceding outcomes, antagonists of both mAChR and nAChR also blocked the increase of IEIs (**Figure 4.6B**, ACSF vs atropine+mecamylamine, $F(1,2521) = 28.15$, $p < 0.0001$, MM GLM, with Tukey post-hoc tests showing no differences between atropine+mecamylamine Pre and Post conditions). Finally, bath application of antagonists did not significantly change glutamate release under baseline conditions in D1-MSNs (**Figure 4.7A** D1-MSNs, $F(4,60) = 1.472$, $p = 0.22$, one-way ANOVA). Together, these results indicate that mAChR, nAChR and DA receptor signaling are all required to mediate the effects of ChIs on glutamate transmission in D1-MSNs.

Next, the mechanisms underlying ChIs-mediated inhibition of glutamate release were assessed in D2-MSNs. Surprisingly, in D2-MSNs the effect of ChI stimulation on IEI length was not significantly different between the ACSF and DA receptor antagonists groups (**Figure 4.6C**, ACSF vs sulpiride+SCH-23390, $F(1,1821) = 0.2625$, $p = 0.6085$, MM GLM), with ChI stimulation significantly lengthening IEI in both groups ($p < 0.05$). This suggested that ChIs exert a direct presynaptic control over glutamate release in D2-MSNs that does not require DA. Interestingly, blocking nAChR signaling in D2-MSNs prevented the ChI stimulation induced lengthening of IEI (**Figure 4.6C** ACSF vs mecamylamine, $F(1,1804) = 25.34$, $p<0.0001$, MM GLM, with Tukey post-hoc tests showing no difference in mecamylamine Pre and Post groups). Recordings in the presence of the mAChR blocker atropine were also significantly different from ACSF control (**Figure 4.6C**

ACSF vs atropine, F(1,1753) = 3.537, p = 0.0402, MM GLM, with Tukey post-hoc tests revealing no difference in the atropine Pre and Post groups). Accordingly, simultaneous application of both nAChR and mAChR antagonists found similar blockage of the ChI effect on IEI (**Figure 4.6C**, ACSF vs atropine+mecamylamine, F(1, 1760) = 55.05, p<0.0001, MM GLM, with Tukey post-hoc tests showing no difference in atropine+mecamylamine Pre vs Post groups). These findings indicate that, unlike in D1-MSNs, ChI-mediated decrease in glutamate release in D2-MSNs is DA-independent but still mediated by both mAChR and nAChR antagonists.

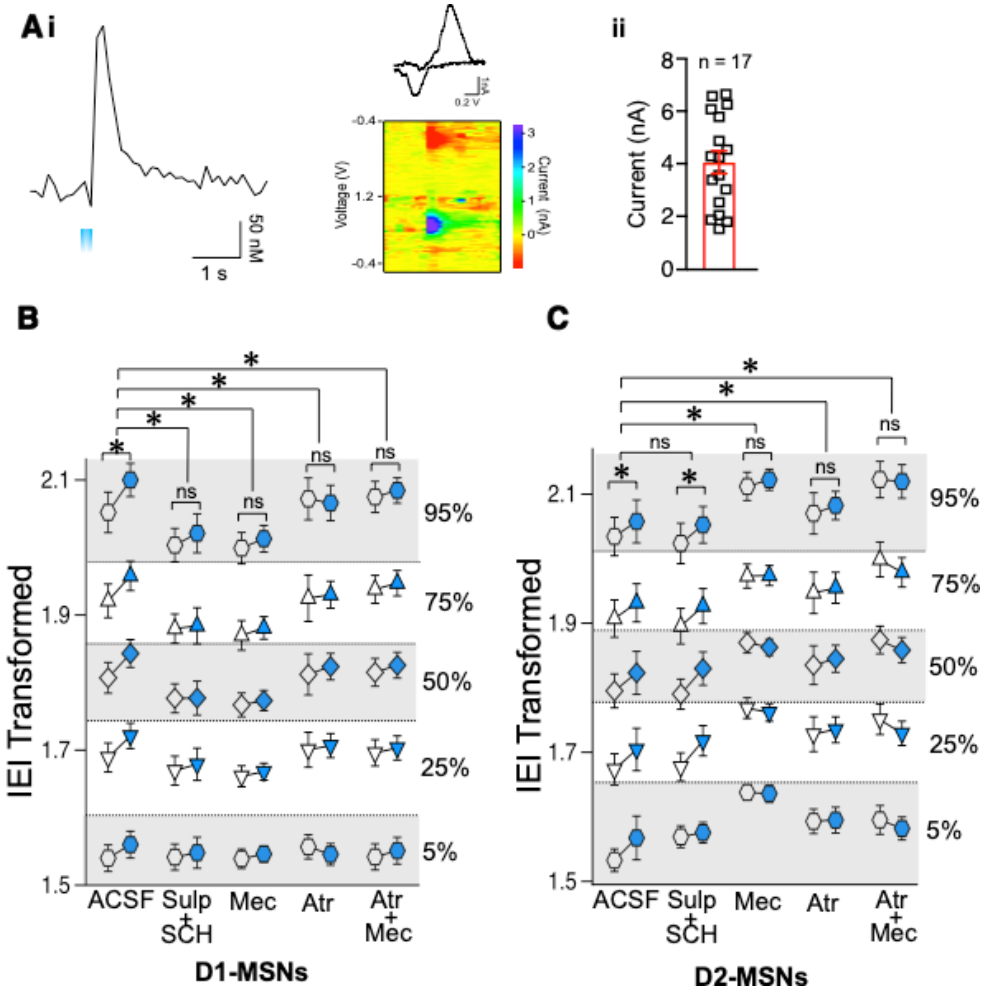

Figure 4.6 | Effects of ChIs on D1- and D2-MSNs glutamate release are mediated through different pathways. A. Optogenetic activation of ChIs evokes dopamine release in NAc as measured by voltammetry. **i**. Representative DA trace and cyclic voltammogram showing characteristic DA waveform. **ii.** DA responses evoked from ChI stimulation scatter plot and average ± SEM showing the range of DA currents from 6 slices and 17 recordings. **B**. Transformed IEI of D1-MSNs sEPSCs shown as percentiles of cumulative distribution. Data for the control group (ACSF) is reproduced from Figure 4.2. IEI is shown before (Pre, white circles) and after (Post, blue circles) ChIs stimulation in control conditions (ACSF) and in presence of antagonists: Sul+SCH (5 uM SCH-23390, D1 receptor antagonist + 1 uM sulpiride, D2 receptor antagonist), Atr (1 uM atropine, mAChR antagonist), Mec (5 uM mecamylamine, nAChR antagonist) and Atr+Mec (atropine + mecamylamine). **C.** Same as B in D2-MSNs. *p < 0.05, ns: no significant difference

In contrast to D1-MSNs, in D2-MSNs, bath application of nicotinic receptors antagonist mecamylamine (without optogenetic stimulation) significantly increased sEPSCs IEIs (**Figure 4.7A**, D2-MSNs mecamylamine, Mann-Whitney U = 21, p = 0.0387, Mann-Whitney test), with no effect of muscarinic or DA receptors antagonists bath application (**Figure 4.7**, D2-MSNs, atropine: p = 0.29, atropine+mecamylamine: p = 0.11, sulpiride+SCH-23390: p = 0.20). This finding provides a possible explanation for the observation that blocking nicotinic receptor with mecamylamine in D2-MSNs increased IEI: bath application of mecamylamine significantly decreased glutamate release, thus reaching a “floor effect” that could not be further decreased by ChIs stimulation (**Figure 4.6C**), indicating high nicotinic receptor sensitivity to the baseline tonic ACh release.

To determine whether the antagonists had similar effects in evoked EPSPs as compared to spontaneous, we recorded eEPSPs in the presence of the cholinergic and dopaminergic antagonists. We found no significant effect of any antagonists during or after ChI stimulation on evoked EPSPs in D1-MSNs (**Figure 4.7B**, F(6,1063) = 0.83, p = 0.54, MM GLM). However, as shown before in **Figure**

4.5C and here in ACSF group, ChI stimulation decreases evoked EPSPs in D2-MSNs, and this effect was blocked by dopaminergic and cholinergic antagonists (**Figure 4.7C**: sulpiride+SCH-23390: $F(2,26.7) = 0.95$, $p = 0.43$, mecamylamine: $F(2,27) = 0.61$, $p = 0.54$, atropine: $F(2,27) = 0.65$, $p = 0.53$, MM GLM).

To further understand the nature of ChI effect on glutamatergic transmission we wanted to determine whether the effect of ChI is due to the stimulation pattern (burst versus tonic). To answer this question, we applied *continuous* 20 Hz stimulation for 2 minutes and measured sEPSCs (**Figures 4.7D-F**). Interestingly, we observed exactly the same response in all the groups tested as with burst stimulation: an increase of inter-event interval in both D1- and D2-MSNs and no change in amplitude of sEPSCs (**Figure 4.7D**, D1-MSNs IEI: $t(9) = 2.74$, $p = 0.023$, paired t-test, Amp: $t(9) = 1.06$, $p = 0.32$ paired t-test; **Figure 4.7E**, D2-MSNs IEI: $t(7) = 3.27$, $p = 0.0136$, paired t-test, Amp: $t(7) = 0.89$, $p = 0.40$, paired t-test), with no change in the control group (**Figure 4.7F**: GFP IEI: $t(9) = 0.54$, $p = 0.60$, Amp: $t(9) = 0.28$, $p = 0.78$, paired t-test). These findings imply that ChI-evoked decrease in glutamatergic transmission is mediated by both, tonic and burst ChI firing.

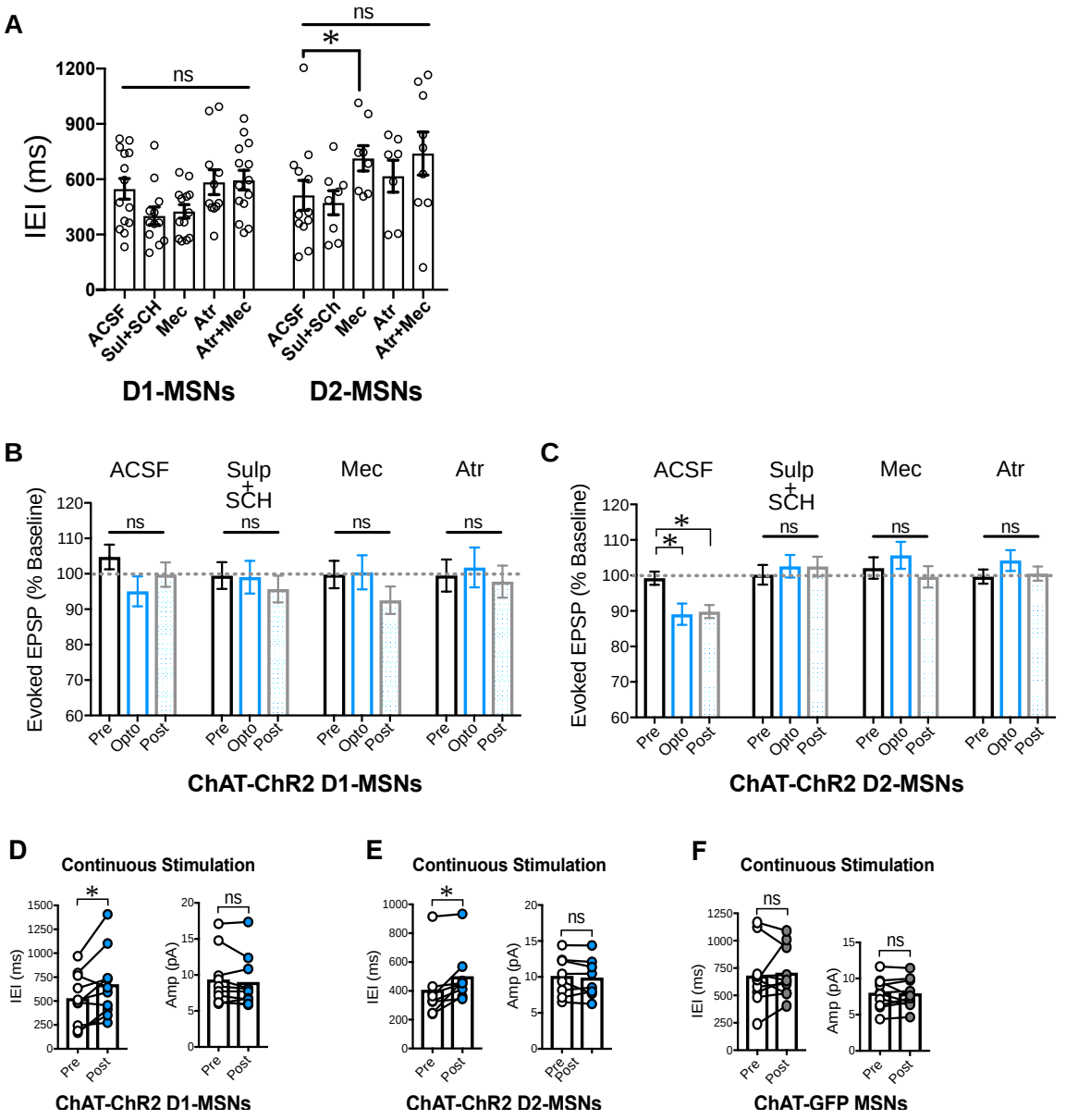

Figure 4.7 | Antagonists and stimulation pattern effect of ChIs stimulation on D1- and D2- MSN glutamatergic transmission. A. Recordings of EPSCs IEIs during the bath application of antagonists. **B-C.** Average evoked EPSPs in D1-MSNs and D2 MSNS before (Pre), during (Opto) and after (Post) ChI optogenetic. **D-F**. Recrodings of sEPSPCs' Inter-event interval (IEI) and amplitude (Amp) before and after 2 minutes of continuous 20Hz ChI stimulation in D1- and D2-MSNs in ChAT-ChR2 mice and undifferentiated MSNs in ChAT-GFP mice. Pre stimulation (white circles) and Post stimulalation (blue circles in ChAT-ChR2 mice or gray circles in ChAT-GFP mice). ACSF (control solution), D1 receptor antagonist sulpiride + D2 receptor antagonist SCH-23390, nAChR antagonist mecamylamine, mAChR antagonist atropine. *p<0.05, ns: no significant difference

Finally, we verified our electrically evoked EPSPs results with optogenetically evoked EPSPs to eliminate the confounding of electric stimulation, which also stimulates other neuron types and projections. To circumvent this potential limitation, we injected virus-delivered Chrimson opsin into PFCx, the brain region known to project robust glutamatergic inputs into the NAc and recorded optogenetically-driven EPSPs (oEPSPs) before and after ChI stimulation. As with electric stimulation, we did not observe significant differences between Pre and Post ChI stimulation in optogenetically-evoked glutamatergic responses (**Figure 4.8A,** average oEPSPs, t(10) = 0.59, p = 0.56, paired t-test, **Figure 4.8B**, timeline of oEPSP response, F(1,284) = 0.46, p = 0.50, 2-way ANOVA, **Figure 4.8C**, average PPR, t(10) = 0.20, p = 0.84, and **Figure 4.8D**, timeline of PPR response F(1,228) = 0.51, p = 0.47, 2-way ANOVA).

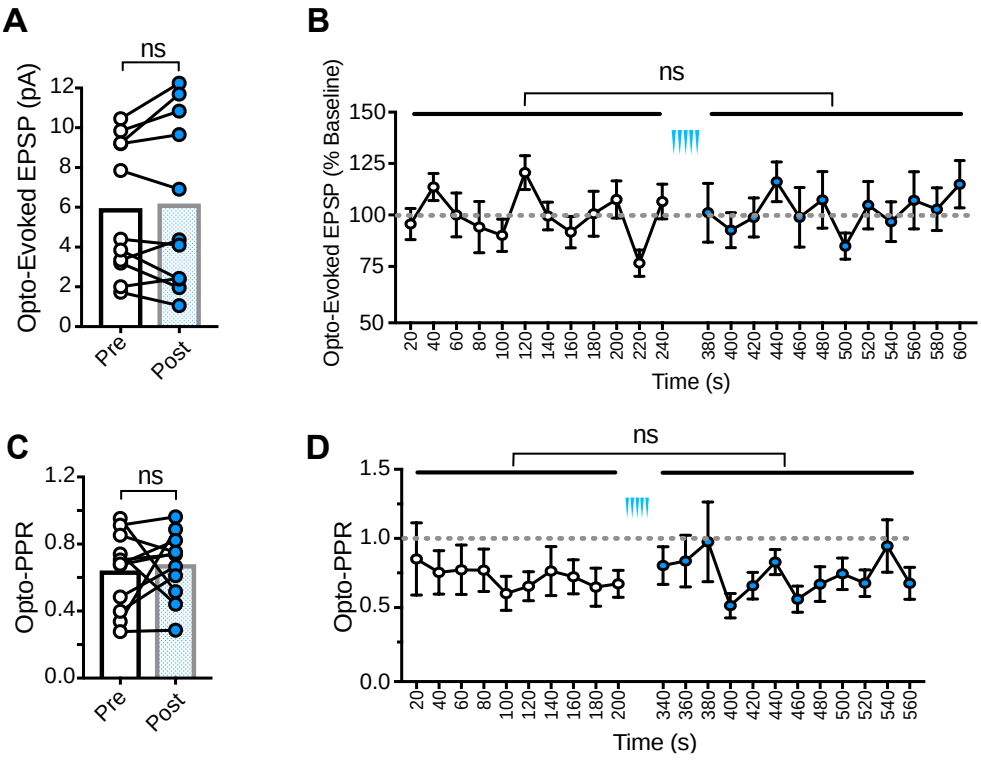

Figure 4.8 | Optogenetically evoked EPSPs in the NAc D1-MSNs with Chrimson opsin injected in PFCx. A. oEPSPs in pre (white circles) and post (blue circles) ChI stimulation showing average pre condition **B**. timeline of EPSP response over 10 minutes . **C, D**. Optogenetically evoked stimulation paired-pulse ratio (PPR) in D1-MSNs averaged for 11 mice.

Binge alcohol drinking effect on ChIs

Considering the profound effect of ChI activation on glutamatergic transmission, we wanted to determine whether alcohol has direct effects on ChIs. We performed whole-cell recordings from ChIs in naïve and DID-treated mice, using the drinking-in-the-dark paradigm, a well-established model of binge alcohol drinking (Rhodes et al., 2005). Interestingly, we observed that while in Naïve mice, majority (68%) were spontaneously firing, after DID treatment, there were many fewer neurons displaying this pattern, with only 24% still spontaneously firing (**Figure 4.9**). These results indicate that DID treatment alters the excitability of ChIs directly.

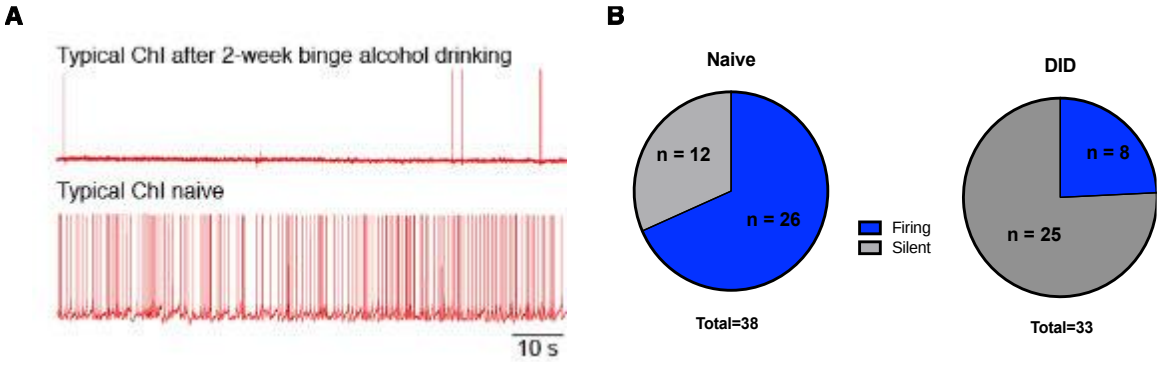

Figure 4.9 | DID modulation of ChI firing pattern. A. Recording from cholinergic interneuron after 2-week mouse binge drinking (DID) and in naïve mouse. **B**. ChIs tend to not fire in the typical spontaneously active firing pattern after alcohol exposure, while in naïve mice 26 out of 38 neurons showed spontaneous firing pattern (68%), only 8 out of 33 neurons recorded were spontaneous firing after DID (24%).

Binge alcohol drinking selectively reverses the effect of ChI-mediated glutamatergic synaptic transmission in D1-MSNs

The effects of preceding alcohol exposure on the ChI control of MSN excitability was assessed using the drinking-in-the-dark (DID) paradigm. The DID paradigm allows mice to drink 20% alcohol for 2h starting 2h into the dark phase for 5 consecutive days per week (**Figure 4.10A**). After 2 weeks of drinking either 20% alcohol (DID group) or water (Naïve group), sEPSCs were recorded in D1- and D2-MSNs before and after optogenetic stimulation. As previously shown in Figs. 4.2 and 4.3, we constructed cumulative distribution plots for D1-MSNs (**Figures 4.10B** (Naïve) and **C** (DID)) and D2-MSNs (**Figures 4.10D** (Naïve) and **E** (DID)). Surprisingly, unlike in Naïve conditions, the effect of alcohol exposure on ChI regulation of sEPSC IEI length was significantly different in D1- and D2-MSNs (**Figure 4.10F**, $F(1,4778) = 12.08$, $p = 0.0005$, MM GLM, 3-way interaction between optogenetic treatment, alcohol treatment and cell type). Tukey post-hoc tests revealed that in naïve D1-MSNs, ChI activation increased IEI while in DID exposed D1-MSNs, IEIs were significantly decreased, thus reversing the ChI effect on glutamatergic transmission. Conversely, ChI activation resulted in longer IEIs in D2-MSNs of both naïve and DID exposed mice. Interestingly, the effects of alcohol treatment seen in D1-MSNs depended on the size of IEI (**Figure 4.10F** D1-MSNs, $F(4,2374) = 3.900$, $p = 0.0037$), with post-hoc tests revealing differences in the 75 and 95 percentiles, but not other intervals, indicating that the alcohol effect was especially pronounced at the longest IEIs. In D2-MSNs there was no

relationship between IEI size and the effect of alcohol, and all percentiles of IEI were equally affected by alcohol.

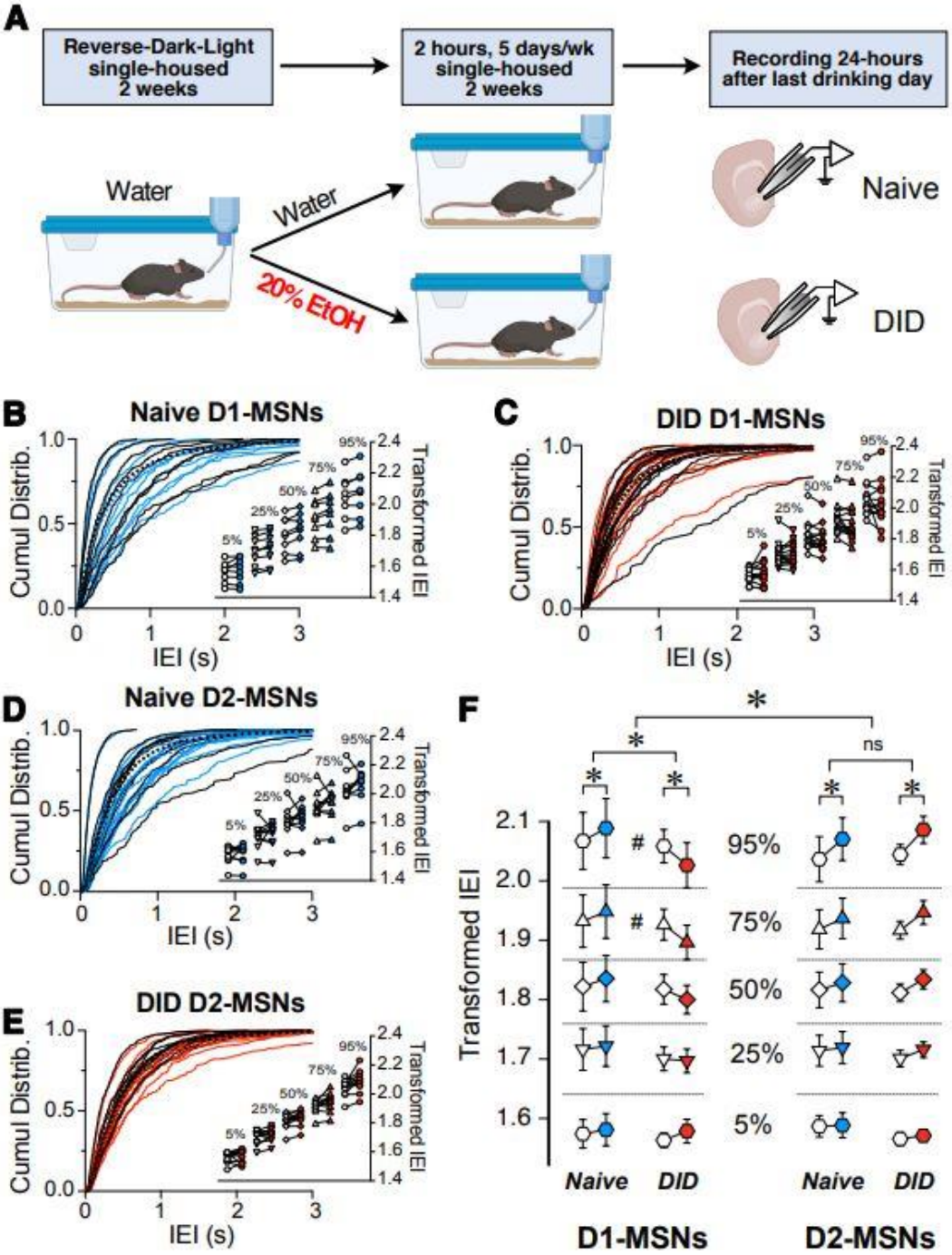

Figure 4.10 | Binge alcohol drinking differentially affects the control by ChI on glutamate release in D1 and D2R MSNs. A. Schematic of drinking in the dark (DID) treatment. Mice were single-housed at 4-5 weeks of age and placed into reversed dark-light schedule to habituate for 2 weeks and then given either water (Naïve group) or 20% EtOH (DID group) each day for 2 hours, 5 days a week for 2 weeks. Brain slices were then isolated, and MSN sEPSCs recorded. **B:** Cumulative frequency distribution of D1-MSN IEI of sEPSCs in ChAT-ChR2 mice group before (Pre, black traces) and after (Post, blue traces) ChI optogenetic stimulation. Each solid line represents a neuron. Average traces for Pre and Post conditions are shown in dotted black and blues lines, respectively. **Inset.** Cumulative distributions of D1-MSNs EPSCs IEIs in ChAT-ChR2 mice broken into percentiles of distribution to quantify median (50%), shoulders (25 and 75%), and extreme values (5 and 94%) of distribution, that are 1^10 transformed to normalize the distribution.**C.** Same as B in DID mice. Black and red traces indicate IEI before and after ChI stimulation, respectively. (n = 14). **D.** Cumulative frequency distribution of D2-MSN IEI of sEPSCs in ChAT-ChR2 mice before (Pre, black traces) and after (Post, blue traces) ChI optogenetic stimulation. Each solid line represents a neuron. Average traces are shown in dotted black and blues lines for Pre and Post conditions, respectively. **Inset.** Cumulative distributions of ChAT-ChR2 D2-MSNs EPSCs IEIs broken into percentiles of distribution to quantify median (50%), shoulders (25 and 75%), and extreme values (5 and 94%) of distribution, that are 1^10 transformed to normalize the distribution. (n = 10)**. E.** Same as B in DID mice. Black and red traces indicate IEI before and after ChI, respectively. (n = 11)**. F.** Percentiles of cumulative distribution of transformed IEIs of EPSCs in Naïve ChAT-ChR2 (Pre, white circles, Post, blue circles) and DID ChAT-ChR2 (Pre, white circles, Post, red circles) in D1- and D2-MSNs. *p < 0.05, #p < 0.05, ns: no significant difference

These results demonstrate that previous alcohol exposure selectively inverts the effect of ChI activation on D1-MSNs from reducing to increasing glutamate release onto D1-MSNs, while not changing the regulation of D2-MSNs. There was no significant difference in DID D1-MSNs sEPSC amplitude (**Figure 4.11A**, t(13) = 1.46, p = 0.168, paired t-test) or in DID D2-MSNs sEPSC amplitude (**Figure 4.11B**, t(10) = 0.69, p = 0.503, paired t-test).

To determine whether alcohol changes ChI mediation of evoked EPSPs, we recorded eEPSPs before, during and after ChI stimulation in DID mice. We did not observe significant difference in eEPSPs during and post ChI stimulation compared to baseline when averaged per treatment in DID D1-MSNs (**Figure**

4.11C, F(1.57,14.14) = 0.91, p = 0.40) or over time (**Figure 4.11D**, F(2,573 = 1.01, p = 0.365, RM one-way ANOVA). We also did not observe an effect in DID D2-MSNs (average eEPSPs **Figure 4.11E**, F(1.16,6.95) = 1.27, p = 0.308, RM one-way ANOVA and eEPSPs over time **Figure 4.11F**, F(2,427) = 3.23, p = 0.063 MM GLM). Interestingly, we did observe a significant difference in alcohol treatment on ChI effect, as compared to naïve ChI treatment in **Figure 4.5E**, but this difference was only present *during* stimulation, not *after* (**Figure 4.11G**, F(2,427) = 3.23, p = 0.042, MM GLM, with interaction of ChI effect and alcohol treatment, Tukey post-hoc). There was no effect of alcohol treatment in DID D1-MSNs (F(2,573) = 1.01, p = 0.364, not shown).

The DID paradigm involved a 24-hour interval after the last drinking bout before sEPSC recordings. We were curious whether recording sEPSCs immediately after the last drinking session (immediate recording DID, IR-DID) would produce different results. Interestingly, recordings performed immediately after the drinking session produced the same results as recordings 24-hours after the last drinking session, with D1 MSNs no longer showing an increase in sEPSCs IEIs (IR-DID D1-MSNs, **Figure 4.11H**, t(14) = 0.24, p = 0.81, paired t-test for IEIs and t(14) = 1.45, p = 0.168, paired t-test for Amp). D2-MSNs still showed significant increase in IEI after ChI stimulation (IR-DID D2-MSNs, **Figure 4.11I**, t(9) = 2.76, p = 0.022, paired t-test, with no difference in Amp, t(9) = 1.54, p = 0.159, paired t-test).

Finally, we compared whether our baseline sEPSCs IEI is altered during the different conditions that were used as baseline (Pre) for different experiments (**Figure 4.11J**). We compared baseline (Pre) sEPSCs in both D1- and D2-MSNs in Naïve, Naïve that were single-house and kept in reverse-dark-light conditions (RDL-Naïve, Controls for DID), DID and IR-DID conditions (recorded immediately after last drinking bout) and did not see any differences in these baseline conditions in D1 ($F(3,46) = 0.90$, $p = 0.444$, one-way ANOVA) or for D2-MSNs ($F(3,41) = 0.32$, $p = 0.814$, one-way ANOVA).

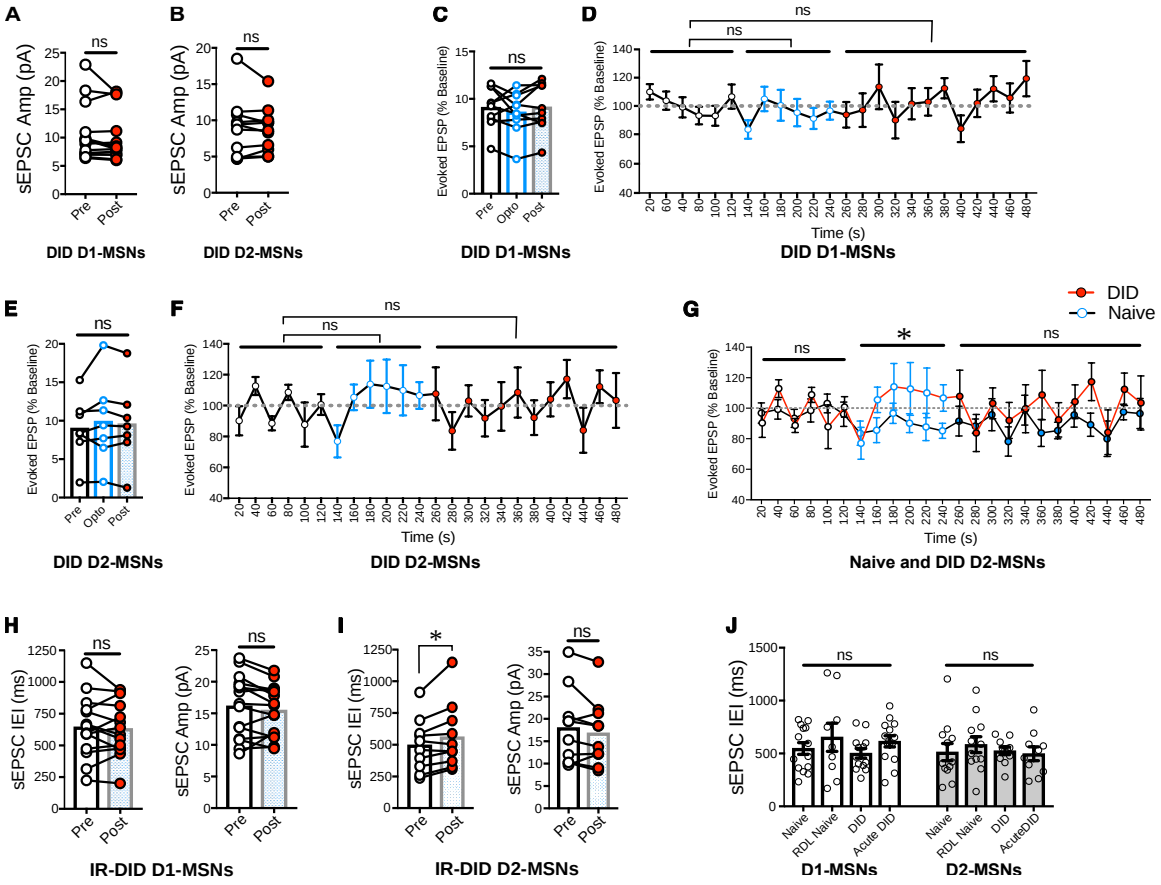

Figure 4.11 | Binge alcohol drinking effect on ChI stimulation in D1- and D2-MSNs. **A.** Amplitudes of DID D1-MSNs sEPSCs before (Pre, white circles) and after (Post, red circles) ChI optogenetic stimulation in ChAT.ChR2 mice (n = 14). Each symbol represents one MSN. **B.** Amplitudes of DID D2-MSNs sEPSCs before (Pre, white circles) and after

(Post, red circles) ChI stimulation in ChAT.ChR2 mice (n = 11). Each symbol represents an MSN. **C, D.** Average and timeline of evoked EPSPs in DID D1-MSNs (Pre, white circle), during (Opto, blue circle), and after (Post, red circle) ChI optogenetic stimulation, recorded every 15 s for 8 mins. **E, F**. Average and timeline of evoked EPSPs in DID D2-MSNs (Pre, white circle), during (Opto, blue circle), and after (Post, red circle) ChI optogenetic stimulation, recorded every 15 s for 8 mins. **G**. Graph of evoked EPSPs in D2-MSNs reproduced from previous panel **F** (DID) and naïve group from Figure 4.5E to show the effect of alcohol as compared to naïve and DID groups. Naïve, blue line, DID, red line. **H, I.** Immediate recording after the last DID session (IR-DID) D1- and D2-MSN sEPSC IEIs and Amplitude recorded in mice that underwent 2-weeks DID. **J.** Baseline comparisons of sEPSCs (Pre) conditions throghought different experiments (Naïve, reverse-dark-light (RDL) Naïve, DID and IR-DID). *p<0.05, ns: no significant difference

Receptors mediating alcohol alteration of ChI effect on D1-MSNs.

Given the effects of previous alcohol exposure on ChI regulation of glutamate release in D1-MSNs, the next objective was to identify receptors mediating these effects. Interestingly, in DID-exposed D1-MSNs, recording in the presence of D1- and D2-antagonists seemed to block the effect of DID (**Figure 4.12A** ACSF vs sulpiride+SCH-23390, $F(1,2331) = 40.49$, $p < 0.0001$, MM GLM). This increase of IEI length following ChI stimulation in the presence of dopamine receptor antagonists in DID-exposed D1-MSNs was reminiscent of the naïve D1-MSN groups (**Figures 4.10F and 4.2**), indicating an important role of DA receptors in alcohol's effect on ChI-modulated glutamate release. In the presence of mAChR antagonist atropine, ChI effect of sEPSC IEI was also significantly different from ACSF condition (**Figure 4.12A** ACSF vs atropine, $F(1,2495) = 25.1129$, $p < 0.0001$, MM GLM, with Tukey post hoc showing a significant IEI decrease only in ACSF group, but no significant difference between Pre vs Post groups in the atropine group). Finally, recording in the presence of nAChR antagonist mecamylamine also abolished the effect of ChIs, and was significantly different from ACSF (**Figure**

4.12A ACSF vs mecamylamine, F(1,2577) = 6.281, p = 0.0123, MM GLM, with Tukey Post hoc similarly showing only a significant difference in the ACSF group). The most parsimonious interpretation of these results is that the influence of previous alcohol exposure on the ChI-mediated glutamate release in D1-MSNs mostly depends on dopaminergic signaling with additional influences from both nAChR and mAChR signals.

Interestingly, the application of bath antagonists in DID D1-MSNs changed only during mecamylamine treatment compared to ACSF (**Figure 4.12B**, mecamylamine, Mann-Whitney U = 22, p = 0.0065), while the other antagonists were not different from ACSF group (**Figure 4.12B**, atropine: p = 0.693, sulpiride+SCH-23390: p = 0.896). This is in stark contrast from naïve D1-MSN group, where mecamylamine treatment did not change the baseline, but is reminiscent of naïve D2-MSN group, where mecamylamine also increased IEIs (**Figure 4.7A**).

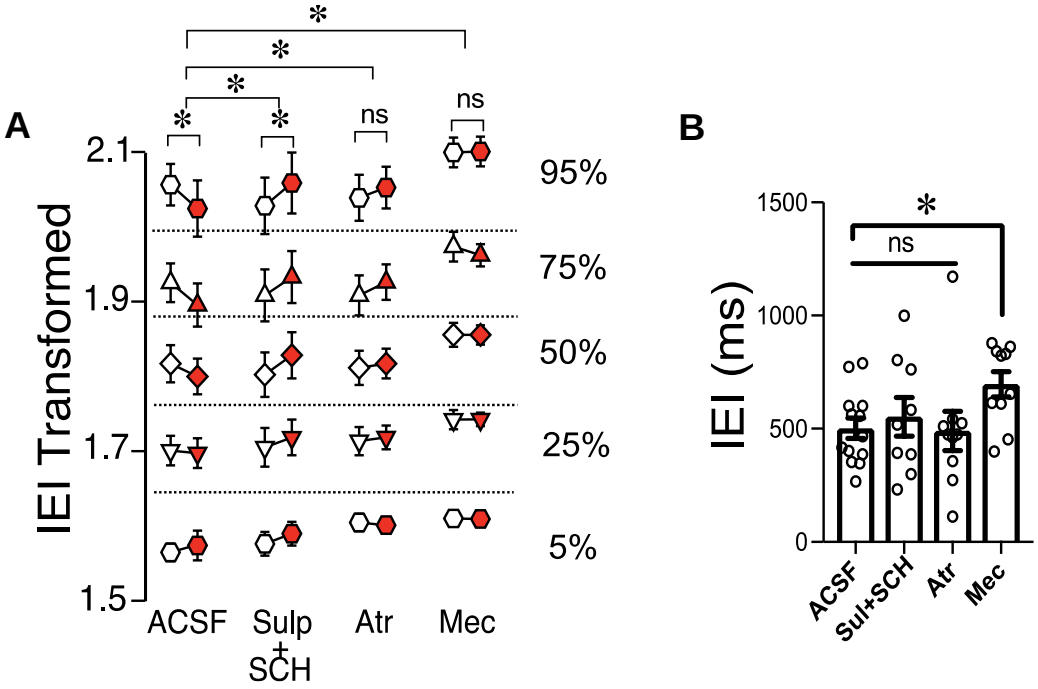

Figure 4.12 | Effects of ChI stimulation in DID D1-MSNs in the presence of antagonists. A. IEI in DID D1-MSNs EPSCs shown as percentiles of cumulative distribution. Data for the control group (ACSF) is reproduced from Figure 4.10. Each group of Pre (white circles) and Post (red circles) column is recorded either without (ACSF) or with the bath presence of antagonists. **B.** sEPSCs IEIs in D1-MSNs in presence of ACh and DA receptors antagonists in DID mice. Average sEPSCs IEIs in DID D1-MSNs recorded in ACSF (control solution) and in presence of dopamine D1 and D2 receptor antagonists sul+SCH (5 uM SCH-23390, D1 receptor antagonist + 1 uM sulpiride, D2 receptor antagonist), Atr (1 uM atropine, mAChR antagonist), Mec (5 uM mecamylamine, nAChR antagonist). *p<0.05, ns: no significant difference

ChI optogenetic stimulation in vivo in the NAc increases alcohol consumption in mice.

Since binge alcohol drinking modulates the ChI-mediated synaptic transmission onto MSNs *ex vivo*, we next tested whether optogenetic stimulation of ChIs in freely-moving animals altered alcohol consumption. Fiber optic cannulas were implanted into the NAc of 4-5 weeks old mice that were allowed to recover and

habituate to our reverse-light-dark room for 3 weeks before being optogenetically stimulated during the first 4 days of alcohol exposure (**Figures 4.13A and B**). From the very first day, the volume of alcohol consumed by stimulated ChAT.ChR2 mice group (**Figure 4.13C**, ChR2) was markedly larger compared to mice in the non-stimulated ChR2 group (**Figure 4.13C**, ChR2 NS) and stimulated ChAT.cre controls (**Figure 4.13C**, $F(2, 22) = 7.685$, $p = 0.0029$, MM GLM, with Tukey post-hoc tests showing ChR2 group significantly different from both control groups). The pattern of alcohol consumption was determined using lickometers by measuring the number and timing of licks of the drinking spout delivering alcohol (**Figure 4.13D**). The total number of licks in stimulated ChR2 mice during the 4 days was significantly increased compared to the non-stimulated and Cre control groups (**Figure 4.13E**, $F(2,22) = 6.50$, $p = 0.0061$, MM GLM). The increase in alcohol drinking was likely due to the increased frequency of consumption measured as the licking bout IEI was dramatically reduced in the ChR2 group (**Figure 4.13F**, $F(2,20) = 5.376$, $p = 0.0135$, one-way ANOVA), and licks were highly correlated with the amount of alcohol consumed (**Figure 4.14A**). General locomotor activity of a subgroup of mice was measured using a passive infrared activity monitoring system and compared to alcohol licks during the same time interval (**Figures 4.13G, H**). This comparison illustrated that the increased drinking in the stimulated ChR2 mice could not be explained through a general increase in activity levels in these mice (**Figure 4.13H**; ChR2: $R2 = 0.134$, $p = 0.122$; Cre controls: $R2 = 0.023$, $p = 0.472$). The increased alcohol consumption observed in stimulated ChR2 mice

was specific to alcohol consumption and did not extend to the consumption of saccharin (**Figure 4.13I**, F(1,47) = 1.53, p = 0.22, RM two-way ANOVA, **Figure 4.14B**, F(1,47) = 1.78, p = 0.93, RM two-way ANOVA), and water (**Figure 4.13J**, F(1,45) = 0.33, p = 0.57, RM two-way ANOVA, **Figure 4.14C**, F(1,49) = 0.03, p = 0.87, RM two-way ANOVA).

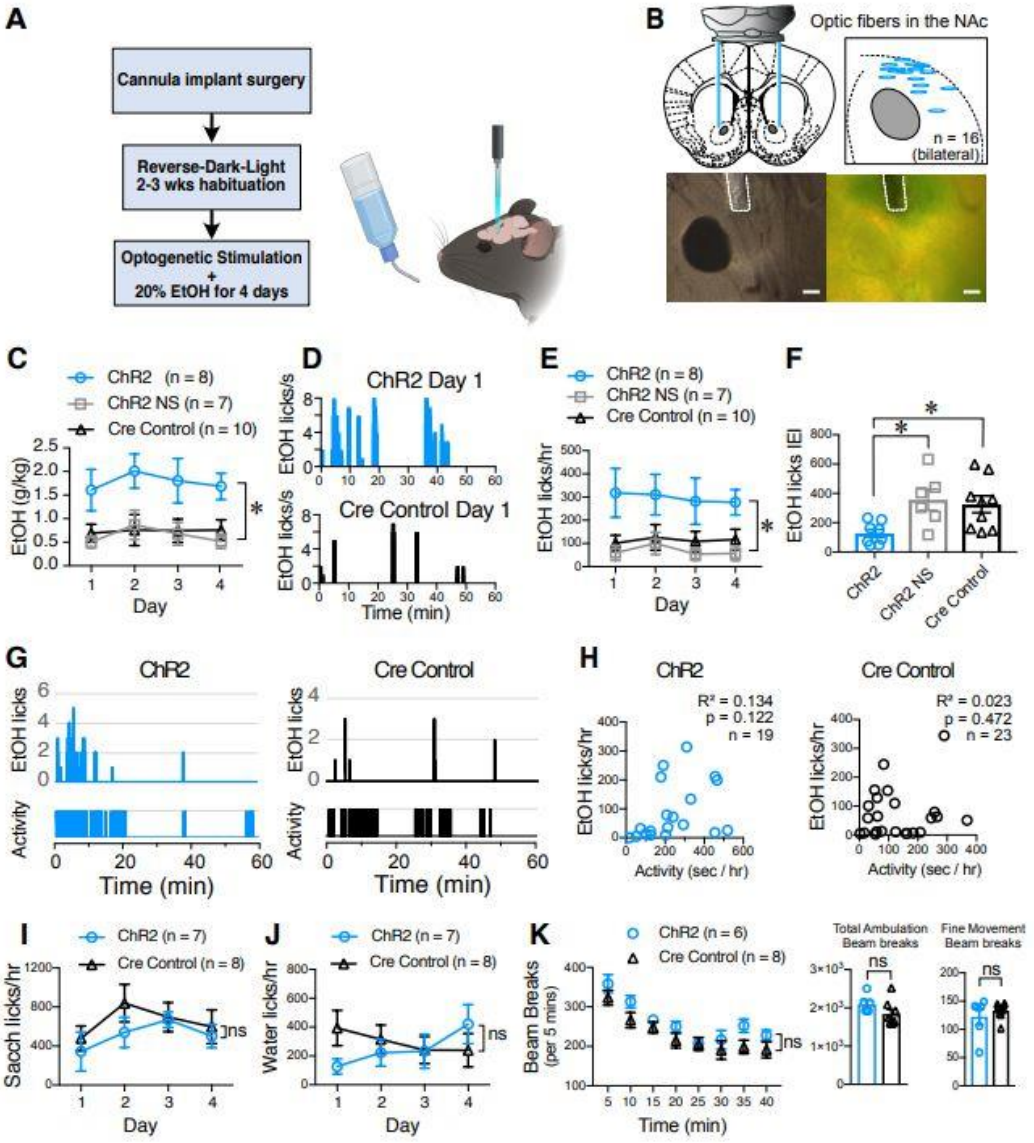

Figure 4.13 | ChI optogenetic stimulation increases EtOH consumption. A. Schematic of the DID behavioral experiment. ChAT.ChR2 and ChAT.cre mice underwent fiber optic implant in the NAc surgery at 4-5 weeks of age, recovered and habituated to reverse-dark-light schedule. ChAT.ChR2 and ChAT.cre mice were optogenetically stimulated during 4 days of 20% alcohol exposure and tethered to the fiber cord while ChAT.ChR2 not stimulated (NS) mice were only tethered to the fiber cord. **B.** Schematic of the bilateral optic fiber cannula implant in the NAc (top left panel), locations of bilateral implants in 8 ChR2 mice that were used for the experiment (top right panel), example image of cannula placement in DIC (bottom left panel) and fluorescent light (bottom right panel). **C.** Average daily alcohol consumption over 4 days in optically stimulated ChR2 mice (ChR2), non-stimulated ChR2 mice (ChR2 NS) and stimulated ChAT-cre mice (Cre controls). **D.** Graphs of alcohol licks during 1st hour period in representative stimulated (top graph, blue bars) and non-stimulated ChR2 mice (bottom, gray bars). **E.** Daily average of alcohol licks over 4 days of alcohol exposure in optically stimulated ChR2 mice (ChR2), non-stimulated ChR2 mice (ChR2 NS) and stimulated ChAT-cre mice (Cre controls). **F.** Frequency of alcohol licks as measured by average licking bout inter-event interval (IEI) per mouse over a 4-day period. **G.** Representative plots of mouse activity as measured by passive infrared (PIR) activity monitoring system and corresponding EtOH licks in ChR2 (Left graphs, blue bars) and Cre control mice (right graphs, black bars). **H.** The number of licks is not correlated with mice locomotor activity in ChR2 (blue symbols) and Cre control groups (black symbols). **I**. Saccharin consumption measured as number of licks/hr over 4 days in 1 hr-long optogenetically stimulated ChR2 (blue circles) and Cre control mice (black triangles). **J.** Water consumption measured as number of licks/hr over 4 days in 1 hr-long optogenetically stimulated ChR2 and Cre control mice. **K.** Ambulatory activity test of ChR2 and Cre control mice during ChI optogenetic stimulation. Ambulation time course shows average beam breaks every 5 mins for 40 mins of the test. Total Ambulation shows the total beam breaks in 40 min, fine movement shows grooming activity and vertical ambulation shows rearing activity. *$p < 0.05$, ns: no significant difference.

Finally, stimulated ChR2 and Cre control mice (**Figure 4.13K**) did not differ in ambulation time course ($F(7,84) = 0.80$, $p = 0.59$, RM two-way ANOVA), total ambulation ($t(12) = 1.63$, $p = 0.13$, Student's t-test), fine movement ($t(12) = 1.12$, $p = 0.28$, Student's t-test), or vertical motion (rearing, **Figure 4.14D**, $t(12) = 0.8$, $p = 0.44$, Student's t-test). These results demonstrate that optogenetic stimulation of ChIs specifically altered alcohol consumption, without affecting water and saccharin drinking, an effect that was not due to increased activity level.

Given the robust results of ChI stimulation on mouse drinking behavior, we wanted to determine whether this effect is specific to the days of stimulation and whether in can be reversed. We observed that after ChIs are no longer stimulated, mice do not have a long-term change in the drinking pattern and showed no difference to ChAT-cre or non-stimulated controls (**Figure 4.14E**). We then tested whether we can inhibit alcohol drinking with ChI inhibition with Halorhodopsin, but did not see a significant difference in consumption (**Figure 4.14F**). Finally, we wanted to test whether we can increase mouse drinking in ChI stimulation after they were already exposed to alcohol for 8 days. We observed that after mice had prior experience with alcohol, ChI stimulation did not increase their drinking on alcohol drinking days 9-12 (**Figure 4.14G**). These results indicate the ChI effect is specific to the first several days of alcohol exposure and does not persist after ChIs are no longer stimulated.

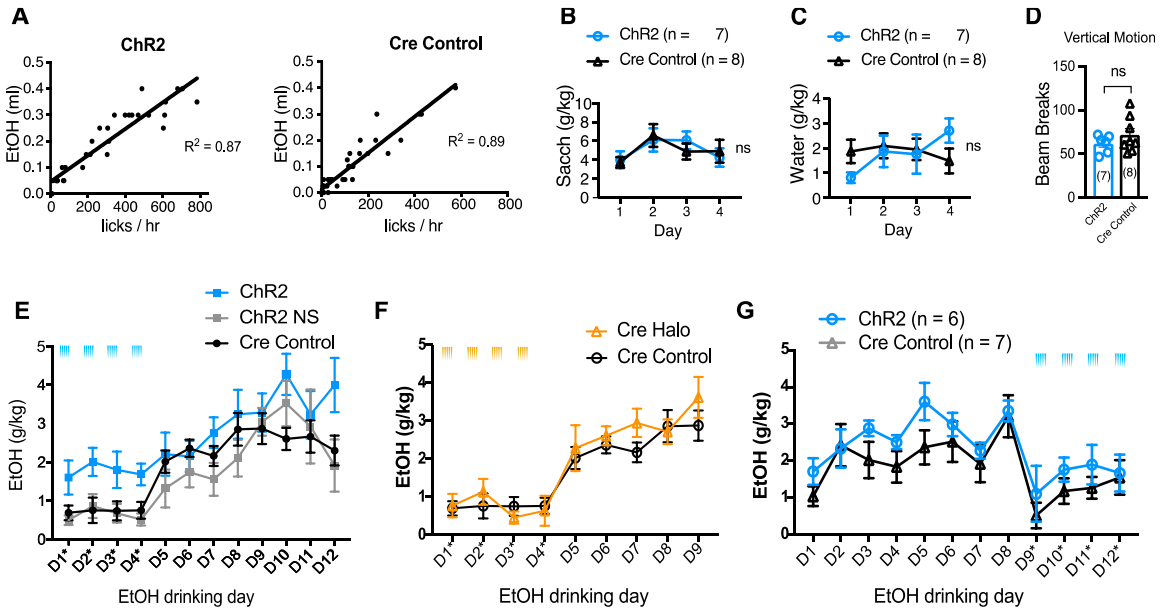

Figure 4.14 | ChI optogenetic stimulation and EtOH consumption behavior. A. Graph shows strong correlation between the volume of EtOH consumed and the number of licks in ChAT.ChR2 (ChR2) and ChAT.cre mice (Cre control). **B.** 0.3% Saccharine consumed (g/kg) during 1-hr long ChI optogenetic stimulation in ChAT.ChR2 and ChAT.cre mice. **C.** Water consumed (g/kg) during 1 hr-long ChI optogenetic stimulation in ChAT.ChR2 and ChAT.cre mice. **D:** Vertical motion (rearing) in ChAT.ChR2 and ChAT.cre mice during ChI optogenetic stimulation. *p<0.05, ns: no significant difference. **E**. First 4 days same data as in Figure above, panel C, days 5-12 (D5-D12) shows continuation of drinking following cessation of stimulation. **F**. Mice drinking alcohol for 9 days during ChI optogenetic inhibition during the first 4 days (Cre Control n = 10, Cre Halo n = 8). **G**. Mice drinking alcohol for 8 days prior to being stimulated at drinking days 9-12 (D9-12). No significant effect was observed in any of the treatments E-G.

Finally, to summarize, we show here that ChIs control glutamatergic synaptic transmission in both D1- and D2-MSNs in alcohol-naïve mice, though the underlying regulatory mechanisms differ. While in naïve mice, ChI stimulation decrease glutamatergic transmission in both D1- and D2-MSNs, after 2-week alcohol exposure, D2-MSNs are still attenuated while D1-MSNs showed an increase in glutamatergic presynaptic transmission (**Figure 4.15**).

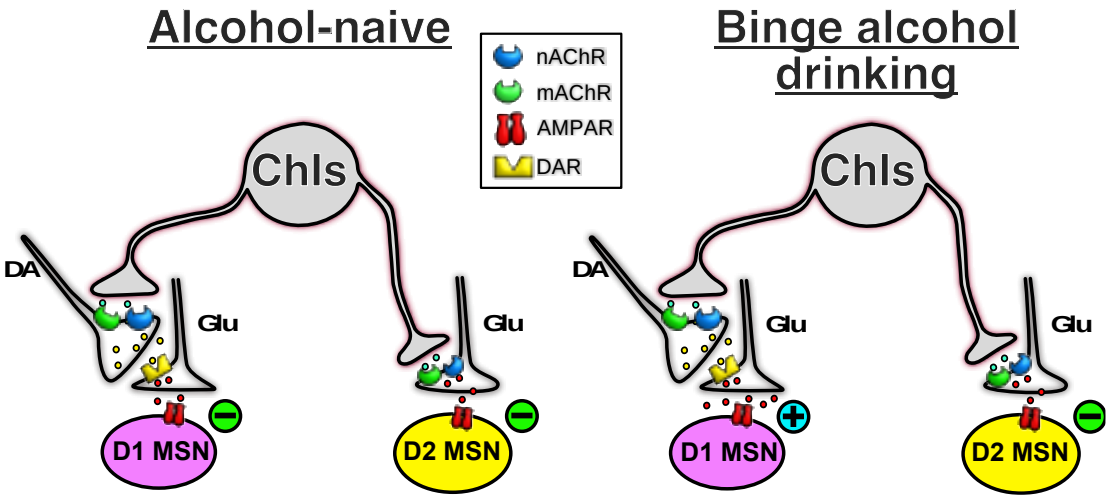

Figure 4.15 | Simplified schematic of ChI effect on glutamatergic neurotransmission in MSNs in naïve and alcohol binge drinking mice. In naïve mice, ChIs decrease glutamatergic neurotransmission onto both D1-and D2-MSNs presynaptically (left). However, in Binge alcohol drinking mice, ChI activation increased glutamtergic neurotransmission, but only in D1-MSNs, while in D2-MSNs the glutamatergic transmission remained decreased after ChI activation.

Discussion

As the sole output neurons of the NAc, D1- and D2-MSNs, are a key part of the neurobiological mechanisms underlying drug addiction (Soares-Cunha et al., 2020) and altering their excitability will likely be an important part of any future treatments of alcohol addiction (Cheng et al., 2017). Despite making up only 1-2% of the NAc neuronal population, ChIs provide a promising avenue as they fulfill a key integrative role modulating the activity of MSNs (Kravitz et al., 2012). The data presented here show that ChIs control glutamatergic synaptic transmission in both D1- and D2-MSNs in alcohol-naïve mice, though the underlying regulatory mechanisms differ (Naïve, **Figure 4.15, left**). While the ChI-driven decrease of glutamate release onto D1-MSNs is mediated by nicotinic and muscarinic ACh receptors and DA receptors, ChIs control of glutamate release onto D2-MSNs likely stems from ChIs directly synapsing on glutamatergic terminals through nicotinic and muscarinic ACh signals. Surprisingly, prior alcohol exposure results in a switch where the effect of ChIs activity inverts from inhibiting to potentiating glutamatergic transmission in D1-MSNs while the inhibitory effect in D2-MSNs remains unchanged (**Figure 4.15, right**). Based on this dramatic change of its influence on D1-MSNs we hypothesized that altering ChI activity could be used to modulate alcohol drinking behavior. In line with this hypothesis, ChI optogenetic stimulation *in vivo* increased alcohol consumption in mice without altering locomotor activity, saccharin or water consumption. Together, these findings

identify NAc ChIs as key modulators of D1- and D2-MSNs excitability and suggest this cell population as a promising target of future addiction treatment strategies.

ChIs decrease glutamate release in D1- and D2-MSNs through different mechanisms.

Our finding that ChIs inhibit MSN glutamatergic synaptic transmission through a presynaptic mechanism confirms previous reports showing that acetylcholine receptor (AChR) agonists reduce the probability of glutamate release in the striatum (Malenka & Kocsis, 1988; Barral, Galarraga, & Bargas, 1999; Higley et al., 2009; Licheri et al., 2018). Similarly, direct stimulation of ChIs depressed electrically evoked EPSCs, an effect also attributed to presynaptic cholinergic receptors (Pakhotin & Bracci, 2007; Lee, Finkelstein, Choi, & Witten, 2016), although a postsynaptic effect was also reported (Calabresi et al., 2000). Despite decades of research striving to understand how ChIs regulate glutamatergic synaptic transmission in MSNs, the mechanisms mediating their effects on D1- and D2-MSNs glutamatergic synaptic transmission is still poorly understood (Cox & Witten, 2019; Joshua et al., 2008). Our study provides evidence that ChIs employ different mechanisms to regulate glutamate release onto D1- and D2-MSNs. Specifically, our data demonstrates the influence of DA on ChIs' regulation of glutamate release in D1- but not D2-MSNs. The role of DA is supported by data from several groups showing that ChIs evoke DA release (Threlfell et al., 2012; Cachope et al., 2012; Wang et al., 2014; Shin et al., 2015), likely through α*β2

nAChR expressed on DA terminals (Threlfell et al., 2012; Yorgason et al., 2017). In addition to nAChRs, we found that mAChRs also contribute to the ChIs-mediated decrease of glutamate release in D1-MSNs, possibly through M5 mAChR (Shin et al., 2015; Grilli et al., 2008; Kuroiwa et al., 2012; Bendor et al., 2010), as shown in previous studies (de Rover et al., 2002; Pancani et al., 2014; Ding et al., 2010). Our study also indicates that, upon its release, DA binds to DA receptors located presynaptically on glutamatergic terminals where it decreases glutamate neurotransmission, a finding supported by several studies (Dumartin et al., 2007; Nicola et al., 1996; Nicola & Malenka, 1997; Nicola & Deadwyler, 2000; Wang et al., 2012b). This action of DA is likely by promoting adenosine efflux via A1 adenosine receptors (A1Rs)(Ciruela et al., 2006; Harvey & Lacey, 1997). While our study confirms the role of DA and ACh receptors in regulating glutamatergic synaptic transmission, it provides key additional information as to how these neurotransmitters work together to regulate glutamate release onto D1-MSNs.

A key finding is that, as opposed to D1-MSNs, DA receptors do not contribute to ChI-mediated decrease of glutamate release in D2-MSNs. Instead, ChIs appear to send direct projections to glutamatergic terminals synapsing onto D2-MSNs, an effect that our pharmacological experiments suggest is mediated by mAChRs. Although performed in conditions that did not differentiate D1- from D2-MSNs, several groups reported a similar contribution of mAChRs on glutamate release in the striatum (Higley et al., 2009; Calabresi et al., 2000; Pancani et al., 2014; Ding et al., 2010). Specifically, M2-4 mAChR located presynaptically on

glutamatergic terminals directly decrease glutamate release by inhibition of P/Q-type voltage-gated calcium channels (VGCCs) and reduction of action potential–induced Ca^{2+} increases in the bouton (Higley et al., 2009; Calabresi et al., 2000; Pancani et al., 2014). We have also found that application of 1 µM nicotinic antagonist mecamylamine decreases sEPSCs in D2-MSNs. However, much ambiguity still exists on the nicotinic effect on glutamate release. $\alpha 4\beta 2$ nAChR antagonist has been shown to increase glutamate release (Howe, Young, Bekheet, & Kozak, 2016), while 1 µM and 10 µM nicotine application was shown to decrease sEPSCs frequency (Licheri et al., 2018), and 2 µM nicotine was found not to change sEPSCs frequency (de Rover et al., 2002). Finally, we have found that ChIs inhibited, albeit moderately (i.e., <10%), electrically evoked EPSPs in D2-MSNs only, mirroring a similarly small reduction of EPSCs in unidentified MSNs (Pakhotin & Bracci, 2007). These results emphasize the importance of distinguishing between striatal D1- and D2-MSNs when assessing their function in basal ganglia function.

Alcohol exposure changes ChI control of the D1/D2 MSNs output balance

Unlike other drugs of abuse, alcohol does not have a single receptor, making identifying its targets difficult. Acute alcohol exposure modulates striatal output through ChIs (Adermark et al., 2011b) and inhibits ChIs firing (Blomeley et al., 2011), while chronic alcohol use reduces density of cholinergic varicosities (Pereira et al., 2014). We found that ChIs' stimulation increases alcohol

consumption *in vivo*, while 2-week alcohol administration reverses the ChI control of glutamate release in D1-MSNs from inhibition to potentiation. Our finding is in line with previous studies showing that repeated exposure to alcohol potentiated D1-MSNs glutamatergic transmission (Strong et al., 2020; Cheng et al., 2017; Kircher, Aziz, Mangieri, & Morrisett, 2019; Ji et al., 2017). In addition to increasing glutamate release from terminals synapsing on D1-MSNs, chronic alcohol exposure was shown to act post-synaptically by increasing of spines density in dendrites of NAc and dorsal striatum MSNs (Nestby et al., 1999; Laguesse, Morisot, Phamluong, Sakhai, & Ron, 2018; Uys et al., 2016). Interestingly, glutamatergic transmission in D2-MSNs was not affected in binge alcohol drinking mice. Although this finding is somewhat surprising, Chen et al. reported that chronic alcohol exposure did not alter evoked EPSCs amplitude but increased GABAergic neurotransmission in dorsal striatal D2-MSNs (Cheng et al., 2017). Although we can only speculate about the specific origin of NAc D2-MSNs inhibitory inputs, it is worth noting that MSNs are mostly inhibited by GABAergic interneurons that are also under the control of ChIs (de Rover et al., 2002; Witten et al., 2010). If true, this would strengthen the putative central role that ChIs play in regulating excitability of D1- and D2-MSNs through glutamatergic and GABAergic synaptic transmission, respectively, and in shaping the overall message sent to downstream brain regions.

The mechanism responsible for reversing ChIs-mediated inhibition of glutamate release in D1-MSNs is unclear. Because DA is responsible for the ChIs-

mediated decrease of glutamate release, increase of frequency observed in DID mice may result from alcohol either decreasing DA release (Karkhanis, Rose, Huggins, Konstantopoulos, & Jones, 2015) and/or impairing nAChR (Hillmer et al., 2014) and mAChRs function (Costa & Guizzetti, 1999). Taken together, our findings offer a putative mechanism explaining why nAChR antagonists decrease alcohol consumption when administered ip (Hendrickson et al., 2009; Ericson, Löf, Stomberg, & Söderpalm, 2009; Hendrickson, Zhao-Shea, Pang, Gardner, & Tapper, 2010), as well as directly into the NAc (Feduccia et al., 2014).

In summary, our study delineates a new understanding of the NAc circuitry and its effect on alcohol drinking behavior. ChIs likely induce DA release, which drives further alcohol consumption. Since ChI activation is what mediates this DA release, ChI stimulation *in vivo* will result in more DA released, driving the continuation of drinking after the very first sip (Beckley et al., 2016). On the other hand, after 2 weeks of daily alcohol exposure, ChIs preferentially and repeatedly stimulate D1-MSNs, which leads to disbalance between D1- and D2-MSNs, potentiating the D1-MSNs “go” direct pathway and inhibiting the M2-MSNs “no-go” indirect pathway. ChI-mediated reciprocal strengthening of “go” and inhibition of “no-go” pathways could be a core element of compulsive increase of drinking over time and transitioning to addiction (Koob et al., 1994; Kravitz et al., 2012). Therefore, inhibition of ChIs could be a future therapeutic target to treatment of alcohol use disorder.

Acknowledgment

This work was supported by the National Institute on Alcohol Abuse and Alcoholism AA020501 (GM) and the National Institute of General Medical Sciences T32GM135751 (TL).

Chapter V

Discussion

Chapter V: Discussion

Summary

This thesis sought to identify the circuitry of the NAc responsible for integrating incoming signals, and how this process is impaired by binge alcohol drinking. First, we investigated how MSNs integrate glutamatergic signals originating in the prefrontal cortex (PFCx) and basolateral amygdala (BLA), and how it is impaired after binge alcohol drinking (Chapter II). Then, we examined the local modulation of glutamatergic inputs by cholinergic interneurons in naïve and binge drinking mice (Chapter IV). Finally, we developed the hierarchical model of spontaneous synaptic transmission for statistical analysis of glutamatergic signals and their modulation (Chapter III).

Chapter II focuses on the characterization of PFCx and BLA inputs and reciprocal gating mechanism in the NAc. The NAc is considered to be a key mediator of the effects of drugs of abuse such as alcohol (Scofield et al., 2016). Within the NAc, MSNs serve as integrators of potentially conflicting cognitive and emotional information (Lara & Wallis, 2015; Wassum & Izquierdo, 2015), such as those coming from PFCx and BLA, respectively. The present study confirms that core NAc MSNs receive converging inputs from the PFCx and BLA. It was further established that the relative timing of input signals determines the subsequent MSN output. Thus, in EtOH-naïve mice, BLA and PFCx inputs reciprocally inhibit each other, but the strength of this reciprocal inhibition is asymmetric, with PFCx gating of BLA being stronger than the reverse (**Figure 2.2**). These findings extend

previous findings by Calhoon and O'Donnell showing bidirectional gating between thalamic and PFCx afferents in anesthetized rats (Calhoon & O'Donnell, 2013). We also found that even a single, very small PFCx-EPSP is capable of gating BLA input (**Figure 2.3**), showing high sensitivity of the gating phenomena. The phenomenon of this gating could be that, as EPSPs travel to the soma following synaptic induction distally, they get subjected to the strong filtering by the dendrites' cable properties, resulting in a depression of the detected EPSPs amplitude (Rall, 1959). The mechanism of gating is likely mediated by AMPA receptors, as neither DA receptors and mGluRs, nor NMDA receptors are recruited during synaptic gating (**Figure 2.5**), but could not be confirmed, as AMPA antagonists would block EPSPs, the very synaptic events we need to study gating.

It was proposed by Bechara and colleagues that hyperactivity of the "emotional" amygdala overriding the "executive" PFCx as the underlying cause of drug addiction (Bechara, 2005). In support of this theory, we found that stimulation of BLA, but not PFCx, projections to NAc abolished an increase in alcohol drinking behavior (**Figure 2.6**). Interestingly, using a Pavlovian conditioning protocol, Millan and colleagues reported that activation of the BLA to NAc pathway blocked alcohol consumption triggered by cue-conditioned alcohol-seeking behavior (Millan et al., 2017). Our results suggest that synaptic gating plays a role in circuit remodeling following alcohol exposure. Our electrophysiology data shows that two-week alcohol exposure strengthens BLA control of PFCx, while PFCx control of BLA remains unchanged (**Figure 2.6**). The alteration of BLA input to the NAc

responsible for modifying alcohol consumption behavior might be the result of changes in direct synapses with MSNs or the inhibition of PFCx projecting inputs to MSNs. Further studies are necessary to identify the exact mechanism and targets of this effect.

To further address the mechanism responsible for the modulation of glutamatergic synaptic transmission in NAc MSNs in EtOH-naïve and binge alcohol drinking mice, I studied the role of the cholinergic interneurons. Because this work relied heavily on measuring spontaneous excitatory postsynaptic currents (sEPSCs), we developed a new statistical analysis detailed in Chapter III. Spontaneous synaptic events, such as amplitude and inter-event interval, are stochastic by nature and follow Poisson distribution (**Figure 3.1**). Most of studies have used a single value for the average of all events in a neuron and performed classical parametric statistics. There are two main problems with this approach: first, reducing 300+ events into a single value entails the major loss of information, since treatments can differentially affect small or large events. Some studies also perform the Kolmogorov-Smirnoff test to assess the “distribution” of the events. However, K-S test is a non-parametric test that assesses a single non-defined deviation between datasets, and is impossible to use if higher-order analysis with more than two groups (such as ANOVA) is required. Secondly, when a single average value of the neuron is taken for parametric statistics, such as t-test or one-way ANOVA, several neurons are usually recorded from the same slice, and several slices from the same animal, and these relationships are not considered

(Aarts et al., 2014; Yu et al., 2021). Therefore, 1) a data set was collected to determine hierarchical relationships between individual measurements (**Figure 3.1**), 2) a new hierarchical statistical approach was developed and tested to capture the distribution of the spontaneous events by dividing the timeline of all 300+ events per neuron into 10-15 equal intervals of 25 consecutive events and from each interval extracting median (50%), shoulders (25 and 75%) and extreme (5 and 95%) values (**Figure 3.3**); and 3) logarithmically transforming these Poisson distribution events to ensure that residuals adhere to a normal distribution and performing mixed-effect general linear model with animal ID, slice ID, neuron ID, and time interval as random variables (**Figures 3.2 and 3.4**). This approach was developed to enable statistical analysis on sEPSC data sets in Chapter IV after being validated on previously published data (**Figure 3.4**).

In Chapter IV I investigated the mechanism of local circuity control of glutamatergic inputs onto MSNs by cholinergic interneurons (ChIs). We found that optogenetic stimulation of ChIs attenuates spontaneous excitatory post-synaptic currents (sEPSCs) in MSNs expressing dopamine D1 and D2 receptors (D1- and D2-MSNs, respectively; **Figures 4.2 and 4.4**). Interestingly, only D2-MSNs displayed reduced evoked EPSPs by activation of ChIs (**Figure 4.5**). We further determined that while ChI stimulation decreases sEPSCs in both D1- and D2-MSNs, receptors mediating this change differed. In D1-MSNs, the decrease of sEPSC frequency required activation of the DA receptors, as well as mAChRs and nAChRs. In contrast, in D2-MSNs, the decrease of sEPSC frequency was not

affected by DA receptor blockers, indicating that glutamatergic inputs to D2-MSNs are regulated directly by cholinergic terminals (**Figure 4.6**).

After 2-week binge drinking exposure, cholinergic stimulation reversed from reduction to potentiation of sEPSCs in D1-MSN, while still attenuating D2-MSN EPSCs (**Figure 4.10**). This finding implies that alcohol facilitates a switch in cholinergic modulation of D1- vs. D2-MSN output, signifying potential direct vs. indirect pathways dysregulation. Furthermore, direct stimulation of ChIs in freely moving mice increased their alcohol consumption, while not affecting saccharin or water consumption or locomotor activity (**Figure 4.13**), indicating direct involvement of cholinergic interneurons in the alcohol consumption behavior. The remainder of this chapter will interpret the results of Chapter IV and discuss implication for future studies.

Cholinergic interneurons decrease glutamate release onto MSNs in the NAc

Our initial finding of ChI stimulation decreasing MSN spontaneous glutamatergic synaptic transmission was anticipated. Indeed, ACh-mediated inhibition of glutamate release in the striatum in pharmacological drug application was reported in several studies (Malenka & Kocsis, 1988; Barral et al., 1999; Higley et al., 2009; Licheri et al., 2018). A similar depression of glutamatergic synaptic transmission on evoked EPSCs was reported following direct stimulation of ChIs, and also found the effect to be presynaptic (Pakhotin & Bracci, 2007). However, a study by Calabresi and collegues showed postsynaptic mAChR activation on MSN

dendrites decreasing glutamate release (Calabresi et al., 2000). Interestingly, TTX was found to decrease both amplitude and frequency of miniature EPSCs (mEPSCs), and the presence of TTX abolished ACh-mediated decrease in glutamate release, indicating AP-dependency of this phenomenon (de Rover et al., 2002).

Surprisingly, while the decrease of spontaneous release was found in both D1- and D2-MSNs (**Figures 4.2 and 4.4**), we found a decrease in electrically evoked EPSPs (eEPSPs) only in D2-MSNs (**Figure 4.5**). Interestingly, Pakhotin and Bracci reported a decrease in eEPSPs only within 80 ms of ChI stimulation. In contrast, we found that ChI optogenetic stimulation decreased eEPSPs both *during* and four minutes *after* ChI stimulation (**Figure 4.5**). This effect is likely due to the difference in the methodology of ChI stimulation: Pakhotin and Bracci manually stimulated a single ChI, while we used optogenetic stimulation that likely synchronously activated many neurons (Pakhotin & Bracci, 2007). The other difference could be due to the differences between dorsal and ventral striatum circuitry and the receptors involved in ChI mediation of glutamate release (Stuber et al., 2010). We verified that the lack of effect in D1-MSNs was not the due to an off-target effect of electric stimulation by repeating the experiment with optogenetically evoked PFCx-mediated EPSPs with Chrimson. We saw no effect of ChI activation on glutamate release onto D1-MSNs from PFCx terminals (**Figure 4.8**). The findings that only D2-MSNs had a decrease in eEPSPs underscore the importance of differentiating D1- and D2-MSNs, as one study found that ChI

stimulation decreased evoked EPSPs (Pakhotin & Bracci, 2007), while another study found no effect (Lee et al., 2016), with both studies not differentiating D1- and D2-MSNs.

The differential effect of ChI stimulation on spontaneous *vs.* evoked glutamatergic transmission was surprising. Evoked responses capture action potential-dependent neurotransmission, or synchronyous neurotransmitter release; while spontaneous release happens independently of action potentials (Kavalali et al., 2015). And although both techniques measure glutamate release, some differences with molecular machinery and type of information they carry has been observed (Guzikovski & Kavalali, 2021). In terms of molecular machinery, it has been shown that evoked and spontaneous release involves distinct vesicle pools, different localization in the synaptic cleft, different subunits of the SNARE complexes, distinct post-synaptic targets and possibly different synapses (Guzikovski & Kavalali, 2021). In terms of information transfer, since evoked or synchronuous release is action potential- or stimulus-dependent, it has been associated with transmitting precise timing information across synapses, while spontaneous, or asynchronuous release was shown to be associated with short-term plasticity, homeostatic plasticity and synapse development (Guzikovski & Kavalali, 2021). Our findings that spontaneous EPSCs were affected by ChI stimulation in both D1- and D2-MSNs, while evoked EPSPs were affected by ChI stimulation only in D2-MSNs outlines that it is likely that ChIs have differential affect on MSNs depending on the type of information they are transmitting – plasticity in

both D1- and D2-MSNs, while modulating the precise timing of salient stimuli only to D2-MSNs. To better understand the role of ChIs in glutamatergic modulation, paired-pulse ratio (PPR) experiment would be insightful. PPR is recorded by having two consecutive evoked EPSCs at 50-400 ms intervals. Paired-pulse facilitation (PPF) is indicative of decrease of the probability of the neurotransmitter release, paired-pulse depression (PPD) is indicative of an increase in the probability of the neurotransmitter release presynaptically (Pennartz, Boeijinga, Kitai, & Lopes da Silva, 1991). Performing this experiment would further elucidate whether evoked responses act pre- or post-synaptically and the role of ChIs in controlling different types of gluamatergic neurotransmission.

We have determined that not only phasic, but tonic ChI stimulation decreased glutamate release (**Figure 4.7D-F**). The tonic stimulation was achieved by 2-minutes of continuous 20 Hz light activation. This same stimulation pattern was used for ChIs optogenetic stimulation in previous studies (Witten et al., 2010; Lee et al., 2016). We have determined that tonic stimulation is unnecessary and wreaks havoc in DA release (personal communication with Yanfeng Zhang, S. Cragg lab), and would be uninterpretable in terms of receptor activation versus desensitization, which is often the case with agonist application (Hendrickson et al., 2013). Therefore, our burst stimulation paradigm is physiological, as it is the burst of ChI activity that encodes incoming salient stimuli (Ding et al., 2010), and has a defined role in triggering DA release (**Figure 4.6**) (Threlfell et al., 2012; Cachope et al., 2012). Future experiments would need to establish the exact length

of the ChI activation effect. We have measured as long as 10 minutes post-stimulation and still observed a decrease in sEPSCs. It would be beneficial to measure the persistence of this effect at 20-40 minutes, the usual timeframe used for short-term, plasticity measurements, such as spike-timing dependent plasticity (STDP) (Ji et al., 2017).

To fully understand ChI modulation of glutamate release, it would be necessary to optogenetically inhibit ChIs and record spontaneous and evoked EPSCs. Although similar to antagonists, this study would determine the temporal effect of the ChI mechanism. Witten and colleagues have found that ChI inhibition increases firing of the majority of MSNs *in vivo*, therefore it would be very interesting to elucidate this mechanism *in vitro* and record D1- and D2-MSN spontaneous and evoked EPSCs after optogenetically silencing ChIs using ChAT.cre mouse line paired with AAV.DIO.Halorhodopsin virus injection into the NAc, or a ChAT.Halorhodopsin mouse line.

Finally, as reported in the literature (de Rover et al., 2002; de Rover, Lodder, Smidt, & Brussaard, 2006; Witten et al., 2010), ChIs modulate GABAergic IPSCs, but their effect on D1- vs. D2-MSNs is unknown. Therefore, experiments using the same ChI optogenetic stimulation protocol but recording IPSCs in D1- and D2-MSNs would determine whether ChIs exert their effect through GABAergic interneurons in concert with or in opposition to the glutamatergic effect, and whether differences exist between D1- and D2-MSN.

ChI stimulation has differential mechanism of action in D1- and D2-MSNs

When elucidating the ChI effects on MSNs, researchers rarely distinguish between D1- and D2-MSNs. Potential differences between dorsal and ventral striatum are also rarely considered. When examining ChI innervation of glutamatergic presynaptic transmission onto MSNs, several pathways have been reported and can be roughly divided between ChI terminals synapsing either directly onto glutamatergic terminals or indirectly, through DA terminals (Bonsi et al., 2011; Lim et al., 2014; Gonzales & Smith, 2015). Moreover, very scant evidence exists whether these innervations differ between D1- and D2-MSNs. Our results show that although ChI stimulation decreases glutamatergic transmission in both D1- and D2-MSNs, the mechanism is quite different (**Figure 4.6**). In D1-MSNs, ChI-mediated glutamate decrease was abolished by D1+D2 receptor antagonists, while in D2-MSNs, the presence of D1+D2 receptor antagonists did not affect ChI-mediated glutamate decrease, indicative that DA receptors only mediate ChI effect on D1-MSNs. Pharmacological application of mAChR agonists has been previously found to decrease sEPSC frequency (de Rover et al., 2002; Ding et al., 2010; Pancani et al., 2014). In both D1- and D2-MSNs, it has been found that mAChR agonist application decreases glutamate presynaptically (Ding et al., 2010; Pancani et al., 2014), but identifying the location of these receptors has been a challenge.

(a) *D1-MSN mechanism*: Our finding that ChI-mediated decrease of glutamate release was blocked by D1+D2 receptor antagonists points to ChI

synapsing onto VTA DA terminals, which, in turn, synapse onto glutamatergic presynaptic terminals. The fact that the nAChR blocker, mecamylamine, produced the same result confirms that DA receptor activation is mediated by ACh release (Exley et al., 2008; Exley & Cragg, 2008). It has long been established that ChI stimulation induces DA release in dorsal and ventral striatum (Threlfell et al., 2012; Cachope et al., 2012; Wang et al., 2014). Therefore, in D1-MSNs, ChI stimulation activated β2* nAChRs on DA terminals, which, in turn, released DA (Threlfell et al., 2012; Yorgason et al., 2017). Accordingly, several studies reported the expression of D1 receptors located presynaptically on glutamatergic terminals that inhibit excitatory synaptic potentials (Nicola et al., 1996; Nicola & Malenka, 1997; Nicola et al., 2000; Dumartin et al., 2007). Additionally, DA decreases glutamate release through D1 receptors located on corticoaccumbal terminals (Ciruela et al., 2006; Wang et al., 2012b), possibly by promoting adenosine efflux via A1 adenosine receptors (A1Rs) (Harvey & Lacey, 1997). Interestingly, we have shown that although either DA or nicotinic receptor blockade was required to abolish ChI-mediated glutamate decrease, it was not sufficient, as mAChR antagonist also abolished ChI effects on glutamate. mAChRs are known to filter DA signaling by decreasing low intensity DA release (DA releave evoked by low-frequncy electric stimuli, <10 Hz), but enhancing high intensity DA release (<20 Hz) (Threlfell et al., 2010; Threlfell & Cragg, 2011). mAChRs are also located on both DA and glutamatergic terminals. M5 mAChRs located on DA terminals were shown to enhance DA release (Grilli et al., 2008; Bendor et al., 2010; Kuroiwa et al., 2012),

while M2-4 mAChR located presynaptically on glutamatergic terminals directly decrease glutamate release, most likely by inhibition of P/Q-type VGCC and reduction of action potential–induced Ca^{2+} increases in the bouton (Calabresi et al., 2000; Higley et al., 2009; Pancani et al., 2014).

(b) *D2-MSN mechanism*: As opposed to D1-MSNs, where DA receptor antagonists block ChI control of glutamate release, in D2-MSNs, ChI stimulation still decreased glutamate release in the presence of DA receptor antagonists (**Figure 4.6**). These results point to ChIs acting directly on cholinergic receptors on glutamatergic terminals, and not through DA receptors. Accordingly, we found that the application of mAChR antagonist atropine abolished the ChI-mediated glutamate decrease, an observation supported by previous studies of mAChRs located directly on glutamatergic terminals and similarly decreasing glutamate release (Calabresi et al., 2000; Higley et al., 2009; Ding et al., 2010; Pancani et al., 2014). Interestingly, we have found that blocking nAChR also abolished ChI-mediated glutamate release, however, unlike all the other antagonists, bath application of nAChR antagonist mecamylamine significantly decreased glutamate release, indicating that nAChRs are sensitive to baseline, tonic ACh level. These nAChRs are likely located on glutamatergic terminals, as application of DA receptor antagonists did not change sEPSCs frequency. This result aligns with previous findings that nAChRs located on glutamatergic terminals enhance glutamate release (Grilli et al., 2008; Zappettini et al., 2014; Blomeley, Cains, & Bracci, 2015). Therefore, it is likely that after our bath mecamylamine application,

glutamate decrease reached a “floor effect” and could not be further affected by ChI stimulation. We have also found that unlike spontaneous EPSCs, ChI-mediated decrease in evoked EPSPs was blocked by DA and AChR antagonists in D2-MSNs. This difference between the receptors mediating ChI effect on spontaneous versus evoked glutamate release exemplifies the complexity of cholinergic modulatory mechanisms. The likely explanation is that the decrease of evoked EPSPs stemmed from ACh direct and indirect action on post-synaptic ACh and DA receptors on the MSNs, as well as D2 receptors on ChIs (Lim et al., 2014).

Interestingly, while $\alpha4\beta2$ nAChRs appear to act as a “brake” for glutamate release, $\alpha7$ nAChRs enhance glutamate release (Howe et al., 2016; Assous, 2021; Campos, Alfonso, & Durán, 2010), and while 1 μM and 10 μM of nicotine was shown to decrease sEPSCs frequency (Licheri et al., 2018), 30 μM caused potentiation of glutamatergic transmission (Zappettini et al., 2014). We have found that bath mecamylamine application only affects D2-MSNs, while ChI stimulation decreases glutamate release on both D1- and D2-MSNs, thus providing a partial explanation for how different subpopulations could give contrasting results. Finally, other pathways, such as nitric oxide (Blomeley et al., 2015) and nAChRs located on astrocytes have been shown to decrease glutamate release (Licheri et al., 2018). These results emphasize the important caveats when interpreting data from bath application of receptor agonists and optogenetic stimulations of neurons while determining the effect on said receptors, as well as the importance of distinguishing D1- and D2-MSNs in the striatum.

To determine whether D1 or D2 receptors mediated ChI effect, follow up experient with application of either D1 (SCH-23390) or D2 (sulpiride) receptor antagonists are required. However, these experiments will not determine the location of DA receptors. To verify that DA receptors on the presynaptic glutmatergic incoming terminals are involved and whether different receptors are located on different inputs to D1- vs. D2-MSNs, usage of mouse transgenic lines would be necessary. To test for the presence of the D1 receptor, $Drd1^{loxP}$ mouse line would be used in conjunction with AAV.cre virus (or specific VGlut promoter cre virus) that would be injected into the nuclei projecting glutamatergic terminals into the NAc, such as PFCx, BLA or Hippocampus. $Drd1^{loxP}$ mouse line would be crossed with ChAT.ChR2 line to stimualate ChIs and DrD2.tdTomato to distinguish D1- and D-MSNs. Following virus expression, the cre virus would disrupt D1 receptor functioning, but only in incoming glutamatergic terminals and ChIs would be stimulated as in previous experiments. The experimental condition with the dysregulated D1 receptor on the glutamatergic transmission would be compared to condition with the intact D1 receptor glutamatergic transmission in D1- and D2-MSNs following ChI optogenetic stimulation. Alternatively, $Drd1^{loxP}$ could be crossed with VGlut1-IRES-Cre knock-in mouse line to eliminate repeated viral injection and thus specifically disrupt D1 receptor function in all of the glutamatergic projections. The caviat of this approach is the fact that all the mice would lack functional D1 receptors their whole life and could show compensatory mechanism. To alleviate that, conditional cre mice line could be used. To

determine whether ChI effect involves D2 receptors on glutamatergic terminals, the above experiment would be repeated with Drd2$^{loxP/loxP}$ mouse line (combined with same cre virus injection), crossed with ChAT.ChR2.eYFP and DrD1.tdTomato, to still be able to distinguish D1- and D2-MSNs. To determine whether the effect of ChIs on evoked glutamate release involves D1 or D2 receptors, the above experiments (with DA receptors floxed mice) would be combined with injection of Chrimson virus into PFCx or other nuclei projecting to the NAc and recording optogenetically evoked EPSPs from D1- or D2-MSNs.

Finally, it is possible that the observed effects or lack of changes during recording were caused by uncontrolled variables, such as recording conditions (temperature, timing, cell health, etc), drug efficacies, or adequate statistical power for analysis. Some variables, such as ChR2 activation with light has been verified and other variables were addressed in Chapter III, such as experimenter, timing and statistical analysis. Other limitations, however, still could have given confounding results, such as drug efficacy, which has not been tested in this data set and used at the concentrations reported in the literature. Further experiments testing the efficacy of the antagonists would be beneficial to validate these results.

Binge alcohol drinking changes ChI excitability

Given our intriguing findings about ChI modulation of glutamatergic transmission, the effect of alcohol on ChI excitability was determined. To investigate how ChIs are affected by alcohol, we recorded ChI firing in naïve and binge-alcohol drinking

mice. As can be seen in **Figure 4.5,** while 68% of naïve ChIs were spontaneous firing, alcohol reduced that number to 24%, indicating a reduction in cholinergic tone. This finding could be explained by the reported reduction of ChI firing rate following acute alcohol administration (Blomeley et al., 2011). However, this could also be explained by a reported increase of ChI firing after acute alcohol administration (Yorgason et al., 2022), as a compensatory mechanism after 2 weeks of alcohol exposure. It has been reported that after 30 days of intermittent alcohol exposure, the number and density of ChIs is reduced (Vetreno, Broadwater, Liu, Spear, & Crews, 2014; Galaj, Kipp, Floresco, & Savage, 2019), therefore, although initial ethanol exposure could increase ChIs excitability as measured by firing increases (Yorgason et al., 2022) and an increase in c-Fos immunoreactivity (Herring et al., 2004), the longer-term effect of alcohol seems to attenuate ChI transmission (Pereira et al., 2014). Therefore, the possible mechanism could be that after repeated alcohol exposure, there is a decrease of ChI firing, which in turn decreases ChI control over DA release. This dysregulation of DA release would have opposing effects on D1 and D2 receptors, thus leading to the imbalance between the two pathways.

However, the direct effect of alcohol on ChI excitability was not tested, and whether ChIs respond differently to first versus repeated alcohol exposure. The observed decrease of ChIs firing after 2-week mice alcohol consumption could be caused not by alcohol itself, but by the 24-hour withdrawal after the last drinking bout. To test this hypothesis, brain slices would be extracted immediately after the

last drinking bout, and 50 mM of ethanol would be added to all the solutions and during recordings, as this concentration is closest to 0.08% BAC. Recording ChIs firing rate at these conditions of acute alcohol presence would most closely capture the effects of alcohol on ChIs excitability during alcohol consumption. These results would be compared to recordings of ChIs firing without bath alcohol after 2-week binge drinking, ChI firing with acute bath alcohol in naïve mice and ChI firing after first day of 2-hour alcohol exposure to determine the timing of the alcohol effect on ChI excitability.

ChI control of the D1/D2 MSNs output balance is altered by binge alcohol drinking

We found that optogenetic stimulation of ChIs *in vivo* increased alcohol consumption in the first four days of exposure (**Figure 4.13**). This finding is in accordance with other studies reporting ChI stimulation having a reinforcing effect on drugs of abuse such as cocaine (Witten et al., 2010; Lee et al., 2016). Interestingly, our *ex vivo* study elucidated that binge alcohol drinking reversed the ChI control of glutamate release in D1-MSNs from attenuation to potentiation with no change in D2-MSNs, which were still attenuated (**Figure 4.10**). These observations provide a potential explanation for the observed increase in consumption: potentiation of D1-MSN excitability has been associated with an increase in alcohol consumption (Renteria, Buske, & Morrisett, 2018; Kircher et al., 2019; Strong et al., 2020), while D2-MSN activation had no impact on alcohol

consumption (Strong et al., 2020). Interestingly, Wang and collegues reported that alcohol exposure increased glutamatergic transmission in D1-, but not D2-MSNs in the dorsal striatum (Wang et al., 2015). We have observed an increase in D1-, but not D2-MSN glutamatergic transmission only after ChI stimulation with no differences between naïve and DID sEPSCs (**Figure 4.11J**). This is possibly because of stronger ChI control over MSN output in ventral, compared to dorsal striatum (Threlfell & Cragg, 2011; Gonzales & Smith, 2015; Marche, Martel, & Apicella, 2017). Moreover, it was reported that previous alcohol consumption potentiated both excitatory glutamatergic transmission in D1-MSNs and inhibitory GABAergic transmission in D2-MSNs (Cheng et al., 2017). Interestingly, ChIs were also found to increase GABAergic transmission (de Rover et al., 2002; de Rover et al., 2006; Witten et al., 2010), which is how they could be controlling D2-MSNs following alcohol exposure. Assessing the effect of ChI stimulation on GABAergic transmission onto D1- and D2-MSNs would involved recording spontaneous inhibitory post-synaptic currents (sIPSCs) and would be achieved by recoridngs in the presence of glutamtergic transmission blockers. It would be expected that ChI effect on sIPSCs would be directly opposite of the effect on sEPSCs: ChI stimulation would increase sIPSCs and ChI inhibition would decrease sIPSCs. It would be especially important to discern the effect of ChI stimulation and inhibition on D1- vs. D2-MSNs in naïve and DID mice, as this has not been reported in literature.

Based on our findings, it is likely that ChIs drive the D1-/D2-MSN differentiation and strengthen D1-MSN pathway after 2-week alcohol exposure. This finding also explains why cholinergic blockers decrease alcohol consumption: numerous studies showed that nAChR antagonists decrease alcohol consumption when administered systemically i.p. (Ericson et al., 2009; Hendrickson et al., 2009; Hendrickson et al., 2010; Hendrickson et al., 2013), as well as nAChR antagonists application directly into the NAc (Feduccia et al., 2014). Therefore, it is likely that ChIs regulate alcohol-induced modulation of striatal output (Adermark et al., 2011b). Consistent with this, we found that binge alcohol drinking altered ChI control of D1-MSN excitability, and this change was blocked by AChR antagonists (**Figure 4.12**). A big difference between our *ex vivo* DID recordings and *in vivo* alcohol consumption was timing of alcohol exposure, since ChI effect on MSN excitability was observed after two weeks of drinking (**Figure 4.10**), while ChI stimulation *in vivo* increased alcohol consumption during the first hour of alcohol consumption (**Figure 4.13**). Initial hypothesis that even one hour of ChI stimulation would produce long-lasting changes in glutamatergic transmission was disproven when alcohol consumption was no longer increased in the absence of ChI stimulation (**Figure 4.14E**). Alternatively, repeated alcohol exposure could alter ChI effect on GABAergic neurotransmission from GABAergic INs onto MSNs, since alcohol is known to potentiate nAChR and GABAA receptors (Olsen et al., 2014). Repeated alcohol exposure was shown to alter the activity of mAChR (Costa & Guizzetti, 1999) and increase the release of [^{3}H]ACh (Nestby et al., 1997;

Nestby et al., 1999). We further found that ChI-mediated increase in glutamatergic transmission in D1-MSNs in DID mice was also DA-dependent, as ChI effect in the presence of DA receptor antagonists was reversed back to the naïve state (**Figures 4.12, 4.10 and 4.2**), again emphasizing DA as being the key player in alcohol effects on the striatal output (Clarke & Adermark, 2015).

Unlike spontaneous EPSCs, in evoked EPSPs alcohol treatment abolished ChI-induced glutamate attenuation in D2-MSNs, with no effect on evoked EPSPs in D1-MSNs (**Figure 4.7**), emphasizing the differential effect of ChI stimulation on spontaneous versus evoked glutamate release. Interestingly, although most studies posit that D1-MSNs activity primarily mediates approach behaviors while D2-MSNs are involved in aversion and punishment (Hikida et al., 2016), recent studies outline that both D1- and D2-MSNs are involved in reward and aversion behaviors (Soares-Cunha et al., 2020). Furthermore, activation of D2-MSNs increases motivational behavior (Soares-Cunha et al., 2018), while application of both, D1 and D2 receptor antagonists together, but not separately, reduces quinine resistant EtOH drinking (Sneddon, Schuh, Frankel, & Radke, 2021). Therefore, ChI control of different modes of glutamatergic transmission, such as evoked or spontaneous, could encode different aspects of motivated behavior by D1-/D2-MSNs. Furthermore, our observed silencing of ChI firing after DID exposure could feed into a feedback loop, where ChI stimulation increases alcohol consumption, which in turn decreases ChI firing and promotes other compensatory mechanisms, such as DA dysregulation.

Althouth we have recorded ChI effect on glutmatergic transmission in DID mice (24 hours after the last drinking session) and immediately after the last drinking session (IR-DID), it could not be ruled out that observed effect could be due not to alcohol itself, but to the alcohol removal. To address this possibility, recordings need to be performed in the presence of acute EtOH in the bath (50 mM) in the naïve and DID-exposed mice. In the case of the DID-exposed mice, recordings performed immediately after the last drinking bout need to be performed on the brain slices continuously exposed to EtOH in the bath, as to not trigger alcohol withdrawal processes.

To understand why alcohol treatment preferentially altered ChI modulation of D1- and not D2-MSNs, several hypotheses should be considered. Alcohol treatment enhances postsynaptic D1 receptor-electrically stimulated cAMP production (Nestby et al., 1999), and EtOH drinking increases the prevalence of dendritic spines and dendritic shaft diameter of medium spiny neurons in the NAc (Uys et al., 2016), signaling an increase in synaptic connectivity. ChI stimulation increases DA release, and while many studies found moderate-to-high EtOH concentrations to decrease evoked DA release (Yorgason et al., 2022), others found an increase in DA after EtOH exposure (Nestby et al., 1997; Nestby et al., 1999; Loftén et al., 2020). This discrepancy has been attributed to different factors, such as frequency of DA stimulation (Robinson et al., 2009; Yorgason et al., 2014), the concentration of EtOH (Gao et al., 2019), and the amount of days of alcohol exposure: during the 2nd day of drinking DA transients were decreased, but during

the 9th day of drinking DA transients were increased in the NAc (Liu et al., 2020). ChIs are likely to be mediating alcohol effects on DA and DA receptors, since alcohol-induced DA elevation was blocked by the combination of muscarinic and nicotinic antagonists (Loftén et al., 2020) and cholinergic depletion decreased alcohol-induced DA elevation (Loftén et al., 2020). A future experiment is necessary to determine the effect of ChI-mediated DA release after 2-week binge alcohol drinking. The follow up experiment would be to record ChI-evoked DA transients using FSCV in the slices of naïve and DID mice. Moreover, to answer whether acute alcohol has an effect of ChI-evoked DA transients, the recordings in naïve and DID slices have to be also made before and in the presence of acute alcohol in the bath, as outlined above for the ChI recording conditions. To further elucidate and settle some of the disparities in the field regarding alcohol effect on DA and ACh, experiments involving DA release and concentration during DID paradigm would be necessary, such as *in vivo* voltammetry measuring DA release and GCaMP photometry recording from ChIs in the NAc during the alcohol consumption tasks.

Finally, as opposed to the study by Witten and collegues who found opposing effects on cocaine preference during ChI stimulation and inhibition (Witten et al., 2010), we could not decrease alcohol intake by optogenetic ChI silencing (**Figure 4.14F**). This could be due to several factors, such as a) a “floor effect”, since our control mice consumed scant amount of alcohol, therefore could not be further inhibited, b) insufficient silencing of interneurons, since the

uninfected ChIs would still be firing, and c) inherent differences between cocaine and alcohol mechanism of action. Additionally, the inherent caviat of this behavioral setup was that mice were tethered to the optic fiber cables throughout the optogenetic stimulation protocol and this discomfort suppressed alcohol consumption compared to unconnected mice (Ji et al., 2017). Despite mice habituating to the connecting cables for four days and for one hour every day prior to the drinking session, the alcohol intake was increased by all groups of mice when the cables were removed on the 5th day of drinking (**Figure 4.14E, F**). The same pattern of decreased drinking was observed when mice got tethered to the cables on day nine of drinking versus eight days of drinking untethered (**Figure 4.14G**). Although this cable attachment artifact could not be alleviated, increased precision of ChI activation could lessen the impact of this caviat. To do that, it is necessary to determine the precise timing of ChI activation during mouse drinking behavior (e.g. before, during or after the drinking bout) and whether it changes depending on the day of alcohol exposure. This can be achieved by GCaMP photometry recording of ChIs activation during DID paradigm and then delivering ChI stimulation or inhibition only during ChI activation phases.

To further validate that ChI optogenetic stimulation changes glutamatergic synaptic neurotransmission in D1-/D2-MSNs, future experiments would involve recording from MSNs in mice that had ChIs stimulated during alcohol exposure. To elucidate which receptors are most important for ChI effects on alcohol consumption, *in vivo* experiments involving application of different DAergic and

cholinergic antagonists during optogenetic ChI stimulation is necessary. Importantly, the antagonists need to be applied to NAc specifically, and not systemically, as other areas such as VTA would contribute to drinking behavior (Hendrickson et al, 2013). To do that, cannulas consisting of connecting ports for AChR and DA receptors antagonists application and optogenetic fibers need to be implanted for behavioral experiments. Finally, a potential caveat to many current optogenetic experiments is that the same stimulation pattern is used whether the mouse is drinking or not. To circumvent this problem, a closed-loop optogenetic strategy is necessary for stimulation or inhibition of ChIs only when the mouse is drinking. This pattern of stimulation or inhibition would recapitulate conditioning that takes place during learning and could lead to an alcohol use disorder.

Conclusions

This study delineates a new understanding of the NAc circuitry and its effect on alcohol behavior: It is likely that alcohol induces DA release, which drives further alcohol consumption, and since ChI activation is what mediates this DA release, when ChIs are stimulated *in vivo*, more DA is released, contributing to a feedback loop. Therefore, after 2-weeks of alcohol consumption, ChIs preferentially and repeatedly potentiate D1-MSNs, which leads to imbalance between D1- and D2-MSNs, “go” and “no-go” pathways, and increased alcohol consumption over time (Koob & Volkow, 2016). Novel therapies aimed at blocking AChR and ChI firing may be beneficial for reducing alcohol use disorder.

Bibliography

Aalto, S., Ingman, K., Alakurtti, K., Kaasinen, V., Virkkala, J., Någren, K., Scheinin, H. (2015). Intravenous ethanol increases dopamine release in the ventral striatum in humans: PET study using bolus-plus-infusion administration of [(11)C]raclopride. *J Cereb Blood Flow Metab*, *35*(3), 424-431. doi:10.1038/jcbfm.2014.209

Aarts, E., Verhage, M., Veenvliet, J. V., Dolan, C. V., & van der Sluis, S. (2014). A solution to dependency: using multilevel analysis to accommodate nested data. *Nat Neurosci*, *17*(4), 491-496. doi:10.1038/nn.3648

Abrahao, K. P., Salinas, A. G., & Lovinger, D. M. (2017). Alcohol and the Brain: Neuronal Molecular Targets, Synapses, and Circuits. *Neuron*, *96*(6), 1223-1238. doi:10.1016/j.neuron.2017.10.032

Abudukeyoumu, N., Hernandez-Flores, T., Garcia-Munoz, M., & Arbuthnott, G. W. (2019). Cholinergic modulation of striatal microcircuits. *Eur J Neurosci*, *49*(5), 604-622. doi:10.1111/ejn.13949

Ade, K. K., Wan, Y., Chen, M., Gloss, B., & Calakos, N. (2011). An Improved BAC Transgenic Fluorescent Reporter Line for Sensitive and Specific Identification of Striatonigral Medium Spiny Neurons. Front Syst Neurosci, 5, 32. doi:10.3389/fnsys.2011.00032

Adermark, L., Clarke, R. B., Olsson, T., Hansson, E., Söderpalm, B., & Ericson, M. (2011a). Implications for glycine receptors and astrocytes in ethanol-induced elevation of dopamine levels in the nucleus accumbens. *Addict Biol*, *16*(1), 43-54. doi:10.1111/j.1369-1600.2010.00206.x

Adermark, L., Clarke, R. B., Söderpalm, B., & Ericson, M. (2011b). Ethanol-induced modulation of synaptic output from the dorsolateral striatum in rat is regulated by cholinergic interneurons. *Neurochem Int*, *58*(6), 693-699. doi:10.1016/j.neuint.2011.02.009

Albin, R. L., Young, A. B., & Penney, J. B. (1989). The functional anatomy of basal ganglia disorders. *Trends Neurosci*, *12*(10), 366-375. doi:10.1016/0166-2236(89)90074-x

Albuquerque, E. X., Pereira, E. F., Castro, N. G., Alkondon, M., Reinhardt, S., Schröder, H., & Maelicke, A. (1995). Nicotinic receptor function in the mammalian central nervous system. Ann N Y Acad Sci, 757, 48-72. doi:10.1111/j.1749-6632.1995.tb17464.x

Albuquerque, E. X., Pereira, E. F., Alkondon, M., & Rogers, S. W. (2009). Mammalian nicotinic acetylcholine receptors: from structure to function. *Physiol Rev*, *89*(1), 73-120. doi:10.1152/physrev.00015.2008

Alexander, G. E., & Crutcher, M. D. (1990). Functional architecture of basal ganglia circuits: neural substrates of parallel processing. *Trends Neurosci*, *13*(7), 266-271. doi:10.1016/0166-2236(90)90107-l

Aosaki, T., Kimura, M., & Graybiel, A. M. (1995). Temporal and spatial characteristics of tonically active neurons of the primate's striatum. *J Neurophysiol*, *73*(3), 1234-1252. Retrieved from

https://www.ncbi.nlm.nih.gov/entrez/query.fcgi?cmd=Retrieve&db=PubMed&dopt=Citation&list_uids=7608768

Aosaki, T., Miura, M., Suzuki, T., Nishimura, K., & Masuda, M. (2010). Acetylcholine-dopamine balance hypothesis in the striatum: an update. *Geriatr Gerontol Int*, *10 Suppl 1*, S148-57. doi:10.1111/j.1447-0594.2010.00588.x

Aosaki, T., Tsubokawa, H., Ishida, A., Watanabe, K., Graybiel, A. M., & Kimura, M. (1994). Responses of tonically active neurons in the primate's striatum undergo systematic changes during behavioral sensorimotor conditioning. *J Neurosci*, *14*(6), 3969-3984. Retrieved from https://www.ncbi.nlm.nih.gov/entrez/query.fcgi?cmd=Retrieve&db=PubMed&dopt=Citation&list_uids=8207500

Aschauer, D. F., Kreuz, S., & Rumpel, S. (2013). Analysis of transduction efficiency, tropism and axonal transport of AAV serotypes 1, 2, 5, 6, 8 and 9 in the mouse brain. *PLoS One*, *8*(9), e76310. doi:10.1371/journal.pone.0076310

Assous, M. (2021). Striatal cholinergic transmission. Focus on nicotinic receptors' influence in striatal circuits. *Eur J Neurosci*, *53*(8), 2421-2442. doi:10.1111/ejn.15135

Atallah, H. E., McCool, A. D., Howe, M. W., & Graybiel, A. M. (2014). Neurons in the ventral striatum exhibit cell-type-specific representations of outcome during learning. *Neuron*, *82*(5), 1145-1156. doi:10.1016/j.neuron.2014.04.021

Barral, J., Galarraga, E., & Bargas, J. (1999). Muscarinic presynaptic inhibition of neostriatal glutamatergic afferents is mediated by Q-type Ca2+ channels. *Brain Res Bull*, *49*(4), 285-289. doi:10.1016/s0361-9230(99)00061-1

Bassareo, V., Cucca, F., Frau, R., & Di Chiara, G. (2017). Changes in Dopamine Transmission in the Nucleus Accumbens Shell and Core during Ethanol and Sucrose Self-Administration. *Front Behav Neurosci*, *11*, 71. doi:10.3389/fnbeh.2017.00071

Beaulieu, J. M., & Gainetdinov, R. R. (2011). The physiology, signaling, and pharmacology of dopamine receptors. *Pharmacol Rev*, *63*(1), 182-217. doi:10.1124/pr.110.002642

Bechara, A. (2005). Decision making, impulse control and loss of willpower to resist drugs: a neurocognitive perspective. *Nat Neurosci*, *8*(11), 1458-1463. doi:10.1038/nn1584

Beckley, J. T., Laguesse, S., Phamluong, K., Morisot, N., Wegner, S. A., & Ron, D. (2016). The First Alcohol Drink Triggers mTORC1-Dependent Synaptic Plasticity in Nucleus Accumbens Dopamine D1 Receptor Neurons. *J Neurosci*, *36*(3), 701-713. doi:10.1523/JNEUROSCI.2254-15.2016

Bendor, J., Lizardi-Ortiz, J. E., Westphalen, R. I., Brandstetter, M., Hemmings, H. C., Sulzer, D., . . . Greengard, P. (2010). AGAP1/AP-3-dependent endocytic recycling of M5 muscarinic receptors promotes dopamine release. *EMBO J*, *29*(16), 2813-2826. doi:10.1038/emboj.2010.154

Bennett, B. D., Callaway, J. C., & Wilson, C. J. (2000). Intrinsic membrane properties underlying spontaneous tonic firing in neostriatal cholinergic interneurons. *J Neurosci*, *20*(22), 8493-8503. Retrieved from https://www.ncbi.nlm.nih.gov/entrez/query.fcgi?cmd=Retrieve&db=PubMed&dopt=Citation&list_uids=11069957

Bennett, B. D., & Wilson, C. J. (1998). Synaptic regulation of action potential timing in neostriatal cholinergic interneurons. *J Neurosci*, *18*(20), 8539-8549. Retrieved from https://www.ncbi.nlm.nih.gov/entrez/query.fcgi?cmd=Retrieve&db=PubMed&dopt=Citation&list_uids=9763496

Bennett, B. D., & Wilson, C. J. (1999). Spontaneous activity of neostriatal cholinergic interneurons in vitro. *J Neurosci*, *19*(13), 5586-5596. Retrieved from https://www.ncbi.nlm.nih.gov/entrez/query.fcgi?cmd=Retrieve&db=PubMed&dopt=Citation&list_uids=10377365

Berlanga, M. L., Olsen, C. M., Chen, V., Ikegami, A., Herring, B. E., Duvauchelle, C. L., & Alcantara, A. A. (2003). Cholinergic interneurons of the nucleus accumbens and dorsal striatum are activated by the self-administration of cocaine. *Neuroscience*, *120*(4), 1149-1156. Retrieved from https://www.ncbi.nlm.nih.gov/entrez/query.fcgi?cmd=Retrieve&db=PubMed&dopt=Citation&list_uids=12927219

Berridge, K. C. (2007). The debate over dopamine's role in reward: the case for incentive salience. *Psychopharmacology (Berl)*, *191*(3), 391-431. doi:10.1007/s00213-006-0578-x

Bliss, T. V., & Lomo, T. (1973). Long-lasting potentiation of synaptic transmission in the dentate area of the anaesthetized rabbit following stimulation of the perforant path. *J Physiol*, *232*(2), 331-356. doi:10.1113/jphysiol.1973.sp010273

Blomeley, C. P., Cains, S., & Bracci, E. (2015). Dual Nitrergic/Cholinergic Control of Short-Term Plasticity of Corticostriatal Inputs to Striatal Projection Neurons. *Front Cell Neurosci*, *9*, 453. doi:10.3389/fncel.2015.00453

Blomeley, C. P., Cains, S., Smith, R., & Bracci, E. (2011). Ethanol affects striatal interneurons directly and projection neurons through a reduction in cholinergic tone. *Neuropsychopharmacology*, *36*(5), 1033-1046. doi:10.1038/npp.2010.241

Bodhinathan, K., & Slesinger, P. A. (2013). Molecular mechanism underlying ethanol activation of G-protein-gated inwardly rectifying potassium channels. *Proc Natl Acad Sci U S A*, *110*(45), 18309-18314. doi:10.1073/pnas.1311406110

Boileau, I., Assaad, J. M., Pihl, R. O., Benkelfat, C., Leyton, M., Diksic, M., . . . Dagher, A. (2003). Alcohol promotes dopamine release in the human nucleus accumbens. *Synapse*, *49*(4), 226-231. doi:10.1002/syn.10226

Bolam, J. P., Wainer, B. H., & Smith, A. D. (1984). Characterization of cholinergic neurons in the rat neostriatum. A combination of choline acetyltransferase immunocytochemistry, Golgi-impregnation and electron microscopy. Neuroscience, 12(3), 711-718. doi:10.1016/0306-4522(84)90165-9

Bonsi, P., Cuomo, D., Martella, G., Madeo, G., Schirinzi, T., Puglisi, F., . . . Pisani, A. (2011). Centrality of striatal cholinergic transmission in Basal Ganglia function. *Front Neuroanat*, *5*, 6. doi:10.3389/fnana.2011.00006

Brady, A. M., Glick, S. D., & O'Donnell, P. (2005). Selective disruption of nucleus accumbens gating mechanisms in rats behaviorally sensitized to methamphetamine. *J Neurosci*, *25*(28), 6687-6695. doi:10.1523/JNEUROSCI.0643-05.2005

Brady, A. M., & O'Donnell, P. (2004). Dopaminergic modulation of prefrontal cortical input to nucleus accumbens neurons in vivo. *J Neurosci*, *24*(5), 1040-1049. doi:10.1523/JNEUROSCI.4178-03.2004

Brimblecombe, K. R., Threlfell, S., Dautan, D., Kosillo, P., Mena-Segovia, J., & Cragg, S. J. (2018). Targeted Activation of Cholinergic Interneurons Accounts for the Modulation of Dopamine by Striatal Nicotinic Receptors. *eNeuro*, *5*. doi:10.1523/ENEURO.0397-17.2018

Britt, J. P., Benaliouad, F., McDevitt, R. A., Stuber, G. D., Wise, R. A., & Bonci, A. (2012). Synaptic and behavioral profile of multiple glutamatergic inputs to the nucleus accumbens. *Neuron*, *76*(4), 790-803. doi:10.1016/j.neuron.2012.09.040

Brog, J. S., Salyapongse, A., Deutch, A. Y., & Zahm, D. S. (1993). The patterns of afferent innervation of the core and shell in the "accumbens" part of the rat ventral striatum: immunohistochemical detection of retrogradely transported fluoro-gold. *J Comp Neurol*, *338*(2), 255-278. doi:10.1002/cne.903380209

Brown, M. T., Tan, K. R., O'Connor, E. C., Nikonenko, I., Muller, D., & Lüscher, C. (2012). Ventral tegmental area GABA projections pause accumbal cholinergic interneurons to enhance associative learning. *Nature*, *492*(7429), 452-456. doi:10.1038/nature11657

Brown, P., & Molliver, M. E. (2000). Dual serotonin (5-HT) projections to the nucleus accumbens core and shell: relation of the 5-HT transporter to amphetamine-induced neurotoxicity. *J Neurosci*, *20*(5), 1952-1963. Retrieved from https://pubmed.ncbi.nlm.nih.gov/10684896

Budygin, E. A., Phillips, P. E., Wightman, R. M., & Jones, S. R. (2001). Terminal effects of ethanol on dopamine dynamics in rat nucleus accumbens: an in vitro voltammetric study. *Synapse*, *42*(2), 77-79. doi:10.1002/syn.1101

Burkhardt, J. M., & Adermark, L. (2014). Locus of onset and subpopulation specificity of in vivo ethanol effect in the reciprocal ventral tegmental area-nucleus accumbens circuit. *Neurochem Int*, *76*, 122-130. doi:10.1016/j.neuint.2014.07.006

Cachope, R., Mateo, Y., Mathur, B. N., Irving, J., Wang, H. L., Morales, M., . . . Cheer, J. F. (2012). Selective activation of cholinergic interneurons enhances accumbal phasic dopamine release: setting the tone for reward processing. *Cell Rep*, *2*(1), 33-41. doi:10.1016/j.celrep.2012.05.011

Calabresi, P., Centonze, D., Gubellini, P., Pisani, A., & Bernardi, G. (2000). Acetylcholine-mediated modulation of striatal function. *Trends Neurosci*, *23*(3), 120-126. Retrieved from https://www.ncbi.nlm.nih.gov/entrez/query.fcgi?cmd=Retrieve&db=PubMed&dopt=Citation&list_uids=10675916

Calhoon, G. G., & O'Donnell, P. (2013). Closing the gate in the limbic striatum: prefrontal suppression of hippocampal and thalamic inputs. *Neuron*, *78*(1), 181-190. doi:10.1016/j.neuron.2013.01.032

Callaway, C. W., Hakan, R. L., & Henriksen, S. J. (1991). Distribution of amygdala input to the nucleus accumbens septi: an electrophysiological investigation. *Journal of Neural Transmission …*. Retrieved from https://link.springer.com/article/10.1007/BF01253391

Campos, F., Alfonso, M., & Durán, R. (2010). In vivo modulation of alpha7 nicotinic receptors on striatal glutamate release induced by anatoxin-A. *Neurochem Int*, *56*(6-7), 850-855. doi:10.1016/j.neuint.2010.03.010

Cardinal, R. N., & Everitt, B. J. (2004). Neural and psychological mechanisms underlying appetitive learning: links to drug addiction. *Curr Opin Neurobiol*, *14*(2), 156-162. doi:10.1016/j.conb.2004.03.004

Cardinal, R. N., Parkinson, J. A., Hall, J., & Everitt, B. J. (2002). Emotion and motivation: the role of the amygdala, ventral striatum, and prefrontal cortex. *Neurosci Biobehav Rev*, *26*(3), 321-352. doi:10.1016/s0149-7634(02)00007-6

Carelli, R. M., & Ijames, S. G. (2000). Nucleus accumbens cell firing during maintenance, extinction, and reinstatement of cocaine self-administration behavior in rats. *Brain Res*, *866*(1-2), 44-54. doi:10.1016/s0006-8993(00)02217-4

Carpenedo, R., Pittaluga, A., Cozzi, A., Attucci, S., Galli, A., Raiteri, M., & Moroni, F. (2001). Presynaptic kynurenate-sensitive receptors inhibit glutamate release. *Eur J Neurosci*, *13*(11), 2141-2147. doi:10.1046/j.0953-816x.2001.01592.x

Chanaday, N. L., & Kavalali, E. T. (2018). Presynaptic origins of distinct modes of neurotransmitter release. Curr Opin Neurobiol, 51, 119-126. doi:10.1016/j.conb.2018.03.005

Cheng, Y., Huang, C. C. Y., Ma, T., Wei, X., Wang, X., Lu, J., & Wang, J. (2017). Distinct Synaptic Strengthening of the Striatal Direct and Indirect Pathways Drives Alcohol Consumption. *Biol Psychiatry*, *81*(11), 918-929. doi:10.1016/j.biopsych.2016.05.016

Cho, R. W., Buhl, L. K., Volfson, D., Tran, A., Li, F., Akbergenova, Y., & Littleton, J. T. (2015). Phosphorylation of Complexin by PKA Regulates Activity-

Dependent Spontaneous Neurotransmitter Release and Structural Synaptic Plasticity. Neuron, 88(4), 749-761. doi:10.1016/j.neuron.2015.10.011

Chuhma, N., Tanaka, K. F., Hen, R., & Rayport, S. (2011). Functional connectome of the striatal medium spiny neuron. J Neurosci, 31(4), 1183-1192. doi:10.1523/JNEUROSCI.3833-10.2011

Ciruela, F., Casadó, V., Rodrigues, R. J., Luján, R., Burgueño, J., Canals, M., . . . Franco, R. (2006). Presynaptic control of striatal glutamatergic neurotransmission by adenosine A1-A2A receptor heteromers. *J Neurosci*, *26*(7), 2080-2087. doi:10.1523/JNEUROSCI.3574-05.2006

Clarke, R., & Adermark, L. (2015). Dopaminergic Regulation of Striatal Interneurons in Reward and Addiction: Focus on Alcohol. *Neural Plast*, *2015*, 814567. doi:10.1155/2015/814567

Clarke, R. B., & Adermark, L. (2010). Acute ethanol treatment prevents endocannabinoid-mediated long-lasting disinhibition of striatal output. *Neuropharmacology*, *58*(4-5), 799-805. doi:10.1016/j.neuropharm.2009.12.006

Coleman, L. G., He, J., Lee, J., Styner, M., & Crews, F. T. (2011). Adolescent binge drinking alters adult brain neurotransmitter gene expression, behavior, brain regional volumes, and neurochemistry in mice. *Alcohol Clin Exp Res*, *35*(4), 671-688. doi:10.1111/j.1530-0277.2010.01385.x

Collins, A. L., Aitken, T. J., Greenfield, V. Y., Ostlund, S. B., & Wassum, K. M. (2016). Nucleus Accumbens Acetylcholine Receptors Modulate Dopamine and Motivation. *Neuropsychopharmacology*, *41*(12), 2830-2838. doi:10.1038/npp.2016.81

Costa, L. G., & Guizzetti, M. (1999). Muscarinic cholinergic receptor signal transduction as a potential target for the developmental neurotoxicity of ethanol. *Biochem Pharmacol*, *57*(7), 721-726. doi:10.1016/s0006-2952(98)00278-0

Cox, J., & Witten, I. B. (2019). Striatal circuits for reward learning and decision-making. *Nat Rev Neurosci*, *20*(8), 482-494. doi:10.1038/s41583-019-0189-2

Crabbe, J. C., Harris, R. A., & Koob, G. F. (2011). Preclinical studies of alcohol binge drinking. *Ann N Y Acad Sci*, *1216*, 24-40. doi:10.1111/j.1749-6632.2010.05895.x

Crespo, J. A., Sturm, K., Saria, A., & Zernig, G. (2006). Activation of muscarinic and nicotinic acetylcholine receptors in the nucleus accumbens core is necessary for the acquisition of drug reinforcement. *J Neurosci*, *26*(22), 6004-6010. doi:10.1523/JNEUROSCI.4494-05.2006

Cui, S. Z., Wang, S. J., Li, J., Xie, G. Q., Zhou, R., Chen, L., & Yuan, X. R. (2011). Alteration of synaptic plasticity in rat dorsal striatum induced by chronic ethanol intake and withdrawal via ERK pathway. *Acta Pharmacol Sin*, *32*(2), 175-181. doi:10.1038/aps.2010.199

Cuzon Carlson, V. C., Seabold, G. K., Helms, C. M., Garg, N., Odagiri, M., Rau, A. R., . . . Grant, K. A. (2011). Synaptic and morphological neuroadaptations in the putamen associated with long-term, relapsing alcohol drinking in

primates. *Neuropsychopharmacology*, *36*(12), 2513-2528. doi:10.1038/npp.2011.140

D'Souza, M. S. (2015). Glutamatergic transmission in drug reward: implications for drug addiction. *Front Neurosci*, *9*, 404. doi:10.3389/fnins.2015.00404

Dalley, J. W., Cardinal, R. N., & Robbins, T. W. (2004). Prefrontal executive and cognitive functions in rodents: neural and neurochemical substrates. *Neurosci Biobehav Rev*, *28*(7), 771-784. doi:10.1016/j.neubiorev.2004.09.006

Dautan, D., Huerta-Ocampo, I., Witten, I. B., Deisseroth, K., Bolam, J. P., Gerdjikov, T., & Mena-Segovia, J. (2014). A major external source of cholinergic innervation of the striatum and nucleus accumbens originates in the brainstem. *J Neurosci*, *34*(13), 4509-4518. doi:10.1523/JNEUROSCI.5071-13.2014

de Rover, M., Lodder, J. C., Kits, K. S., Schoffelmeer, A. N., & Brussaard, A. B. (2002). Cholinergic modulation of nucleus accumbens medium spiny neurons. *Eur J Neurosci*, *16*(12), 2279-2290. Retrieved from https://www.ncbi.nlm.nih.gov/entrez/query.fcgi?cmd=Retrieve&db=PubMed&dopt=Citation&list_uids=12492422

de Rover, M., Lodder, J. C., Smidt, M. P., & Brussaard, A. B. (2006). Pitx3 deficiency in mice affects cholinergic modulation of GABAergic synapses in the nucleus accumbens. *J Neurophysiol*, *96*(4), 2034-2041. doi:10.1152/jn.00333.2006

Delfs, J. M., Zhu, Y., Druhan, J. P., & Aston-Jones, G. S. (1998). Origin of noradrenergic afferents to the shell subregion of the nucleus accumbens: anterograde and retrograde tract-tracing studies in the rat. *Brain Res*, *806*(2), 127-140. doi:10.1016/s0006-8993(98)00672-6

DePoy, L., Daut, R., Brigman, J. L., MacPherson, K., Crowley, N., Gunduz-Cinar, O., . . . Holmes, A. (2013). Chronic alcohol produces neuroadaptations to prime dorsal striatal learning. *Proc Natl Acad Sci U S A*, *110*(36), 14783-14788. doi:10.1073/pnas.1308198110

Di Chiara, G. (2002). Nucleus accumbens shell and core dopamine: differential role in behavior and addiction. *Behav Brain Res*, *137*(1-2), 75-114. Retrieved from https://www.ncbi.nlm.nih.gov/entrez/query.fcgi?cmd=Retrieve&db=PubMed&dopt=Citation&list_uids=12445717

(2013). *Diagnostic and statistical manual of mental disorders : DSM-5.* (Fifth edition. ed.).

Ding, J. B., Guzman, J. N., Peterson, J. D., Goldberg, J. A., & Surmeier, D. J. (2010). Thalamic gating of corticostriatal signaling by cholinergic interneurons. *Neuron*, *67*(2), 294-307. doi:10.1016/j.neuron.2010.06.017

Ding, Y., Won, L., Britt, J. P., Lim, S. A., McGehee, D. S., & Kang, U. J. (2011). Enhanced striatal cholinergic neuronal activity mediates L-DOPA-induced dyskinesia in parkinsonian mice. Proc Natl Acad Sci U S A, 108(2), 840-845. doi:10.1073/pnas.1006511108

Dobrunz, L. E., & Stevens, C. F. (1997). Heterogeneity of release probability, facilitation, and depletion at central synapses. *Neuron*, *18*(6), 995-1008. doi:10.1016/s0896-6273(00)80338-4

Dopico, A. M., Bukiya, A. N., & Martin, G. E. (2014). Ethanol modulation of mammalian BK channels in excitable tissues: molecular targets and their possible contribution to alcohol-induced altered behavior. *Front Physiol*, *5*, 466. doi:10.3389/fphys.2014.00466

Dumartin, B., Doudnikoff, E., Gonon, F., & Bloch, B. (2007). Differences in ultrastructural localization of dopaminergic D1 receptors between dorsal striatum and nucleus accumbens in the rat. *Neurosci Lett*, *419*(3), 273-277. doi:10.1016/j.neulet.2007.04.034

Duvoisin, R. C. (1967). Cholinergic-anticholinergic antagonism in parkinsonism. Arch Neurol, 17(2), 124-136. doi:10.1001/archneur.1967.00470260014002

Eglen, R. M. (2005). Muscarinic receptor subtype pharmacology and physiology. *Prog Med Chem*, *43*, 105-136. doi:10.1016/S0079-6468(05)43004-0

Ericson, M., Blomqvist, O., Engel, J. A., & Söderpalm, B. (1998). Voluntary ethanol intake in the rat and the associated accumbal dopamine overflow are blocked by ventral tegmental mecamylamine. *Eur J Pharmacol*, *358*(3), 189-196. doi:10.1016/s0014-2999(98)00602-5

Ericson, M., Löf, E., Stomberg, R., & Söderpalm, B. (2009). The smoking cessation medication varenicline attenuates alcohol and nicotine interactions in the rat mesolimbic dopamine system. *J Pharmacol Exp Ther*, *329*(1), 225-230. doi:10.1124/jpet.108.147058

Exley, R., Clements, M. A., Hartung, H., McIntosh, J. M., & Cragg, S. J. (2008). Alpha6-containing nicotinic acetylcholine receptors dominate the nicotine control of dopamine neurotransmission in nucleus accumbens. *Neuropsychopharmacology*, *33*(9), 2158-2166. doi:10.1038/sj.npp.1301617

Exley, R., & Cragg, S. J. (2008). Presynaptic nicotinic receptors: a dynamic and diverse cholinergic filter of striatal dopamine neurotransmission. *Br J Pharmacol*, *153 Suppl 1*, S283-97. doi:10.1038/sj.bjp.0707510

Feduccia, A. A., Simms, J. A., Mill, D., Yi, H. Y., & Bartlett, S. E. (2014). Varenicline decreases ethanol intake and increases dopamine release via neuronal nicotinic acetylcholine receptors in the nucleus accumbens. *Br J Pharmacol*, *171*(14), 3420-3431. doi:10.1111/bph.12690

Finch, D. M. (1996). Neurophysiology of converging synaptic inputs from the rat prefrontal cortex, amygdala, midline thalamus, and hippocampal formation onto single neurons of the caudate/putamen and nucleus accumbens. *Hippocampus*, *6*(5), 495-512. doi:10.1002/(SICI)1098-1063(1996)6:5<495::AID-HIPO3>3.0.CO;2-I

Francis, T. C., Yano, H., Demarest, T. G., Shen, H., & Bonci, A. (2019). High-Frequency Activation of Nucleus Accumbens D1-MSNs Drives Excitatory Potentiation on D2-MSNs. *Neuron*. doi:10.1016/j.neuron.2019.05.031

Franklin, T. R., Wang, Z., Wang, J., Sciortino, N., Harper, D., Li, Y., . . . Childress, A. R. (2007). Limbic activation to cigarette smoking cues

independent of nicotine withdrawal: a perfusion fMRI study. Neuropsychopharmacology, 32(11), 2301-2309. doi:10.1038/sj.npp.1301371

French, S. J., & Totterdell, S. (2002). Hippocampal and prefrontal cortical inputs monosynaptically converge with individual projection neurons of the nucleus accumbens. *J Comp Neurol*, *446*(2), 151-165. doi:10.1002/cne.10191

French, S. J., & Totterdell, S. (2003). Individual nucleus accumbens-projection neurons receive both basolateral amygdala and ventral subicular afferents in rats. *Neuroscience*, *119*(1), 19-31. doi:10.1016/s0306-4522(03)00150-7

Galaj, E., Kipp, B. T., Floresco, S. B., & Savage, L. M. (2019). Persistent Alterations of Accumbal Cholinergic Interneurons and Cognitive Dysfunction after Adolescent Intermittent Ethanol Exposure. *Neuroscience*, *404*, 153-164. doi:10.1016/j.neuroscience.2019.01.062

Gallagher, M., & Chiba, A. A. (1996). The amygdala and emotion. *Curr Opin Neurobiol*, *6*(2), 221-227. doi:10.1016/s0959-4388(96)80076-6

Gao, F., Chen, D., Ma, X., Sudweeks, S., Yorgason, J. T., Gao, M., . . . Wu, J. (2019). Alpha6-containing nicotinic acetylcholine receptor is a highly sensitive target of alcohol. *Neuropharmacology*, *149*, 45-54. doi:10.1016/j.neuropharm.2019.01.021

Gerfen, C. R., & Surmeier, D. J. (2011). Modulation of striatal projection systems by dopamine. *Annu Rev Neurosci*, *34*, 441-466. doi:10.1146/annurev-neuro-061010-113641

Gonzales, K. K., & Smith, Y. (2015). Cholinergic interneurons in the dorsal and ventral striatum: anatomical and functional considerations in normal and diseased conditions. *Ann N Y Acad Sci*, *1349*, 1-45. doi:10.1111/nyas.12762

Goto, Y., & Grace, A. A. (2008). Limbic and cortical information processing in the nucleus accumbens. *Trends Neurosci*, *31*(11), 552-558. doi:10.1016/j.tins.2008.08.002

Grafen, A., & Hails, R. (2002). Modern statistics for the life sciences. *sidalc.net*. Retrieved from http://www.sidalc.net/cgi-bin/wxis.exe/?IsisScript=sibe01.xis&method=post&formato=2&cantidad=1&expresion=mfn=025194

Granger, A. J., Wallace, M. L., & Sabatini, B. L. (2017). Multi-transmitter neurons in the mammalian central nervous system. *Curr Opin Neurobiol*, *45*, 85-91. doi:10.1016/j.conb.2017.04.007

Graybiel, A. M. (2000). The basal ganglia. *Curr Biol*, *10*(14), R509-11. doi:10.1016/s0960-9822(00)00593-5

Greif, G. J., Lin, Y. J., Liu, J. C., & Freedman, J. E. (1995). Dopamine-modulated potassium channels on rat striatal neurons: specific activation and cellular expression. *J Neurosci*, *15*(6), 4533-4544. Retrieved from https://www.ncbi.nlm.nih.gov/entrez/query.fcgi?cmd=Retrieve&db=PubMed&dopt=Citation&list_uids=7790922

Griffin, W. C., Haun, H. L., Hazelbaker, C. L., Ramachandra, V. S., & Becker, H. C. (2014). Increased extracellular glutamate in the nucleus accumbens promotes excessive ethanol drinking in ethanol dependent mice. *Neuropsychopharmacology*, *39*(3), 707-717. doi:10.1038/npp.2013.256

Grilli, M., Patti, L., Robino, F., Zappettini, S., Raiteri, M., & Marchi, M. (2008). Release-enhancing pre-synaptic muscarinic and nicotinic receptors co-exist and interact on dopaminergic nerve endings of rat nucleus accumbens. *J Neurochem*, *105*(6), 2205-2213. doi:10.1111/j.1471-4159.2008.05307.x

Groenewegen, H. J., Wright, C. I., Beijer, A. V., & Voorn, P. (1999). Convergence and segregation of ventral striatal inputs and outputs. *Ann N Y Acad Sci*, *877*, 49-63. doi:10.1111/j.1749-6632.1999.tb09260.x

Guzikowski, N. J., & Kavalali, E. T. (2021). Nano-Organization at the Synapse: Segregation of Distinct Forms of Neurotransmission. Front Synaptic Neurosci, 13, 796498. doi:10.3389/fnsyn.2021.796498

Haber, S. N. (2003). The primate basal ganglia: parallel and integrative networks. *J Chem Neuroanat*, *26*(4), 317-330. doi:10.1016/j.jchemneu.2003.10.003

Harvey, J., & Lacey, M. G. (1997). A postsynaptic interaction between dopamine D1 and NMDA receptors promotes presynaptic inhibition in the rat nucleus accumbens via adenosine release. *J Neurosci*, *17*(14), 5271-5280. Retrieved from https://pubmed.ncbi.nlm.nih.gov/9204911

Heinz, A., Siessmeier, T., Wrase, J., Hermann, D., Klein, S., Grüsser, S. M., . . . Bartenstein, P. (2004). Correlation between dopamine D(2) receptors in the ventral striatum and central processing of alcohol cues and craving. *Am J Psychiatry*, *161*(10), 1783-1789. doi:10.1176/appi.ajp.161.10.1783

Hendrickson, L. M., Guildford, M. J., & Tapper, A. R. (2013). Neuronal nicotinic acetylcholine receptors: common molecular substrates of nicotine and alcohol dependence. *Front Psychiatry*, *4*, 29. doi:10.3389/fpsyt.2013.00029

Hendrickson, L. M., Zhao-Shea, R., Pang, X., Gardner, P. D., & Tapper, A. R. (2010). Activation of alpha4* nAChRs is necessary and sufficient for varenicline-induced reduction of alcohol consumption. *J Neurosci*, *30*, 10169-10176. doi:10.1523/JNEUROSCI.2601-10.2010

Hendrickson, L. M., Zhao-Shea, R., & Tapper, A. R. (2009). Modulation of ethanol drinking-in-the-dark by mecamylamine and nicotinic acetylcholine receptor agonists in C57BL/6J mice. *Psychopharmacology (Berl)*, *204*(4), 563-572. doi:10.1007/s00213-009-1488-5

Hernandez-Lopez, S., Tkatch, T., Perez-Garci, E., Galarraga, E., Bargas, J., Hamm, H., & Surmeier, D. J. (2000). D2 dopamine receptors in striatal medium spiny neurons reduce L-type Ca2+ currents and excitability via a novel PLC[beta]1-IP3-calcineurin-signaling cascade. *J Neurosci*, *20*(24), 8987-8995. Retrieved from https://www.ncbi.nlm.nih.gov/entrez/query.fcgi?cmd=Retrieve&db=PubMed&dopt=Citation&list_uids=11124974

Herring, B. E., Mayfield, R. D., Camp, M. C., & Alcantara, A. A. (2004). Ethanol-induced Fos immunoreactivity in the extended amygdala and hypothalamus of the rat brain: focus on cholinergic interneurons of the nucleus accumbens. *Alcohol Clin Exp Res*, *28*(4), 588-597. Retrieved from https://www.ncbi.nlm.nih.gov/entrez/query.fcgi?cmd=Retrieve&db=PubMed&dopt=Citation&list_uids=15100610

Higley, M. J., Gittis, A. H., Oldenburg, I. A., Balthasar, N., Seal, R. P., Edwards, R. H., . . . Sabatini, B. L. (2011). Cholinergic interneurons mediate fast VGluT3-dependent glutamatergic transmission in the striatum. *PLoS One*, *6*(4), e19155. doi:10.1371/journal.pone.0019155

Higley, M. J., Soler-Llavina, G. J., & Sabatini, B. L. (2009). Cholinergic modulation of multivesicular release regulates striatal synaptic potency and integration. *Nat Neurosci*, *12*(9), 1121-1128. doi:10.1038/nn.2368

Hikida, T., Kaneko, S., Isobe, T., Kitabatake, Y., Watanabe, D., Pastan, I., & Nakanishi, S. (2001). Increased sensitivity to cocaine by cholinergic cell ablation in nucleus accumbens. *Proc Natl Acad Sci U S A*, *98*(23), 13351-13354. doi:10.1073/pnas.231488998

Hikida, T., Morita, M., & Macpherson, T. (2016). Neural mechanisms of the nucleus accumbens circuit in reward and aversive learning. *Neurosci Res*, *108*, 1-5. doi:10.1016/j.neures.2016.01.004

Hillmer, A. T., Tudorascu, D. L., Wooten, D. W., Lao, P. J., Barnhart, T. E., Ahlers, E. O., . . . Christian, B. T. (2014). Changes in the α4β2* nicotinic acetylcholine system during chronic controlled alcohol exposure in nonhuman primates. *Drug Alcohol Depend*, *138*, 216-219. doi:10.1016/j.drugalcdep.2014.01.027

Hollander, J. A., Ijames, S. G., Roop, R. G., & Carelli, R. M. (2002). An examination of nucleus accumbens cell firing during extinction and reinstatement of water reinforcement behavior in rats. *Brain Res*, *929*(2), 226-235. Retrieved from https://www.ncbi.nlm.nih.gov/entrez/query.fcgi?cmd=Retrieve&db=PubMed&dopt=Citation&list_uids=11864628

Hopf, F. W., Bowers, M. S., Chang, S. J., Chen, B. T., Martin, M., Seif, T., . . . Bonci, A. (2010). Reduced nucleus accumbens SK channel activity enhances alcohol seeking during abstinence. *Neuron*, *65*(5), 682-694. doi:10.1016/j.neuron.2010.02.015

Howe, W. M., Young, D. A., Bekheet, G., & Kozak, R. (2016). Nicotinic receptor subtypes differentially modulate glutamate release in the dorsal medial striatum. *Neurochem Int*, *100*, 30-34. doi:10.1016/j.neuint.2016.08.009

Humphries, M. D., & Prescott, T. J. (2010). The ventral basal ganglia, a selection mechanism at the crossroads of space, strategy, and reward. *Prog Neurobiol*, *90*(4), 385-417. doi:10.1016/j.pneurobio.2009.11.003

Hyman, S. E., Malenka, R. C., & Nestler, E. J. (2006). Neural mechanisms of addiction: the role of reward-related learning and memory. *Annu Rev Neurosci*, *29*, 565-598. doi:10.1146/annurev.neuro.29.051605.113009

Ikemoto, S. (2007). Dopamine reward circuitry: two projection systems from the ventral midbrain to the nucleus accumbens-olfactory tubercle complex. *Brain Res Rev*, *56*(1), 27-78. doi:10.1016/j.brainresrev.2007.05.004

Jeanes, Z. M., Buske, T. R., & Morrisett, R. A. (2014). Cell type-specific synaptic encoding of ethanol exposure in the nucleus accumbens shell. *Neuroscience*, *277*, 184-195. doi:10.1016/j.neuroscience.2014.06.063

Ji, X., & Martin, G. E. (2012). New rules governing synaptic plasticity in core nucleus accumbens medium spiny neurons. *Eur J Neurosci*, *36*(12), 3615-3627. doi:10.1111/ejn.12002

Ji, X., Saha, S., Kolpakova, J., Guildford, M., Tapper, A. R., & Martin, G. E. (2017). Dopamine Receptors Differentially Control Binge Alcohol Drinking-Mediated Synaptic Plasticity of the Core Nucleus Accumbens Direct and Indirect Pathways. *J Neurosci*, *37*(22), 5463-5474. doi:10.1523/JNEUROSCI.3845-16.2017

Ji, X., Saha, S., & Martin, G. E. (2015). The origin of glutamatergic synaptic inputs controls synaptic plasticity and its modulation by alcohol in mice nucleus accumbens. *Front Synaptic Neurosci*, *7*, 12. doi:10.3389/fnsyn.2015.00012

Joel, D., & Weiner, I. (2000). The connections of the dopaminergic system with the striatum in rats and primates: an analysis with respect to the functional and compartmental organization of the striatum. *Neuroscience*, *96*(3), 451-474. doi:10.1016/s0306-4522(99)00575-8

Joshua, M., Adler, A., Mitelman, R., Vaadia, E., & Bergman, H. (2008). Midbrain dopaminergic neurons and striatal cholinergic interneurons encode the difference between reward and aversive events at different epochs of probabilistic classical conditioning trials. *J Neurosci*, *28*(45), 11673-11684. doi:10.1523/JNEUROSCI.3839-08.2008

Jr, F. J. M. (1951). The Kolmogorov-Smirnov test for goodness of fit. *Journal of the American statistical Association*. Retrieved from https://www.tandfonline.com/doi/abs/10.1080/01621459.1951.10500769

Kandel, E. R., Schwartz, J. H., Jessell, T. M., & Siegelbaum…, S. (2000). *Principles of neural science*.

Karkhanis, A. N., Rose, J. H., Huggins, K. N., Konstantopoulos, J. K., & Jones, S. R. (2015). Chronic intermittent ethanol exposure reduces presynaptic dopamine neurotransmission in the mouse nucleus accumbens. *Drug Alcohol Depend*, *150*, 24-30. doi:10.1016/j.drugalcdep.2015.01.019

Kasanetz, F., & Manzoni, O. J. (2009). Maturation of excitatory synaptic transmission of the rat nucleus accumbens from juvenile to adult. *J Neurophysiol*, *101*(5), 2516-2527. doi:10.1152/jn.91039.2008

Katz, B. (1969). The release of neural transmitter substances. *Thomas*, *Springfield, IL*.

Kauer, J. A., & Malenka, R. C. (2007). Synaptic plasticity and addiction. *Nat Rev Neurosci*, *8*(11), 844-858. doi:10.1038/nrn2234

Kavalali, E. T. (2015). The mechanisms and functions of spontaneous neurotransmitter release. Nat Rev Neurosci, 16(1), 5-16. doi:10.1038/nrn3875

Kawaguchi, Y., Wilson, C. J., Augood, S. J., & Emson, P. C. (1995). Striatal interneurones: chemical, physiological and morphological characterization. *Trends Neurosci*, *18*(12), 527-535. Retrieved from https://www.ncbi.nlm.nih.gov/entrez/query.fcgi?cmd=Retrieve&db=PubMed&dopt=Citation&list_uids=8638293

Kebabian, J. W., & Calne, D. B. (1979). Multiple receptors for dopamine. Nature, 277(5692), 93-96. doi:10.1038/277093a0

Kircher, D. M., Aziz, H. C., Mangieri, R. A., & Morrisett, R. A. (2019). Ethanol Experience Enhances Glutamatergic Ventral Hippocampal Inputs to D1 Receptor-Expressing Medium Spiny Neurons in the Nucleus Accumbens Shell. *J Neurosci*, *39*(13), 2459-2469. doi:10.1523/JNEUROSCI.3051-18.2019

Klapoetke, N. C., Murata, Y., Kim, S. S., Pulver, S. R., Birdsey-Benson, A., Cho, Y. K., . . . Boyden, E. S. (2014). Independent optical excitation of distinct neural populations. *Nat Methods*, *11*(3), 338-346. doi:10.1038/nmeth.2836

Klenowski, P. M. (2018). Emerging role for the medial prefrontal cortex in alcohol-seeking behaviors. *Addict Behav*, *77*, 102-106. doi:10.1016/j.addbeh.2017.09.024

Kolpakova, J., Marvel-Zuccola, J. D., Futai, K., & Martin…, G. E. (2022). EPHierStats: a statistical tool to model the hierarchical relationships in electrophysiological data. *bioRxiv*. Retrieved from https://www.biorxiv.org/content/10.1101/2022.03.23.485501

Kolpakova, J., van der Vinne, V., Giménez-Gómez, P., Le, T., You, I. J., Zhao-Shea, R., . . . Martin, G. E. (2021). Binge Alcohol Drinking Alters Synaptic Processing of Executive and Emotional Information in Core Nucleus Accumbens Medium Spiny Neurons. *Front Cell Neurosci*, *15*, 742207. doi:10.3389/fncel.2021.742207

Kombian, S. B., & Malenka, R. C. (1994). Simultaneous LTP of non-NMDA- and LTD of NMDA-receptor-mediated responses in the nucleus accumbens. *Nature*, *368*(6468), 242-246. doi:10.1038/368242a0

Koob, G. F., Ahmed, S. H., Boutrel, B., Chen, S. A., Kenny, P. J., Markou, A., . . . Sanna, P. P. (2004). Neurobiological mechanisms in the transition from drug use to drug dependence. *Neurosci Biobehav Rev*, *27*(8), 739-749. doi:10.1016/j.neubiorev.2003.11.007

Koob, G. F., & Le Moal, M. (1997). Drug abuse: hedonic homeostatic dysregulation. *Science*, *278*(5335), 52-58. doi:10.1126/science.278.5335.52

Koob, G. F., Rassnick, S., Heinrichs, S., & Weiss, F. (1994). Alcohol, the reward system and dependence. *EXS*, *71*, 103-114. doi:10.1007/978-3-0348-7330-7_11

Koob, G. F., & Volkow, N. D. (2010). Neurocircuitry of addiction. *Neuropsychopharmacology*, *35*(1), 217-238. doi:10.1038/npp.2009.110

Koob, G. F., & Volkow, N. D. (2016). Neurobiology of addiction: a neurocircuitry analysis. *Lancet Psychiatry*, *3*(8), 760-773. doi:10.1016/S2215-0366(16)00104-8

Kravitz, A. V., Tye, L. D., & Kreitzer, A. C. (2012). Distinct roles for direct and indirect pathway striatal neurons in reinforcement. *Nat Neurosci*, *15*(6), 816-818. doi:10.1038/nn.3100

Krieger, H., Young, C. M., Anthenien, A. M., & Neighbors, C. (2018). The Epidemiology of Binge Drinking Among College-Age Individuals in the United States. *Alcohol Res*, *39*(1), 23-30. Retrieved from https://pubmed.ncbi.nlm.nih.gov/30557145

Kupchik, Y. M., Brown, R. M., Heinsbroek, J. A., Lobo, M. K., Schwartz, D. J., & Kalivas, P. W. (2015). Coding the direct/indirect pathways by D1 and D2 receptors is not valid for accumbens projections. *Nat Neurosci*, *18*(9), 1230-1232. doi:10.1038/nn.4068

Kupchik, Y. M., & Kalivas, P. W. (2017). The Direct and Indirect Pathways of the Nucleus Accumbens are not What You Think. *Neuropsychopharmacology*, *42*(1), 369-370. doi:10.1038/npp.2016.160

Kuroiwa, M., Hamada, M., Hieda, E., Shuto, T., Sotogaku, N., Flajolet, M., . . . Nishi, A. (2012). Muscarinic receptors acting at pre- and post-synaptic sites differentially regulate dopamine/DARPP-32 signaling in striatonigral and striatopallidal neurons. *Neuropharmacology*, *63*(7), 1248-1257. doi:10.1016/j.neuropharm.2012.07.046

Laguesse, S., Morisot, N., Phamluong, K., Sakhai, S. A., & Ron, D. (2018). mTORC2 in the dorsomedial striatum of mice contributes to alcohol-dependent F-Actin polymerization, structural modifications, and consumption. *Neuropsychopharmacology*, *43*(7), 1539-1547. doi:10.1038/s41386-018-0012-1

Lalumiere, R. T. (2014). Optogenetic dissection of amygdala functioning. *Front Behav Neurosci*, *8*, 107. doi:10.3389/fnbeh.2014.00107

Lara, A. H., & Wallis, J. D. (2015). The Role of Prefrontal Cortex in Working Memory: A Mini Review. *Front Syst Neurosci*, *9*, 173. doi:10.3389/fnsys.2015.00173

Lau, C. G., & Zukin, R. S. (2007). NMDA receptor trafficking in synaptic plasticity and neuropsychiatric disorders. *Nat Rev Neurosci*, *8*(6), 413-426. doi:10.1038/nrn2153

Le Moine, C., & Bloch, B. (1995). D1 and D2 dopamine receptor gene expression in the rat striatum: sensitive cRNA probes demonstrate prominent segregation of D1 and D2 mRNAs in distinct neuronal populations of the dorsal and ventral striatum. *J Comp Neurol*, *355*(3), 418-426. doi:10.1002/cne.903550308

LeDoux, J. E. (2000). Emotion circuits in the brain. *Annu Rev Neurosci*, *23*, 155-184. doi:10.1146/annurev.neuro.23.1.155

Lee, J., Finkelstein, J., Choi, J. Y., & Witten, I. B. (2016). Linking Cholinergic Interneurons, Synaptic Plasticity, and Behavior during the Extinction of a

Cocaine-Context Association. *Neuron*, *90*(5), 1071-1085. doi:10.1016/j.neuron.2016.05.001

Lee, J. H., Ribeiro, E. A., Kim, J., Ko, B., Kronman, H., Jeong, Y. H., . . . Kim, J. H. (2020). Dopaminergic Regulation of Nucleus Accumbens Cholinergic Interneurons Demarcates Susceptibility to Cocaine Addiction. *Biol Psychiatry*, *88*(10), 746-757. doi:10.1016/j.biopsych.2020.05.003

Licheri, V., Lagström, O., Lotfi, A., Patton, M. H., Wigström, H., Mathur, B., & Adermark, L. (2018). Complex Control of Striatal Neurotransmission by Nicotinic Acetylcholine Receptors via Excitatory Inputs onto Medium Spiny Neurons. *J Neurosci*, *38*(29), 6597-6607. doi:10.1523/JNEUROSCI.0071-18.2018

Lim, S. A., Kang, U. J., & McGehee, D. S. (2014). Striatal cholinergic interneuron regulation and circuit effects. *Front Synaptic Neurosci*, *6*, 22. doi:10.3389/fnsyn.2014.00022

Limpert, E., Stahel, W. A., & Abbt, M. (2001). Log-normal distributions across the sciences: keys and clues: on the charms of statistics, and how mechanical models resembling gambling machines offer a link to a …. *BioScience*. Retrieved from https://academic.oup.com/bioscience/article-abstract/51/5/341/243981

Lin, J. Y., Chung, K. K., de Castro, D., Funk, G. D., & Lipski, J. (2004). Effects of muscarinic acetylcholine receptor activation on membrane currents and intracellular messengers in medium spiny neurones of the rat striatum. *Eur J Neurosci*, *20*(5), 1219-1230. doi:10.1111/j.1460-9568.2004.03576.x

Liu, L., Hendrickson, L. M., Guildford, M. J., Zhao-Shea, R., Gardner, P. D., & Tapper, A. R. (2013a). Nicotinic acetylcholine receptors containing the α4 subunit modulate alcohol reward. *Biol Psychiatry*, *73*(8), 738-746. doi:10.1016/j.biopsych.2012.09.019

Liu, L., Zhao-Shea, R., McIntosh, J. M., & Tapper, A. R. (2013b). Nicotinic acetylcholine receptors containing the α6 subunit contribute to ethanol activation of ventral tegmental area dopaminergic neurons. *Biochem Pharmacol*, *86*(8), 1194-1200. doi:10.1016/j.bcp.2013.06.015

Liu, Y., Jean-Richard-Dit-Bressel, P., Yau, J. O., Willing, A., Prasad, A. A., Power, J. M., . . . McNally, G. P. (2020). The Mesolimbic Dopamine Activity Signatures of Relapse to Alcohol-Seeking. *J Neurosci*, *40*(33), 6409-6427. doi:10.1523/JNEUROSCI.0724-20.2020

Lobo, M. K., Covington, H. E., Chaudhury, D., Friedman, A. K., Sun, H., Damez-Werno, D., . . . Nestler, E. J. (2010). Cell type-specific loss of BDNF signaling mimics optogenetic control of cocaine reward. *Science*, *330*(6002), 385-390. doi:10.1126/science.1188472

Lobo, M. K., Karsten, S. L., Gray, M., Geschwind, D. H., & Yang, X. W. (2006). FACS-array profiling of striatal projection neuron subtypes in juvenile and adult mouse brains. *Nat Neurosci*, *9*(3), 443-452. doi:10.1038/nn1654

Löf, E., Ericson, M., Stomberg, R., & Söderpalm, B. (2007). Characterization of ethanol-induced dopamine elevation in the rat nucleus accumbens. *Eur J Pharmacol*, *555*(2-3), 148-155. doi:10.1016/j.ejphar.2006.10.055

Loftén, A., Adermark, L., Ericson, M., & Söderpalm, B. (2020). An acetylcholine-dopamine interaction in the nucleus accumbens and its involvement in ethanol's dopamine-releasing effect. *Addict Biol*, e12959. doi:10.1111/adb.12959

Lograno, D. E., Matteo, F., Trabucchi, M., Govoni, S., Cagiano, R., Lacomba, C., & Cuomo, V. (1993). Effects of chronic ethanol intake at a low dose on the rat brain dopaminergic system. *Alcohol*, *10*(1), 45-49. doi:10.1016/0741-8329(93)90052-p

Lovinger, D. M., & Roberto, M. (2013). Synaptic effects induced by alcohol. *Curr Top Behav Neurosci*, *13*, 31-86. doi:10.1007/7854_2011_143

Lovinger, D. M., White, G., & Weight, F. F. (1989). Ethanol inhibits NMDA-activated ion current in hippocampal neurons. *Science*, *243*(4899), 1721-1724. doi:10.1126/science.2467382

Lu, X. Y., Ghasemzadeh, M. B., & Kalivas, P. W. (1998). Expression of D1 receptor, D2 receptor, substance P and enkephalin messenger RNAs in the neurons projecting from the nucleus accumbens. *Neuroscience*, *82*(3), 767-780. doi:10.1016/s0306-4522(97)00327-8

Lüscher, C., & Malenka, R. C. (2011). Drug-evoked synaptic plasticity in addiction: from molecular changes to circuit remodeling. *Neuron*, *69*(4), 650-663. doi:10.1016/j.neuron.2011.01.017

Ma, T., Barbee, B., Wang, X., & Wang, J. (2017). Alcohol induces input-specific aberrant synaptic plasticity in the rat dorsomedial striatum. *Neuropharmacology*, *123*, 46-54. doi:10.1016/j.neuropharm.2017.05.014

Ma, T., Cheng, Y., Roltsch Hellard, E., Wang, X., Lu, J., Gao, X., . . . Wang, J. (2018). Bidirectional and long-lasting control of alcohol-seeking behavior by corticostriatal LTP and LTD. *Nat Neurosci*, *21*(3), 373-383. doi:10.1038/s41593-018-0081-9

Ma, Y. Y., Lee, B. R., Wang, X., Guo, C., Liu, L., Cui, R., . . . Dong, Y. (2014). Bidirectional modulation of incubation of cocaine craving by silent synapse-based remodeling of prefrontal cortex to accumbens projections. *Neuron*, *83*(6), 1453-1467. doi:10.1016/j.neuron.2014.08.023

Macpherson, T., Morita, M., & Hikida, T. (2014). Striatal direct and indirect pathways control decision-making behavior. Front Psychol, 5, 1301. doi:10.3389/fpsyg.2014.01301

Malarkey, E. B., & Parpura, V. (2008). Mechanisms of glutamate release from astrocytes. *Neurochem Int*, *52*(1-2), 142-154. doi:10.1016/j.neuint.2007.06.005

Malenka, R. C., & Bear, M. F. (2004). LTP and LTD: an embarrassment of riches. *Neuron*, *44*(1), 5-21. doi:10.1016/j.neuron.2004.09.012

Malenka, R. C., & Kocsis, J. D. (1988). Presynaptic actions of carbachol and adenosine on corticostriatal synaptic transmission studied in vitro. *J*

Neurosci, *8*(10), 3750-3756. Retrieved from https://www.ncbi.nlm.nih.gov/entrez/query.fcgi?cmd=Retrieve&db=PubMed&dopt=Citation&list_uids=2848109

Manabe, T., Renner, P., & Nicoll, R. A. (1992). Postsynaptic contribution to long-term potentiation revealed by the analysis of miniature synaptic currents. *Nature*, *355*(6355), 50-55. doi:10.1038/355050a0

Manzoni, O., Michel, J. M., & Bockaert, J. (1997). Metabotropic glutamate receptors in the rat nucleus accumbens. *Eur J Neurosci*, *9*(7), 1514-1523. doi:10.1111/j.1460-9568.1997.tb01506.x

Mao, W., Salzberg, A. C., Uchigashima, M., Hasegawa, Y., Hock, H., Watanabe, M., . . . Futai, K. (2018). Activity-Induced Regulation of Synaptic Strength through the Chromatin Reader L3mbtl1. *Cell Rep*, *23*(11), 3209-3222. doi:10.1016/j.celrep.2018.05.028

Marche, K., Martel, A. C., & Apicella, P. (2017). Differences between Dorsal and Ventral Striatum in the Sensitivity of Tonically Active Neurons to Rewarding Events. *Front Syst Neurosci*, *11*, 52. doi:10.3389/fnsys.2017.00052

Margrie, T. W., Brecht, M., & Sakmann, B. (2002). In vivo, low-resistance, whole-cell recordings from neurons in the anaesthetized and awake mammalian brain. *Pflugers Arch*, *444*(4), 491-498. doi:10.1007/s00424-002-0831-z

Martin, G., Nie, Z., & Siggins, G. R. (1997). Metabotropic glutamate receptors regulate N-methyl-D-aspartate-mediated synaptic transmission in nucleus accumbens. *J Neurophysiol*, *78*(6), 3028-3038. doi:10.1152/jn.1997.78.6.3028

Martin, G. E. (2010). BK channel and alcohol, a complicated affair. *Int Rev Neurobiol*, *91*, 321-338. doi:10.1016/S0074-7742(10)91010-6

Martinez, D., Gil, R., Slifstein, M., Hwang, D. R., Huang, Y., Perez, A., . . . Abi-Dargham, A. (2005). Alcohol dependence is associated with blunted dopamine transmission in the ventral striatum. *Biol Psychiatry*, *58*(10), 779-786. doi:10.1016/j.biopsych.2005.04.044

Maurice, N., Mercer, J., Chan, C. S., Hernandez-Lopez, S., Held, J., Tkatch, T., & Surmeier, D. J. (2004). D2 dopamine receptor-mediated modulation of voltage-dependent Na+ channels reduces autonomous activity in striatal cholinergic interneurons. *J Neurosci*, *24*(46), 10289-10301. doi:10.1523/JNEUROSCI.2155-04.2004

McClintick, J. N., McBride, W. J., Bell, R. L., Ding, Z. M., Liu, Y., Xuei, X., & Edenberg, H. J. (2016). Gene Expression Changes in Glutamate and GABA-A Receptors, Neuropeptides, Ion Channels, and Cholesterol Synthesis in the Periaqueductal Gray Following Binge-Like Alcohol Drinking by Adolescent Alcohol-Preferring (P) Rats. *Alcohol Clin Exp Res*, *40*(5), 955-968. doi:10.1111/acer.13056

McCool, B. A. (2011). Ethanol modulation of synaptic plasticity. *Neuropharmacology*, *61*(7), 1097-1108. doi:10.1016/j.neuropharm.2010.12.028

McDaid, J., McElvain, M. A., & Brodie, M. S. (2008). Ethanol effects on dopaminergic ventral tegmental area neurons during block of Ih: involvement of barium-sensitive potassium currents. *J Neurophysiol*, *100*(3), 1202-1210. doi:10.1152/jn.00994.2007

McGehee, D. S., & Role, L. W. (1995). Physiological diversity of nicotinic acetylcholine receptors expressed by vertebrate neurons. Annu Rev Physiol, 57, 521-546. doi:10.1146/annurev.ph.57.030195.002513

Melendez-Zaidi, A. E., Lakshminarasimhah, H., & Surmeier, D. J. (2019). Cholinergic modulation of striatal nitric oxide-producing interneurons. *Eur J Neurosci*. doi:10.1111/ejn.14528

Meredith, G. E., & Totterdell, S. (1999). Microcircuits in nucleus accumbens' shell and core involved in cognition and reward. *Psychobiology*. Retrieved from https://link.springer.com/article/10.3758/BF03332112

Millan, E. Z., Kim, H. A., & Janak, P. H. (2017). Optogenetic activation of amygdala projections to nucleus accumbens can arrest conditioned and unconditioned alcohol consummatory behavior. *Neuroscience*, *360*, 106-117. doi:10.1016/j.neuroscience.2017.07.044

Miller, E. K. (2000). The prefrontal cortex and cognitive control. *Nat Rev Neurosci*, *1*, 59-65. doi:10.1038/35036228

Mishra, D., Zhang, X., & Chergui, K. (2012). Ethanol disrupts the mechanisms of induction of long-term potentiation in the mouse nucleus accumbens. *Alcohol Clin Exp Res*, *36*(12), 2117-2125. doi:10.1111/j.1530-0277.2012.01824.x

Mullikin-Kilpatrick, D., & Treistman, S. N. (1994). Ethanol inhibition of L-type Ca2+ channels in PC12 cells: role of permeant ions. *Eur J Pharmacol*, *270*(1), 17-25. doi:10.1016/0926-6917(94)90076-0

Myslivecek, J. (2021). Two Players in the Field: Hierarchical Model of Interaction between the Dopamine and Acetylcholine Signaling Systems in the Striatum. *Biomedicines*, *9*(1). doi:10.3390/biomedicines9010025

Nestby, P., Vanderschuren, L. J., De Vries, T. J., Hogenboom, F., Wardeh, G., Mulder, A. H., & Schoffelmeer, A. N. (1997). Ethanol, like psychostimulants and morphine, causes long-lasting hyperreactivity of dopamine and acetylcholine neurons of rat nucleus accumbens: possible role in behavioural sensitization. *Psychopharmacology (Berl)*, *133*(1), 69-76. Retrieved from https://www.ncbi.nlm.nih.gov/entrez/query.fcgi?cmd=Retrieve&db=PubMed&dopt=Citation&list_uids=9335083

Nestby, P., Vanderschuren, L. J., De Vries, T. J., Mulder, A. H., Wardeh, G., Hogenboom, F., & Schoffelmeer, A. N. (1999). Unrestricted free-choice ethanol self-administration in rats causes long-term neuroadaptations in the nucleus accumbens and caudate putamen. *Psychopharmacology (Berl)*, *141*(3), 307-314. Retrieved from https://www.ncbi.nlm.nih.gov/entrez/query.fcgi?cmd=Retrieve&db=PubMed&dopt=Citation&list_uids=10027512

Nicola, S. M. (2007). The nucleus accumbens as part of a basal ganglia action selection circuit. *Psychopharmacology (Berl)*, *191*(3), 521-550. doi:10.1007/s00213-006-0510-4

Nicola, S. M., & Deadwyler, S. A. (2000). Firing rate of nucleus accumbens neurons is dopamine-dependent and reflects the timing of cocaine-seeking behavior in rats on a progressive ratio schedule of reinforcement. *J Neurosci*, *20*(14), 5526-5537. Retrieved from https://www.ncbi.nlm.nih.gov/entrez/query.fcgi?cmd=Retrieve&db=PubMed&dopt=Citation&list_uids=10884336

Nicola, S. M., Kombian, S. B., & Malenka, R. C. (1996). Psychostimulants depress excitatory synaptic transmission in the nucleus accumbens via presynaptic D1-like dopamine receptors. *J Neurosci*, *16*(5), 1591-1604. Retrieved from https://www.ncbi.nlm.nih.gov/entrez/query.fcgi?cmd=Retrieve&db=PubMed&dopt=Citation&list_uids=8774428

Nicola, S. M., & Malenka, R. C. (1997). Dopamine depresses excitatory and inhibitory synaptic transmission by distinct mechanisms in the nucleus accumbens. *J Neurosci*, *17*(15), 5697-5710. Retrieved from https://www.ncbi.nlm.nih.gov/entrez/query.fcgi?cmd=Retrieve&db=PubMed&dopt=Citation&list_uids=9221769

Nicola, S. M., Surmeier, J., & Malenka, R. C. (2000). Dopaminergic modulation of neuronal excitability in the striatum and nucleus accumbens. *Annu Rev Neurosci*, *23*, 185-215. doi:10.1146/annurev.neuro.23.1.185

Nishio, M., & Narahashi, T. (1990). Ethanol enhancement of GABA-activated chloride current in rat dorsal root ganglion neurons. *Brain Res*, *518*(1-2), 283-286. doi:10.1016/0006-8993(90)90982-h

Nona, C. N., & Nobrega, J. N. (2018). A role for nucleus accumbens glutamate in the expression but not the induction of behavioural sensitization to ethanol. *Behav Brain Res*, *336*, 269-281. doi:10.1016/j.bbr.2017.09.024

O'Donnell, P., & Grace, A. A. (1995). Synaptic interactions among excitatory afferents to nucleus accumbens neurons: hippocampal gating of prefrontal cortical input. *J Neurosci*, *15*(5 Pt 1), 3622-3639. Retrieved from https://pubmed.ncbi.nlm.nih.gov/7751934

Olson, P. A., Tkatch, T., Hernandez-Lopez, S., Ulrich, S., Ilijic, E., Mugnaini, E., . . . Surmeier, D. J. (2005). G-protein-coupled receptor modulation of striatal CaV1.3 L-type Ca2+ channels is dependent on a Shank-binding domain. *J Neurosci*, *25*(5), 1050-1062. doi:10.1523/JNEUROSCI.3327-04.2005

Olsen, R. W., Li, G. D., Wallner, M., Trudell, J. R., Bertaccini, E. J., Lindahl, E., . . . Davies, D. L. (2014). Structural models of ligand-gated ion channels: sites of action for anesthetics and ethanol. Alcohol Clin Exp Res, 38(3), 595-603. doi:10.1111/acer.12283

Otsu, Y., Shahrezaei, V., Li, B., Raymond, L. A., Delaney, K. R., & Murphy, T. H. (2004). Competition between phasic and asynchronous release for

recovered synaptic vesicles at developing hippocampal autaptic synapses. J Neurosci, 24(2), 420-433. doi:10.1523/JNEUROSCI.4452-03.2004

Owesson-White, C. A., Cheer, J. F., Beyene, M., Carelli, R. M., & Wightman, R. M. (2008). Dynamic changes in accumbens dopamine correlate with learning during intracranial self-stimulation. *Proc Natl Acad Sci U S A*, *105*(33), 11957-11962. doi:10.1073/pnas.0803896105

Pakhotin, P., & Bracci, E. (2007). Cholinergic interneurons control the excitatory input to the striatum. *J Neurosci*, *27*(2), 391-400. doi:10.1523/JNEUROSCI.3709-06.2007

Pancani, T., Bolarinwa, C., Smith, Y., Lindsley, C. W., Conn, P. J., & Xiang, Z. (2014). M4 mAChR-mediated modulation of glutamatergic transmission at corticostriatal synapses. *ACS Chem Neurosci*, *5*(4), 318-324. doi:10.1021/cn500003z

Pascoli, V., Cahill, E., Bellivier, F., Caboche, J., & Vanhoutte, P. (2014). Extracellular signal-regulated protein kinases 1 and 2 activation by addictive drugs: a signal toward pathological adaptation. *Biol Psychiatry*, *76*(12), 917-926. doi:10.1016/j.biopsych.2014.04.005

Pati, D., Kelly, K., Stennett, B., Frazier, C. J., & Knackstedt, L. A. (2016). Alcohol consumption increases basal extracellular glutamate in the nucleus accumbens core of Sprague-Dawley rats without increasing spontaneous glutamate release. *Eur J Neurosci*, *44*(2), 1896-1905. doi:10.1111/ejn.13284

Peled, E. S., Newman, Z. L., & Isacoff, E. Y. (2014). Evoked and spontaneous transmission favored by distinct sets of synapses. Curr Biol, 24(5), 484-493. doi:10.1016/j.cub.2014.01.022

Pennartz, C. M., Boeijinga, P. H., Kitai, S. T., & Lopes da Silva, F. H. (1991). Contribution of NMDA receptors to postsynaptic potentials and paired-pulse facilitation in identified neurons of the rat nucleus accumbens in vitro. *Exp Brain Res*, *86*(1), 190-198. doi:10.1007/BF00231053

Pennartz, C. M., Dolleman-Van der Weel, M. J., Kitai, S. T., & Lopes da Silva, F. H. (1992). Presynaptic dopamine D1 receptors attenuate excitatory and inhibitory limbic inputs to the shell region of the rat nucleus accumbens studied in vitro. *J Neurophysiol*, *67*(5), 1325-1334. doi:10.1152/jn.1992.67.5.1325

Pereira, P. A., Neves, J., Vilela, M., Sousa, S., Cruz, C., & Madeira, M. D. (2014). Chronic alcohol consumption leads to neurochemical changes in the nucleus accumbens that are not fully reversed by withdrawal. *Neurotoxicol Teratol*, *44*, 53-61. doi:10.1016/j.ntt.2014.05.007

Perez, M. F., White, F. J., & Hu, X. T. (2006). Dopamine D(2) receptor modulation of K(+) channel activity regulates excitability of nucleus accumbens neurons at different membrane potentials. *J Neurophysiol*, *96*(5), 2217-2228. doi:10.1152/jn.00254.2006

Pisani, A., Martella, G., Tscherter, A., Bonsi, P., Sharma, N., Bernardi, G., & Standaert, D. G. (2006). Altered responses to dopaminergic D2 receptor activation and N-type calcium currents in striatal cholinergic interneurons in

a mouse model of DYT1 dystonia. *Neurobiol Dis*, *24*(2), 318-325. doi:10.1016/j.nbd.2006.07.006

Quarta, D., Ciruela, F., Patkar, K., Borycz, J., Solinas, M., Lluis, C., . . . Ferré, S. (2007). Heteromeric nicotinic acetylcholine-dopamine autoreceptor complexes modulate striatal dopamine release. *Neuropsychopharmacology*, *32*(1), 35-42. doi:10.1038/sj.npp.1301103

Rahman, S., & Prendergast, M. A. (2012). Cholinergic receptor system as a target for treating alcohol abuse and dependence. *Recent Pat CNS Drug Discov*, *7*(2), 145-150. Retrieved from https://www.ncbi.nlm.nih.gov/entrez/query.fcgi?cmd=Retrieve&db=PubMed&dopt=Citation&list_uids=22574675

Rall, W. (1959). Branching dendritic trees and motoneuron membrane resistivity. *Exp Neurol*, *1*, 491-527. doi:10.1016/0014-4886(59)90046-9

Renteria, R., Buske, T. R., & Morrisett, R. A. (2018). Long-term subregion-specific encoding of enhanced ethanol intake by D1DR medium spiny neurons of the nucleus accumbens. *Addict Biol*, *23*(2), 689-698. doi:10.1111/adb.12526

Renteria, R., Maier, E. Y., Buske, T. R., & Morrisett, R. A. (2017). Selective alterations of NMDAR function and plasticity in D1 and D2 medium spiny neurons in the nucleus accumbens shell following chronic intermittent ethanol exposure. *Neuropharmacology*, *112*(Pt A), 164-171. doi:10.1016/j.neuropharm.2016.03.004

Rhodes, J. S., Best, K., Belknap, J. K., Finn, D. A., & Crabbe, J. C. (2005). Evaluation of a simple model of ethanol drinking to intoxication in C57BL/6J mice. *Physiol Behav*, *84*(1), 53-63. doi:10.1016/j.physbeh.2004.10.007

Robbe, D., Alonso, G., Chaumont, S., Bockaert, J., & Manzoni, O. J. (2002). Role of p/q-Ca2+ channels in metabotropic glutamate receptor 2/3-dependent presynaptic long-term depression at nucleus accumbens synapses. *J Neurosci*, *22*(11), 4346-4356. Retrieved from https://pubmed.ncbi.nlm.nih.gov/12040040

Robinson, D. L., Howard, E. C., McConnell, S., Gonzales, R. A., & Wightman, R. M. (2009). Disparity between tonic and phasic ethanol-induced dopamine increases in the nucleus accumbens of rats. *Alcohol Clin Exp Res*, *33*(7), 1187-1196. doi:10.1111/j.1530-0277.2009.00942.x

Robinson, T. E., & Berridge, K. C. (1993). The neural basis of drug craving: an incentive-sensitization theory of addiction. *Brain Res Brain Res Rev*, *18*(3), 247-291. Retrieved from https://www.ncbi.nlm.nih.gov/entrez/query.fcgi?cmd=Retrieve&db=PubMed&dopt=Citation&list_uids=8401595

Root, D. H., Melendez, R. I., Zaborszky, L., & Napier, T. C. (2015). The ventral pallidum: Subregion-specific functional anatomy and roles in motivated behaviors. *Prog Neurobiol*, *130*, 29-70. doi:10.1016/j.pneurobio.2015.03.005

Rosenkranz, J. A., & Grace, A. A. (1999). Modulation of basolateral amygdala neuronal firing and afferent drive by dopamine receptor activation in vivo. *J*

Neurosci, *19*(24), 11027-11039. Retrieved from https://pubmed.ncbi.nlm.nih.gov/10594083

Sacks, J. J., Gonzales, K. R., Bouchery, E. E., Tomedi, L. E., & Brewer, R. D. (2015). 2010 National and State Costs of Excessive Alcohol Consumption. *Am J Prev Med*, *49*(5), e73-e79. doi:10.1016/j.amepre.2015.05.031

Sakmann, B., & Neher, E. (1984). Patch clamp techniques for studying ionic channels in excitable membranes. *Annu Rev Physiol*, *46*, 455-472. doi:10.1146/annurev.ph.46.030184.002323

Schilaty, N. D., Hedges, D. M., Jang, E. Y., Folsom, R. J., Yorgason, J. T., McIntosh, J. M., & Steffensen, S. C. (2014). Acute ethanol inhibits dopamine release in the nucleus accumbens via α6 nicotinic acetylcholine receptors. *J Pharmacol Exp Ther*, *349*(3), 559-567. doi:10.1124/jpet.113.211490

Schuckit, M. A. (1994). Low level of response to alcohol as a predictor of future alcoholism. *Am J Psychiatry*, *151*(2), 184-189. doi:10.1176/ajp.151.2.184

Schuckit, M. A., Smith, T. L., Hesselbrock, V., Bucholz, K. K., Bierut, L., Edenberg, H., . . . Trim, R. (2008). Clinical implications of tolerance to alcohol in nondependent young drinkers. *Am J Drug Alcohol Abuse*, *34*(2), 133-149. doi:10.1080/00952990701877003

Schulz, J. M., & Reynolds, J. N. (2013). Pause and rebound: sensory control of cholinergic signaling in the striatum. *Trends Neurosci*, *36*(1), 41-50. doi:10.1016/j.tins.2012.09.006

Scofield, M. D., Heinsbroek, J. A., Gipson, C. D., Kupchik, Y. M., Spencer, S., Smith, A. C., . . . Kalivas, P. W. (2016). The Nucleus Accumbens: Mechanisms of Addiction across Drug Classes Reflect the Importance of Glutamate Homeostasis. *Pharmacol Rev*, *68*(3), 816-871. doi:10.1124/pr.116.012484

Scofield, M. D., & Kalivas, P. W. (2014). Astrocytic dysfunction and addiction: consequences of impaired glutamate homeostasis. *Neuroscientist*, *20*(6), 610-622. doi:10.1177/1073858413520347

Shen, W., Flajolet, M., Greengard, P., & Surmeier, D. J. (2008). Dichotomous dopaminergic control of striatal synaptic plasticity. *Science*, *321*(5890), 848-851. doi:10.1126/science.1160575

Shin, J. H., Adrover, M. F., Wess, J., & Alvarez, V. A. (2015). Muscarinic regulation of dopamine and glutamate transmission in the nucleus accumbens. *Proc Natl Acad Sci U S A*, *112*(26), 8124-8129. doi:10.1073/pnas.1508846112

Sneddon, E. A., Schuh, K. M., Frankel, J. W., & Radke, A. K. (2021). The contribution of medium spiny neuron subtypes in the nucleus accumbens core to compulsive-like ethanol drinking. *Neuropharmacology*, *187*, 108497. doi:10.1016/j.neuropharm.2021.108497

Soares-Cunha, C., Coimbra, B., Domingues, A. V., Vasconcelos, N., Sousa, N., & Rodrigues, A. J. (2018). Nucleus Accumbens Microcircuit Underlying D2-MSN-Driven Increase in Motivation. *eNeuro*, *5*(2). doi:10.1523/ENEURO.0386-18.2018

Soares-Cunha, C., de Vasconcelos, N. A. P., Coimbra, B., Domingues, A. V., Silva, J. M., Loureiro-Campos, E., . . . Rodrigues, A. J. (2020). Nucleus accumbens medium spiny neurons subtypes signal both reward and aversion. *Mol Psychiatry*, *25*(12), 3241-3255. doi:10.1038/s41380-019-0484-3

Söderpalm, B., Ericson, M., Olausson, P., Blomqvist, O., & Engel, J. A. (2000). Nicotinic mechanisms involved in the dopamine activating and reinforcing properties of ethanol. *Behav Brain Res*, *113*(1-2), 85-96. Retrieved from https://www.ncbi.nlm.nih.gov/entrez/query.fcgi?cmd=Retrieve&db=PubMed&dopt=Citation&list_uids=10942035

Söderpalm, B., Lidö, H. H., & Ericson, M. (2017). The Glycine Receptor-A Functionally Important Primary Brain Target of Ethanol. *Alcohol Clin Exp Res*, *41*(11), 1816-1830. doi:10.1111/acer.13483

Song, S., Miller, K. D., & Abbott, L. F. (2000). Competitive Hebbian learning through spike-timing-dependent synaptic plasticity. *Nat Neurosci*, *3*(9), 919-926. doi:10.1038/78829

Spanagel, R. (2009). Alcoholism: a systems approach from molecular physiology to addictive behavior. *Physiol Rev*, *89*(2), 649-705. doi:10.1152/physrev.00013.2008

Spano, P. F., Govoni, S., & Trabucchi, M. (1978). Studies on the pharmacological properties of dopamine receptors in various areas of the central nervous system. Adv Biochem Psychopharmacol, 19, 155-165. Retrieved from https://pubmed.ncbi.nlm.nih.gov/358777

Spiga, S., Talani, G., Mulas, G., Licheri, V., Fois, G. R., Muggironi, G., . . . Diana, M. (2014). Hampered long-term depression and thin spine loss in the nucleus accumbens of ethanol-dependent rats. *Proc Natl Acad Sci U S A*, *111*(35), E3745-54. doi:10.1073/pnas.1406768111

Stephens, D. N., & Duka, T. (2008). Review. Cognitive and emotional consequences of binge drinking: role of amygdala and prefrontal cortex. *Philos Trans R Soc Lond B Biol Sci*, *363*(1507), 3169-3179. doi:10.1098/rstb.2008.0097

Stigler, S. M. (1997). Regression towards the mean, historically considered. *Statistical methods in medical research*. Retrieved from https://journals.sagepub.com/doi/abs/10.1177/096228029700600202

Strong, C. E., Hagarty, D. P., Brea Guerrero, A., Schoepfer, K. J., Cajuste, S. M., & Kabbaj, M. (2020). Chemogenetic selective manipulation of nucleus accumbens medium spiny neurons bidirectionally controls alcohol intake in male and female rats. *Sci Rep*, *10*(1), 19178. doi:10.1038/s41598-020-76183-2

Stuber, G. D., Hnasko, T. S., Britt, J. P., Edwards, R. H., & Bonci, A. (2010). Dopaminergic terminals in the nucleus accumbens but not the dorsal striatum corelease glutamate. *J Neurosci*, *30*(24), 8229-8233. doi:10.1523/JNEUROSCI.1754-10.2010

Stuber, G. D., Sparta, D. R., Stamatakis, A. M., van Leeuwen, W. A., Hardjoprajitno, J. E., Cho, S., . . . Bonci, A. (2011). Excitatory transmission from the amygdala to nucleus accumbens facilitates reward seeking. *Nature*, *475*(7356), 377-380. doi:10.1038/nature10194

Südhof, T. C. (2013). Neurotransmitter release: the last millisecond in the life of a synaptic vesicle. Neuron, 80(3), 675-690. doi:10.1016/j.neuron.2013.10.022

Surmeier, D. J., Bargas, J., Hemmings, H. C., Nairn, A. C., & Greengard, P. (1995). Modulation of calcium currents by a D1 dopaminergic protein kinase/phosphatase cascade in rat neostriatal neurons. *Neuron*, *14*(2), 385-397. Retrieved from https://www.ncbi.nlm.nih.gov/entrez/query.fcgi?cmd=Retrieve&db=PubMed&dopt=Citation&list_uids=7531987

Surmeier, D. J., Ding, J., Day, M., Wang, Z., & Shen, W. (2007). D1 and D2 dopamine-receptor modulation of striatal glutamatergic signaling in striatal medium spiny neurons. *Trends Neurosci*, *30*(5), 228-235. doi:10.1016/j.tins.2007.03.008

Surmeier, D. J., Eberwine, J., Wilson, C. J., Cao, Y., Stefani, A., & Kitai, S. T. (1992). Dopamine receptor subtypes colocalize in rat striatonigral neurons. *Proc Natl Acad Sci U S A*, *89*(21), 10178-10182. Retrieved from https://www.ncbi.nlm.nih.gov/entrez/query.fcgi?cmd=Retrieve&db=PubMed&dopt=Citation&list_uids=1332033

Surmeier, D. J., & Graybiel, A. M. (2012). A feud that wasn't: acetylcholine evokes dopamine release in the striatum. *Neuron*, *75*(1), 1-3. doi:10.1016/j.neuron.2012.06.028

Taylor, S. R., Badurek, S., Dileone, R. J., Nashmi, R., Minichiello, L., & Picciotto, M. R. (2014). GABAergic and glutamatergic efferents of the mouse ventral tegmental area. *J Comp Neurol*, *522*(14), 3308-3334. doi:10.1002/cne.23603

Tepper, J. M., Tecuapetla, F., Koós, T., & Ibáñez-Sandoval, O. (2010). Heterogeneity and diversity of striatal GABAergic interneurons. *Front Neuroanat*, *4*, 150. doi:10.3389/fnana.2010.00150

Threlfell, S., Clements, M. A., Khodai, T., Pienaar, I. S., Exley, R., Wess, J., & Cragg, S. J. (2010). Striatal muscarinic receptors promote activity dependence of dopamine transmission via distinct receptor subtypes on cholinergic interneurons in ventral versus dorsal striatum. *J Neurosci*, *30*(9), 3398-3408. doi:10.1523/JNEUROSCI.5620-09.2010

Threlfell, S., & Cragg, S. J. (2011). Dopamine signaling in dorsal versus ventral striatum: the dynamic role of cholinergic interneurons. *Front Syst Neurosci*, *5*, 11. doi:10.3389/fnsys.2011.00011

Threlfell, S., Lalic, T., Platt, N. J., Jennings, K. A., Deisseroth, K., & Cragg, S. J. (2012). Striatal dopamine release is triggered by synchronized activity in cholinergic interneurons. *Neuron*, *75*(1), 58-64. doi:10.1016/j.neuron.2012.04.038

Tomsovic, M. (1974). “Binge” and continuous drinkers. Characteristics and treatment follow-up. *Q J Stud Alcohol*, *35*(2), 558-564. Retrieved from https://pubmed.ncbi.nlm.nih.gov/4431895

Trantham-Davidson, H., Burnett, E. J., Gass, J. T., Lopez, M. F., Mulholland, P. J., Centanni, S. W., . . . Chandler, L. J. (2014). Chronic alcohol disrupts dopamine receptor activity and the cognitive function of the medial prefrontal cortex. *J Neurosci*, *34*(10), 3706-3718. doi:10.1523/JNEUROSCI.0623-13.2014

Tritsch, N. X., Ding, J. B., & Sabatini, B. L. (2012). Dopaminergic neurons inhibit striatal output through non-canonical release of GABA. *Nature*, *490*(7419), 262-266. doi:10.1038/nature11466

Tritsch, N. X., & Sabatini, B. L. (2012). Dopaminergic modulation of synaptic transmission in cortex and striatum. *Neuron*, *76*(1), 33-50. doi:10.1016/j.neuron.2012.09.023

Tuesta, L. M., Fowler, C. D., & Kenny, P. J. (2011). Recent advances in understanding nicotinic receptor signaling mechanisms that regulate drug self-administration behavior. *Biochem Pharmacol*, *82*(8), 984-995. doi:10.1016/j.bcp.2011.06.026

Turrigiano, G. (2011). Too many cooks? Intrinsic and synaptic homeostatic mechanisms in cortical circuit refinement. *Annual review of neuroscience*. Retrieved from https://www.annualreviews.org/doi/abs/10.1146/annurev-neuro-060909-153238

Uys, J. D., McGuier, N. S., Gass, J. T., Griffin, W. C., Ball, L. E., & Mulholland, P. J. (2016). Chronic intermittent ethanol exposure and withdrawal leads to adaptations in nucleus accumbens core postsynaptic density proteome and dendritic spines. *Addict Biol*, *21*(3), 560-574. doi:10.1111/adb.12238

VanDemark, K. L., Guizzetti, M., Giordano, G., & Costa, L. G. (2009). Ethanol inhibits muscarinic receptor-induced axonal growth in rat hippocampal neurons. *Alcohol Clin Exp Res*, *33*(11), 1945-1955. doi:10.1111/j.1530-0277.2009.01032.x

Vertes, R. P., & Hoover, W. B. (2008). Projections of the paraventricular and paratenial nuclei of the dorsal midline thalamus in the rat. *J Comp Neurol*, *508*(2), 212-237. doi:10.1002/cne.21679

Vetreno, R. P., Broadwater, M., Liu, W., Spear, L. P., & Crews, F. T. (2014). Adolescent, but not adult, binge ethanol exposure leads to persistent global reductions of choline acetyltransferase expressing neurons in brain. *PLoS One*, *9*(11), e113421. doi:10.1371/journal.pone.0113421

Volkow, N. D., Koob, G. F., & McLellan, A. T. (2016). Neurobiologic Advances from the Brain Disease Model of Addiction. *N Engl J Med*, *374*(4), 363-371. doi:10.1056/NEJMra1511480

Volkow, N. D., & Morales, M. (2015). The Brain on Drugs: From Reward to Addiction. *Cell*, *162*(4), 712-725. doi:10.1016/j.cell.2015.07.046

Voorn, P., Vanderschuren, L. J., Groenewegen, H. J., Robbins, T. W., & Pennartz, C. M. (2004). Putting a spin on the dorsal-ventral divide of the striatum. *Trends Neurosci*, *27*(8), 468-474. doi:10.1016/j.tins.2004.06.006

Wang, J., Ben Hamida, S., Darcq, E., Zhu, W., Gibb, S. L., Lanfranco, M. F., . . . Ron, D. (2012a). Ethanol-mediated facilitation of AMPA receptor function in the dorsomedial striatum: implications for alcohol drinking behavior. *J Neurosci*, *32*(43), 15124-15132. doi:10.1523/JNEUROSCI.2783-12.2012

Wang, J., Cheng, Y., Wang, X., Roltsch Hellard, E., Ma, T., Gil, H., . . . Ron, D. (2015). Alcohol Elicits Functional and Structural Plasticity Selectively in Dopamine D1 Receptor-Expressing Neurons of the Dorsomedial Striatum. *J Neurosci*, *35*(33), 11634-11643. doi:10.1523/JNEUROSCI.0003-15.2015

Wang, L., Zhang, X., Xu, H., Zhou, L., Jiao, R., Liu, W., . . . Zhou, Z. (2014). Temporal components of cholinergic terminal to dopaminergic terminal transmission in dorsal striatum slices of mice. *J Physiol*, *592*(16), 3559-3576. doi:10.1113/jphysiol.2014.271825

Wang, W., Darvas, M., Storey, G. P., Bamford, I. J., Gibbs, J. T., Palmiter, R. D., & Bamford, N. S. (2013). Acetylcholine encodes long-lasting presynaptic plasticity at glutamatergic synapses in the dorsal striatum after repeated amphetamine exposure. *J Neurosci*, *33*(25), 10405-10426. doi:10.1523/JNEUROSCI.0014-13.2013

Wang, W., Dever, D., Lowe, J., Storey, G. P., Bhansali, A., Eck, E. K., . . . Bamford, N. S. (2012b). Regulation of prefrontal excitatory neurotransmission by dopamine in the nucleus accumbens core. *J Physiol*, *590*(16), 3743-3769. doi:10.1113/jphysiol.2012.235200

Warner-Schmidt, J. L., Schmidt, E. F., Marshall, J. J., Rubin, A. J., Arango-Lievano, M., Kaplitt, M. G., . . . Greengard, P. (2012). Cholinergic interneurons in the nucleus accumbens regulate depression-like behavior. *Proc Natl Acad Sci U S A*, *109*(28), 11360-11365. doi:10.1073/pnas.1209293109

Wassum, K. M., & Izquierdo, A. (2015). The basolateral amygdala in reward learning and addiction. *Neurosci Biobehav Rev*, *57*, 271-283. doi:10.1016/j.neubiorev.2015.08.017

Watabe-Uchida, M., Zhu, L., Ogawa, S. K., Vamanrao, A., & Uchida, N. (2012). Whole-brain mapping of direct inputs to midbrain dopamine neurons. Neuron, 74(5), 858-873. doi:10.1016/j.neuron.2012.03.017

Weight, F. F., Lovinger, D. M., & White, G. (1991). Alcohol inhibition of NMDA channel function. *Alcohol Alcohol Suppl*, *1*, 163-169. Retrieved from https://pubmed.ncbi.nlm.nih.gov/1726982

Weight, F. F., Peoples, R. W., Wright, J. M., Lovinger, D. M., & White, G. (1993). Ethanol action on excitatory amino acid activated ion channels. *Alcohol Alcohol Suppl*, *2*, 353-358. Retrieved from https://pubmed.ncbi.nlm.nih.gov/7538302

Weiner, J. L., & Valenzuela, C. F. (2006). Ethanol modulation of GABAergic transmission: the view from the slice. *Pharmacol Ther*, *111*(3), 533-554. doi:10.1016/j.pharmthera.2005.11.002

Wess, J. (1996). Molecular biology of muscarinic acetylcholine receptors. *Crit Rev Neurobiol*, *10*(1), 69-99. doi:10.1615/critrevneurobiol.v10.i1.40

Wieland, S., Du, D., Oswald, M. J., Parlato, R., Köhr, G., & Kelsch, W. (2014). Phasic dopaminergic activity exerts fast control of cholinergic interneuron firing via sequential NMDA, D2, and D1 receptor activation. *J Neurosci*, *34*(35), 11549-11559. doi:10.1523/JNEUROSCI.1175-14.2014

Wilcox, M. V., Cuzon Carlson, V. C., Sherazee, N., Sprow, G. M., Bock, R., Thiele, T. E., . . . Alvarez, V. A. (2014). Repeated binge-like ethanol drinking alters ethanol drinking patterns and depresses striatal GABAergic transmission. *Neuropsychopharmacology*, *39*(3), 579-594. doi:10.1038/npp.2013.230

Williams, M. J., & Adinoff, B. (2008). The role of acetylcholine in cocaine addiction. *Neuropsychopharmacology*, *33*(8), 1779-1797. doi:10.1038/sj.npp.1301585

Wise, R. A. (2002). Brain reward circuitry: insights from unsensed incentives. *Neuron*, *36*(2), 229-240. doi:10.1016/s0896-6273(02)00965-0

Witten, I. B., Lin, S. C., Brodsky, M., Prakash, R., Diester, I., Anikeeva, P., . . . Deisseroth, K. (2010). Cholinergic interneurons control local circuit activity and cocaine conditioning. *Science*, *330*(6011), 1677-1681. doi:10.1126/science.1193771

Wu, J., Gao, M., & Taylor, D. H. (2014). Neuronal nicotinic acetylcholine receptors are important targets for alcohol reward and dependence. *Acta Pharmacol Sin*, *35*(3), 311-315. doi:10.1038/aps.2013.181

Xia, J. X., Li, J., Zhou, R., Zhang, X. H., Ge, Y. B., & Ru Yuan, X. (2006). Alterations of rat corticostriatal synaptic plasticity after chronic ethanol exposure and withdrawal. *Alcohol Clin Exp Res*, *30*(5), 819-824. doi:10.1111/j.1530-0277.2006.00095.x

Yan, Z., Flores-Hernandez, J., & Surmeier, D. J. (2001). Coordinated expression of muscarinic receptor messenger RNAs in striatal medium spiny neurons. *Neuroscience*, *103*(4), 1017-1024. doi:10.1016/s0306-4522(01)00039-2

Yasuda, R. P., Ciesla, W., Flores, L. R., Wall, S. J., Li, M., Satkus, S. A., . . . Wolfe, B. B. (1993). Development of antisera selective for m4 and m5 muscarinic cholinergic receptors: distribution of m4 and m5 receptors in rat brain. *Mol Pharmacol*, *43*(2), 149-157. Retrieved from https://pubmed.ncbi.nlm.nih.gov/8429821

Yawata, S., Yamaguchi, T., Danjo, T., Hikida, T., & Nakanishi, S. (2012). Pathway-specific control of reward learning and its flexibility via selective dopamine receptors in the nucleus accumbens. *Proc Natl Acad Sci U S A*, *109*(31), 12764-12769. doi:10.1073/pnas.1210797109

Yin, H. H., Park, B. S., Adermark, L., & Lovinger, D. M. (2007). Ethanol reverses the direction of long-term synaptic plasticity in the dorsomedial striatum. *Eur J Neurosci*, *25*(11), 3226-3232. doi:10.1111/j.1460-9568.2007.05606.x

Yorgason, J. T., Ferris, M. J., Steffensen, S. C., & Jones, S. R. (2014). Frequency-dependent effects of ethanol on dopamine release in the nucleus accumbens. *Alcohol Clin Exp Res*, *38*(2), 438-447. doi:10.1111/acer.12287

Yorgason, J. T., Rose, J. H., McIntosh, J. M., Ferris, M. J., & Jones, S. R. (2015). Greater ethanol inhibition of presynaptic dopamine release in C57BL/6J than DBA/2J mice: Role of nicotinic acetylcholine receptors. *Neuroscience*, *284*, 854-864. doi:10.1016/j.neuroscience.2014.10.052

Yorgason, J. T., Wadsworth, H. A., Anderson, E. J., Williams, B. M., Brundage, J. N., Hedges, D. M., . . . Steffensen, S. C. (2022). Modulation of dopamine release by ethanol is mediated by atypical GABA. *Addict Biol*, *27*(1), e13108. doi:10.1111/adb.13108

Yorgason, J. T., Zeppenfeld, D. M., & Williams, J. T. (2017). Cholinergic Interneurons Underlie Spontaneous Dopamine Release in Nucleus Accumbens. *J Neurosci*, *37*(8), 2086-2096. doi:10.1523/JNEUROSCI.3064-16.2017

Yoshimoto, K., McBride, W. J., Lumeng, L., & Li, T. K. (1992). Alcohol stimulates the release of dopamine and serotonin in the nucleus accumbens. *Alcohol*, *9*(1), 17-22. Retrieved from https://www.ncbi.nlm.nih.gov/entrez/query.fcgi?cmd=Retrieve&db=PubMed&dopt=Citation&list_uids=1370758

Yu, Z., Guindani, M., Grieco, S. F., Chen, L., Holmes, T. C., & Xu, X. (2021). Beyond t test and ANOVA: applications of mixed-effects models for more rigorous statistical analysis in neuroscience research. *Neuron*. Retrieved from https://www.sciencedirect.com/science/article/pii/S089662732100845X

Zappettini, S., Grilli, M., Olivero, G., Chen, J., Padolecchia, C., Pittaluga, A., . . . Marchi, M. (2014). Nicotinic α7 receptor activation selectively potentiates the function of NMDA receptors in glutamatergic terminals of the nucleus accumbens. *Front Cell Neurosci*, *8*, 332. doi:10.3389/fncel.2014.00332

Zhang, W. H., Cao, K. X., Ding, Z. B., Yang, J. L., Pan, B. X., & Xue, Y. X. (2019). Role of prefrontal cortex in the extinction of drug memories. *Psychopharmacology (Berl)*, *236*(1), 463-477. doi:10.1007/s00213-018-5069-3

Zhang, X. F., Hu, X. T., & White, F. J. (1998). Whole-cell plasticity in cocaine withdrawal: reduced sodium currents in nucleus accumbens neurons. *J Neurosci*, *18*(1), 488-498. Retrieved from https://pubmed.ncbi.nlm.nih.gov/9412525

Zhou, F. M., Liang, Y., & Dani, J. A. (2001). Endogenous nicotinic cholinergic activity regulates dopamine release in the striatum. *Nat Neurosci*, *4*(12), 1224-1229. doi:10.1038/nn769

Zhou, F. M., Wilson, C. J., & Dani, J. A. (2002). Cholinergic interneuron characteristics and nicotinic properties in the striatum. *J Neurobiol*, *53*(4), 590-605. doi:10.1002/neu.10150

Zorumski, C. F., Mennerick, S., & Izumi, Y. (2014). Acute and chronic effects of ethanol on learning-related synaptic plasticity. *Alcohol*, *48*(1), 1-17. doi:10.1016/j.alcohol.2013.09.045

Zuo, Y., Kuryatov, A., Lindstrom, J. M., Yeh, J. Z., & Narahashi, T. (2002). Alcohol modulation of neuronal nicotinic acetylcholine receptors is alpha subunit dependent. *Alcohol Clin Exp Res*, *26*(6), 779-784. Retrieved from https://pubmed.ncbi.nlm.nih.gov/12068245